INFORMATION TO USERS

This material was produced from a microfilm copy of the original document. While the most advanced technological means to photograph and reproduce this document have been used, the quality is heavily dependent upon the quality of the original submitted.

The following explanation of techniques is provided to help you understand markings or patterns which may appear on this reproduction.

1. The sign or "target" for pages apparently lacking from the document photographed is "Missing Page(s)". If it was possible to obtain the missing page(s) or section, they are spliced into the film along with adjacent pages. This may have necessitated cutting thru an image and duplicating adjacent pages to insure you complete continuity.

2. When an image on the film is obliterated with a large round black mark, it is an indication that the photographer suspected that the copy may have moved during exposure and thus cause a blurred image. You will find a good image of the page in the adjacent frame.

3. When a map, drawing or chart, etc., was part of the material being photographed the photographer followed a definite method in "sectioning" the material. It is customary to begin photoing at the upper left hand corner of a large sheet and to continue photoing from left to right in equal sections with a small overlap. If necessary, sectioning is continued again — beginning below the first row and continuing on until complete.

4. The majority of users indicate that the textual content is of greatest value, however, a somewhat higher quality reproduction could be made from "photographs" if essential to the understanding of the dissertation. Silver prints of "photographs" may be ordered at additional charge by writing the Order Department, giving the catalog number, title, author and specific pages you wish reproduced.

5. PLEASE NOTE: Some pages may have indistinct print. Filmed as received.

Xerox University Microfilms
300 North Zeeb Road
Ann Arbor, Michigan 48106

Downloaded from SHAREOK. Persistent Handle URL: https://hdl.handle.net/11244/3851

75-6531

KUMAR, Subodh, 1936-
A STUDY OF THE EFFECTS OF SIMULATED WEATHERING AND REPEATED LOADS ON FOUR LIME STABILIZED OKLAHOMA SHALES.

The University of Oklahoma, Ph.D., 1974
Engineering, civil

Xerox University Microfilms, Ann Arbor, Michigan 48106

THIS DISSERTATION HAS BEEN MICROFILMED EXACTLY AS RECEIVED.

THE UNIVERSITY OF OKLAHOMA

GRADUATE COLLEGE

A STUDY OF THE EFFECTS OF SIMULATED WEATHERING AND REPEATED LOADS ON FOUR LIME STABILIZED OKLAHOMA SHALES

A DISSERTATION

SUBMITTED TO THE GRADUATE FACULTY

in partial fulfillment of the requirements for the

degree of

DOCTOR OF PHILOSOPHY

BY

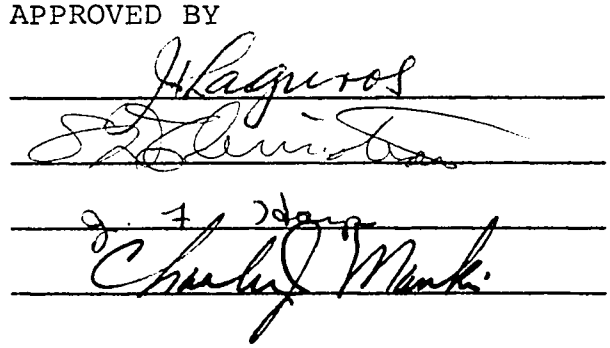
SUBODH KUMAR

Norman, Oklahoma

1974

A STUDY OF THE EFFECTS OF SIMULATED WEATHERING AND REPEATED LOADS ON FOUR LIME STABILIZED OKLAHOMA SHALES

APPROVED BY



DISSERTATION COMMITTEE

ABSTRACT

The current methods of pavement design are based on the durability characteristics of pavement materials, nature of traffic loads and predicted volume of traffic. However, these methods do not take into account the effects of the climatic conditions existing during construction and the gradual changes due to climatic and traffic induced stresses after construction.

In the present investigation, it is attempted to develop the testing procedures to simulate the combined effects of climatic and traffic induced stresses and evaluate the performance of subgrade materials under the criteria of wet-dry cycles and repetitive loading. Four Oklahoma shales, varying in texture and mineralogy, were selected. They were treated with the addition of 1, 2, 4 and 6 percent lime. Each shale-lime combination was subjected to 5, 15, 30 and 50 wet-dry weathering cycles, and tested under cyclic loading in the form of repetitive split tensile strength tests.

Addition of lime improved strength characteristics and reduced shrinkage in relation to the amount of clay content in the shale and amount of lime. The destructive effect of wet-dry cycles was greater on untreated shales than on the

lime treated shales, and it became minimal with increasing amounts of lime. To determine the failure of samples in repeated load split tensile strength tests, the diametral strain proved to be a very good criterion. However, the strength gain of shale lime mix appears to depend on the humidity, matrix porosity, progress of shale lime reaction and amount and nature of reaction products. Addition of lime to shale significantly alters the character of the shale. However, alternate wetting and drying results in material properties which are significantly different from those of the raw and of the lime stabilized shale. This study indicated that the use of shales in pavement construction needs to follow new design criteria which consider the continuous changes under environmental conditions and repetitive loads taking place in the lime stabilized shale mass.

ACKNOWLEDGMENTS

A significant part of this investigation was conducted under OURI Project 1677 which was under contract with the Oklahoma Department of Highways (Study 68-03-2). The author wishes to acknowledge the help of Messrs. Williard McCasland and Curtis J. Hayes of the Research and Development Division, Oklahoma Department of Highways for collecting and making available the shales used in this study.

The author is extremely grateful to his major professor Dr. Joakim G. Laguros for his advice, guidance, interest and supervision related to this investigation and to the author's academic program. The author is sincerely thankful to Dr. Sherril D. Christian, Professor, Department of Chemistry, Dr. James F. Harp, Associate Professor, Department of Civil Engineering and Environmental Science, and Dr. Charles J. Mankin, Director, School of Geology and Geophysics, for their general guidance and taking time out to serve on the author's Graduate Program Advisory Committee.

Thanks are due also Dr. Ghassan Al-Rawi and Messrs. Vahe Aprahamian, Suresh Chandra, Bobby D. Hanks, Johnny D. James, Howard C. Martin, Shailendra K. Saksena, Thomas C. Wisehart and Mohsin Zaidi for their help at various stages of

this investigation, and to Ms. Bobbie Everidge for her excellent and efficient typing of the manuscript.

Very special thanks are due Dr. Manickam Annamalai for his constant counsel, critique, friendship and help during all phases of the author's graduate study program at the University of Oklahoma.

The author wishes to express his great admiration for his dear wife, Nipha, for her love, patience and help in preparation of the manuscript for this dissertation.

TABLE OF CONTENTS

		Page
LIST OF TABLES		ix
LIST OF ILLUSTRATIONS		xi
Chapter		
I.	INTRODUCTION	1
II.	REVIEW OF LITERATURE	3
	Moisture Content	5
	Repeated Load Testing	8
	Split Tensile Strength Test	12
	Crack and Crack Propagation	25
	Lime Stabilization	27
III.	SELECTION OF MATERIALS	33
IV.	TESTING PROCEDURE	37
	Preparation of Mix	37
	Moisture Density Relationship	38
	Preparation of Samples	38
	Application of Wet-Dry Cycles	43
	Repeated Load Split Tensile Strength Test	47
	Determination of Liquid Limit	58
	Determination of Plastic Limit	58
	X-Ray Diffraction Analysis	58
V.	PRESENTATION AND DISCUSSION OF TEST DATA	60
	Maximum Dry Density and Optimum Moisture Content	61
	Preparation of Samples	64
	Application of Wet-Dry Cycles	66
	Repeated Load Split Tensile Strength Test	73
	Atterberg Limit Tests	99
	X-Ray Diffraction Analysis	102
	General Discussion	113

TABLE OF CONTENTS--Continued

Chapter		Page
VI.	CONCLUSIONS	119
VII.	SUGGESTIONS FOR FURTHER RESEARCH	123
REFERENCES		125
APPENDICES		133
A:	DERIVATION OF EXPRESSIONS FOR DETERMINING THE STRESSES IN THE SPLIT TENSILE STRENGTH TEST SPECIMEN UNDER VERTICAL DIAMETRAL COMPRESSION	134
B:	CIRCUIT DIAGRAMS FOR ELECTRICAL CONNECTIONS	144
C:	SHRINKAGES OF SHALE AND SHALE LIME MIX SAMPLES	148
D:	TEST DATA FOR SHALE AND SHALE LIME MIX SAMPLES	153
E:	EFFECT OF AMOUNT OF LIME ON DIAMETRAL STRAIN OF SAMPLES	170
F:	EFFECT OF WET-DRY CYCLES ON DIAMETRAL STRAIN OF SAMPLES	187
G:	EFFECTS OF AMOUNT OF LIME AND OF WET-DRY CYCLES ON THE LIQUID LIMIT VALUES OF SHALES AND SHALE LIME MIXES	204
H:	EFFECTS OF AMOUNT OF LIME AND OF WET-DRY CYCLES ON THE PLASTICITY INDEX VALUES OF SHALES AND SHALE LIME MIXES	211

LIST OF TABLES

Tables		Page
3.1	Geologic Information on Shales	36
3.2	Engineering Property Data of Shales	36
4.1	Maximum Dry Density and Optimum Moisture Content Values at Various Amounts of Lime	39
5.1	Optimum, Average Molding and End of Cycle Moisture Contents for Various Shale Lime Combinations	67
5.2	Average Shrinkage (%) of Samples	69
5.3	Example of Shrinkage (%) at the End of Wet-Dry Cycles for Various Shales at 4 Percent Lime Addition	71
5.4	Effect of Load on the Diametral Strain of Some Shale and Shale Lime Samples	82
5.5	Effect of Frequency of Load Application on the Diametral Strain of Some Shale and Shale Lime Samples	86
5.6	Clay Mineral Composition of Shales	90
5.7	X-Ray Identification d-Spacing for Clays, Clay Associated Minerals, Lime and Lime Clay Reaction Products	104
D.1	Test Data for Shale and Shale Lime Mix Samples. Shale No. 13, Test Condition: Humid	154
D.2	Test Data for Shale and Shale Lime Mix Samples. Shale No. 13, Test Condition: Dry	156
D.3	Test Data for Shale and Shale Lime Mix Samples. Shale No. 15, Test Condition: Humid	158

LIST OF TABLES--Continued

Table		Page
D.4	Test Data for Shale and Shale Lime Mix Samples. Shale No. 15, Test Condition: Dry	160
D.5	Test Data for Shale and Shale Lime Mix Samples. Shale No. 21, Test Condition: Humid	162
D.6	Test Data for Shale and Shale Lime Mix Samples. Shale No. 21, Test Condition: Dry	164
D.7	Test Data for Shale and Shale Lime Mix Samples. Shale No. 24, Test Condition: Humid	166
D.8	Test Data for Shale and Shale Lime Mix Samples. Shale No. 24, Test Condition: Dry	168
G.1	Effects of Amount of Lime and of Wet-Dry Cycles on the Liquid Limit Values of Shales and Shale Lime Mixes	205
H.1	Effects of Amount of Lime and of Wet-Dry Cycles on the Plasticity Index Values of Shales and Shale Lime Mixes	212

LIST OF ILLUSTRATIONS

Figure		Page
2.1	Forces Acting on a Disk and Location of Point (x,y) in Split Tensile Strength Test	16
2.2	Distribution of Stresses S_x and S_y along Coordinate Axes x and y in a Disk Under Vertical Diametral Compression	18
2.3	Geometrical Configuration and Locations of Points (x_e,y_e) and (x_1,y_1) on a Disk Deformed by Distance d Along Vertical Diameter in Split Tensile Strength Test	22
2.4	Distribution of Stresses S_x and S_y Along Coordinate Axes for Sample Under Deformation in Split Tensile Strength Test (Deformation = 0.02 x Diameter) . . .	24
3.1	Location and Identification of Selected Shale Samples	35
4.1	Change in Maximum Dry Density Values with the Addition of Lime	40
4.2	Change in Optimum Moisture Content Value with the Addition of Lime	41
4.3	Details of Sample Molding Apparatus	42
4.4	Wet-Dry Cycles for Oklahoma	45
4.5	Equipment for Cyclic Split Tensile Strength Test	48
4.6	Load Cell	50
4.7	Displacement Strain Gage	50
4.8	Arrangement of Load Cell and Displacement Strain Gage During Testing	52

LIST OF ILLUSTRATIONS--Continued

Figure		Page
4.9	Detailed View of Sample Under Test	52
4.10	A Sample of Recordings Obtained from Sanborn Strip Chart Recorder	54
5.1	Relationship Between Maximum Dry Density and Optimum Moisture Content for all Shales and Shale Lime Combinations	63
5.2	Example of Diametral Strain, Load and Frequency Relationships for Repeated Load Split Tensile Strength Test	75
5.3	Example of Stress, Load and Frequency Relationships for Repeated Load Split Tensile Strength Test	76
5.4	Three Zones of a Typical Strain-Frequency-Load Graph	78
5.5	Examples of Three Common Types of Strain-Frequency-Load Graphs	78
5.6	Example of Bending Points on Strain-Frequency-Load Graph	78
5.7	General Diametral Strain-Load Relationship	85
5.8	General Diametral Strain-Frequency Relationship	85
5.9	Selected X-Ray Diffraction Patterns for Shale 13 and its Lime Combinations	107
5.10	Selected X-Ray Diffraction Patterns for Shale 15 and its Lime Combinations	108
5.11	Selected X-Ray Diffraction Patterns for Shale 21 and its Lime Combinations	110
5.12	Selected X-Ray Diffraction Patterns for Shale 24 and its Lime Combinations	112
B.1	Circuit Diagram for SBEL Soil Dynamic Testing Machine (From Reference SBEL, 1970)	145

LIST OF ILLUSTRATIONS--Continued

Figure		Page
B.2	Half Bridge Connection to Preamplifier (From Reference Hewlett-Packard, 1967b)	146
B.3	Circuit Diagram Showing Connection Between Dwell Monitor and Atomic Strip Chart Recorder	147
C.1	Shrinkage of Shale and Shale Lime Mix Samples for Shale 13 at the End of Wet-Dry Cycles and of 120-Day Curing	149
C.2	Shrinkage of Shale and Shale Lime Mix Samples for Shale 15 at the End of Wet-Dry Cycles and of 120-Day Curing	150
C.3	Shrinkage of Shale and Shale Lime Mix Samples for Shale 21 at the End of Wet-Dry Cycles and of 120-Day Curing	151
C.4	Shrinkage of Shale and Shale Lime Mix Samples for Shale 24 at the End of Wet-Dry Cycles and of 120-Day Curing	152
E.1	Effect of Amount of Lime on Diametral Strain at Failure for Humid Samples of Shale 13	171
E.2	Effect of Amount of Lime on Diametral Strain at Failure for Humid Samples of Shale 13	172
E.3	Effect of Amount of Lime on Diametral Strain at Failure for Dry Samples of Shale 13	173
E.4	Effect of Amount of Lime on Diametral Strain at Failure for Dry Samples of Shale 13	174
E.5	Effect of Amount of Lime on Diametral Strain at Failure for Humid Samples of Shale 15	175
E.6	Effect of Amount of Lime on Diametral Strain at Failure for Humid Samples of Shale 15	176

LIST OF ILLUSTRATIONS--Continued

Figure		Page
E.7	Effect of Amount of Lime on Diametral Strain at Failure for Dry Samples of Shale 15	177
E.8	Effect of Amount of Lime on Diametral Strain at Failure for Dry Samples of Shale 15	178
E.9	Effect of Amount of Lime on Diametral Strain at Failure for Humid Samples of Shale 21	179
E.10	Effect of Amount of Lime on Diametral Strain at Failure for Humid Samples of Shale 21	180
E.11	Effect of Amount of Lime on Diametral Strain at Failure for Dry Samples of Shale 21	181
E.12	Effect of Amount of Lime on Diametral Strain at Failure for Dry Samples of Shale 21	182
E.13	Effect of Amount of Lime on Diametral Strain at Failure for Humid Samples of Shale 24	183
E.14	Effect of Amount of Lime on Diametral Strain at Failure for Humid Samples of Shale 24	184
E.15	Effect of Amount of Lime on Diametral Strain at Failure for Dry Samples of Shale 24	185
E.16	Effect of Amount of Lime on Diametral Strain at Failure for Dry Samples of Shale 24	186
F.1	Effect of Wet-Dry Cycles on Diametral Strain at Failure for Humid Samples of Shale 13	188
F.2	Effect of Wet-Dry Cycles on Diametral Strain at Failure for Humid Samples of Shale 13	189

LIST OF ILLUSTRATIONS--Continued

Figure		Page
F.3	Effect of Wet-Dry Cycles on Diametral Strain at Failure for Dry Samples of Shale 13	190
F.4	Effect of Wet-Dry Cycles on Diametral Strain at Failure for Dry Samples of Shale 13	191
F.5	Effect of Wet-Dry Cycles on Diametral Strain at Failure for Humid Samples of Shale 15	192
F.6	Effect of Wet-Dry Cycles on Diametral Strain at Failure for Humid Samples of Shale 15	193
F.7	Effect of Wet-Dry Cycles on Diametral Strain at Failure for Dry Samples of Shale 15	194
F.8	Effect of Wet-Dry Cycles on Diametral Strain at Failure for Dry Samples of Shale 15	195
F.9	Effect of Wet-Dry Cycles on Diametral Strain at Failure for Humid Samples of Shale 21	196
F.10	Effect of Wet-Dry Cycles on Diametral Strain at Failure for Humid Samples of Shale 21	197
F.11	Effect of Wet-Dry Cycles on Diametral Strain at Failure for Dry Samples of Shale 21	198
F.12	Effect of Wet-Dry Cycles on Diametral Strain at Failure for Dry Samples of Shale 21	199
F.13	Effect of Wet-Dry Cycles on Diametral Strain at Failure for Humid Samples of Shale 24	200
F.14	Effect of Wet-Dry Cycles on Diametral Strain at Failure for Humid Samples of Shale 24	201

LIST OF ILLUSTRATIONS--Continued

Figure		Page
F.15	Effect of Wet-Dry Cycles on Diametral Strain at Failure for Dry Samples of Shale 24	202
F.16	Effect of Wet-Dry Cycles on Diametral Strain at Failure for Dry Samples of Shale 24	203
G.1	Effect of Amount of Lime on Liquid Limit Values for Shale 13	206
G.2	Effect of Amount of Lime on Liquid Limit Values for Shale 15	207
G.3	Effect of Amount of Lime on Liquid Limit Values for Shale 21	208
G.4	Effect of Amount of Lime on Liquid Limit Values for Shale 24	209
G.5	Change in Liquid Limit Values with the Amount of Lime for 120-Day Cured Samples	210
H.1	Effect of Amount of Lime on Plasticity Index Values for Shale 13	213
H.2	Effect of Amount of Lime on Plasticity Index Values for Shale 15	214
H.3	Effect of Amount of Lime on Plasticity Index Values for Shale 21	215
H.4	Effect of Amount of Lime on Plasticity Index Values for Shale 24	216
H.5	Change in Plasticity Index Values with Amount of Lime for 120-Day Cured Samples	217

CHAPTER I

INTRODUCTION

Attempts at improvements in the design of pavements have classically resulted in increased pavement thickness; however, the problem of pavement failure has not been obliterated. The current methods of pavement design do take into consideration the stability and durability of subgrade material; still, the problem of pavement design is not approached from a realistic point of view since design methods have not as yet been developed to take account of the effects of the conditions existing during construction and then during the life of the subgrade material under a pavement.

During grading operations, soil is excavated from its original location and transported to the fill site. The soil is then spread in thin layers and compacted to maximum dry density at optimum moisture content. In certain cases, especially in Oklahoma, the subgrade soil must be stabilized. After completion of grading operations, the road is left unpaved for a certain period of time. During this period climatic and environmental factors act on the subgrade soil. High temperatures and low relative humidity conditions cause

drying of the compacted soil. On the other hand, precipitation and frost action tend to increase subgrade moisture content. In Oklahoma freezing of subgrades is not a major problem except in the northwest section; thus, increases in moisture content are due primarily to precipitation and high relative humidity conditions.

A number of wet-dry cycles precede the paving operations. After the placement of the pavement structure, the moisture content levels in the subgrade soil vary within small ranges; however, the pavement is now subjected to the action of traffic loads. The intensity and frequency of such load applications are dictated by traffic conditions but their effect on pavements is difficult to evaluate accurately.

Under the influence of climate and traffic related factors changes take place in the subgrade material. These changes are expected to be primarily physical in nature and their effects would be manifested by variations in the plastic and strength properties of soil material which in turn affect the stability, durability and performance of pavement.

The scope of this study was twofold. First, to employ laboratory experiments which simulate more realistically the events that occur in the earlier life of a subgrade material, and second, to evaluate the effects of weathering and repetitive loading on four raw and lime stabilized shales of Oklahoma.

CHAPTER II

REVIEW OF LITERATURE

The performance of a pavement structure, to a great extent, is dependent upon that of its subgrade. Any changes in the properties of the materials constituting the subgrade may significantly influence the durability and the riding quality of a pavement. Thus, logically, in modern times there has been increased activity in the research related to the physical properties of the soils subjected to load characteristics based on traffic parameters.

The anticipated traffic is calculated in terms of the average number of equivalent 18-kip single axle loads (Equivalent Wheel Loads, EWL) expected per day in a traffic lane during the design life of a pavement (Asphalt Institute, 1963; Chastain, 1962). Traffic on highways varies both in the number of vehicles and in the magnitude of the axle loadings. These factors affect the structural requirements of a pavement and since they occur in infinite number of combinations, they make even the most elaborate traffic pattern estimates, at best, approximate. Even though the design of a pavement is based on employing the 18-kip EWL,

the designs are not restricted to that load; in fact, heavier loads are often encountered on primary and interstate highways (Asphalt Institute, 1963). Additional parameters in the pavement design are the index and strength property values of the subgrade soil; hence, any study of pavement stresses must take into account the varying characteristics of the subgrade soil on which the pavement structure rests (Venkatasubramanian, 1964). Thus, in the evaluation of subgrade material, all the factors which may adversely affect its load supporting capacity must be considered.

When subjected to stress, the resistance of a soil to deformation depends on interaction among its constituent particles. The stress response of a soil mass is thus dependent on its microstructure, the present state of which is a result of the actions among various intrinsic and environmental factors (Foster and De, 1971). While the physicochemical properties of the soil are the major factors determining the nature of the electrical forces between adjacent particles, the structure of compacted highway subgrade soil is determined largely by the moisture content and the type and amount of compaction (Nalzeny and Li, 1967). Prediction of pavement performance, however, requires a knowledge of the behavior of the subgrade soils under conditions representative of those that are expected to occur in the field. For fine grained soils these conditions include not only the initial placement conditions but also the traffic

patterns and environmental features of the area in which they exist (Sauer and Monismith, 1968). These factors are as important and in many cases more important than the soil variability factor (Yoder, 1969). Under these conditions, the factor which influences the characteristics of a soil most is the moisture content.

Moisture Content

Sherif (1966) from his experiments on the deformation and flow properties of clay soils concluded that the clay structure was very similar to metal structure; the effect of moisture content in clay being analogous to the effect of temperature on metal. For moisture contents below the plastic limit, Sherif found clay to behave as a work hardened viscoelastic plastic material; for moisture contents above the plastic limit, after certain stress levels, excessive deformations occur and the behavior of clay beyond these levels depends on the rate of shear with the strength of soil decreasing as the rate of shear decreases (Sherif, 1966). Kriezek and Kondner (1964) observed that for any given value of dynamic strain amplitude value, the dynamic stress amplitude value increased as the moisture content of the sample decreased and thus, the dynamic stress-strain data are significantly affected by variation in moisture content even within small ranges. Their test data showed, for example, that at 4.0×10^{-4} cm dynamic strain amplitude, the values of

dynamic stress amplitude were 20 percent greater at 32.3 percent moisture content and 60 percent greater than at 30.6 percent moisture content compared to that at 34.0 percent moisture content level.

Normally, at the time of its placement the subgrade soil is compacted at or about its optimum moisture content to obtain the desired density and stability (Sauer and Monsmith, 1968). From then on, however, the moisture variations depend upon the environmental and climatological factors. Aitchison and Richards (1965) attribute the moisture conditions at any point beneath or adjacent to a roadway to a combination of the regional effects--in which climate and regional geology or pedology would be dominant--and the local effects--in which construction, local topography and hydrology would be dominant.

Theoretically, moisture movement under transient conditions could be described by a differential equation. The solution of such an equation would make it possible to calculate the rates of moisture changes as well as the moisture distribution for any particular point at any particular time. The physical processes of water transport, however, depend not only on the moisture gradient but also on parameters such as the concentration of dissolved salts and the thermal gradient. The development of an adequate expression to describe combined moisture and heat transfer in porous media has proved to be a formidable task (Saare and Nevander, 1967).

Venkatasubramanian (1964) found that under subgrades the diurnal variation of temperature was almost negligible but that there was appreciable seasonal variation. Russam (1970) measured the effect of seasonal changes under vegetation and under areas covered by relatively impervious surfaces and concluded that large seasonal changes could occur under natural vegetation but when ground is covered by a relatively impervious surface the seasonal moisture changes are reduced and except for a zone close to the pavement edge, the moisture conditions tend to a relatively stable value. From their studies Marks and Haliburton (1969) found that variations in the moisture content under roadway surfaces occur on an annual basis and that soil type had no noticeable effect on these subgrade moisture variations. In the United Kingdom, Uppal (1965) has established that in the areas abounding in silty clays, the maximum saturation that a subgrade normally attains is substantially below 100 percent. In heavy rainfall areas of India and for 'black cotton soils' the moisture content in an uncovered area was found to be between 6 percent and 23 percent while under a covered surface 2.5 feet from the edge of the road the moisture content was 13 percent during the dry season and 16 percent after the monsoon; at a distance of 5.0 feet from the edge these values were 12 percent and 15 percent, respectively. While the range in variation of the moisture content of the uncovered surface from dry to wet season is of the order of about 15

percent in the top two to three feet of the subgrade this range is reduced to about 3 percent to 4 percent after the subgrade has been provided with a sealed surface pavement (Uppal, 1965).

As is obvious, the data presented above do consider moisture distribution and variation in subgrades under pavements; however, in no case have the data been collected for that phase of construction during which the subgrade is left exposed to the effects of environment and climate for a considerable period of time between its compaction and construction of pavement over it.

Repeated Load Testing

After the construction of pavement over a subgrade the strength and deformation characteristics of the subgrade soil are affected by the repeated application of stresses induced by wheel loads moving over the pavement. In general, the effect of such loads on soils is not satisfactorily predictable by conventional strength tests.

Larew and Leonards (1962) report that for a given set of sample conditions, a given level of repeated axial load ultimately produced greater deformation than a static or gradually applied load of equal magnitude. Also, two different soils with initial conditions which produced nearly identical stress - strain curves in static triaxial tests developed entirely different total and elastic deformations

in the repeated load triaxial tests. Further, the soil specimens might suddenly fail after withstanding a number of repetitive deviator stresses of the same magnitude. Thus, the load deformation characteristics of a soil determined by static load tests may not be indicative of its behavior under repeated load conditions.

At small frequency and magnitude of repeated stress, a material shows high plasticity. Increases in both the frequency and the level of stress cause the behavior to progressively become more elastic. From their experiments with sand-asphalt beams, Moavenzadeh and Carnaghi (1966) and on soils, Seed, et al. (1967) concluded that as the number of load applications increased, the deflection per load cycle decreased. In other words, as the load applications increased the material tended to become more elastic. At higher stresses, however, the effect of load repetition may be completely lost. Pretorius and Monismith (1972) measured tensile and compressive strains from flexural tests made on soil-cement beams and observed that the strain remained constant over a large number of stress applications after which the rate of change of strain started to increase. Once the strain rate started to change, it did so at an increasing rate until complete rupture was attained. Soderman, et al. (1968) noted a decrease in the value of the elastic modulus of a clay till subjected to repeated load applications and attributed this to the breakdown of the soil structure as the specimen

developed large strains near failure. An interesting observation of the Pretorius and Monismith experiment was that the specimens did not fail even after one million applications of load and exhibited a constant strain output during the entire test. When the specimens were failed under a higher stress, the strain history remained essentially unchanged and the effect of previously induced damage was comparatively insignificant.

At lower strains, the soil specimens exhibit elastic behavior until the initiation of crack formation. Increase in both, the frequency and the level of repeated stress, cause increase in the 'ultimate strength' of soils, however, the effect of repeated stress in this case is rather insignificant (Kawakami and Ogawa, 1964). In the experiments conducted by Larew and Leonards (1962) on clays, for the frequency range of one to twenty applications per minute, the specimen deformation depended on the number of stress applications but was independent of the frequency of application, provided the saturation was not too high. For a low degree of saturation, the strength and stiffness of clay soils was increased by stress repetitions. At higher degrees of saturation, the strength did not increase appreciably although stiffness did. The stiffening effect was gradually reduced with increasing deviator stress and was finally destroyed by large sample deformations. Seed, et al. (1967) found that for small number of stress applications the soil exhibited increasing

elasticity as the time interval between compaction and testing increased. However, after a large number of stress applications, because of thixotropic changes and deformation occurring during repeated load application, the effects of aging are reduced and the results are the same for the specimens tested immediately after compaction as for specimens tested after a delay.

Just as in the case for static strength tests, the bending points on the stress - strain curves for repeated load tests indicate occurrence of slip and the presence of more than one bending point may be attributable to the 'step-strain phenomenon' (Kawakami and Ogawa, 1964).

From their studies on the effect of various parameters on the behavior of soils under repeated load, Seed, et al. (1967) observed that:

1. The method of compaction which produced dispersed structure in a soil produced lower modulus of resilient deformation.
2. As the degree of saturation at compaction increased, the resilient deformation at a particular stress level increased and the resilient modulus decreased, and
3. As the moisture content of soil increased, the resilience increased and conversely as the density increased the resilience decreased.

Most of the repeated load tests, however, are conducted under essentially a constant load cycle wherein maximum

and minimum stress levels are held approximately constant during each application of load (Lenzen, et al., 1968). This differs greatly from the actual field conditions in that the highway pavement subgrades are subjected to significantly variable loadings.

Split Tensile Strength Test

When a layer of subgrade material undergoes varying strains under a load traveling on the pavement, its area immediately below the load is compressed while the areas in front and behind the load undergo tension. On the underside of the layer the strain pattern is just the opposite (Hong, 1967). With increasing velocity of the load, the point of maximum deflection starts to fall more and more behind the load, but the general pattern of strains remains the same (Thompson, 1963). A relatively large magnitude of tensile strain compared to a small compressive strain develops at the underside of the layer and it is from this side, most probably, that the crack formation initiates (Hong, 1967). Peattie (1962) considered the vertical compressive stress at the topside of the surface and horizontal tensile strain at the underside of a layer to be the critical factors in the design of flexible pavements. Thus, for the design of subgrades, taking into account the cumulative action of the repetitive traffic loading the tension parameters at the bottom of layer appear to be the critical factors. These

parameters can be measured in the laboratory using either the flexural test or the tension tests. Generally, the tension tests require much less material and samples can be molded using the compaction equipment commonly available in most soil laboratories. Since the failure in tension test samples starts inside the soil mass, the wall effects and the effects of surface conditions are not the determining factors; thus, using tensile tests in some ways has distinct advantages.

The most commonly used tension tests are the direct tensile strength and split tensile strength tests. The results from direct tensile strength tests are greatly influenced by the end constraints; also in such tests failure of specimen can occur along any surface. In split tensile strength tests, the surface of failure for all soil and concrete like materials is pretty well defined and is located in the neighborhood of the vertical diametral plane of the specimen. For ceramic materials splitting strength is proportional to the compressive strength (Popovics, 1967) while failure of concrete by splitting is controlled by its tensile strength and is dependent on its composition as well as the level of applied stress. Using the split tensile strength test, Carniero and Barcellos (1953) found a significant correlation between the tensile and the compressive strengths of concrete and that a mathematical function relationship existed between these two types of strengths. For stabilized

soils Metcalf and Frydman (1962) have shown that their split tensile strengths are 1/12 to 1/10 times their unconfined compressive strengths. Under repetitive load conditions the split tensile strength test results are but little affected by the constraints at or near the ends of the specimen. It is also a more satisfactory test than those in which the platens come in contact with the specimen since the platen contact can cause significant dispersion in test values and provoke uncertainty as to what is actually being measured. Thus, split tensile strength test appears to be preferred test to measure the tensile strength parameters of soils.

For the split tensile strength test it is assumed that the stresses and strains at all times and at all points remain within the elastic range and in particular Hooke's Law holds up to the failure (Peltier, 1954). Timoshenko and Goodier (1951) have analyzed the stresses in a circular disk loaded vertically by concentrated loads acting along diametral plane. They have also analyzed the case wherein the loads are concentrated but act along a vertical chord not in the diametral plane. Frocht (1961) has considered the same two cases but provided more detailed expressions to the generalized equations put forward by Timoshenko and Goodier. A detailed treatment involving split tensile strength test has been provided by Peltier (1954). In his treatment Peltier has considered the cases of:

1. Concentrated loads along two generators in contact with the press platens,
2. Distributed loads in the vicinity of generators in contact, and
3. Constant contact pressure over the contact area in the vicinity of the contact generators.

From the point of view of the theory of elasticity, for a load P acting vertically along a diametral plane of a cylinder of radius R and length L, the stresses at a point (x, y) in the plane of the disk (Figure 2.1) are given by:

$$s_x = \frac{-2P}{\pi L}\left(\frac{(R - y)\,x^2}{r_1^4} + \frac{(R + y)\,x^2}{r_2^4} - \frac{1}{2R}\right) \qquad (2.1)$$

$$s_y = \frac{-2P}{\pi L}\left(\frac{(R - y)^3}{r_1^4} + \frac{(R + y)^3}{r_2^4} - \frac{1}{2R}\right) \qquad (2.2)$$

$$t_{xy} = \frac{2P}{\pi L}\left(\frac{(R - y)^2\,x}{r_1^4} + \frac{(R + y)^2\,x}{r_2^4}\right) \qquad (2.3)$$

where s_x = normal stress in x-direction

s_y = normal stress in y-direction

t_{xy} = shear stress in x-y plane

$r_1^2 = x^2 + (R - y)^2$

$r_2^2 = x^2 + (R + y)^2$

The solutions given above for the normal and shear stresses consist of the sum of three systems:

1. Boussinesq's solution in infinite medium for a load P located at point A (Figure 2.1),

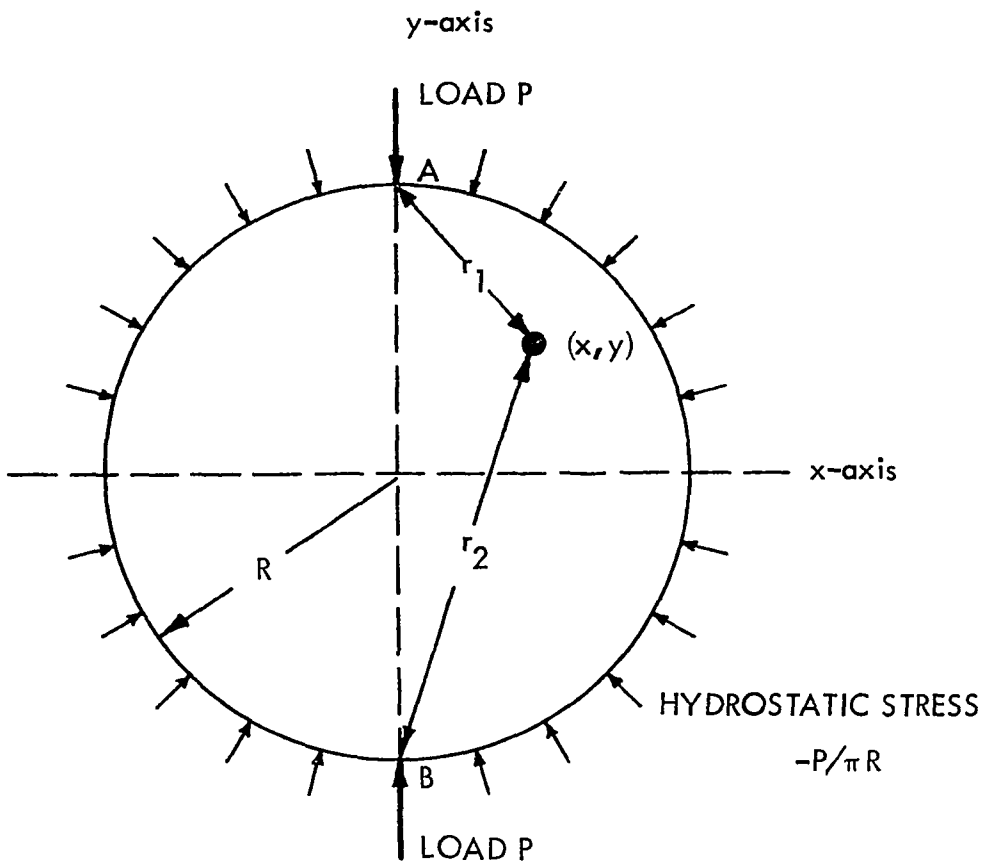


Figure 2.1 Forces acting on a disk and location of point (x,y) in split tensile strength test.

2. Boussinesq's solution in infinite medium for a load P located at point B (Figure 2.1), and
3. A hydrostatic tensile stress of absolute value of $P/\pi R$.

From these equations it is obvious that in the neighborhood of points A and B the stresses are close to those applied by the platens and, thus, the rupture will start from these points.

Along the y-axis, $x = 0$, $r_1 = R - y$ and $r_2 = R + y$ and hence,

$$s_{xy} = \frac{P}{\pi LR} \tag{2.4}$$

$$s_{yy} = \frac{-P}{\pi L}\left(\frac{4R}{R^2 - y^2} - \frac{1}{R}\right) \tag{2.5}$$

$$t_{xyy} = 0 \tag{2.6}$$

The distributions of s_{xy} and s_{yy} are shown on Figure 2.2(a).

Along the x-axis, $y = 0$, $r_1^2 = r_2^2 = x^2 + R^2$ and hence

$$s_{xx} = \frac{-P}{\pi LR}\left(\frac{R^2 - x^2}{R^2 + x^2}\right)^2 \tag{2.7}$$

$$s_{yx} = \frac{P}{\pi LR}\left(\frac{4R^4}{(R^2 + x^2)^2} - 1\right) \tag{2.8}$$

$$t_{xyx} = 0 \tag{2.9}$$

The distributions of s_{xx} and s_{yx} are shown on Figure 2.2(b).

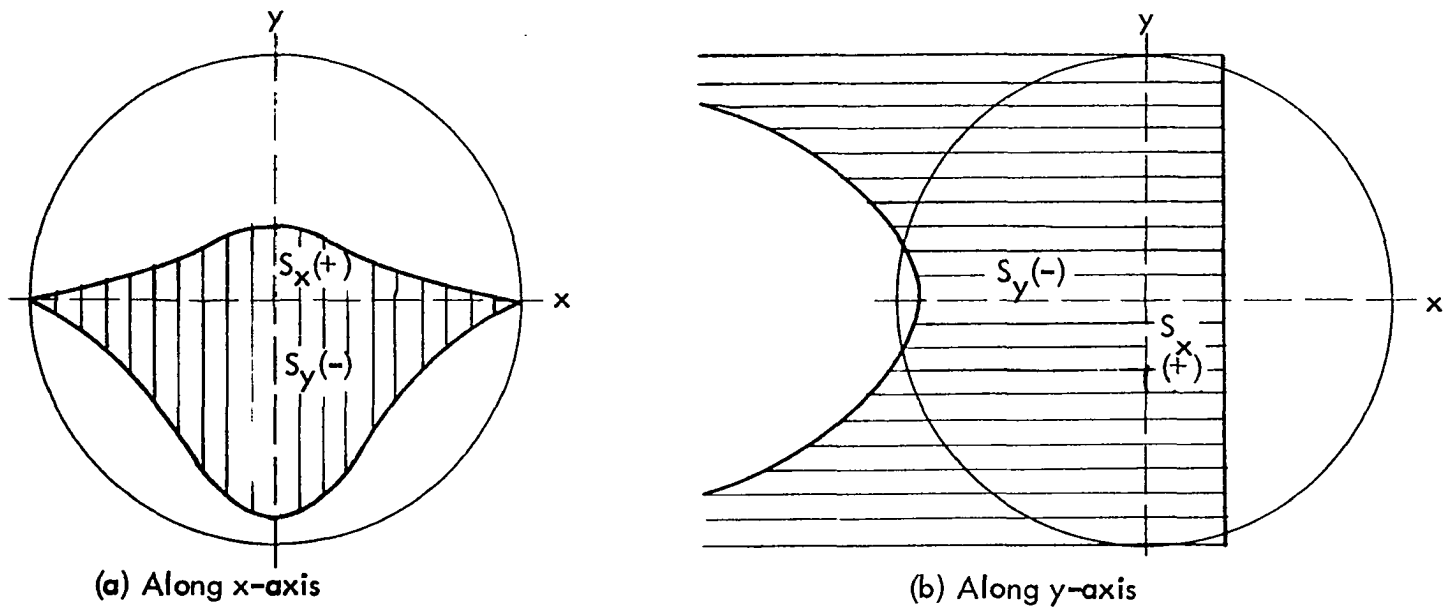


Figure 2.2 Distribution of stresses S_x and S_y along Co-ordinate axes x and y in a disk under vertical diametral compression.

An examination of these expressions indicates that in all cases, irrespective of the values of load P and radius R, the rupture will always start at points A and B. Along the y-axis the minimum value of s_{yy} is $-3s_{xy}$ and occurs at the center of the disk. At the contact points A and B the magnitude of s_{yy} becomes infinitely large. In general, however, the load is applied through a strip of width 'a' and the limiting value of s_{yy} is P/(aL).

Except in the immediate vicinity of the platen contacts, the stresses produced during the test are mainly compressive and they are small in comparison to the compressive strength of the material; thus, they remain well within the elastic range of the material. The principal compressive stress may reach very high magnitudes without having any influence on the rupture (Carneiro and Barcellos, 1953; Peltier, 1954). The tensile stress distribution along the vertical axis is uniform and these tensile stresses are the ones which tend to exceed the elastic limit. However, even when the specimen is deformed the tension remains constant, uniform and proportional to the load in the central part of the specimen. The test thus remains a tensile test until failure ensues. The rupture is always sharp and separation is along the vertical plane containing the generators of contact. For concrete specimens this fact was first verified by Carniero and Barcellos (1953).

The plastic range of tensile stresses and strains is very small for brittle materials. The plasticity of the material generally produces stress relief within the material and the stresses become relatively uniform. The plasticity would, thus, attenuate the effect of very high stresses in the nighborhood of press platens. These stresses tend to displace the zone of rupture from the center toward the boundaries. On the other hand, the stresses vary little in the central zone and are slightly affected by the plasticity of the material (Peltier, 1954), load platen contact, crackings and minute non-homogeneities (Carneiro and Barcellos, 1953).

The expressions presented by Timoshenko and Goodier (1951), Frocht (1961) and Peltier (1954) are of great importance for finding stresses within an elastic body for a given static load. Unfortunately, they take no account of the deformation occurring in the specimen. Thus, they provide no information necessary for the actual split tension test conditions where variations in stresses occur due to the deformation taking place in the vertical diametral dimension. Also, in the case of soil material the point of failure is generally not well defined and is commonly chosen on the basis of engineering judgment.

Hence, in this study an attempt has been made to derive equations taking into account the conditions for elastic deformations assuming that the changes in other

dimensions of the sample remain negligible. From the derivations included in Appendix A, the following expressions were obtained for determining the stresses along the horizontal and the vertical diametral axes of the specimen (Figure 2.3).

Along the x-axis:

$$s_{xx} = \frac{P}{2\pi x_1 L}\left[\frac{2y_1\,(x_e + x_1)}{y_1^2 + (x_e + x_1)^2} - \frac{2y_1\,(x_e - x_1)}{y_1^2 + (x_e - x_1)^2} - 2\arctan\left(\frac{2x_1y_1}{y_1^2 + x_e^2 - x_1^2}\right) + \frac{y_1}{R}\ln\left(\frac{R + x_1}{R - x_1}\right)\right] \tag{2.10}$$

$$s_{yx} = \frac{-P}{2\pi x_1 L}\left[\frac{2y_1\,(x_e + x_1)}{y_1^2 + (x_e + x_1)^2} - \frac{2y_1\,(x_e - x_1)}{y_1^2 + (x_e - x_1)^2} + 2\arctan\left(\frac{2x_1y_1}{y_1^2 + x_e^2 - x_1^2}\right) - \frac{y_1}{R}\ln\left(\frac{R + x_1}{R - x_1}\right)\right] \tag{2.11}$$

$$t_{xyx} = 0$$

Along the y-axis:

$$s_{xy} = \frac{P}{2\pi x_1 L}\left[\frac{2x_1\,(y_1 - y_e)}{(y_1 - y_e)^2 + x_1^2} + \frac{2x_1\,(y_1 + y_e)}{(y_1 + y_e)^2 + x_1^2} - 2\arctan\left(\frac{2x_1y_1}{y_1^2 - x_1^2 - y_e^2}\right) + \frac{y_1}{R}\ln\left(\frac{R + x_1}{R - x_1}\right)\right] \tag{2.12}$$

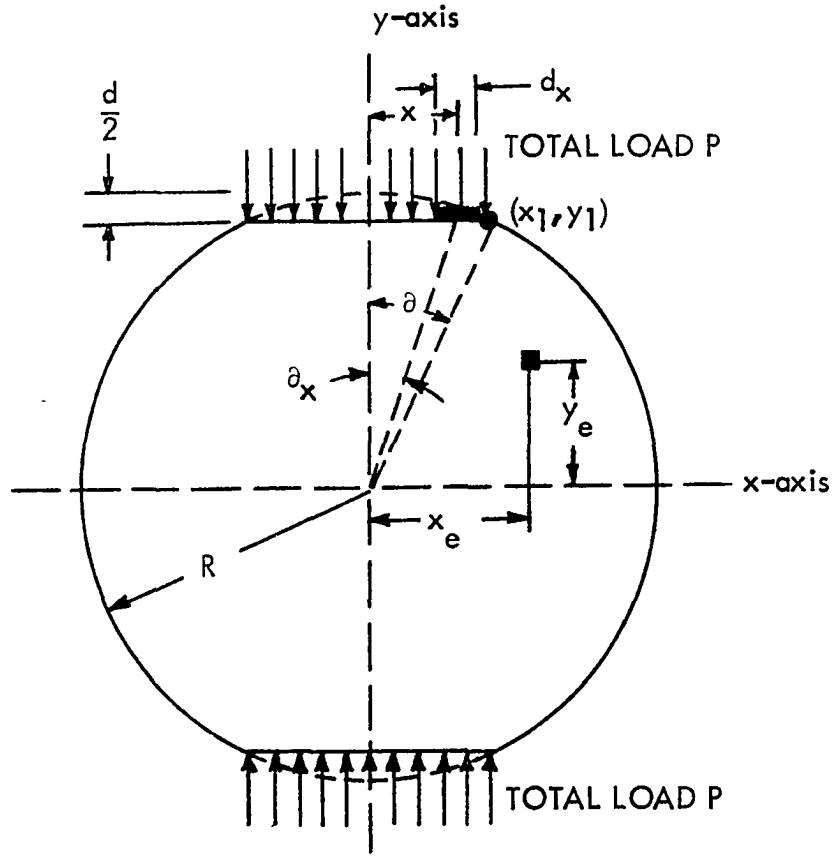


Figure 2.3 Geometrical configuration and locations of points (x_e, y_e) and (x_1, y_1) on a disk deformed by distance d along vertical diameter in split tensile strength test.

$$s_{yy} = \frac{-p}{2\pi x_1 L}\left\{\frac{2x_1\,(y_1 - y_e)}{(y_1 - y_e)^2 + x_1^2} + \frac{2x_1\,(y_1 + y_e)}{(y_1 + y_e)^2 + x_1^2}\right.$$

$$\left. + 2 \arctan\left(\frac{2x_1 y_1}{y_1^2 - x_1^2 - y_e^2}\right) - \frac{y_1}{R} \ln\left(\frac{R + x_1}{R - x_1}\right)\right\} \tag{2.13}$$

$$t_{xyy} = 0$$

where, at a certain instant,

x_1 = half the distance about y-axis along which the total load is applied

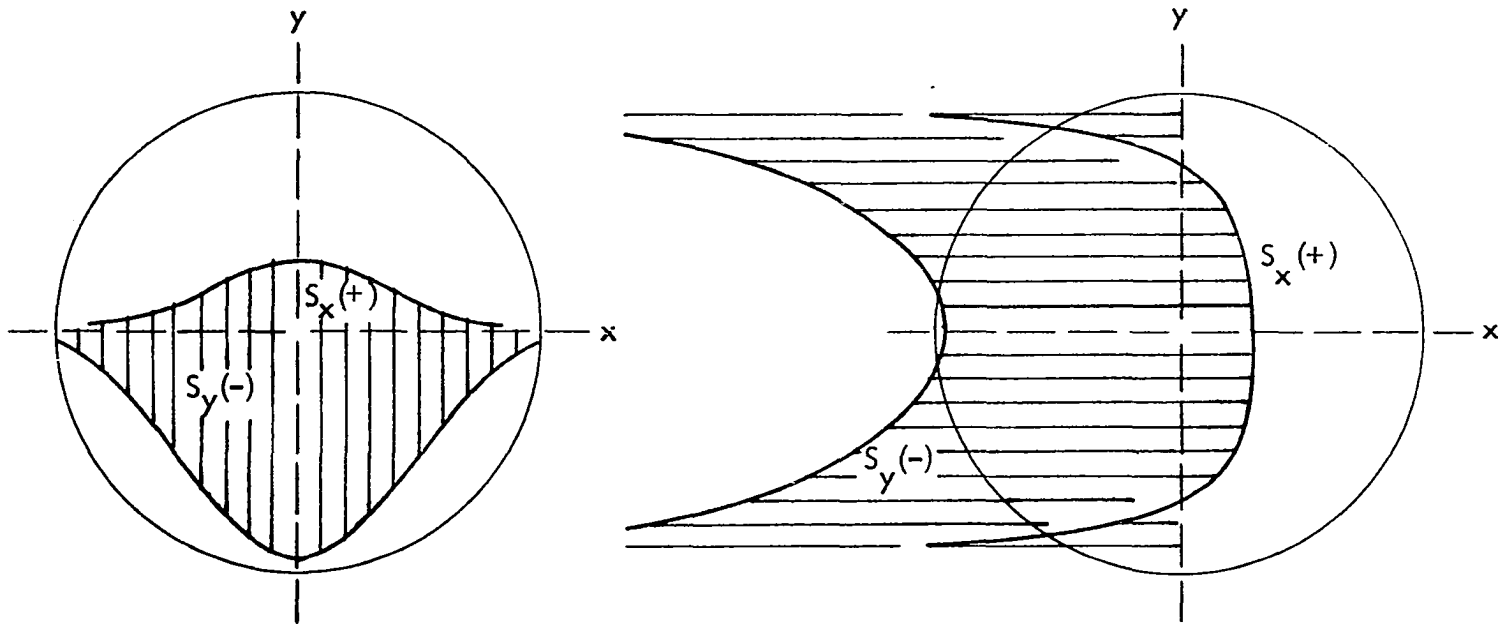
y_1 = half the height of the specimen in the vertical diametral plane

x_e = distance from y-axis of the element under consideration, and

y_e = distance from x-axis of the element under consideration

For an assumed deformation of 2 percent of the diameter and a unit load the distribution of stresses s_{xx}, s_{yx}, s_{xy} and s_{yy} are shown in Figures 2.4(a) and 2.4(b).

As will be observed from these figures, the extreme values of stresses occur either at the center or the ends of the specimen. A list of stresses at the center and the ends is included at the end of Appendix A. It should be pointed out that these equations are not applicable to the case of zero deformation since in the case x_1 becomes equal to radius



(a) Along x-axis

(b) Along y-axis

Figure 2.4 Distribution of stresses S_x and S_y along coordinate axes for sample under deformation in split tensile strength test (deformation = 0.02 x diameter).

R and the natural logarithm term becomes undefined. The great importance of these expressions is that they permit plotting of stress strain diagrams for the split tension test in much the same way these diagrams are plotted for unconfined compressive strength and triaxial compression tests.

A sample computer program to determine the various stresses at the center and the ends and the diametral strain is included at the end of Appendix A.

Crack and Crack Propagation

The tensile strength is considered as the maximum stress which develops in the material at the onset of the failure. The characteristics of deformation developed in the material are used to determine the mode of failure. If a material fails without undergoing a substantial deformation, the failure is termed 'brittle failure'; in case the material undergoes considerable deformation, it suffers a 'ductile failure' (Moavenzadeh, 1967).

Failure of a brittle material under stress takes place through progressive internal cracking. Eventual failure of a material results from a gradual development of internal tension microcracking throughout the specimen. Total failure takes place when the cracks begin to form continuous patterns (Popovics, 1969).

Crack propagation is an important factor in the fatigue failure of any material since the final fracture is

dependent on the extent of crack pattern (Antrim, 1967). According to Griffith's theory (1920) the presence of small inherent cracks and flaws in brittle materials is responsible for stress concentration and stress at certain points could reach a level higher than the average stress level and may eventually exceed the tensile strength of the material (Moavenzadeh, 1967; Popovics, 1969) causing or furthering cracking in the material. For the progressive development of failure in homogeneous brittle materials crack formation causes creation of new surfaces and the strain energy of the specimen is transformed into surface energy. This increases the energy demand to create new surfaces by initiating and propagating cracks. Crack propagation continues until a critical stage is reached. Beyond this stage, the rate of surface energy change is less than the rate of stored energy change. The energy demand for creating new surfaces is now less than the existing strain energy and the propagation of crack will occur at increasing speed until failure occurs (Popovics, 1969).

The mechanism of cracking is basically similar under different types of loadings. Under repeated loading, failure starts at few weak spots and if the propagation of the cracks can be delayed, the crack pattern will develop at a slower rate and failure will be delayed (Antrim, 1967). The internal microcracking starts at a fraction of ultimate load and the cracks are oriented parallel to the direction of loading. The strength of the material decreases when continuous patterns

have developed extensively (Slate and Olsefski, 1963). Current investigations (Stallmeyer and Walker, 1968) of fatigue damage at the microscopic level and in the early stages of stress application suggest that there are differences in the nature of fatigue failure. The delineation between the early and the later stages might be the transition from primary interparticle damage characterized by the progressive breaking of bonds, intrusions, extrusions within grains to intergranular crack formation and propagation. Since the behavior of any soil mass under stress is determined primarily by its mineralogy, characteristics and distribution of its particles, interaction among them and the effect of cementation between them, modifications in the particle interrelationship can be brought about by the use of stabilizing agents. Lime is among the most extensively used stabilizing agents for subgrade construction, particularly with plastic soils in Oklahoma.

Lime Stabilization

Having once started as an aid in maintenance works, lime stabilization of soils has now become a significant step in upgrading substandard soils for highway construction (Eades and Grim, 1966).

Addition of lime to soil increases electrolyte concentration and consequently the pH of the porewater of the soil. Ion exchange between lime and soil particles produces

Ca-clay and causes clay particles to flocculate (Herzog and Mitchell, 1963). Increased pH also makes alumina and silica more soluble and calcium ions react with hydrous alumina to form hydrated calcium aluminate (Diamond and Kinter, 1966; Eades and Grim, 1966). This rather fast reaction is supplemented by comparatively slower reaction of silica with lime to generate hydrated calcium silicate or "tobermorite gel" ($3CaO \cdot 2SiO_2 \cdot 3H_2O$). The gel hardens gradually and imparts strength to the soil lime mix. The reaction products of calcium alumina and silica spall, liberating fresh clay surfaces for further adsorption and reaction (Diamond and Kinter, 1966). X-ray diffraction patterns indicate a destruction of the clay mineral structure by lime (Diamond and Kinter, 1966; Eades and Grim, 1966; Huang and Roderick, 1969), and the soil lime mix continues to exhibit strength gains for a long period of time. The hydration process ceases, like in cement concrete only when moisture content in soil mass reaches a state of equilibrium with the relative humidity of the surrounding air (Pihlajavaara, 1967).

During the initial stages, the formation of very small quantities of cementing products at the points of contact between the edges of one particle and the faces of the adjacent particles is believed to be sufficient to stabilize the flocs so that the index properties are modified; however, the bonding among flocs is not strong enough to provide sufficient strength to the clay mass and thus the clay seems to

have been ameliorated but not stabilized. To stabilize the mix, compaction to minimum void ratio is essential. From the strength point of view, the production of hydrated calcium aluminates and silicates during long term reactions is responsible for the stabilization of soils (Diamond and Kinter, 1966). The further this reaction proceeds, the higher the strength becomes. At any time there may be more than one phase of the reaction present depending on the curing time and temperature (Ruff and Ho, 1966). Hilt and Davidson (1960) have shown that some of the lime is utilized in the early amelioration of clay and thus it does not enter into pozzolanic reaction. Ho and Handy (1963, 1964) indicate that during the initial stages of reaction lime does not show up on differential thermal analysis curves, suggesting its adsorption on clay surface. At higher temperatures and after longer curing periods this effect may be reduced due to the dissolution of clay and the accompanying release of adsorbed calcium.

Ruff and Ho (1966) have shown that the strength of a soil lime mix is not a function of $Ca(OH)_2$ alone. The exact products formed vary according to the type of clay and reaction conditions, particularly temperature (Diamond and Kinter, 1966). Generally, the sample containing the largest amount of acid soluble silica and alumina or the smallest amount of unreacted lime would have the highest strength (Ruff and Ho, 1966). Thus, after the initial stage the

strength increase depends on the amount of lime used and the free lime present at the time of testing. Consequently, higher strengths may be shown at intermediate percentages of lime (Kumar, 1961).

The purity and fineness of lime also have an important influence on the lime requirement of a soil; the finer the lime used, the more the clay mass contracts and the soil is ameliorated in a reduced period of time (McDowell, 1966).

Current construction practices require lime to be mixed and blended with soil at least 24 hours before compaction. Compaction density and moisture contents are usually at or near those specified by the AASHTO Designation T 99-70. Since the strength of the compacted soil lime mix increases continually, the design values adopted are those that correspond to the 90-day curing period results (McDowell, 1966). In the laboratory, comparative results can be obtained by accelerated curing. For lime stabilized clay-gravel and micaceous silty clay soils, Anday (1961) found that 18-hour curing in an oven at 60°C (140°F) was equivalent to 45-day during in the field under summer temperatures.

The effect of lime treatment on soils can be observed by an increase in the number of large voids due to flocculation, resulting in decreased compacted density and increased optimum moisture content. This fact is reflected in increased permeability of soils on treatment with lime (Laguros, 1965). Ranganatham (1961) had arrived at similar conclusions from

consolidation tests. Hilt and Davidson (1960) have shown that the plasticity indices of all soils tested decreased with each increment in the percentage of lime until the material became non-plastic. Addition of lime to black cotton soils of India increased liquid limits and plasticity indices but reduced plastic limits in the 0.0 percent to 0.75 percent lime range; beyond 1.0 percent addition there was a decrease in plasticity index value and addition of lime in 1.5 percent to 2.0 percent range converted the plastic clay into friable soil (Katti and Barve, 1962). Lime addition at these levels, however, does not result in significant strength improvement for the soil.

Uncured lime modified soils behave primarily as cohesive ($\phi = 0$) materials (Neubauer and Thompson, 1972). McDowell (1966) found that in uncured samples addition of 1 percent lime reduced the cohesion materially and further additions of lime resulted in lower cohesion values, not much distinction being noted among mixes containing five to eight percent lime. Proper lime treatment--amount and curing--however results in greatly improved shear strengths of soils (Thompson, 1966). For clay soils substantial improvements are noted in the values of cohesion and the modulus of elasticity (Neubauer and Thompson, 1972), while only minor increases take place in the values of the angle of friction. The maximum cohesiometer values for soil lime mixes are obtained at or near optimum moisture content.

Reaction of lime with cohesive argillaceous material to produce pozzolanic activity requires adequate curing time. Most of the research on soil lime mixes has been concentrated on the evaluation of the properties under these very conditions. Meager data and few research findings are available on the properties of soil lime mixes which have not been so adequately cured and where curing simulates field conditions more realistically. It is from this viewpoint that research must be advanced and techniques developed to evaluate engineering property data on lime stabilized soils and to assess the influence of such stabilization on the design of pavement structures.

CHAPTER III

SELECTION OF MATERIALS

On the basis of their geologic, physiographic and geographic locations, 24 shales were obtained from various parts of Oklahoma for a study involving the predictability of physical changes of clay forming materials (Laguros, 1972). Routine engineering and geologic information related to these shales were obtained at the Soils Laboratory, University of Oklahoma at Norman. The information so obtained was analyzed using the method of 'Factor Analysis' and engineering judgment. Factor analysis uses statistical techniques to obtain correlations among a set of variables so as to resolve this set of variables into a small number of 'factors' and in such a manner that the factors convey all the essential information of the original set of variables (Harman, 1967). This method is uniquely applicable to a classification procedure where data from a large battery of tests are reduced in order to identify a few common factors. The shales were then divided into various groups, shales in each group having similar characteristics. From these groups four shales, each belonging to a different group, were selected for this study.

Locations of these shales are shown in Figure 3.1, and their relevent geologic and engineering information are depicted in Tables 3.1 and 3.2, respectively.

The shales obtained from the field were air dried and then ground to pass U.S. Standard Sieve No. 10. The material passing the No. 10 sieve was used for the investigations of this study.

The shales were stabilized using hydrated lime, U.S.P. (powder) $Ca(OH)_2$ manufactured by Mallinckrodt Chemical Works of St. Louis, Missouri. The maximum limits of impurities for this lime are given as: Acid insoluble substances, 0.5 percent; Arsenic, 0.0003 percent; Carbonates, to pass test; Heavy Metals (as Pb), 0.0010 percent; Mg and Alkali Salts, 4.8 percent; and the Amount of Lime, 95 to 100 percent.

The water used for all tests was distilled water prepared in laboratory.

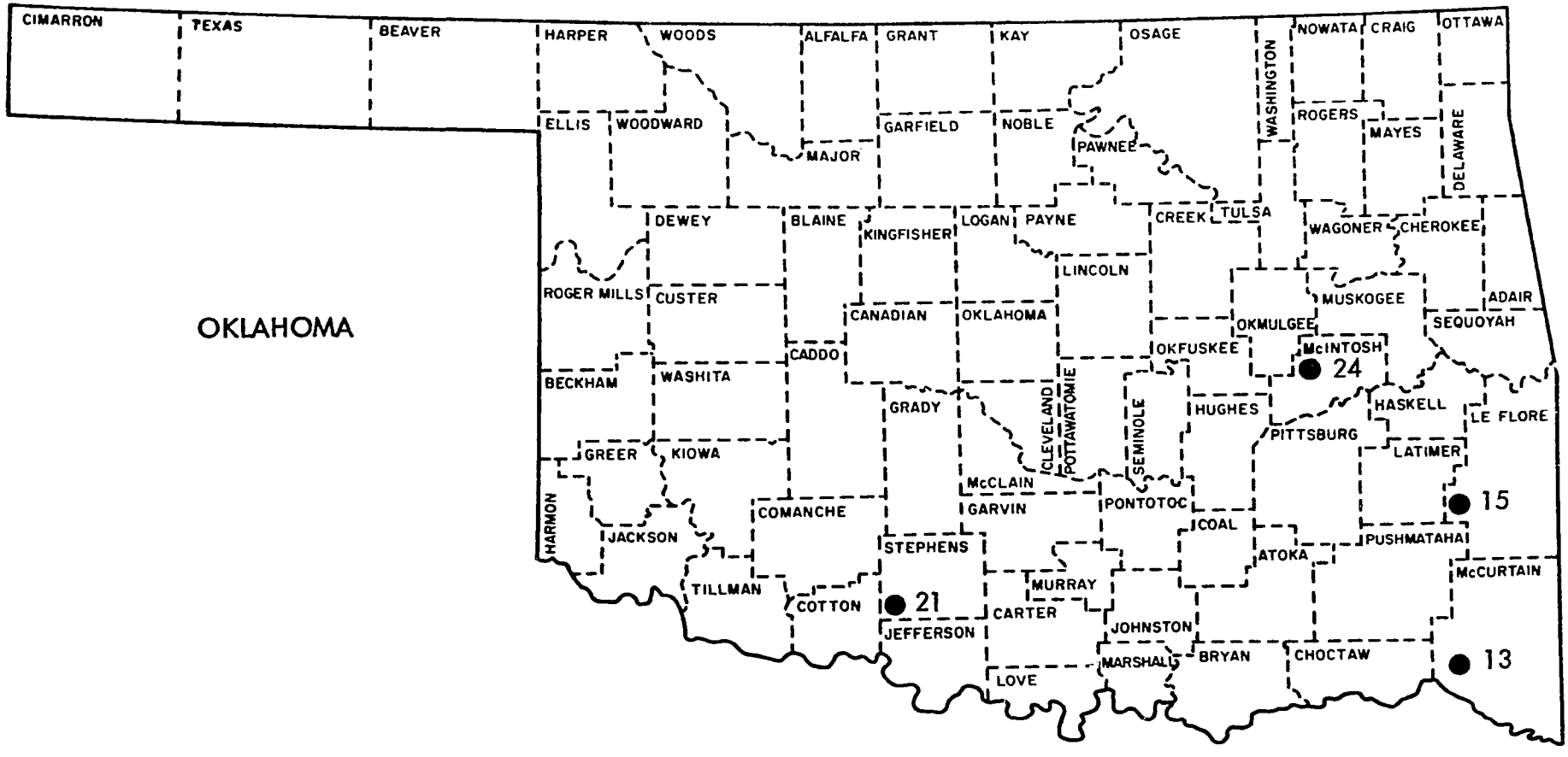


Figure 3.1 Location and identification of selected shale samples.

TABLE 3.1

GEOLOGIC INFORMATION ON SHALES[a]

Shale Number	County	Geologic System	Physiographic Region[b]	Geologic Unit
13	McCurtain	Cretaceous	Red River	Washita
15	LeFlore	Mississippian	Ouachita Mountain	Stanley
21	Stephens	Permian	Red Beds Plains	Claypool
24	McIntosh	Pennsylvanian	Prairie Plains	Senora

[a]From Reference - Laguros, 1972.

[b]From Reference - Sheerar, 1932.

TABLE 3.2

ENGINEERING PROPERTY DATA OF SHALES[a]

Shale Number	Grain Size Analysis, %			Specific Gravity	pH	UCS[b] psi	Volume Change %	AASHTO[c] Class.
	Silt	< 5μ Clay	< 2μ Clay					
13	35	59	48	2.73	5.1	22.5	10.3	A-7(6)
15	9	18	14	2.77	7.9	2.2	0.2	A-1-b
21	49	39	25	2.79	8.5	31.7	6.8	A-6
24	44	23	14	2.73	7.6	26.1	4.4	A-4

[a]From Reference Laguros, 1972.

[b]Unconfined compressive strength.

[c]American Association of State Highway and Transportation Officials Classification.

CHAPTER IV

TESTING PROCEDURE

In a previous investigation (Annamalai, et al., 1970). the lime retention point (Hilt and Davidson, 1960; Ho and Handy, 1963) for the shales 13, 21 and 24 was found to be between 2 and 4 percent of lime on dry soil weight basis. Shale 15 was not included in that investigation; this shale has an AASHTO classification of A-1-b and is not considered suitable for lime stabilization. It was included in this investigation to provide a reference point. The other shales, it will be noted, have AASHTO classifications of A-7(6), A-6 and A-4 in order of effectiveness of lime stabilization on them. For the shales 13, 21 and 24 it was noticed that significant changes take place in maximum dry density, optimum moisture content, plasticity characteristics and unconfined compressive strength between zero percent and three percent lime additions. Thus, percentages of lime adopted for stabilization of shales under this study were 0, 1, 2, 4, and 6.

Preparation of Mix

The hygroscopic moisture content of the shale sample material finer than U.S. Standard Sieve No. 10 was determined

by drying a portion of sample in an oven set at 105°C - 110°C. The weight of the shale material corrected for hygroscopic moisture was then determined along with the amount of lime required by weight. A portion of air dried shale and the required amount of lime were then weighed and mixed together. Water was added to the shale-lime mixture and the whole mix was then thoroughly mixed. The amount of water added depended on the requirements of the particular test; for determining the moisture density relationships it was variable and for the preparation of the samples it was determined from the moisture density relationship data.

Moisture Density Relationship

For all shales and shale lime mixes moisture density relationships were determined in a manner similar to that specified by AASHTO designation T 99-70 (ASTM designation D 698-64 T) with the exception that the Harvard miniature compaction apparatus was used. The values of maximum dry density and corresponding optimum moisture contents for all shales and shale lime mixes are given in Table 4.1 and the relationships of the two parameters with the amount of lime are shown in Figures 4.1 and 4.2, respectively.

Preparation of Samples

Samples were statically compacted in the apparatus shown in detail in Figure 4.3. The dimensions of a sample prepared by this method are diameter 1.35 in and height

TABLE 4.1

MAXIMUM DRY DENSITY AND OPTIMUM MOISTURE CONTENT VALUES AT VARIOUS AMOUNTS OF LIME

Shale Number	Amount of Lime, %				
	0	1	2	4	6
13	109.2[a] (18.3)[b]	103.2 (21.6)	100.9 (21.6)	98.5 (21.6)	98.2 (22.8)
15	119.2 (13.2)	116.0 (15.2)	115.6 (16.1)	113.8 (16.3)	111.8 (16.6)
21	105.2 (21.5)	98.7 (24.0)	98.0 (25.5)	95.0 (25.8)	96.2 (25.3)
24	110.8 (18.0)	105.3 (18.2)	102.6 (20.0)	101.0 (20.2)	100.3 (21.5)

[a]Maximum dry density, pcf.

[b]Optimum moisture content, percent.

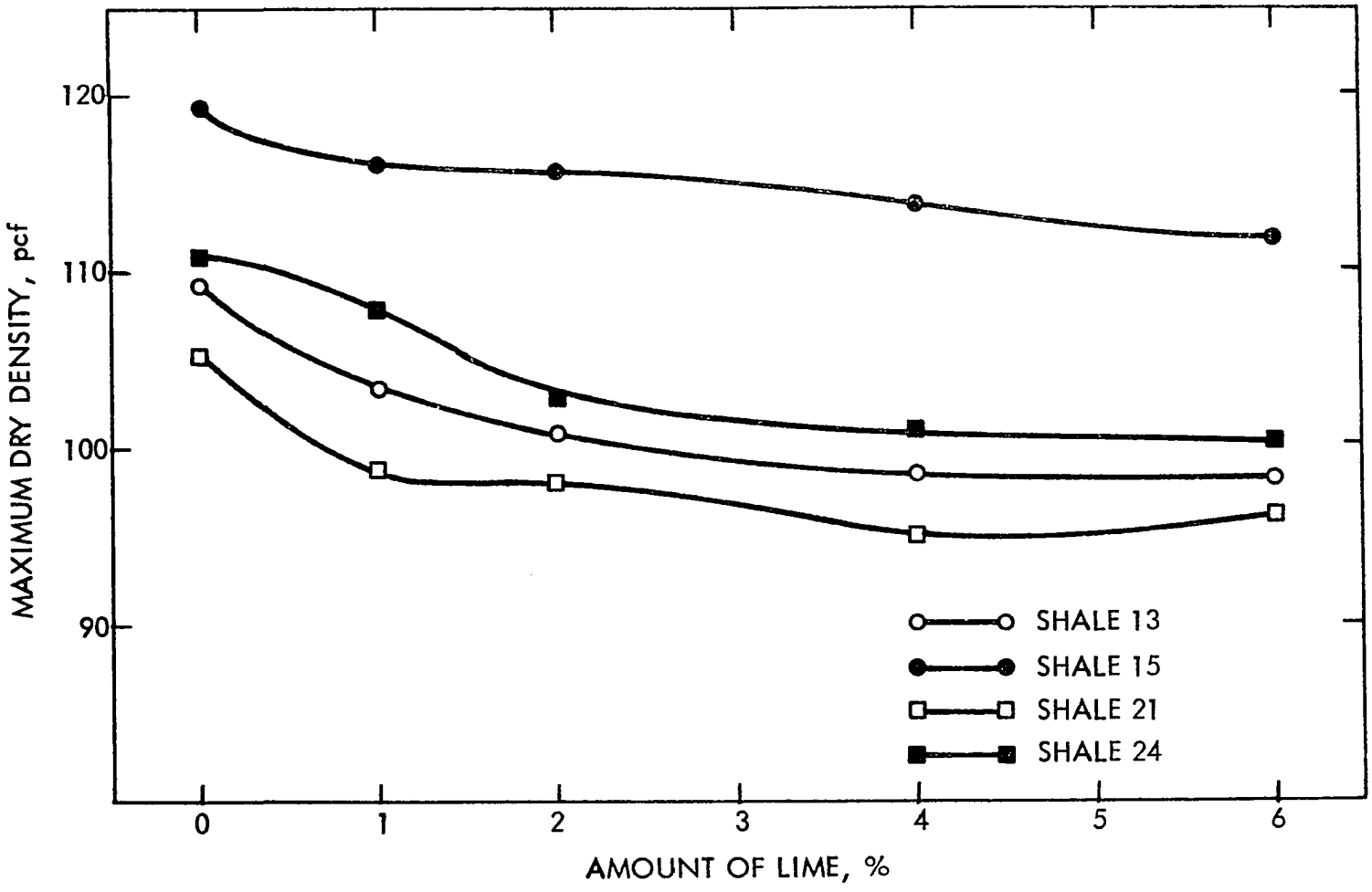


Figure 4.1. Change in maximum dry density values with the addition of lime.

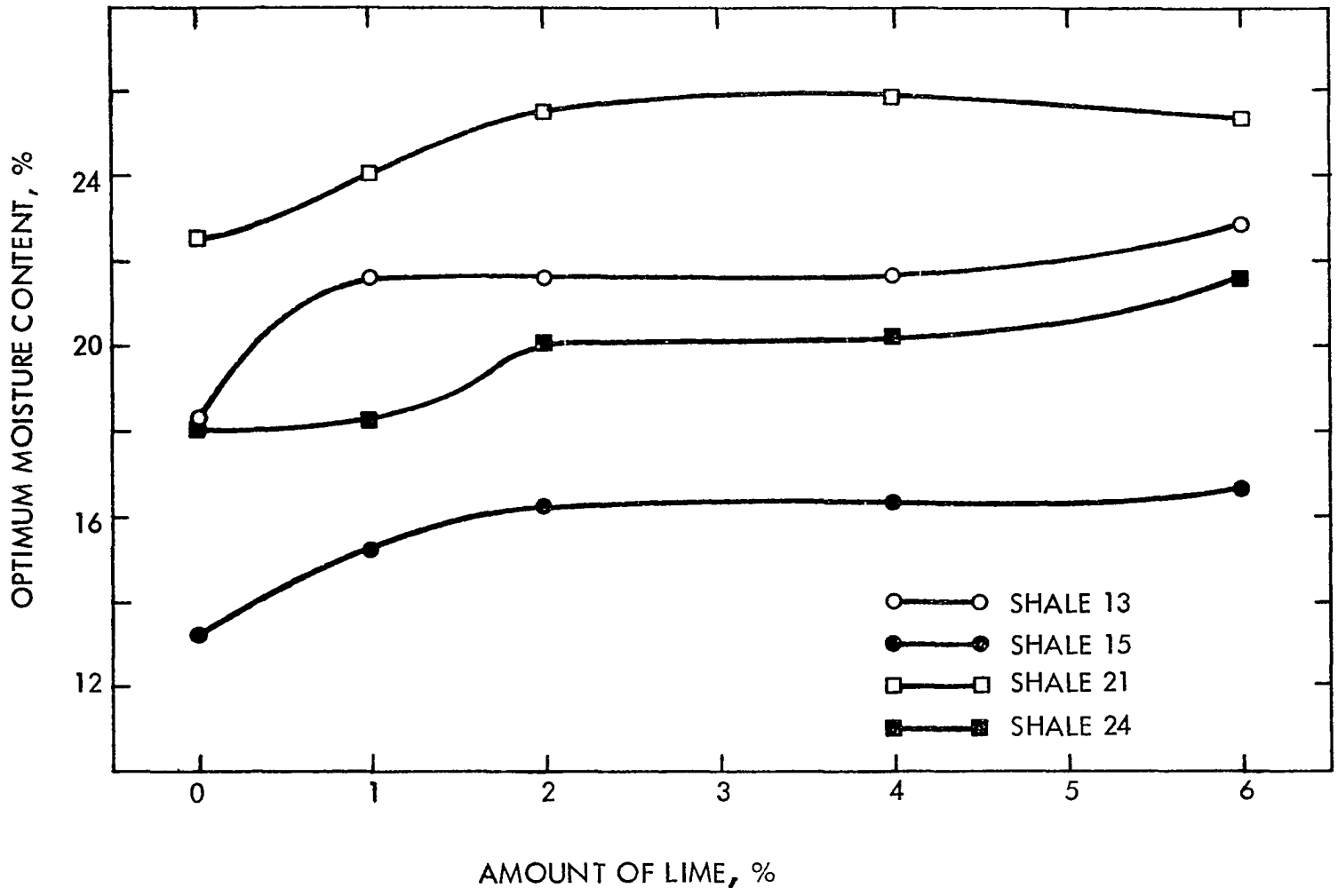


Figure 4. 2 Change in optimum moisture content value with the addition of lime.

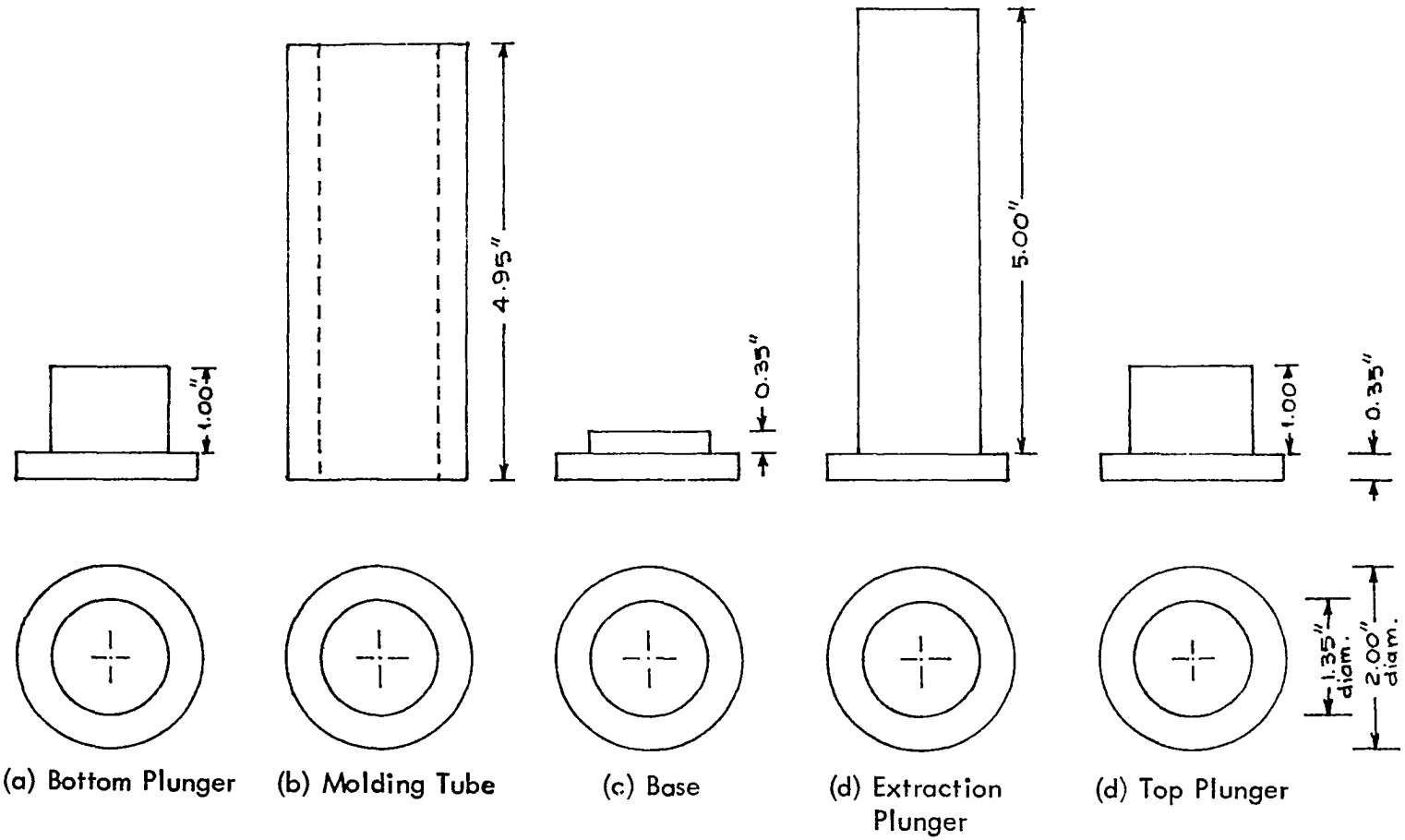


Figure 4.3 Details of sample molding apparatus.

2.95 in; thus the volume of the sample prepared by this apparatus is ten percent greater than that of the sample obtained from Harvard miniature compaction apparatus. Amounts of shale, lime and water required for maximum dry density and optimum moisture conditions were weighed and thoroughly mixed together and then allowed to equilibriate in a humid atmosphere for 24 hours. The calculated amount of mix was poured into the molding tube which was then placed under a compression machine along with the two plungers and compressed until the flanges of plungers were in complete contact with the ends of the tube. The assembly was left under the machine for five minutes after which the load was removed and plungers withdrawn. Using the extraction plunger, the sample was extracted from the molding tube under the pressure applied through hydraulic jack.

The extracted sample was wrapped in Saran wrap, labeled and stored in humidifier. The samples for long term curing were left in humidifier for 120 days but all other samples were stored in it only for 7 days. After the end of the curing period the sample was removed, weighed and its dimensions measured. The sample cured for 7 days was then subjected to wet-dry cycles.

Application of Wet-Dry Cycles

The application of wet-day cycles is expected to simulate the effect of weather on shale samples. To determine

the number of wet-dry cycles, data for the ten year period 1960 through 1969 from 16 locations in Oklahoma were collected and then evaluated (Laguros, 1972). A wet-dry cycle is defined as a dry period in a 24-hour interval; any rainfall less than 0.10 inch is disregarded unless it links two 24-hour periods with at least a total of 0.10 inches of rainfall. The third highest number of cycles is chosen as the 'number of wet-dry cycles.' The number of such cycles for various parts of Oklahoma is shown in Figure 4.4. The range of cycles is 30 to 45. Since the time lapse between construction of subgrade and placement of pavement on it is usually in the range of six months, the number of wet-dry cycles to which the subgrade material is expected to be subjected is in the range of 15 to 25. It was therefore decided to investigate the changes in the shales and the stabilized shales after 0, 5, 15, 30 and 50 wet-dry cycles.

As explained in the following description the samples were tested in split tensile strength test either in 'humid' state or 'dry' state. The samples subjected to zero wet-dry cycles and in humid state were taken out of the humidifier and directly used for strength testing. All other samples were placed in an oven set at 60°C, which corresponds to the maximum temperature in open areas for Oklahoma. The samples were oven dried for 12 hours. After this they were transferred to a humidifier--100 percent relative humidity atmosphere at 22.2°C (72°F)--and kept in it for 24 hours. This

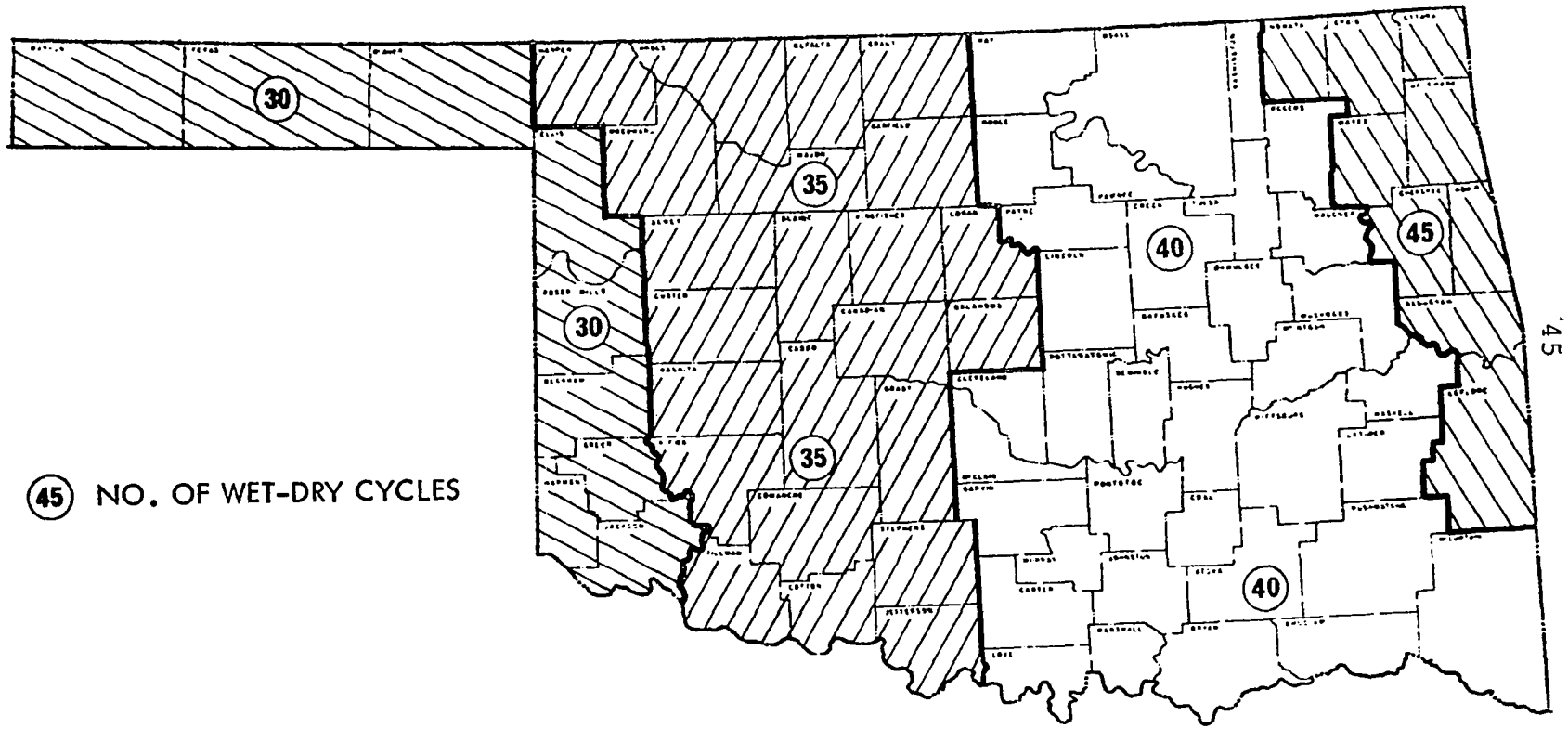


Figure 4.4 Wet-Dry cycles for Oklahoma.

drying and humidifying was continued until the required number of wet-dry cycles was completed. At the end of the cycle samples had moisture content in equilibriation with the humidifier environment. This state was termed as the 'humid' state. For the samples subjected to zero wet-dry cycles the moisture content in the humid state will be approximately equal to their molding or optimum moisture content. Half of the total number of specimens of one type, having same shale and amount of lime combination and having been subjected to the same number of wet-dry cycles, were placed in the oven set at 60°C for further drying for a period of 12 hours. Half of the total number of specimens of one type and subjected to 120-day curing also were dried in this manner. At the end of drying the samples had moisture content in equilibriation with the oven compartment environment and this state of samples was termed the 'dry' state. As would be expected, the moisture content in the dry state was much lower than in the humid state.

Initially, it was proposed to soak the samples in water but none of the samples could stand this severe treatment. Hence, the idea of soaking them was abandoned and substituted by storing them in 100 percent relative humidity atmosphere.

At the end of required weathering treatment the samples were weighed and their heights and diameters measured. After this they were subjected to repeated load split tensile strength testing.

For four shales, five percentages of lime, five wet-dry cycles, two states of testing and two replicates, the total number of samples prepared for this series was 400. Additional 64 samples were prepared for studying the effect of long term curing on the repeated load split tensile strength characteristics of the four shales.

Repeated Load Split Tensile Strength Test

The equipment for this test is shown in Figure 4.5 and it consists of:

1. SBEL soil dynamic testing machine
2. Load cell
3. Displacement strain gage
4. Sanborn strip chart recorder
5. Atomic strip chart recorder.

SBEL Soil Dynamic Testing Machine

This machine has been manufactured by the Structural Behavior Engineering Laboratories of Phoenix, Arizona. The power unit of this machine consists of compressed air, the volume of air required is small. Pulse action is initiated through air solenoid valves which are operated on command by a gearhead variable speed motor and adjustable cams. Essentially, the unit can be called an air over oil system with low volume, high response capability (SBEL, 1970).

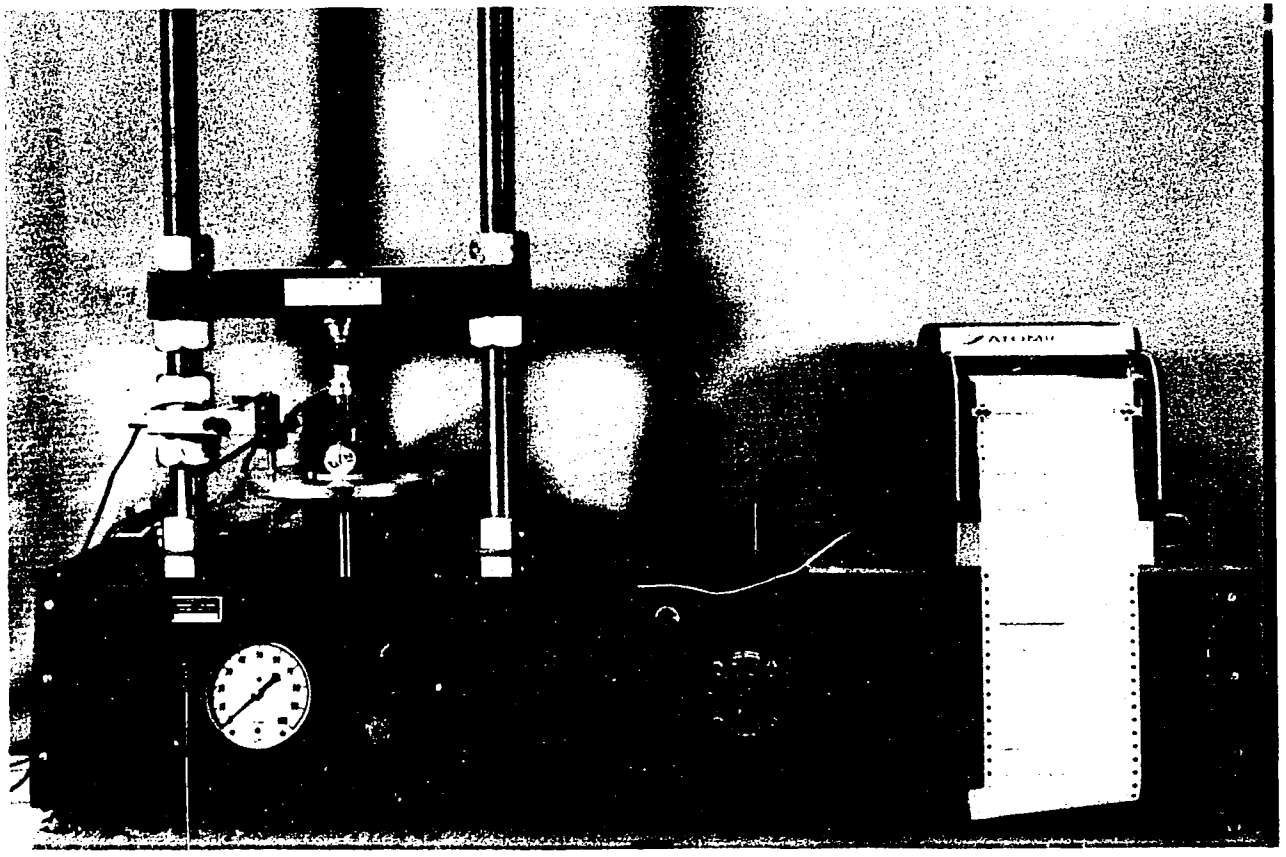


Figure 4.5 Equipment for cyclic split tensile strength test.

The upper crosshead is adjustable within a distance of two feet and contains demountable swivel head. The cross head rests on two posts which are bolts 1-1/2 inch in diameter threaded throughout and mounted 13 inches apart. The base consists of a 9-inch diameter demountable platen.

The front panel of the machine provides controls for line pressure, air regulation, dwell time and pulse rate. Also provided on the front panel are AC power switch, dwell time monitor outlets, load releases exhaust control, gage shut-off and solenoid by-pass. (Figure 4.5 shows the front view of the machine.)

The machine is capable of applying up to 1250 lb load and has a maximum ram throw of 2 inches. The dwell time can be varied continuously between 0.05 sec to 10 sec and the maximum pulse count capability is limited to 10,000. The frequency of load application can be varied within a wide range but is restricted to 2.4, 3, 4, 6, 12, 24, 30, 40, 60 and 120 cycles per minute.

The circuit diagram for the machine, taken from SBEL, 1970, is shown in Figure B.1 (Appendix B).

Load Cell

An aluminum load cell was made locally. It consists of an aluminum piece cut to the dimensions shown in Figure 4.6. It was anticipated that the loads to be applied would be low; hence, attempt was made to make the cell as thin as

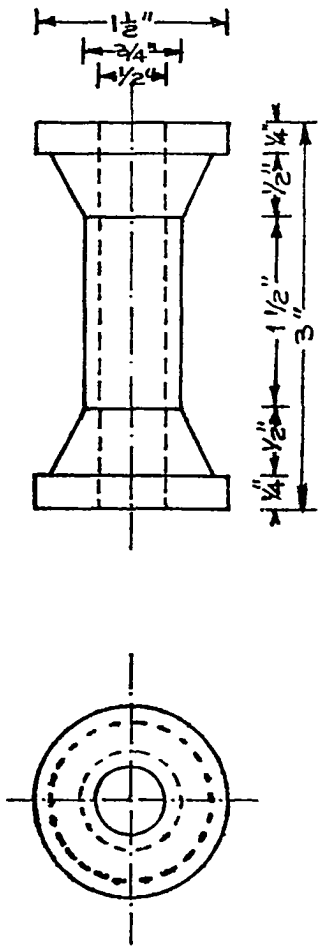


Figure 4.6 Load cell

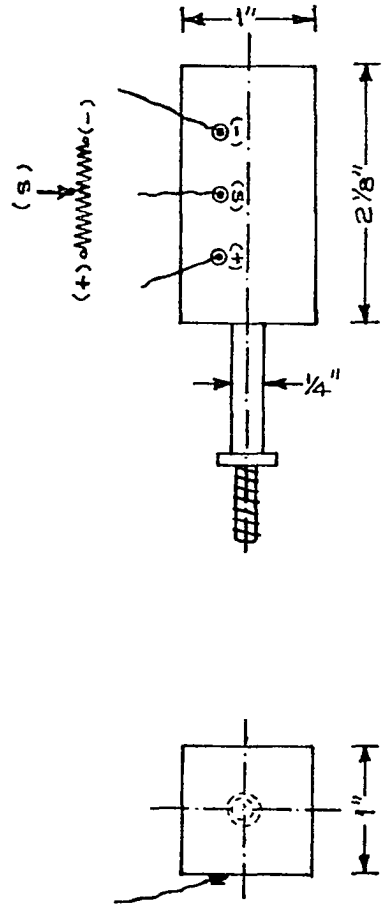


Figure 4.7 Displacement strain gage

possible. The load cell in question is only 1/8-inch thick. SR-4 strain gages (Type A-7, resistance 120 ohms; manufactured by the BLH Electronics, Inc., of Waltham, Massachusetts) are glued to the external surface of the cell at about mid height. The connection of the strain gages to the preamplifier is in the manner shown in Figure B.2 (Appendix B). The cell is fixed to the cross head of the soil dynamic testing machine (Figure 4.8).

Displacement Strain Gage

The strain gage is linear motion, infinite resolution potentiometer (Model 111, Computer Instruments Corporation, Hampstead, Long Island, New York). As shown in Figure 4.7, the gage has a body 1 inch square and 2-1/8 inches high. The displacement shaft is 1/4 inch in diameter and can move to a maximum distance of 1 inch. The shaft is spring loaded and is set to measure the deflections of the lower platen. The body of the gage is held in place by a connecting unit attached to one of the threaded posts of the soil dynamic testing machine (Figures 4.8 and 4.9). The electrical connections of the gage to the preamplifier are similar to those shown in Figure B.2 (Appendix B).

Sanborn Strip Chart Recorder

The Sanborn two-channel recording system Model 296 used during this investigation is a recording electronic voltmeter with direct writing facility. Inkless recordings

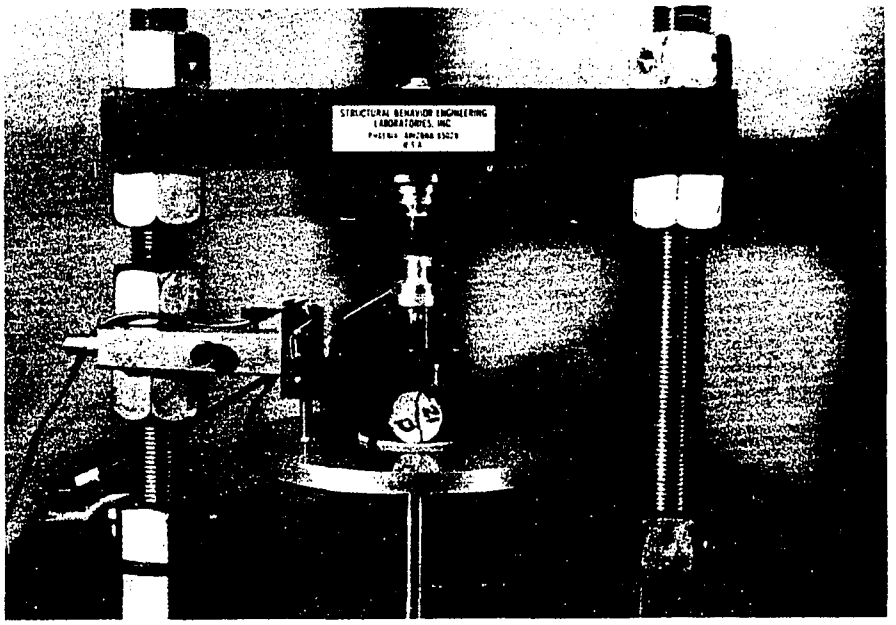


Figure 4.8 Arrangement of load cell and displacement strain gage during testing.

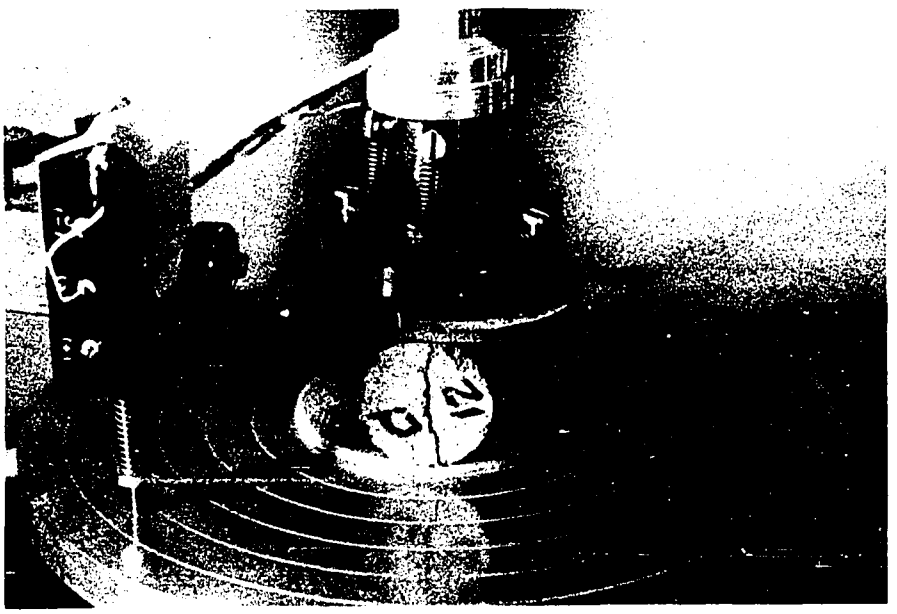


Figure 4.9 Detailed view of sample under test.

are made by hot wire writing arms on heat sensitive paper chart (Hewlett-Packard, 1967b). Input for the recording unit is provided by the load cell and the displacement strain gage through carrier preamplifier 350-1100 C. Both the recorder and the preamplifier are supplied in one mobile unit manufactured by the Sanborn Division of the Hewlett-Packard Company, Waltham, Massachusetts.

Throughout this study, only the lowest chart speed (5 mm/sec) was used since the trial runs did not indicate that any significant additional information could be obtained at faster speeds. Also, the amount of chart paper consumed at faster speeds was excessive. A sample of recordings is shown in Figure 4.10.

The carrier preamplifier is a phase sensitive electronic voltmeter which operates in conjunction with an external device sensitive to the physical variable to be measured. The preamplifier supplies an excitation voltage to the transducer, the transducer returns a signal to the preamplifier. The amplitude of the signal represents the amplitude of the physical variable to be measured and the signal phasing with respect to reference indicates the sense (positive or negative) of the physical variable. The preamplifier interprets this signal in terms of load units and direction and shows this information on the recording chart (Hewlett-Packard, 1967a).

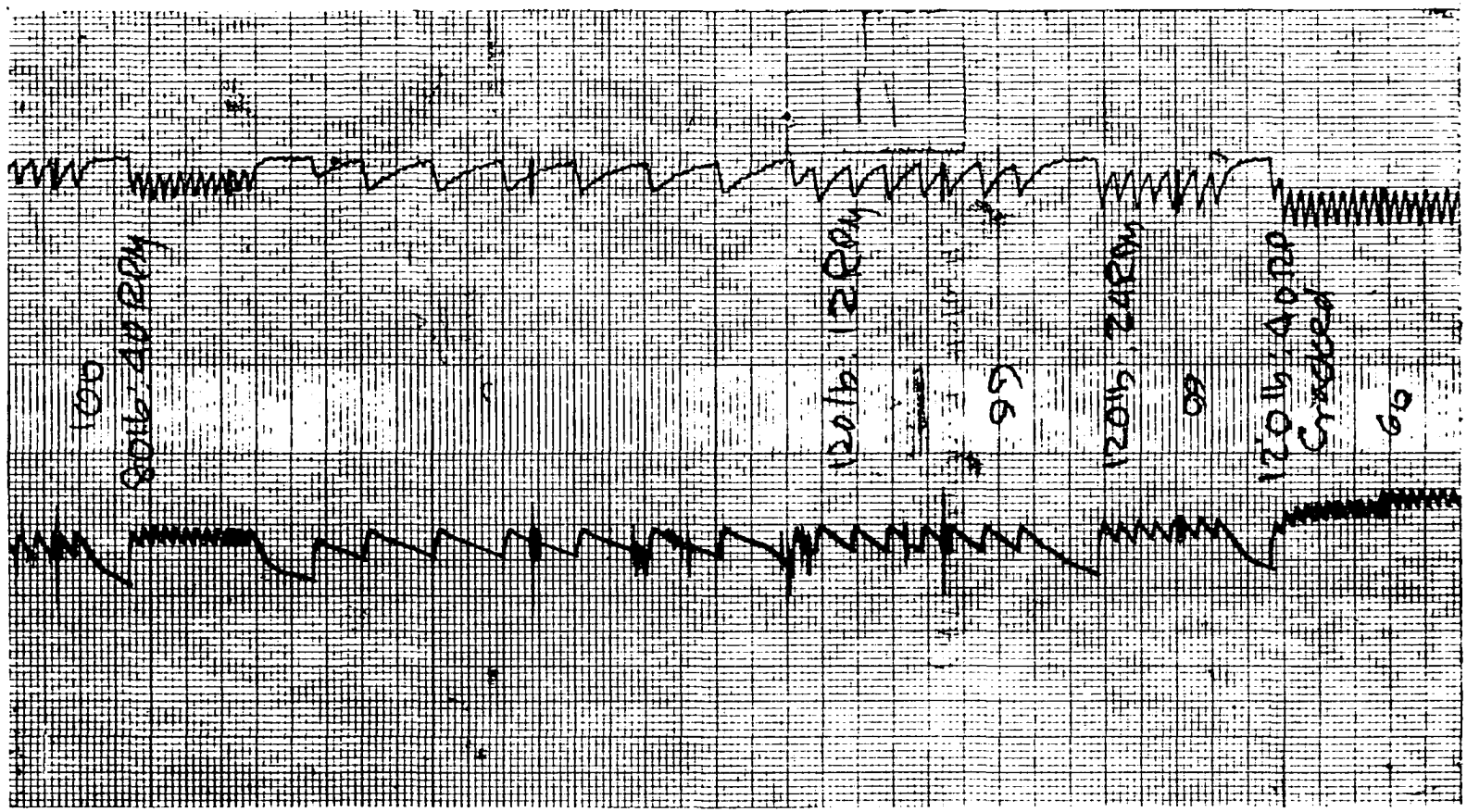


Figure 4.10 A sample of recordings obtained from Sanborn strip chart recorder.

Atomic Strip Chart Recorder

This unit is basically a single channel graphic direct current milliammeter. Electric current flowing through a coil, suspended in a strong magnetic field, causes the coil to turn to an equilibrium position. Calibrated springs resist the coil movement and cause writing arm to deflect providing ink recordings on a chart paper.

The chart speed used during this investigation was 1.5 inches/min, the maximum available on the instrument. The pulse characteristics of the split tensile strength test are relayed to this recorder by means of the arrangement shown in Figure B.3 (Appendix B).

Before starting the series of experiments both the load cell and the displacement strain gage were calibrated. In the case of the load cell it was properly connected to the preamplifier and the recording system and put under the proving ring assembly of a compression testing machine. For known magnitudes of loads, deflections on the strip chart were noted. Relationship between the load and the chart deflection was then determined graphically. The displacement strain gage was attached to a micrometer screw gage and for known displacements of the strain gage shaft the chart deflections were noted. As in the previous case, the relationship between the shaft movement and chart deflections was determined graphically.

Hard board pieces 1/16-inch in thickness and 3 inches in diameter were attached to the top and bottom platen of the machine. In order to prevent rolling and slipping of the samples away from the central axes, the hard board pieces were profiled to accept the 1.35 inch diameter cylindrical samples placed lengthwise on the lower platen.

After its weight, height and diameter were determined the sample was placed on the profiled hard board attached to the lower platen. The lower platen was then brought to the mid height of its throw, the maximum throw being 2 inches. The upper crosshead was then adjusted, by turning the nuts on the threaded posts, until the profiled surface on the upper platen just came in contact with the cylindrical surface of the specimen.

After making the machine ready for operation, the line pressure was adjusted at a low value (2 psig). The dwell was set at 1.0 sec and the frequency of load application was set at 6 applications per minute (APM). Right after this the recording unit, the atomic chart recorder and the pulse switch were turned on. The pressure gage was then immediately set to apply 40 lb load on the sample. The load, APM and line pressure relationships were determined previously on cylindrical aluminum samples.

After 100 load applications, the pulse switch was briefly turned off and the frequency of load application

changed to 12 APM and the pressure gage adjusted to apply 40 lb load at this frequency. Again the load was applied 100 times. In this manner the frequency of load application was varied to 6, 12, 24 and 40 APM and the loads of 40, 80, 120 and 160 lb were applied at each one of the frequencies. The load was kept constant while the frequencies were varied after each 100 load applications and then the whole procedure was repeated with greater and greater loads.

The range of frequency was limited between 6 APM and 40 APM. No useful information was obtained on trial samples tested under frequency of load application lower than 6 APM. For frequencies higher than 40 APM the information obtained was not considered to be reliable. Also at the 60 APM and higher frequency settings the time period of load application became equal or less than the dwell time of 1.0 sec and a continuous, rather than a wave, curve was obtained on the strip chart.

One millimeter division on the strip chart represented a 20 lb load and with the thickness of lines produced by writing arms of the Sanborn strip chart recorder, it was difficult to determine the load accurately at that level and the percentage of error was considered high. Hence, the load of 40 lb was adopted as the minimum level of load application. Application of load at 160 lb level and 40 APM frequency was beyond the capacity of the machine so the testing had to be terminated at 160 lb load and 24 APM frequency.

The test was continued until failure occurred. Initiation of any cracks visible to the eye was noted on the strip chart, as soon as it became noticeable. For those samples which did not fail, the tests were continued to the end (160 lb load and 24 APM frequency).

After the completion of the split tensile strength test, the sample was removed from the lower platen of the machine and allowed to air dry. Several days later the sample was broken and ground to pass U.S. Standard Sieve No. 10. A major portion of this material was used for the determination of liquid limit and plastic limit, and a small portion was used for x-ray analysis to determine the changes in clay mineralogy.

Determination of Liquid Limit

Tests for this purpose on all the shales and shale lime mixes were conducted in accordance with the AASHTO designation T 89-68.

Determination of Plastic Limit

Plastic limits for all shales and shale lime mixes were determined in accordance with the AASHTO designation T 90-70.

X-Ray Diffraction Analysis

The mineralogical composition of all shales and shale lime mixes was determined by x-ray diffraction method using

Cu K-alpha radiation. Material used for analysis was that passed U.S. Standard Sieve No. 200. X-ray patterns were obtained using Norelco x-ray diffractometer unit with the rate of scanning set at 2 degrees per minute. The alterations in mineralogical composition were determined using 'area under the peak' method (Gillott, 1968). Other data relative to diffractometer include: kV = 40, mA = 20, Ratemeter 100 cycles per sec, Standard Deviation of 3 percent, and Chart Speed of 1/2 inch per min.

CHAPTER V

PRESENTATION AND DISCUSSION OF TEST DATA

For the variety of parameters considered, an inordinate number of samples would have been necessary had a statistical evaluation been made for every shale type, each percentage of lime and each testing condition included in this investigation. The variety of testing itself is expected to present an initial overall pattern, additional details for which, if desired, could be obtained by subsequent testing.

The main feature of this study was the determination of the properties of the four shales, raw as well as stabilized, under and after various loads and load frequency applications and the effect of simulated weathering on these load parameters. No attempt, however, was made to determine the classic S-N curves for any sample since for a certain load and a certain load application frequency this would have indicated only the allowable number of load applications on a sample, a figure of no practical significance in highway pavement design.

Maximum Dry Density and Optimum Moisture Content

The first step in any study on the effects of stabilization of soils is to determine the relationships of maximum dry density and optimum moisture content with the amount of lime added to the soil. This study on shales confirms the earlier findings of various investigators that lime treatment causes a decrease in maximum dry density of clayey soils. For all shales included in this study, on addition of lime, the density decreased rapidly at first and then the rate of decrease in density dropped with increasing amount of lime, no significant difference being noticeable beyond 4 percent level of lime treatment (Table 4.1, Figure 4.1). The maximum dry density values in the case of Shale 24, for example, are 110.8 pcf for no treatment, 105.3 pcf at 1 percent, 101.0 pcf at 4 percent and 100.3 at 6 percent level of lime treatment. This study also confirms that lime treatment causes increase in the optimum moisture content. On addition of lime the optimum moisture content values increased rapidly at first and then the rate of increase in optimum moisture content value dropped with the increasing amount of lime (Table 4.1, Figure 4.2). No significant changes were found to occur in the optimum moisture content values beyond 2 percent lime addition; for example, for Shale 24 the optimum moisture content values are 18.0 percent for no treatment, 20.0 percent at 2 percent and 21.5 percent at 6 percent level of lime treatment.

For soils, in general, the higher maximum dry density values are associated with lower moisture content values and vice versa. This type of relationship is valid in this study not only for the raw shales but also for all their lime stabilized combinations. The regression equation obtained for this relationship is:

$$MDD = 143.916 - 1.933\ (OMC)$$

where MDD = maximum dry density, pcf,

OMC = optimum moisture content, percent

The coefficient of correlation for this equation is 0.952. This relationship is shown graphically in Figure 5.1. Similar relationships were obtained by Annamalai (1974) and Laguros (1972) for twenty-four similar untreated shales.

The orders in which the maximum dry density and optimum moisture content curves appear are very much as expected except for the Shale 21. Shale 21 has an AASHTO classification of A-6 while the Shale 13 has an AASHTO classification of A-7(6) and thus maximum dry density curve for the Shale 21 will be expected to be on the higher density side. This, however, is not the case. To explain this behavior the parameter 'activity coefficient' was considered. The moisture density relationships for soils depend not only on their particle size distribution but also on their plasticity characteristics and the parameter combining these two factors is known as 'activity coefficient.' It is defined (Skempton, 1953) as

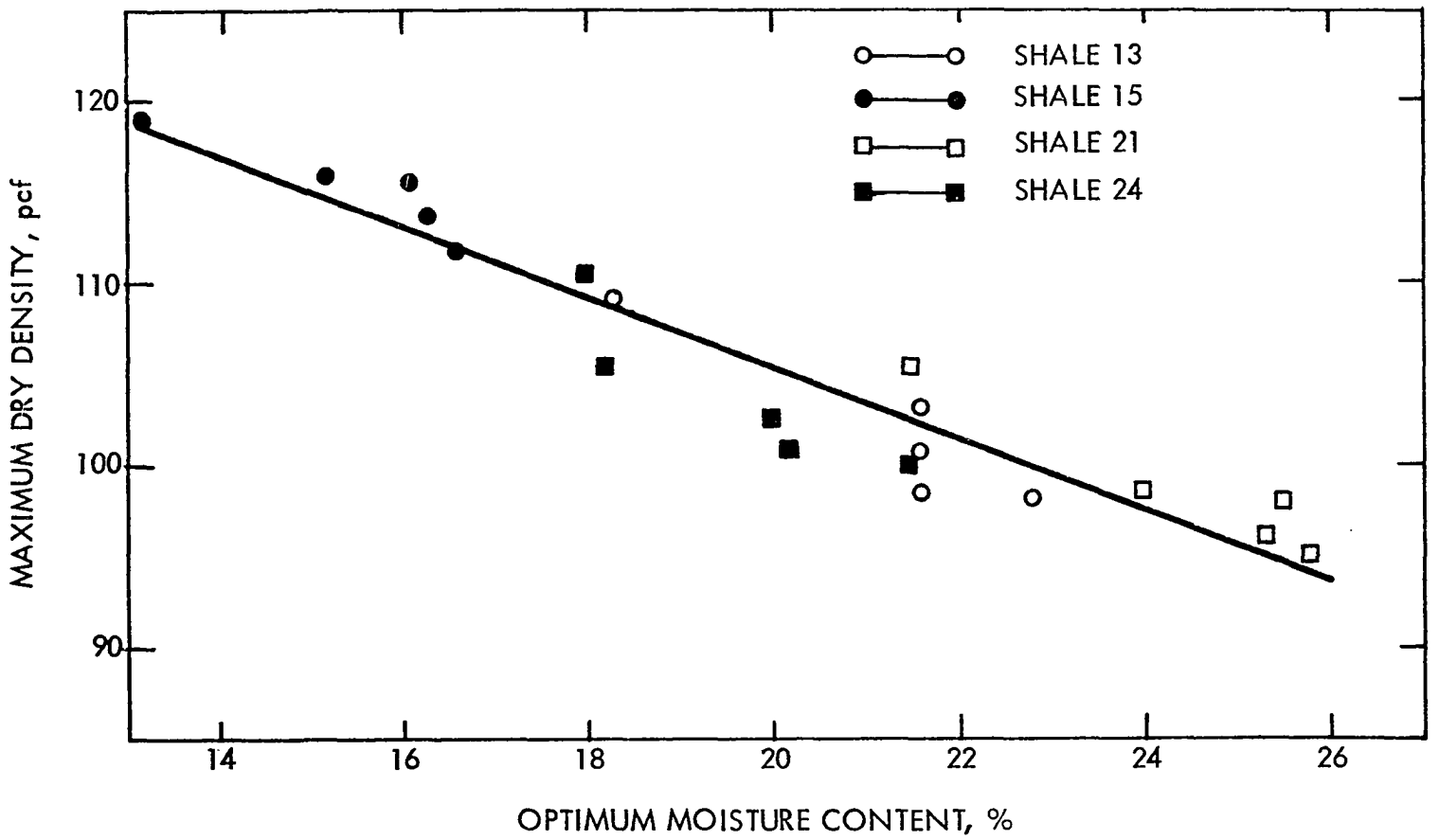


Figure 5.1 Relationship between maximum dry density and optimum moisture content for all shales and shale lime combinations.

$$\text{Activity Coefficient} = \frac{\text{Plasticity Index}}{\text{Clay Content (Percent} < 2 \text{ micron)}}$$

The values for activity coefficients from the data of Laguros (1972) were found to be 0.48 for Shale 13, 0.14 for Shale 15, 0.56 for Shale 21 and 0.43 for Shale 24.

It is now obvious that the order in which the maximum dry density and the optimum moisture content curves occur is directly related to their activity coefficients.

The decreases in maximum dry density and increases in optimum moisture content values are attributed to flocculation of clay particles brought about by ion exchange between them and the lime particles. Small percentages of lime are easily adsorbed on the clay particles. As the amount of lime increases, the rate of adsorption decreases due to the smaller surface area of clay particles available for adsorption and consequent flocculation.

Preparation of Samples

Visual examination of compacted samples indicated slight increase in densification toward the ends of the specimens. Ejection of samples, using the extraction plunger, also seems to have caused some increase in density. In general, it may be stated that the process of static compaction used in this study had high reproducibility. The height of the specimen is designed to be 2.95 inches; the extreme values of height noted for all samples were 3.035 inches and

2.808 inches, indicating less than 5 percent variation from the ideal height dimension. The mean value of height was 2.965 inches with a standard deviation of 0.048 inch indicating possible rebounds of specimens having a mean value of 0.015 inch or about 0.5 percent.

For all shales and shale lime combinations the weights of ideal samples were calculated on the basis of maximum dry density and optimum moisture content data depicted in Table 4.1. To take care of losses small amounts of shale or shale and lime mix and water were added to the mix used for molding of specimens. For all samples the mean weight was found to be 0.36 gm above the ideal with a standard deviation of 0.74 gm. Sixteen samples showed excessive differences between the weights of ideal and the actual samples. These differences were in the range of 1.3 gm to 5.2 gm or about 1 percent to 4 percent of the weight of an average sample. Statistical analysis excluding these sixteen samples showed the mean weight to be 0.26 gm above the ideal with a standard deviation of 0.48 gm.

Thus using the size and weight as a basis, it is concluded that most samples were exceptionally uniform. The existence of a density gradient, of any sort, within the sample, however, cannot be confirmed or denied by these statistical analyses.

Application of Wet-Dry Cycles

As explained in the previous chapter, after molding and following the 7 day curing period the samples were subjected to wet-dry cycles. The samples subjected to 120-day moist curing were not included in this series. The wetting of samples was limited to keeping them in 100 percent relative humidity environment. The samples were not allowed to come in contact with water. Drying was effected by placing the samples in an oven set at 60°C temperature.

As would be expected, even after one drying the amounts of moisture content for all samples were well below their optimum or molding moisture contents. The moisture contents for samples tested in humid condition were greater than for those tested in dry condition. In the case of samples not subjected to any drying at all the moisture content remained equal to the molding moisture content. As shown in Table 5.1, the molding moisture contents are very close, within 1 percent, to the optimum moisture contents for all shales and shale lime combinations.

End of cycle moisture contents also were very close. As an example, for Shale 21 and 4 percent lime addition, the samples in humid state had moisture content values of 7.1 percent at the end of 5, 7.8 percent at the end of 15 and 8.2 percent at the end of 50 wet-dry cycles. Also, for a particular shale no significant difference is exhibited by different lime additions on the moisture content at the end of different

TABLE 5.1

OPTIMUM, AVERAGE MOLDING AND END OF CYCLE MOISTURE CONTENTS FOR VARIOUS SHALE LIME COMBINATIONS

Shale Number	Amount of Lime %	Optimum Moisture Content %	Avg. Mold. Moisture Content %	End of Cycle Moist. Content, %	
				Humid[a,b]	Dry[a]
13	0	18.3	18.7	9.3	1.8
	1	21.6	22.0	9.3	1.4
	2	21.6	21.9	9.2	1.7
	4	21.6	21.6	9.2	1.9
	6	22.8	22.5	10.7	2.5
15	0	13.2	14.1	5.4	1.1
	1	15.2	16.0	4.5	1.0
	2	16.1	16.9	5.5	1.6
	4	16.3	17.2	6.2	1.5
	6	16.6	17.4	6.8	1.3
21	0	21.5	21.8	11.4	2.3
	1	24.0	24.4	11.0	2.1
	2	25.5	25.9	10.4	2.2
	4	25.8	25.9	10.7	2.0
	6	25.3	25.2	11.0	2.0
24	0	18.0	18.0	6.7	0.8
	1	18.2	18.4	7.1	1.0
	2	20.0	19.2	6.7	0.8
	4	20.2	20.5	7.7	1.1
	6	21.5	21.0	7.9	0.8

[a]State of specimen at the time of testing.

[b]Does not include samples in humid state not subjected to at least one drying.

wet-dry cycles. In the case of Shale 21 for example, after 30 wet-dry cycles the moisture content values for humid samples were: 6.1 percent for no treatment; 6.3 percent for 1 percent; 6.9 percent for 2 percent; 7.8 percent for 4 percent; and 7.3 percent for 6 percent lime treatment. This observation remains true for samples in both states, the humid and the dry.

The effect of loss of moisture is readily reflected in the volume of sample. The reduction in volume, or shrinkage, is defined here as:

$$\text{Shrinkage, percent} = \frac{(V_i - V_t) \times 100}{V_i}$$

where V_i = volume of sample at the end of 7-day curing period

V_t = volume of sample at the end of the process

As expected, the shrinkage is greater for the samples in dry state than for those in humid state. Shrinkage showed no significant difference among the number of wet-dry cycles. For Shale 13 and 2 percent lime addition, for example, the dry state samples show shrinkage values of 6.2 percent after 5, 6.4 percent after 15, 5.8 percent after 30 and 7.5 percent after 50 wet-dry cycles. The effect of lime addition, however, is very significant. As indicated in Table 5.2 and depicted on Figures C.1 through C.4 (Appendix C), the addition of lime is effective in reducing the

TABLE 5.2

AVERAGE SHRINKAGE (%) OF SAMPLES

Shale Number	Amount of Lime %	End of Wet-Dry Cycles		End of 120-Day Curing	
		Humid[a,b]	Dry[a]	Humid	Dry
13	0	10.9	11.5	1.2	13.3
	1	8.9	11.6	--	--
	2	6.4	8.6	0.0	8.4
	4	5.0	6.4	0.0	7.0
	6	4.5	7.0	0.6	7.0
15	0	2.2	3.5	0.0	2.2
	1	1.8	2.3	--	--
	2	1.5	2.2	0.0	1.8
	4	1.2	1.7	0.0	2.5
	6	1.4	1.8	0.0	2.2
21	0	10.2	13.2	1.2	17.6
	1	7.6	8.8	--	--
	2	6.3	8.0	0.0	9.2
	4	3.7	6.3	0.0	7.8
	6	4.4	6.0	0.0	5.4
24	0	6.2	7.1	1.2	7.9
	1	4.0	5.1	--	--
	2	2.8	3.6	0.0	4.2
	4	2.1	3.8	0.0	3.4
	6	2.0	3.8	0.0	3.7

Note: End of Wet-Dry cycle values contain values for all cycles.

[a]State of specimen at the time of testing.

[b]Does not include samples in humid state not subjected to at least one drying.

shrinkage of samples due to the loss of moisture. Shrinkage occurs rapidly at first and then as the amount of lime increases the rate of shrinkage decreases. For the humid state samples of Shale 13, for example, the shrinkage values were: 10.9 percent at no treatment; 6.4 percent at 2 percent; and 4.5 percent at 6 percent lime treatment. There is no noticeable difference beyond 4 percent lime addition. The values shown in Table 5.2 are averages of eight values for the samples in humid state and of ten values for the samples in dry state. Table 5.3 shows an example of the actual data obtained for various shales at 4 percent lime addition. The data show that even though in some cases there is indication that the shrinkage increases with increasing number of wet-dry cycles, the differences in the values are not obvious in all cases, and in most cases not significant enough to be termed as a trend.

The orders in which the 'end of cycle' moisture content (Table 5.1) and the 'average shrinkage' (Table 5.2) values occur for the four shales can again be related directly to the 'activity coefficient' defined earlier. As more and more shale reacts with the added lime, the shrinkage decreases. However, a greater concentration of the shale lime reaction products, either due to prolonged curing or due to the greater percentage of lime, may reverse this trend since now the shrinkage in the gel, which is the

TABLE 5.3

EXAMPLE OF SHRINKAGE (%) AT THE END OF WET-DRY CYCLES FOR VARIOUS SHALES AT 4 PERCENT LIME ADDITION

Shale Number	Test Condition	Sample Number	Number of Wet-Dry Cycles				
			0	5	15	30	50
13	Humid	1	0.0	4.9	4.0	5.7	6.7
		2	0.0	4.8	4.0	4.9	5.0
	Dry	1	4.3	6.9	7.6	4.0	--[a]
		2	5.7	6.2	6.1	8.5	8.4
15	Humid	1	0.0	1.0	1.7	2.2	1.7
		2	0.0	1.1	0.8	1.9	1.4
	Dry	1	--[a]	1.0	1.3	3.1	2.3
		2	2.0	0.8	1.1	2.7	2.4
21	Humid	1	0.0	3.0	3.1	2.9	5.3
		2	0.0	3.2	3.8	3.9	4.5
	Dry	1	2.9	6.5	6.1	5.9	7.5
		2	7.5	6.9	6.2	6.9	7.2
24	Humid	1	0.0	2.2	1.7	1.9	2.2
		2	0.0	2.1	1.8	2.6	2.5
	Dry	1	3.0	3.5	2.6	5.5	5.2
		2	3.4	3.8	2.7	3.6	5.0

[a]No data available; samples destroyed.

most important reaction product, may become significant. This reversal in trend would be more obvious in predominantly kaolinitic and illitic shales than in the predominantly montmorillonitic shales (George, 1968). This seems to be attested in this investigation, too. The shrinkage values at the end of the wet-dry cycles for Shale 15 are higher for the 6 percent lime treatment level than for the 4 percent treatment level (Table 5.2, Figure C.2 in Appendix C). Shale 24 also shows a similar trend but with much less distinction in values.

George (1968) considered the reduction in volume in clay soils to be a 'structure effect,' the higher the molding moisture content the higher the tendency to form dispersed structure and accordingly the reduction in volume is higher. This concept seems to be valid for untreated shales but not for the shales treated with lime. In the latter case the stabilizing effect of lime becomes more predominant and reverses the molding moisture content and reduction in volume relationship.

On drying, some samples showed cracks, visible especially at the ends of the samples. The cracking was less apparent in the samples made of shale lime mixes. No cracking was obvious in the samples containing lime at or above 2 percent treatment level. This observation confirms the well known beneficial aspects of lime stabilization.

Repeated Load Split Tensile Strength Test

The strength related characteristics of samples in this investigation were effected primarily by two major aspects:

1. Application of wet-dry cycles.
2. Stabilization of shale due to addition of lime.

Increasing the number of wet-dry cycles implies more extensive destruction of the bonds among the particles constituting the sample mass. On the other hand, the increase in the number of wet-dry cycles prolongs the time element and increased bonding results due to the pozzolanic reaction between shale and lime. This observation may help explain the wide range of values related to strength characteristics which are very low, very high, or which do not occur as otherwise would be expected at the end of the most prolonged wet-dry cycles or with the highest lime treatment levels.

The load and displacement graphs produced by the Sanborn recording equipment were continuous and showed the expected wave pattern (Figure 4.10). On the load graph, the maximum amplitude in the interval of one load application indicates the load applied on the total length of the sample. The amplitude of the displacement graph indicates the diametral compression of the sample. For most viscoelastic materials the maximum strain lags behind the maximum stress amplitude in time (Seed, et al., 1967). In this investigation

however, the stress produced was due to the movement of the lower platen of the machine which brought the sample in contact with the load cell assembly, and, thus, the load and the diametral compression had the maxima of their values at the same moment and no lag was noticed in those amplitudes.

For a given load and a load application frequency, the only quantity measured was the diametral compression. As shown by the expressions in Appendix A, the stresses at any point within the sample body are dependent on the diametral deformation and the load. In this investigation since the load was kept constant over a range of load applications the stresses, thus, were primarily dependent upon the diametral strain. It was thus decided to plot the diametral strain against the load and the frequency of load application - applications per minute. A graph of this type is shown in Figure 5.2. For the values corresponding to diametral strains used for this figure, the values of stresses s_{xxc}, s_{yxc}, s_{xye} and s_{yye} are shown in Figure 5.3.

An examination of Figures 5.2 and 5.3 shows that as far as the failure criterion is concerned, the diametral strain graph gives more meaningful results than does any other graph. This was found to be true in all the cases where at least two ranges of load were applied; a sudden increase in the stress values obliterated the effect of failure, if any, when the next higher load was introduced. To determine the behavior of sample material, thus, the diametral strain graphs like those shown in Figure 5.1 were used.

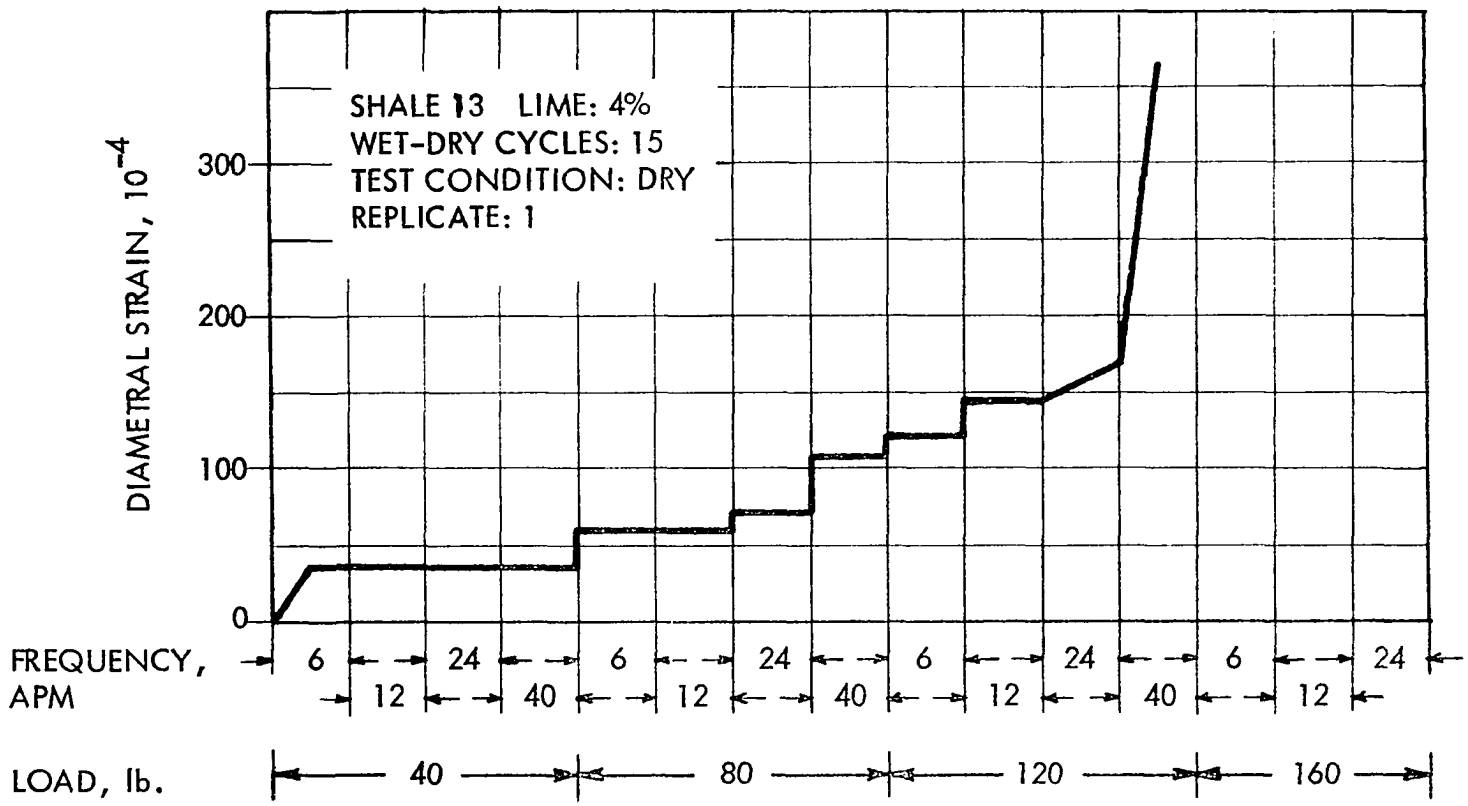


Figure 5.2. Example of diametral strain, load and frequency relationships for repeated load split tensile strength test.

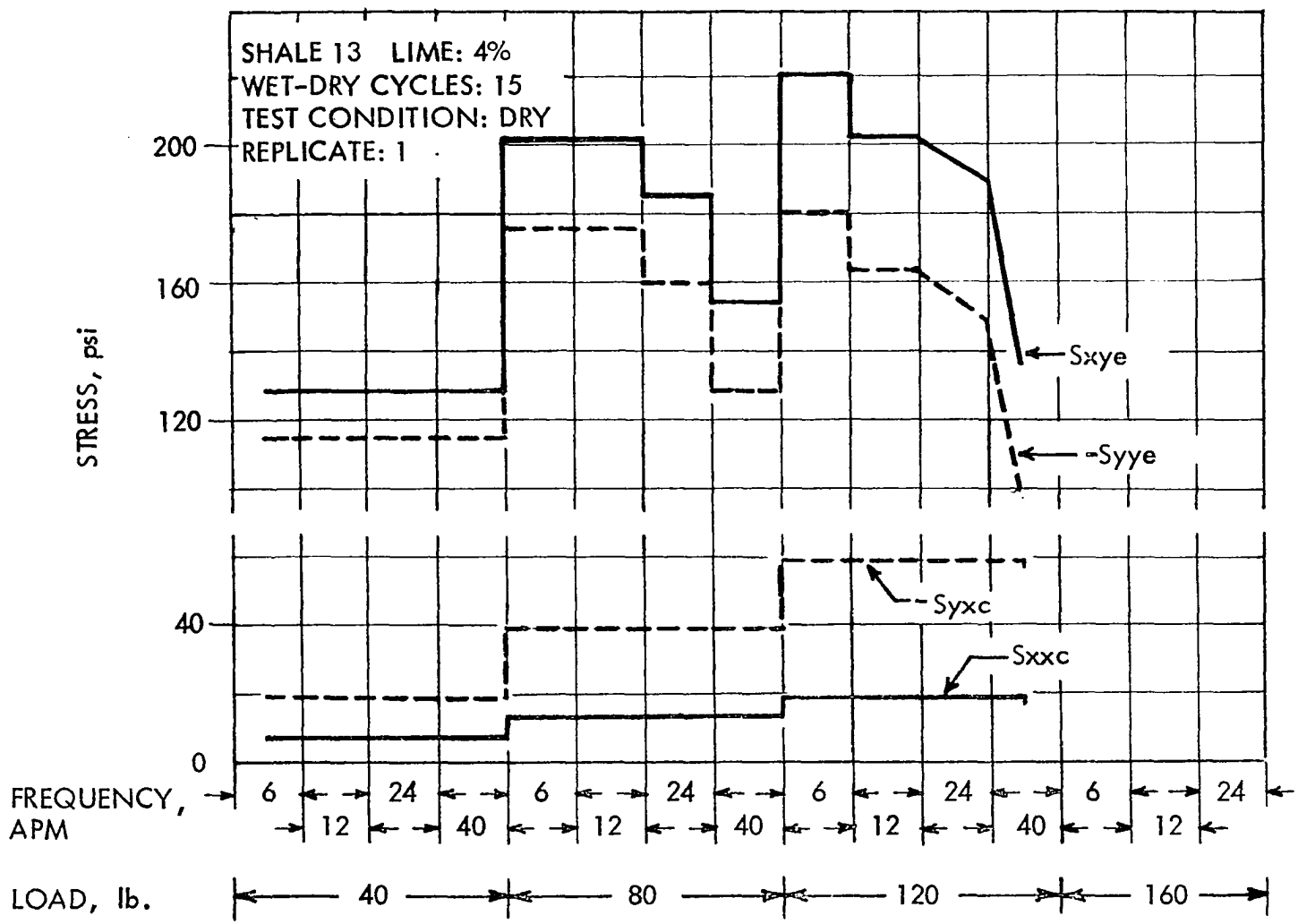


Figure 5.3. Example of stress, load and frequency relationships for repeated load split tensile strength test.

As shown in Figure 5.4, in general, three zones can be identified in these graphs:

1. Initial zone: This zone is limited to the first 50 cycles of the 40 lb load applied at the frequency of 6 applications per minute. It is during this time that the seating of the sample occurs and which in certain instances seems to have caused appreciable sample disturbance. Small flattening of the sample ends was, in general, sufficient to prevent any further sample disturbance. It was not found possible to take this disturbance into account since its exact nature could not be established.
2. Intermediate zone: It is the zone after the initial zone and before the sample failure occurs.
3. Failure zone: The zone in which cracking and failure of sample occurs.

A number of samples showed less than the minimum measurable strength in that they broke at the application of the first impact. No identifiable zones could be established for such samples. For certain other samples the failure zone and the initial zone were the same as the samples failed before 50 cycles of 40 lb load at 6 applications per minute were applied (Figure 5.5, Curve A). For such samples it was difficult to assign any value for diametral strain at failure. In few cases, the failure of samples occurred just outside

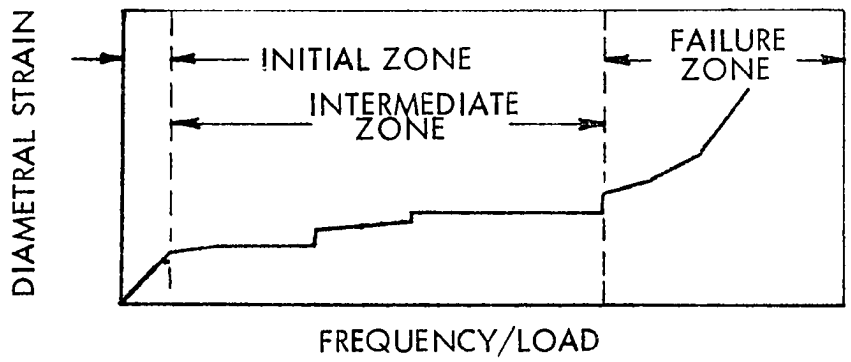


Figure 5.4 Three zones of a typical strain-frequency-load graph.

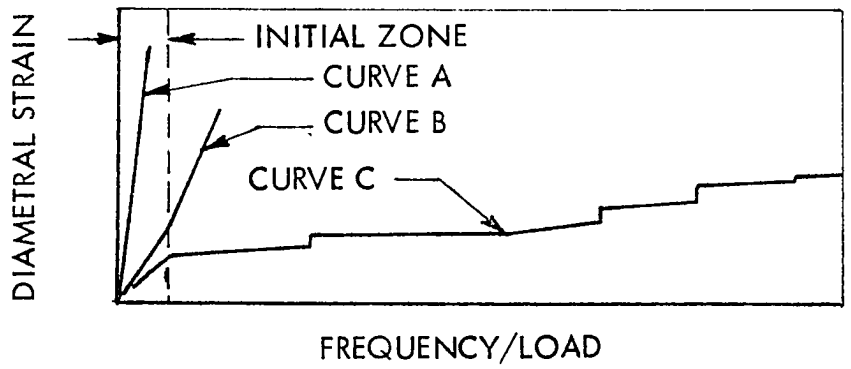


Figure 5.5 Examples of three common types of strain-frequency-load graphs.

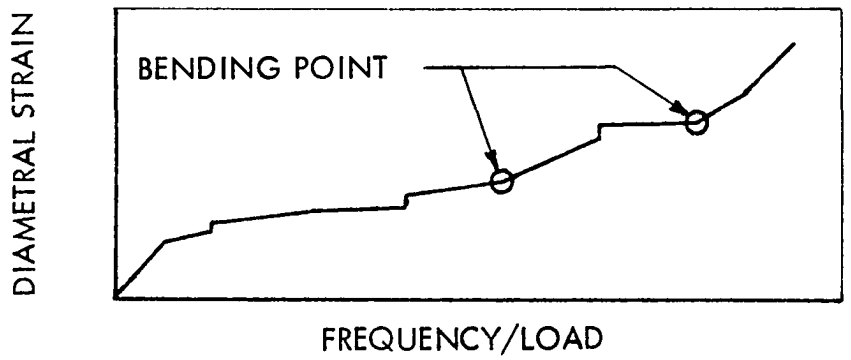


Figure 5.6 Example of bending points on strain-frequency-load graph.

the initial zone (Figure 5.5, Curve B) and thus for the sample of this category there was no intermediate zone. Some samples, especially those in the dry condition, did not fail at all within the range of the testing (Figure 5.5, Curve C). For the samples of this type there was no failure zone. For most of the samples, however, the three zones could be identified in spite of the fact that distinction between the intermediate and the failure zone was not always very obvious.

For the full range of test, as would be expected, the strain progressively increased as a trend with the increasing number of cycles. There, however, were ranges during which the strain did not appreciably change. This may be due partly to the difficulty in discriminating very small differences in deformation values on the graph and partly to the fact that indeed no appreciable deformation did occur in that range.

Within the intermediate zone, for a given load, initially the strain increased with a decreasing rate, this observation is similar to that of Moavenzadeh and Carnaghi (1966) on sand-asphalt beams. This trend continues unless interrupted by a trend of opposite nature in which the strain per cycle starts to increase with the increasing number of cycles (Figure 5.6). It appears that the beginning of this trend or the 'bending point' marks the initiation of crack formation and/or progressive failure with the specimen.

Kawakami and Ogawa (1964) considered the bending point to indicate the beginning of slipping in their rheological model. In their study and in this study a number of samples showed more than one bending point. Kawakami and Ogawa (1964) have attributed this behavior to step-strain phenomenon. If the trend of increasing strain per cycle does not reverse itself soon it is followed by the failure zone. The failure zone is approached only when the cracks become visually identifiable or when the failure strain exceeds a certain limit.

Initiation of cracking identifiable by visual examination was considered to be the start of failure. For the samples for which intermediate zone was clearly identifiable, the failure was taken at the last bending point before complete rupture of the sample was achieved. Furthermore, it was noticed that in the case of samples that failed, the diametral strain had increased by more than 0.0025 over a 50 cycle period.

This observation helped in identifying the failure zones when visual examination was difficult. Thus, a sudden increase in the value of diametral strain by 0.0025 over any 50 cycle period was considered as an additional criterion for failure. For the samples that did not fail within the range of this test, the end of the test value, that is, the diametral strain corresponding to the 160 lb load and 100 cycles applied at the frequency of 24 applications per minute, was taken as the final diametral strain.

Effect of Load

To determine the effect of load on the diametral strain, the data for all the samples that withstood all the four loads and all the frequency levels were collected and have been presented in Table 5.4. The strain values shown cover the frequency range from the beginning of the 12 applications per minute frequency to the end of the 24 applications per minute frequency. The six applications per minute range was discarded since it included the initial zone in the 40 lb load range in which strain value shown on the chart might not have been necessarily due to the compression of the specimen alone. Due to the limitations of the testing machine the tests had to be terminated at the end of 24 applications per minute frequency range for the 160 lb load and thus the 40 applications per minute range was not included for consideration.

There is wide variation in the strain values. The data is insufficient to determine meaningfully the effects of the amounts of lime and the wet-dry cycles. The data, however, are sufficient to give an overall view of the effect of load on the diametral strain. From the total data presented, the average values for diametral strains in the 12 - 24 applications per minute range are found to be: 0.00067 for 40 lb load, 0.00145 for 80 lb load, 0.00148 for 120 lb load, and 0.00192 for 160 lb load.

TABLE 5.4

EFFECT OF LOAD ON THE DIAMETRAL STRAIN OF SOME SHALE AND SHALE LIME SAMPLES

Shale Number	Amount of Lime, %	No. of Wet-Dry Cycles	Test Condition	Replicate	Load, lb			
					40	80	120	160
13	0	0	Dry	2	25[a]	0	13	25
		30	Dry	1	12	13	25	12
				2	0	13	13	38
		50	Dry	1	0	12	12	24
				2	0	11	12	24
		LT[b]	Dry	1	12	37	12	13
	1	0	Dry	1	12	13	0	0
				2	0	0	0	13
		15	Dry	2	12	37	37	0
		30	Dry	1	0	0	0	13
				2	0	0	12	13
		50	Dry	1	12	12	13	12
				2	0	25	13	--
	2	0	Dry	1	00	12	37	12
				2	12	12	12	12
		50	Dry	2	12	12	0	25
		LT	Dry	1	12	12	12	0
	4	0	Dry	1	0	12	0	12
		LT	Humid	1	12	24	12	23
				2	0	11	24	36
			Dry	1	12	12	12	12
	6	0	Dry	1	0	12	35	0
				2	24	24	25	12
		LT	Humid	1	0	12	23	12
				2	0	12	12	35
			Dry	1	0	12	12	12
15	2	LT	Humid	1	0	12	24	23
			Dry	1	12	24	24	48
	4	LT	Humid	1	12	11	12	35
			Dry	1	0	0	11	0
21	0	0	Dry	1	25	12	12	25
				2	0	13	28	38
		15	Dry	1	12	13	25	12
				2	0	25	37	12

[a] Diametral strain x 10^{-4}

[b] LT = Long term (120-day) cured sample.

TABLE 5.4--Continued

Shale Number	Amount of Lime, %	No. of Wet-Dry Cycles	Test Condition	Replicate	Load, lb			
					40	80	120	160
21	0	30	Dry	1	12	24	24	12
				2	12	12	0	36
		50	Dry	1	37	12	0	37
				2	13	38	13	13
	6	LT	Humid	1	0	12	0	0
24	0	0	Dry	1	0	0	12	36
				2	13	24	49	49
		15	Dry	1	0	36	12	0
				2	0	12	0	24
		30	Dry	1	0	0	0	33
				2	0	12	12	25
		50	Dry	1	0	12	12	25
				2	0	24	12	12

Thus, it appears that the greater the load, the greater is the change in diametral strain (Figure 5.7). The difference between the 80 lb and the 120 lb values is very little and appears to be due to the fact that most of the 'bending points' are located in the 80 lb load range.

Effect of Frequency of Load Application

To determine the effect of frequency of load application on the diametral strain, the samples used were the same as those used for determining the effect of load on the diametral strain. The ranges of 80 lb and 120 lb loads were the only ranges that contained all the four frequency levels and did not contain the 'initial zone.' From these two ranges the 80 lb range was chosen arbitrarily to determine the required effects. In this load range diametral strain values were calculated for 100 load applications of each frequency. These values are depicted in Table 5.5 These data, as mentioned earlier, are insufficient to determine the effects of the amount of lime and the wet-dry cycles, but are adequate to provide an overall view of the effect of frequency of load application on the change in diametral strain. The average values of diametral strain were found to be: 0.00127 for 6 APM frequency, 0.00081 for 12 APM frequency, 0.00114 for 24 APM frequency, and 0.00057 for 40 APM frequency.

Thus, the effect of increasing frequency at the same load does appear to be significant. The lower frequency

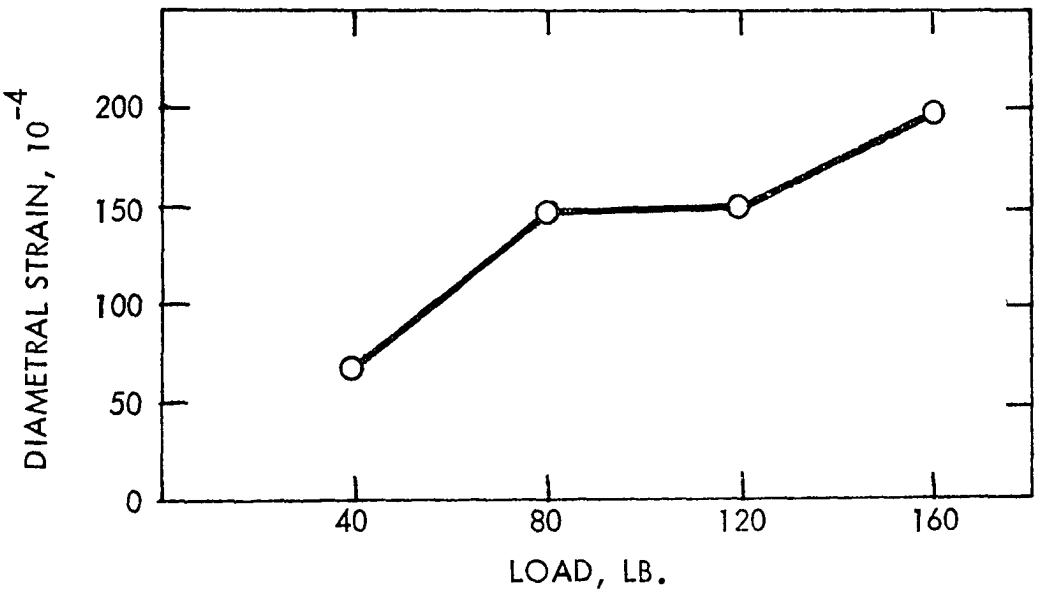


Figure 5.7. General diametral strain-load relationship.

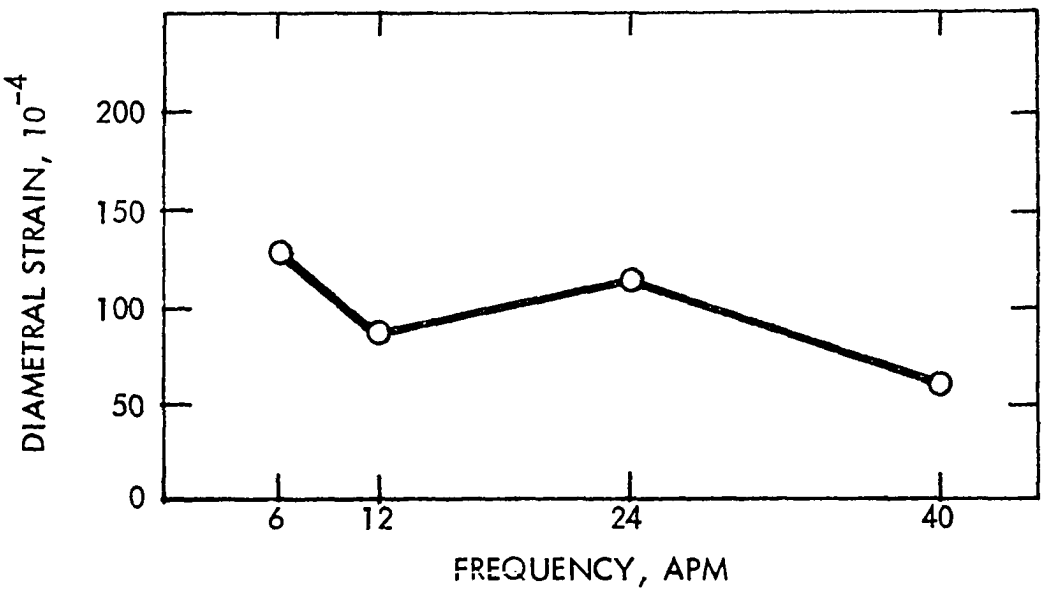


Figure 5.8. General diametral strain-frequency relationship.

TABLE 5.5

EFFECT OF FREQUENCY OF LOAD APPLICATION ON THE DIAMETRAL STRAIN OF SOME SHALE AND SHALE LIME SAMPLES

Shale Number	Amount of Lime, %	No. of Wet-Dry Cycles	Test Condition	Replicate	Frequency, APM[a]			
					6	12	24	40
13	0	0	Dry	2	12[b]	0	0	0
		30	Dry	1	13	12	13	13
				2	12	0	13	12
		50	Dry	1	0	12	12	0
				2	24	0	11	0
		LT[c]	Dry	1	38	0	37	13
	1	0	Dry	1	0	13	0	12
				2	12	0	0	0
		15	Dry	2	12	13	24	0
		30	Dry	1	12	13	0	12
				2	12	0	0	13
		50	Dry	1	0	0	12	12
				2	12	13	12	12
	2	0	Dry	1	37	0	12	0
				2	37	25	0	0
		50	Dry	2	12	12	0	13
		LT	Dry	1	13	0	12	12
	4	0	Dry	1	24	0	12	0
		LT	Humid	1	11	0	24	0
				2	12	0	11	0
			Dry	1	0	12	12	13
	6	0	Dry	1	12	12	12	0
				2	13	12	24	0
		LT	Humid	1	12	0	12	0
				2	12	23	12	0
			Dry	1	24	0	12	0
15	2	LT	Humid	1	23	12	12	0
			Dry	1	0	12	24	11
	4	LT	Humid	1	12	0	11	0
			Dry	1	12	12	0	0

[a] APM = applications per minute.

[b] Diametral strain x 10^{-4}.

[c] LT = Long term (120-day) cured sample.

TABLE 5.5--Continued

Shale Number	Amount of Lime, %	No. of Wet-Dry Cycles	Test Condition	Replicate	Frequency, APM[a] 6	12	24	40
21	0	0	Dry	1	12	13	12	0
				2	38	12	13	0
		15	Dry	1	12	0	13	0
				2	0	24	13	12
		30	Dry	1	13	12	12	12
				2	13	0	12	12
		50	Dry	1	0	13	12	25
				2	12	0	38	0
	6	LT	Humid	1	0	12	0	35
24	0	0	Dry	1	13	0	0	0
				2	12	12	12	0
		15	Dry	1	0	12	24	12
				2	12	13	12	12
		30	Dry	1	12	12	0	0
				2	0	12	12	0
		50	Dry	1	12	12	0	0
				2	12	12	13	0

caused greater diametral strain change and as the frequency of load application increased the change in strain became less (Figure 5.8), unless the sample failure was initiated. In the latter case, the change in the diametral strain increased with increasing frequency of load application. The values for 12 and 24 applications per minute frequencies were in the range where bending points occurred and this may explain their deviation from the expected values.

The data points for the 'humid' state samples are so few that it was not possible to identify the effect the moisture content had on the deformation characteristics of the samples. Kriezek and Kondner (1964) have stated that the stress-strain data for soils was significantly affected by even small variations in moisture content.

The main factors affecting the split tensile strengths of sample are the amount of lime and the effect of wet-dry cycles. Since the diametral strain was to be the criterion to determine the effects of various factors, its values have been provided in Appendix D. The data are arranged in order of shale number, the condition of specimen at the time of split tensile strength test, number of the wet-dry cycles, amount of lime and the replicate number. There were two samples that were prepared and treated in exactly the same manner. In the tables included in Appendix D, a number of data points have not been shown. This is due either to the accidental breaking of the sample or to the failure of sample

in the manners described by either of the curves 'A' or 'B' of Figure 5.5. For the samples that failed in these manners it was difficult to assign any definite value to the failure diametral strain. Even though diametral strain was used as the principal criterion, the other criteria, especially the load and the frequency of load application were not abandoned. On the contrary, these values were extensively used to evaluate the effects of various factors.

Figures showing relationships between the diametral strain and the amount of lime, the number of wet-dry cycles being kept constant are given in Appendix E. The figures showing relationships between the diametral strain and the wet-dry cycles, keeping the amount of lime constant have been included in Appendix F.

Shale 13

The AASHTO classification for this shale is A-7(6) and it contains 48 percent clay size particles among which the predominant clay mineral is montmorillonite (Table 5.6). In the case of 'humid' samples that were not subjected to any prolonged curing or any wet-dry cycles, even small amounts of lime were sufficient to reduce the plasticity characteristics of the shale and introduce brittleness in the sample material. The diametral strain reduced from a high value of 0.0148 for untreated shale to an average value of 0.0048 for the mix containing 1 percent lime. Further additions of lime

TABLE 5.6

CLAY MINERAL COMPOSITION OF SHALES

Shale Number	2-micron Clay, %	Percent Clay Mineral[a]					Other Silicate Minerals
		C	I	K	M	ML	
13	48	--	--	11	89	--	Q
15	14	22	38	40	--	--	Q,F
21	25	6	15	--	22	57	Q,F
24	14	--	68	28	4	--	Q,F

[a]C = Chlorite; F = Feldspar; I = Illite; K = Kaolinite; M = Montmorillonite; ML = Mixed Layer Montmorillonite-Illite; Q = Quartz.

did not materially change either the strain magnitude or the capacity of the shale lime mix to take up greater stresses. For all wet-dry cycles, this effect of lime remained essentially the same. The effect of wet-dry cycles was significant for the untreated shale but not for the treated shale mixes. Even 15 wet-dry cycles were significant in reducing the high average value of 0.0148 for the diametral strain for zero wet-dry cycles to an average value of 0.0074. Not much difference was noticed in the deformation characteristics of the samples after 15 wet-dry cycles.

With the increasing amount of lime and with the increasing number of wet-dry cycles the samples seemed to become more brittle in that they failed at about the same load but under decreasing diametral strains. The sample behavior became significantly brittle even at 1 percent lime

addition. At early stages of curing this effect appears to be due to the utilization of lime for the rapid ameliorative effects without formation of any substantial amount of gel (Diamond and Kinter, 1966; Eades and Grim, 1966).

For the samples cured for 120-days the effect of lime was very much as expected (Figure E.2, Appendix E). Addition of 2 percent lime decreased the diametral strain from an average value of 0.0131 to 0.0071. In addition the samples containing higher percentages of lime were able to carry greater magnitudes of load and greater number of load applications. For the 4 percent and the 6 percent lime mixes, the presence of gel and unreacted lime seems to have contributed some elasticity in the samples. The samples containing 2 percent lime failed at an average diametral strain of 0.0065 under 80 lb load and 6 APM frequency but the sample containing 6 percent lime failed at an average diametral strain of 0.0083 under 160 lb load and 12 APM frequency.

The behavior of 'dry' samples is not much different from the samples of the 'humid' state from the point of view of diametral strain. However, the effects of lime treatment and application of wet-dry cycles are less pronounced. After one drying the diametral strain had an average value of 0.0112 for the untreated shale and a value of 0.0079 for the shale containing 1 percent lime. In the case of humid samples the difference in the diametral strains was 0.0100 while it was only 0.0033 for the dry samples. Application of wet-dry

cycles was effective in reducing the average diametral strain value of 0.112 after one drying to a value of 0.0074 after 5 wet-dry cycles. Beyond 5 cycles, however, no significant differences in the diametral strain values were observed for the untreated and the treated shales.

Compared to the samples in the 'humid' state, the samples of 'dry' state took greater loads and greater number of load applications; also, the crack pattern was slower to develop in these samples. The behavior of the untreated shale under stress was very much elastic and its samples were able to withstand the total range of load and load applications. Addition of lime to shale introduced brittleness and the samples failed under much smaller loads, fewer applications of loads and at smaller diametral strain. For zero number of wet-dry cycles the untreated shale showed an average diametral strain of 0.0112 at the end of test (160 lb load, 24 APM frequency, 100 load applications) while the shale samples containing 6 percent lime showed an average diametral strain of 0.0067 at the load of 80 lb to 120 lb and 12 APM frequency.

During the early stages of weathering (0 and 15 wet-dry cycles) the diametral strain values showed an increase toward the 6 percent lime treatment level (Figure E.3, Appendix E) probably due to the presence of excess unreacted lime in the mix.

For the samples subjected to 120-day curing, the addition of lime and prolonged curing significantly improved

their strength characteristics. All shale-lime mix samples were able to withstand the total range of loads and load applications. The sample seemed to become more elastic with the increase in the amount of lime in that they showed lower diametral strain for the same load parameters (160 lb and 24 APM frequency) the values of diametral strain were 0.0097, 0.0095 and 0.0085 for 2, 4 and 6 percent lime treatments, respectively.

Shale 15

In its natural state this shale is associated with high bearing capacity and high permeability. These characteristics are lost on its being ground up and worked upon; its granular structure is broken down and shale converted into a material exhibiting low strength and plasticity characteristics. A similar finding is reported by Townsend, et al. (1969) for lateritic soils. Addition of lime, in great percentages, could improve the stress-strain characteristics of this shale.

All shale and shale lime samples in 'humid' state exhibited, for zero number of wet-dry cycles, strengths below the minimum measurable and their diametral strain - load - load application frequency graphs resemble curve 'A' of Figure 5.5. For the other wet-dry cycles only the samples of the untreated shale and those containing 6 percent lime showed any measurable strength. There is not much difference

in these samples from the strength standpoint, all samples failing within the 40 lb load zone.

The effect of the addition of lime on 120-day curing was interesting (Table D.3, Appendix D, and Figure E.6, Appendix E). Samples containing 2 percent lime failed in the 160 lb load zone at a diametral strain of 0.0083, but those containing 6 percent lime failed in the 80 lb load zone at a strain of 0.0047 only. The reason for this particular behavior is not immediately apparent. It appears that during prolonged curing increase in the amount of lime provides more contact between the clay and the lime particles and the formation of shale-lime reaction products provides increasing elasticity characteristics to the mix. Shale 15 contains only 14 percent 2-micron size particles, and in addition the clay is predominantly kaolinitic and illitic (Table 5.6) so the surface area available for lime to react is very limited, and when lime is added in excess of 4 percent, some of it remains unreacted, thus contributing to the brittle behavior of the shale-lime mix samples.

The effect of wet-dry cycles could be observed only for the untreated shale and the mix containing 6 percent lime. The untreated shale samples did not indicate any significant difference occurring due to the application of wet-dry cycles. At 6 percent treatment level, the effect of wet-dry cycles was primarily in stabilizing the shale.

Samples gradually became more elastic with the increasing number of wet-dry cycles in that they exhibited smaller diametral strains (Figures F.5 and F.6, Appendix F).

The effect of the amount of lime on the diametral strain for the 'dry' samples is shown by Figures E.7 and E.8 (Appendix E). Even though no significant changes were observed, the treated samples, as a trend, did show increased elasticity with increasing percentage of lime (Table D.4, Appendix D). For 30 wet-dry cycles treated samples failed in the 80 lb load zone, but the average diametral strains were 0.0077, 0.0077, 0.0066 and 0.0048 for 1, 2, 4 and 6 percent lime treatment levels, respectively. Thus, the lime treatment became significant only at 6 percent level, and then also it did not produce a material significantly different from the untreated shale. The wet-dry cycles also did not show any significant effect on the diametral strains or the strength characteristics of the samples.

Shale 21

Shale 21 has an AASHTO classification of A-6 and contains 25 percent less than 2-micron size particles in which the clay particles are predominantly of montmorillonite-illite mixed layer and montmorillonite minerals. The samples that had not been subjected to any wet-dry cycles and contained 0 or 1 percent lime did not show any measurable strength; those containing more lime did. Samples from the

latter mix withstood the same load, 40 lb, and the same load application frequency, up to 40 APM. For the amounts of lime 2 percent or greater, the samples containing greater percentage of lime showed greater diametral strain. Since there had hardly been enough time for shale-lime reaction products to form, the strength gain could only be due to flocculation of the clay. The application of wet-dry cycles and subsequent humidification of samples seemed to have destroyed whatever bond formation took place, and the samples, even after 50 applications of wet-dry cycles, did not show any measurable strength.

The effect of lime on 120-day curing of samples is very much as expected (Table D.5, Appendix D, and Figure E.10, Appendix E); with increasing percentage of lime, the samples showed increasingly elastic behavior.

The strength development in Shale 21 that was destroyed by the humidification of the samples became apparent on removal of water from the shale-lime mix. The untreated shale samples in the 'dry' state exhibited plastic behavior in that they underwent substantial deformation (diametral strain of 0.0151 to 0.0178 for the 160 lb and the 120 lb load, respectively) but under high loads. Increasing amounts of lime made the shale increasingly brittle, and the samples took less loads and failed at smaller average diametral strains.

The effect of wet-dry cycles was most significant on the untreated shale. Increasing number of wet-dry cycles made the material more brittle. As the amount of lime added to the shale was increased, the effect of wet-dry cycles on the samples became less significant. For the 2 percent and the 4 percent lime additions, no significant differences were observed. At 6 percent lime treatment level, the samples exhibited increasingly elastic behavior with the increasing number of wet-dry cycles in that they showed gradually lower diametral strains for the same load.

The 120-day curing did not produce any significant differences. Addition of 2 and 4 percent lime seemed to make the material more plastic, and addition of 6 percent lime tended to make it elastic. In the dry state the untreated material, however, remained more elastic than any treated material.

Shale 24

Shale 24 has an AASHTO classification of A-4 and contains 14 percent 2-micron size particles in which the clay portion basically contains illite and kaolinite.

Examination of Table D.7 (Appendix D), Figures E.13 and E.14 (Appendix E), and Figures F.13 and F.14 (Appendix F) indicated that the addition of lime did not improve the stress-strain characteristics of the samples. The results obtained were very much similar to those obtained for the

humid samples of Shale 15. The flocculation of lime seemed to have provided some plasticity to the shale in the initial stages, but the effect was completely lost when 30 wet-dry cycles had been applied and the samples had undergone humidification; only the untreated shale samples showed any measurable strength for 30 and 50 wet-dry cycles.

After 120-day curing, the untreated shale samples did not show any measurable strength, but all the lime treated shale samples showed equal development of strength; they all took 80 lb load at diametral strains varying from 0.0059 to 0.0071.

The effect of lime in the initial stages was primarily to make the 'dry' samples more plastic (Table D.8 in Appendix D and Figures E.15 and E.16 in Appendix E) in that they show greater strain per unit load. With increasing number of wet-dry cycles, most samples were able to withstand slightly greater loads or greater number of load applications in the same load zone. Samples containing 1 percent lime, after 15 wet-dry cycles, showed average diametral strain of 0.0096 at 80 lb load and 24 APM frequency, while after 50 wet-dry cycles they showed average diametral strain of 0.0072 at 120 lb and 6 to 24 APM frequency. The differences for other samples were not so obvious. The diametral strain values for the untreated shale and the shale containing 1 percent lime increased when the number of wet-dry cycles increased to 5 from 0. Beyond this small region, however, there was no definite

effect of the amount of lime or the wet-dry cycles on the diametral strain. The 120-day curing caused lime-treated samples to have a little less strength than what the untreated shale samples had, but the treated shale samples showed smaller diametral strains. The samples of untreated shale showed a diametral strain of 0.0085 at 120 lb load, while the sample of shale containing 6 percent lime showed a diametral strain of 0.0060 at 80 lb load.

Atterberg Limit Tests

After the completion of split tensile strength tests, the samples were ground and used to determine the liquid limit and plasticity index values. These values were determined only for the samples that had been subjected to 0, 15 and 50 wet-dry cycles. The 120-day curing samples were included to provide the reference values. In all cases, both the 'humid' and the 'dry' test conditions were included. Values for liquid limits are shown in Table G.1 (Appendix G), and their relationships to the amount of lime and wet-dry cycles are shown in Figures G.1 through G.4 (Appendix G). The plasticity index values are shown in Table H.1 (Appendix H), and their relationships to the amount of lime and to the wet-dry cycles are shown in Figures H.1 through H.4 (Appendix H).

An examination of these tables and figures reveals that there is not much difference between the values for the 'humid' and the 'dry' samples. However, there are several instances where the 'humid' samples do show plasticity index

value but the 'dry' samples do not. The reverse is not true. Also, for a particular wet-dry cycle, this occurs for the samples containing lime above a certain percentage. This percentage is different for different shales. This difference in the behavior due to the condition of the samples at the time of the test could be due to the fact that after being subjected to their respective wet-dry cycles, the 'humid' samples were kept in the humidifier and the 'dry' samples were kept in desiccator until the time of testing. Thus, apparently, the lime in the dry samples had less time to react with the shale, and the presence of unreacted lime in the sample could have made it difficult to determine the plastic limit, and thus the plasticity index value of the shale-lime mix.

The effect of wet-dry cycles was found to be insignificant for all percentages of lime for the Shales 13, 21 and 24. For the three wet-dry cycles and the 120-day curing samples, for these three shales the liquid limit values decreased with the addition of lime until the amount of lime was 4 percent. There is no significant difference in the liquid limit values for the 4 percent and the 6 percent lime contents; for Shale 13, the values were between 48 and 53 for the untreated samples, between 35 and 40 at 4 percent lime content, and between 35 and 39 at 6 percent lime content. In the case of Shale 21, the values for untreated shale varied from 41 to 47, and for 4 percent lime content they varied from

31 to 35, while for 6 percent lime content they varied from 29 to 34. For Shale 24, the liquid limit values were between 37 and 42 for the untreated mix, between 30 and 37 for the shale with 4 percent lime content, and between 30 and 36 for the shale containing 6 percent lime.

In contrast to the behavior shown by the other three shales, the liquid limit values for Shale 15 were not significantly influenced by the addition of lime; some increase of liquid limit was noted. Again, there was no significant influence traceable to the wet-dry cycles. Liquid limit values varied from 24 to 26 for the untreated shale and from 24 to 33 for the shale containing 6 percent lime.

After 120-day curing, except for the 'humid' state sample of Shale 13, the 6 percent lime treatment was found to be effective in making the shale non-plastic. It was not possible to determine the liquid limit values for the shales containing 6 percent lime (Figure G.5, Appendix G).

For Shales 13, 21 and 24, the effect of lime on plasticity index values was very much pronounced. The values decreased rapidly with the addition of lime until the lime content reached 2 percent level. After that, the values did not change significantly; however, it was difficult to determine plasticity index values for a great number of samples. For the plasticity index values also there was little difference between the 'humid' and the 'dry' samples, and the effect of wet-dry cycles on these values also was insignificant.

For Shale 13, the plasticity index values were between 28 and 32 for the untreated mix and between 13 and 18 at 2 percent lime treatment level. Shale 21 showed values between 15 and 20 for the untreated material and between 11 and 14 for the shale containing 1 percent lime. In the case of Shale 24, the plasticity index values were between 12 and 19 for the untreated mix and between 8 and 12 for the shale containing 2 percent lime.

Shale 15 showed very little differences even with the increase in the amount of lime, and the plasticity index values varied from 6 to 9 for the untreated mix and from 5 to 8 for 1 percent lime treatment level. After 1 percent level it was very difficult to determine experimentally the plastic limit, and thus the plasticity index values for the majority of samples.

After 120-day curing, the 2 percent lime treatment level was found to have made Shales 13, 21 and 24 non-plastic, and only addition of 1 percent lime treatment level made it extremely difficult to determine the plastic limit values for Shale 15.

X-Ray Diffraction Analysis

The purpose of obtaining the X-ray diffraction patterns was primarily to determine the extent to which the reaction between shale and lime proceeded under the alternating wet-dry conditions and what easily identifiable reaction

products were formed. The clay mineral composition of the shales is shown in Table 5.6.

The d-spacings of various clays, clay associated minerals, lime and lime clay reaction products are given in Table 5.7. The values shown in this table have been taken from various reference indicated therein.

All shale samples contained quartz in quantities sufficient to show its strong characteristic peaks. Most shale samples also contained feldspars for which peaks occur at numerous locations for d-spacings between 3.34 Å and 1.99 Å (ASTM, 1966). Peaks indicated for lime are the same as those for $Ca(OH)_2$, Portlandite. The peaks for Calcite shown in the table identify calcium carbonate ($CaCO_3$) which is produced due to the carbonation of lime in the treated samples.

Lime-kaolinite peaks were reported by Eades and Grim (1962) for a mix cured at 60°C. Experiments conducted by Ho and Handy (1964) on lime stabilized montmorillonite slurry samples showed no peaks for the reaction products, but the intensity of clay mineral peaks diminished with the increasing lime content. On the other hand, Hilt and Davidson (1961) reported new diffraction lines for lime-montmorillonite at 8.11 Å and 7.59 Å.

Among the lime clay reaction products, the tricalcium silicate hydrates, C_3SH or the tobermorites, are the most important. Tobermorites are formed as immediate products in

Filmed as received

without page(s) 104 .

UNIVERSITY MICROFILMS.

almost all reactions in which calcium ions and silicate ions come together. Tobermorites have layered structures, and their crystalline and semicrystalline varieties give characteristic reflections anywhere from 9.0 Å to 14.0 Å (Taylor, 1966). Other reflections reported for tobermorites are given in Table 5.7. The other important lime clay reaction products are (1) CAH, calcium aluminate hydrate; (2) C_3AH, tricalcium aluminate hydrate; (3) C_4AH_n, tetracalcium aluminate hydrate; (4) C_2S, dicalcium silicate; and (5) C_3S, tricalcium silicate.

The 3.34 Å reflections for montmorillonite and illite occur at the location of the strongest basal reflection for quartz and thus had no importance for this investigation.

Since there was considerable overlap in the reflections, the only way to determine the effects of amount of lime and of wet-dry cycles was to compare the diffraction patterns of the treated samples with those of the raw shale and that also with the inherent variability of shale material in mind. From this standpoint, it was decided to obtain diffraction patterns only for the samples of untreated shales and those containing 2 and 6 percent lime among these only those samples which had been subjected to 120-day curing and 0, 15 and 50 wet-dry cycles.

The diffraction patterns for all four shales did not indicate any significant changes with the wet-dry cycles for the untreated material. Patterns for the shale combinations

containing 2 percent lime showed presence of little or no unreacted lime. Calcite peaks could be observed for all wet-dry cycles in most cases. Peaks for both the unreacted lime and the calcite in general became more pronounced for the mixes containing 6 percent lime. The 'dry' samples, in general indicated presence of more unreacted lime than did the 'humid' samples; they also showed stronger calcite peaks and thus indicated presence of greater amount of calcium carbonate.

For the Shale 13 (Figure 5.9), there was some indication of reaction having taken place between lime and kaolinite, but there was no indication for the lime and montmorillonite reaction. Presence of CAH and C_3S was noted at 0 wet-dry cycle stage, and then with time C_2S and C_4AH_n also were formed. At 6 percent level of lime treatment, some reaction of lime with kaolinite as well as montmorillonite is noticeable. The products formed are much the same as formed with the 2 percent lime. The samples subjected to 120-day curing show no lime peaks at both the 2 percent and the 6 percent lime treatment level; also the lime-kaolinite reaction peaks are absent. Reaction between lime and montmorillonite is still indicated and the reaction products include CAH, C_4AH_n and C_2S.

For Shale 15 (Figure 5.10) the calcite peaks became prominent for 6 percent lime content subjected to 50 wet-dry cycles. Reaction, in this case, also seems to start earlier

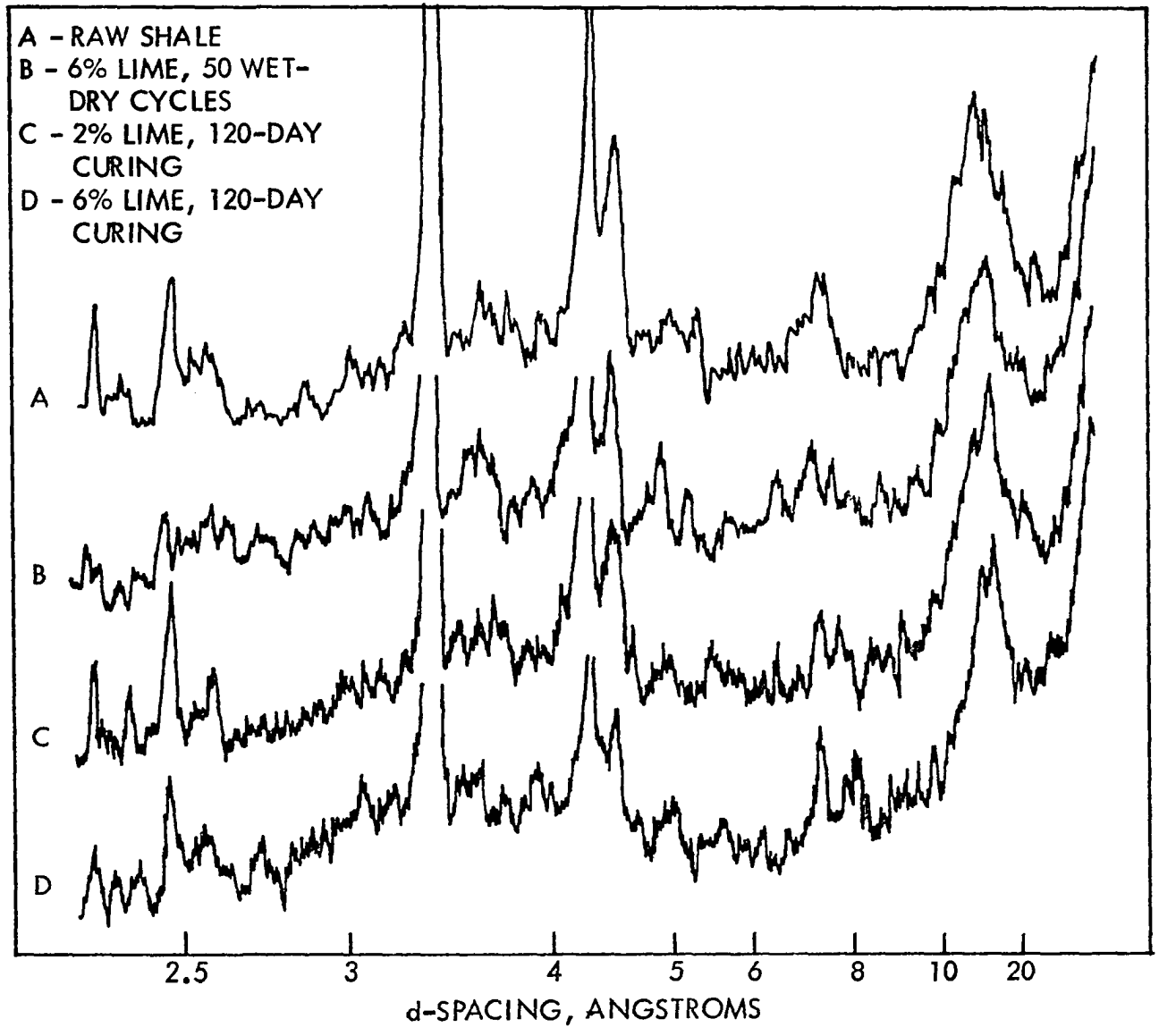


Figure 5.9 Selected x-ray diffraction patterns for shale 13 and its lime combinations.

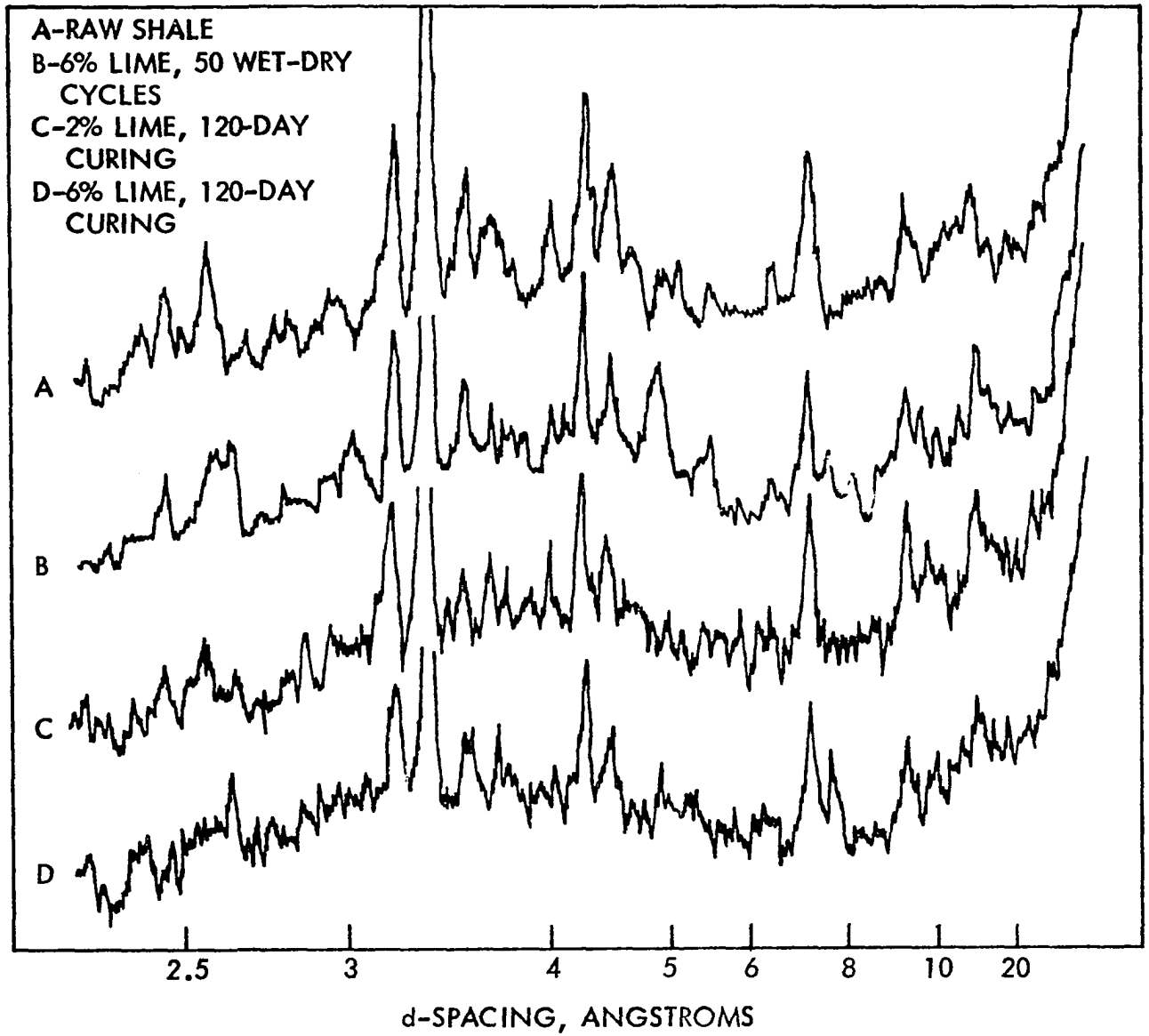


Figure 5.10 Selected x-ray diffraction patterns for shale 15 and its lime combinations.

between lime and kaolinite. There is indication of some lime-montmorillonite type of reaction having taken place, but since the raw shale contained no montmorillonite, this reaction could have been due to association between lime and illite. This assumed lime-illite reaction became noticeable for the samples containing 2 percent lime and subjected to 15 or more wet-dry cycles. For the samples containing 6 percent lime, this reaction is observed for all the wet-dry cycles. The reflections observed indicate presence of CAH, C_4AH_n, C_2S and C_3S, in that order, with increasing lime content and with increasing wet-dry cycles. At 6 percent lime treatment level and for 15 and 50 wet-dry cycles, the quartz peaks were greatly effected. The samples subjected to 120-day curing show very little calcite and presence of very little unreacted lime. The reflections showing reaction between lime and kaolinite are either absent or very weak. The products formed are the same as those described earlier, and they are formed in all samples containing lime.

For Shale 21 (Figure 5.11), little or no unreacted lime was observed in all the treated samples. Some calcite reflections were observed for 2 percent lime combinations at 50 wet-dry cycle treatment, but for the 6 percent lime combination the calcite peaks were prominent for all the wet-dry cycles. CAH, C_4AH_n and C_3S seem to be the initial reaction products, and the reaction between lime and montmorillonite-illite-mixed layer mineral seems to be rapid and significant.

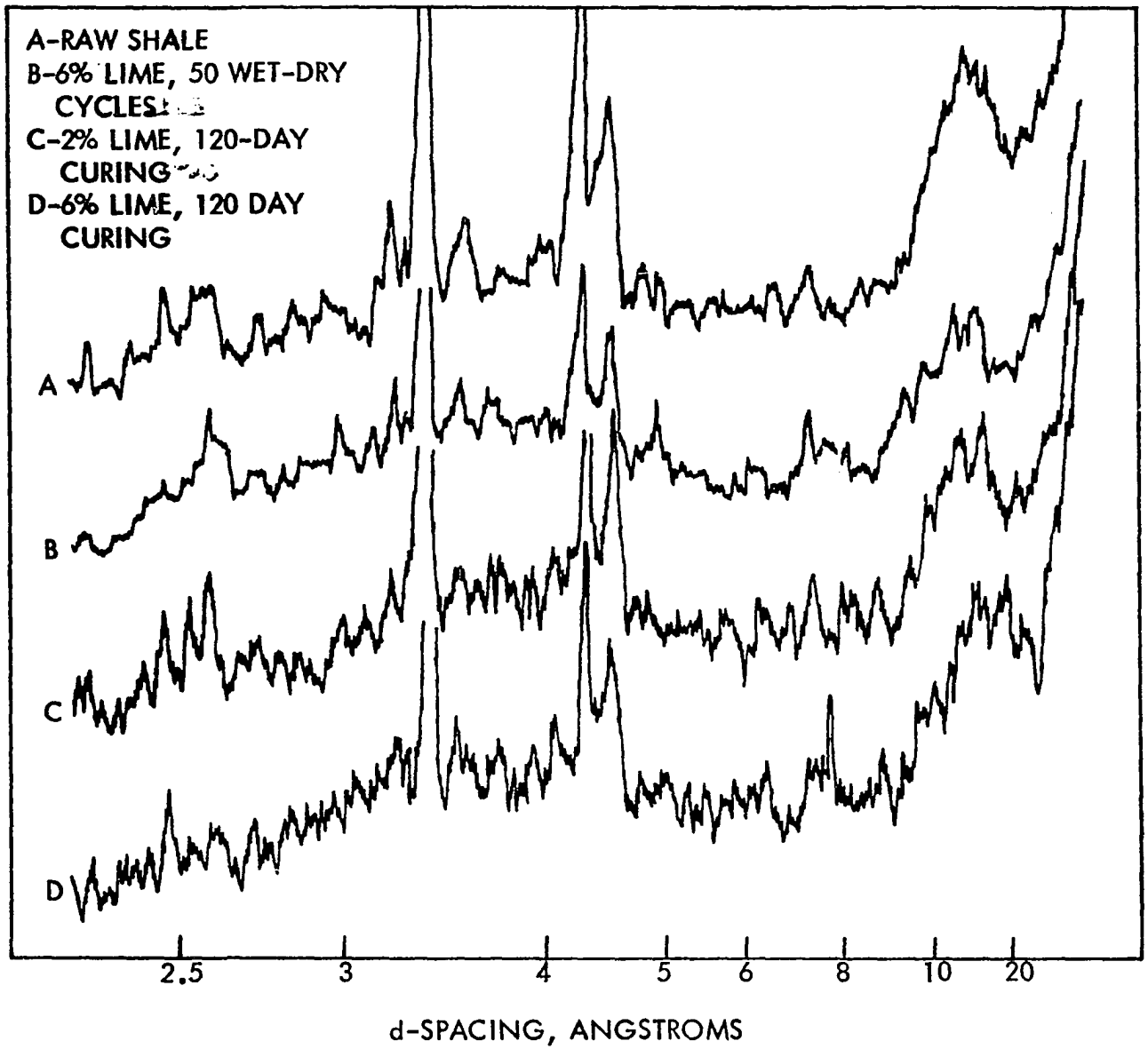


Figure 5.11 Selected x-ray diffraction patterns for shale 21 and its lime combinations.

The 120-day cured samples also did not show presence of any unreacted lime but all showed calcite peaks. These peaks, however, were not as strong as those for the samples containing 6 percent lime and subjected to 15 or 50 wet-dry cycles. There was no significant difference in other reactions.

In the case of Shale 24 (Figure 5.12), at 6 percent lime treatment level the lime peaks were observed for the samples in both the humid and the dry test conditions and not subjected to any wetting or drying, but for the 15 and the 50 wet-dry cycles lime peaks were observed only for the 'dry' samples, not the 'humid' ones. There were no calcite peaks for the samples of zero wet-dry cycles, but for the other wet-dry cycles calcite peaks were easily identifiable. The calcite peaks for the 6 percent lime treatment were more pronounced than for the 2 percent lime treatment. The lime-illite reaction appears earlier on diffraction patterns than do lime-kaolinite reactions. The first reaction products to appear are C_3S and CAH, followed by C_4AH_n and C_2S. The latter products appear either when the number of wet-dry cycles has reached 50 for the mix containing 2 percent lime or when the number of wet-dry cycles has reached 15 for the samples containing 6 percent lime. In the samples cured for 120-days, some calcite appeared on all the diffraction patterns. The 2 percent lime mixes did not show any presence of unreacted lime, but the samples containing 6 percent lime

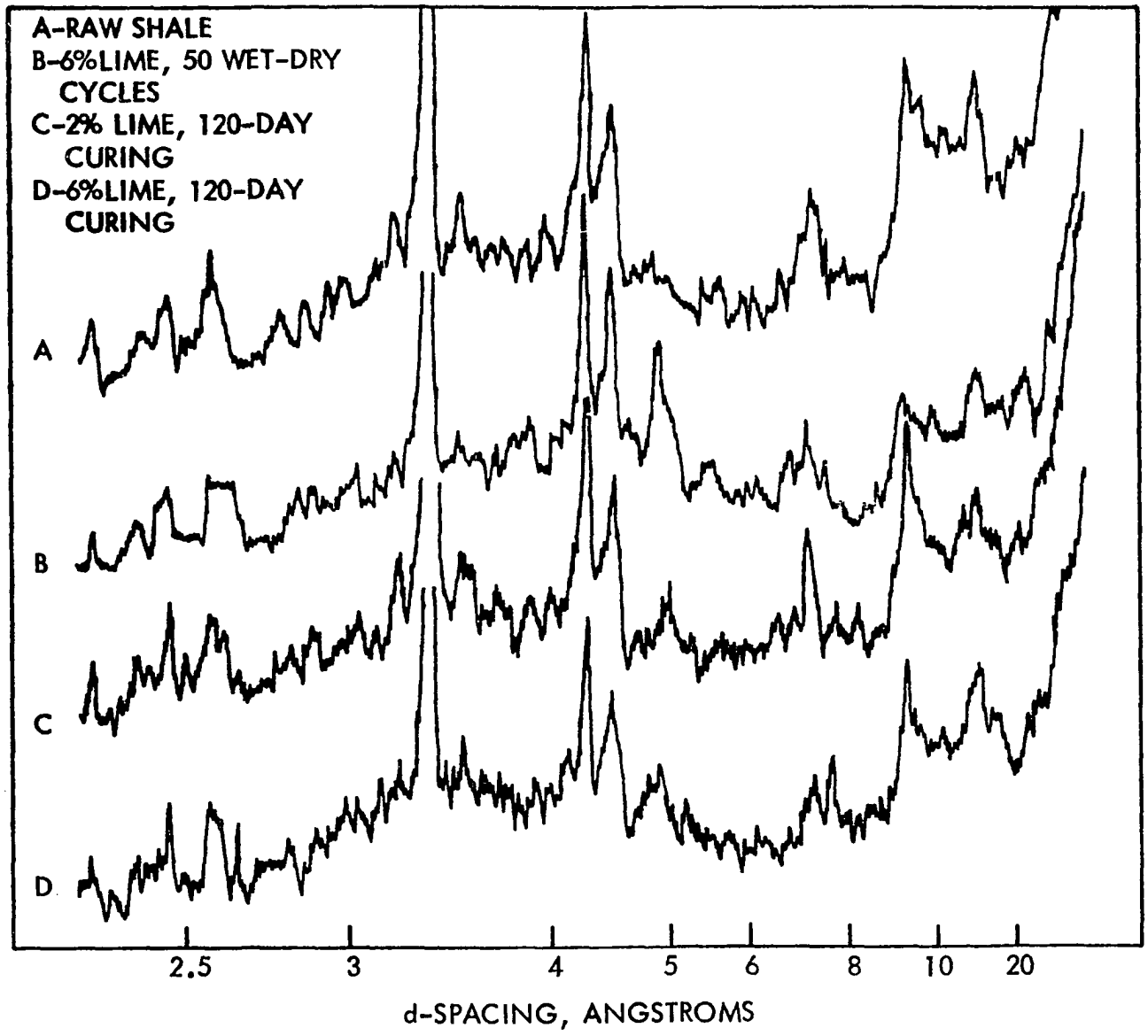


Figure 5.12 Selected x-ray diffraction patterns for shale 24 and its lime combinations.

did. The lime clay reactions and reaction products were similar to those described earlier for the samples subjected to the wet-dry cycles.

General Discussion

The effect of lime on shale must be considered from the point of view of the composition of shale and the type and amount of clay minerals. Addition of lime to a shale would not only cause flocculation of clay particles but would also introduce lime particles in the sand-silt-clay matrix of shale. The strength of this matrix would depend on the 'cardhouse' structure of clays and friction between various particle edges and surfaces. In the presence of moisture, the shale lime reactions would proceed with time, and various reaction products would be formed. The strength of the matrix would now be affected by these reaction products also. The amount of moisture available for shale lime reactions varies continuously in the wet-dry cycling process, and thus the progress of reaction would be much less under this type of weathering than under the constant high humidity conditions. Introduction and removal of moisture from the system in a repetitive pattern causes reversal of stresses between the particles and causes destruction of bonds between the particles. Humidification of sample introduces moisture in the shale lime system, and now the strength of the sample depends not only on the bonds between the particles and the strength of these bonds but also on the porosity of the matrix

and the moisture imbibing characteristics of the shale lime mass.

Shales 15 and 24 each contain only 14 percent clay size particles; their initially porous structure seems to become more so with the application of wet-dry cycles and with the addition of lime. Even a small amount of moisture due to humidification seems to have provided formation of a layer of water thick enough to facilitate the failure of sample at a load of small magnitude. The samples containing 6 percent lime, however, were able to carry greater loads while showing non-plastic characteristics. The X-ray diffraction patterns for these samples indicated presence of many shale lime reaction products, especially the tobermorite gel, and thus the strength of samples is due to the bonds formed by the gel. This strength still is too little and when subjected to humidification samples show some, but not much, resistance to stress.

The strength of the untreated shale samples is obviously due to their less porous structure. The same reasoning seems to hold for the strength of the samples of Shales 13 and 21 containing 1 or 2 percent lime. Also the differences between the Shales 13 and 21 are due to the differences in their clay contents; Shale 13 has 48 percent clay size particles while Shale 21 has only 25 percent particles in this size range.

On drying, the shale particles come closer together and the shear strength of the sample increases. This drying may restrain crack propagation and materially delay the failure of the sample (Antrim, 1967). Presence of shrinkage cracks due to the loss of moisture may contribute to some loss in strength due to reduction in the section carrying load. Shrinkage, or reduction in volume, was significant in Shales 13 and 21, which have higher percentages of clay size particles and in spite of the reduced load carrying section these shales were capable of withstanding the total range of loads and load applications. In the lime treated shales, however, on drying, the dispersed cardhouse structure prevents the particles from coming close together. Thus the shale lime matrix remains porous and exhibits lower strength. In addition, the presence of small amounts of unreacted lime and calcite particles provides additional areas of discontinuity from which cracks may initiate or propagate without requiring much energy. This may explain why some samples containing high percentages of lime exhibited lower strengths for the same wet-dry cycle treatment. The porous structure of lime stabilized shales, however, inhibits the effects of wet-dry cycles and thus provides a more desirable material.

Beyond initial stage the chemical reactions between shale and lime are dependent on time and temperature parameters. Anessi (1970) had found that for long term, high temperature curing, illitic samples tended to be more

significantly modified than montmorillonitic samples. From the strength, plasticity and X-ray diffraction data for the shales subjected to 120-day curing at 22°C (72°F), the contrary was found to be true. After 120-day curing Shale 24, which is predominantly illitic, showed no peak for lime for the sample containing 2 percent lime, but showed strong peaks when the lime content was 6 percent. In the case of Shale 13, which is predominantly montmorillonitic, however, no peaks for lime were observed either at 2 percent or at 6 percent level of lime treatment. Also, the samples subjected to 120-day curing and containing 4 percent or 6 percent lime exhibited greater elasticity in the case of Shale 13 than in the case of Shale 24. It must be noted that this observation was made under conditions different from those under which Anessi's observations were made.

Due to higher surface area available for shale lime reaction, montmorillonites should provide early strength development (Anessi, 1970) and this is the case in this study also. Samples of lime treated Shale 13, in general, are capable of withstanding greater loads and number of load applications than the samples of lime treated Shale 21. Shale 21, in turn, in this case is better than the lime treated Shale 24. With the passage of time, the shales with smaller surface area in Anessi's experiment tended to develop greater strength due to higher concentration of the shale lime reaction products. Such was not the case for the present

study since the shale expected to have smaller surface area showed more brittle behavior and failed at smaller diametral strains under a smaller load and at fewer load applications. Most probably, the wet-dry cycling process and 120-day curing did not carry the shale lime reaction toward completion to the extent that Anessi's experiment did. From the present study it may be concluded that the lime stabilization seems to be more effective with the shale containing higher percent of clay and the shale that has greater montmorillonitic clay content. It must be pointed out that this observation is based on the study of only four shales widely varying in character.

A comparison between the samples subjected to simulated weathering and those subjected to 120-day curing indicated very clearly that even after 50 wet-dry cycles the shale lime reactions were far from complete. The samples cured for 120-days showed superior strength characteristics also. They also showed that shale lime reaction had proceeded to a greater extent in their case. Lime peaks could be identified for the samples of Shales 13 and 21 containing 6 percent lime and which had been subjected to 50 wet-dry cycles. These peaks, however, were absent for similar samples subjected to 120-day curing. The differences between simulated weathering and 120-day curing were however such that they did not significantly show up in the Atterberg limit tests.

Addition of lime was largely ineffective in stabilizing Shale 15. For Shales 13, 21 and 24 even 1 percent lime addition was sufficient to alter their plastic nature to brittle behavior. Addition of 2 percent lime made these shales non-plastic, but until this percentage a great portion of lime seems to have reacted with the shale, since X-ray patterns indicated presence of little or no unreacted lime. At 6 percent lime treatment level, the strength and plasticity characteristics are not significantly different from the same characteristics at 4 percent lime treatment level for these three shales; however, the X-ray diffraction patterns for these shale and 6 percent lime mixes subjected to 50 wet-dry cycles showed strong calcite and unreacted lime peaks indicating that not only much more time was required for the lime to react with the shale but also that some of the lime must be wasted as calcium carbonate which imparts but little strength to the shale lime mass. Thus, for highway construction purposes, towards which this study is directed, the optimum amount of lime seems to be between 2 percent and 6 percent, the exact amount depending on the content and the type of clay in the shale selected for stabilization.

CHAPTER VI

CONCLUSIONS

Present laboratory research was conducted in an attempt to eventually establish design criteria for shales used in highway design. The data obtained from the various tests on four selected Oklahoma shales provide the basis for arriving at the following conclusions.

1. The relationship between the maximum dry density (MDD) and the corresponding optimum moisture content (OMC) for the shales and their lime mixes is given by the regression equation:

$$\text{MDD, pcf} = 143.916 - 1.933\ (\text{OMC}), \text{ percent}$$

2. The order in which shales could be expected to behave is better indicated by the composite parameter of 'activity coefficient' which is defined as:

$$\text{Activity Coefficient} = \frac{\text{Plasticity Index}}{\text{Clay Content (percent} < 2 \text{ micron)}}$$

than either by the amount of clay, its plasticity characteristics or the type of clay minerals taken independently.

3. In split tensile strength tests, where loads are increased in discrete magnitudes and not in a continuous manner, the diametral strain is a very good criterion to determine the failure points. Once the failure points are identified, the limiting stresses may be computed and used to evaluate the strength characteristics of different shales.
4. Atterberg limits are not much affected by the number of wet-dry cycles used in this investigation (up to 50). These limits, however, are significantly affected by the addition of lime. With the addition of 2 percent lime, all shales become non-plastic. Shale 15 became non-plastic even at 1 percent lime addition. The liquid limit does not change significantly for addition of lime in excess of 2 percent.
5. The presence of unreacted lime in the shale lime mix tends to cause brittleness. Samples exhibit increasingly elastic behavior as the amount of unreacted lime decreases.
6. After 50 wet-dry cycles, in all shales much of the lime is utilized for shale lime reaction at the 2 percent lime treatment level. However, at 6 percent treatment level, lime is only partly utilized and X-ray diffraction patterns reveal the presence of unreacted lime and calcite. Tricalcium silicate (C_3S) appears as the first product of shale lime reaction followed by dicalcium silicate (C_2S) and calcium aluminate hydrates (CAH and C_4AH_n).

7. The strength of shale lime mix appears to depend on the matrix porosity, progress of shale lime reaction, amount and nature of reaction products, amount of unreacted lime and the amount of calcite in the mix.
8. Humidification of samples causes loss of strength and thus the dry samples withstand greater loads and more number of load applications than the moist samples. The effect of humidification on loss of strength is greatest for Shale 15 and its lime mixes. This effect decreases with Shale 24, Shale 21 and Shale 13, in that order.
9. Shale 15 has an AASHTO classification of A-1-b and it was found to be unsuitable for lime stabilization. The less than 2 micron size clay contents for Shales 13, 21 and 24 were 48, 25 and 14, respectively. Shales 13, 21 and 24 were found suitable for stabilization. The effect of lime in modifying shale was most significant on Shale 13 and in decreasing order on Shales 21 and 24, respectively.
10. When tested in moist condition, the samples containing higher percentage of lime show greater elasticity after prolonged (120-day) curing.
11. Lime stabilization reduces the magnitude of shrinkage of shale due to loss of moisture.
12. The destructive effect of wet-dry cycles is greater on untreated shales than on the lime treated shales. The greater the percentage of lime in the shale mix, the less is the effect of the wet-dry cycles on the mix.

13. Weathering of untreated shale and addition of lime to it, both reduce the plastic characteristics of shale and introduce brittleness in it.
14. Addition of lime to shale significantly alters the character of shale. However, the extent to which the shale lime reaction proceeds under the simulated weathering conditions of alternate wetting and drying is much less than the extent to which such reactions proceed during prolonged curing at 100 percent humidity conditions. Thus, the material produced by weathering is significantly different not only from the raw shale but also from the stabilized shale mass produced in the laboratory using conventional methods.

CHAPTER VII

SUGGESTIONS FOR FURTHER RESEARCH

Before formulating final design criteria for using shale in highway construction, it is imperative to obtain all information relative to shale characterization under repeated loads and environmental changes. Towards this end, the following suggestions for future research are offered.

1. Study of the effects of hygrometric changes on the cracking pattern and on load deformation characteristics of shales used in highway pavement structures.
2. Effect of lime on pure clay minerals subjected to long term curing at different temperatures and at different humidity conditions.
3. Direct split tensile strength test, with strain gages properly attached to the sample, shales and stabilized materials to determine the validity of the expressions derived in Chapter II for the determination of various principal stresses in split tensile strength test specimens.
4. In as much as lime stabilization renders shales porous, it would be worthwhile to investigate the effect of the

type and amount of clay and of the stabilization processes on the porosity of the shale lime mixes.

REFERENCES

Aitchison, G. D., and Richards, B. G. (1965). A Broad-Scale Study of Moisture Conditions in Pavement Subgrades Throughout Australia, Moisture Equilibria and Moisture Changes in Soils Beneath Covered Areas, A Symposium in Print, G. D. Aitchison, ed., Butterworths, Sydney, Australia, pp. 184-204.

Anday, M. C. (1961). Accelerated Curing for Lime Stabilized Soils, Bulletin 304, Highway Research Board, Washington, DC, January, 1961, pp. 1-13.

Anessi, T. J. (1970). Strength and Consolidation Properties of Raw and Stabilized Oklahoma Shales, A Dissertation, University of Oklahoma, Norman, Oklahoma, Unpublished.

Annamalai, M. (1974). Engineering Properties of Raw and Ultrasonic Treated Oklahoma Shales, A Dissertation, University of Oklahoma, Norman, Oklahoma, Unpublished.

Annamalai, M.; Kumar, S.; Norvell, M.; and Patrick, D. M. (1970). A Study of Three Oklahoma Shales, A Report Prepared for the Department of Civil Engineering and Environmental Science, University of Oklahoma, Norman, Oklahoma, Unpublished.

Antrim, J. D. (1967). The Mechanism of Fatigue in Cement Paste and Plain Concrete, Highway Research Record No. 210, Highway Research Board, Washington, DC, pp. 95-107.

Asphalt Institute.(1963). Thickness Design--Asphalt Pavement Structures for Highways and Streets, Manual Series No. 1 (MS-1), Author, College Park, Maryland.

ASTM (1966). KWIC Guide to the Powder Diffraction File, ASTM Publication PD IS-16K, American Society for Testing and Materials, Philadelphia, Pennsylvania.

Carneiro, F. L. L. B. and Barcellos, A. (1953). Concrete Tensile Strength, Bulletin No. 13, Union of Testing and Research Laboratories for Materials and Structures (R.I.L.E.M.), Paris, France, pp. 97-123.

Chastain, W. E., Sr. (1962). Application of Road Test Formulas in Structural Design of Pavement, Special Report 73, The AASHO Road Test, Proceedings of a Conference held in May 1962 at St. Louis, MO, Highway Research Board, Washington, DC, pp. 299-313.

Diamond, S. and Kinter, E. B. (1966). Mechanism of Soil Lime Stabilization--An Interpretive Review, Public Roads, Vol. 33, No. 12, Bureau of Public Roads, U.S. Department of Commerce, Washington, DC, pp. 260-265.

Eades, J. L. and Grim, R. E. (1966). A Quick Test to Determine Lime Requirements for Lime Stabilization, Highway Research Record No. 139, Highway Research Board, Washington, DC, pp. 61-72.

Eades, J. L.; Nichols, F. P., Jr.; and Grim, R. E. (1962). Formation of New Minerals with Lime Stabilization as Proven by Field Experiments in Virginia, Highway Research Board Bulletin 335, Highway Research Board, Washington, DC, pp. 31-39.

Foster, R. H. and De, P. K. (1971). Optical and Electron Microscopic Investigation of Shear Induced Structures in Lightly Consolidated (Soft) and Heavily Consolidated (Hard) Kaolinite, Clays and Clay Minerals, Journal of the Clay Minerals Society, Vol. 19, No. 1, Oxford, UK, pp. 31-47.

Frocht, M. M. (1961). Photoelasticity, Vol. 2, John Wiley and Sons, Inc., New York, NY.

George, K. P. (1968). Shrinkage Characteristics of Soil Cement Mixtures, Highway Research Record No. 255, Highway Research Board, Washington, DC, pp. 42-58.

Gillott, J. E. (1968). Clay in Engineering Geology, Elsevier Publishing Company, Amsterdam, Holland.

Glenn, G. R. and Handy, R. L. (1963). Lime-Clay Mineral Reaction Products, Highway Research Record No. 29, Highway Research Board, Washington, DC, pp. 70-82.

Griffith, A. A. (1920). The Phenomena of Rupture and Flow in Solids, Philosophical Transactions, Series A, Vol. 221, Royal Society of London, London, UK, pp. 163-198.

Grim, R. E. (1968). Clay Mineralogy, Second Edition, McGraw-Hill Book Company, New York, NY.

Harman, H. H. (1967). Modern Factor Analysis, Second Edition, University of Chicago Press, Chicago, IL.

Herzog, A. and Mitchell, J. K. (1963). Reactions Accompanying Stabilization of Clay with Cement, Highway Research Record No. 36, Highway Research Board, Washington, DC, pp. 146-171.

Hewlett-Packard, Sanborn Division (1967a). 296 Two Channel Recording System, Operating and Service Manual; IM-296-2, Waltham, Massachusetts.

Hewlett-Packard, Sanborn Division (1967b). 350-1100 C Carrier Preamplifier, Operating and Service Manual; IM-350-1100C-1, Waltham, Massachusetts.

Hilt, G. H. and Davidson, D. T. (1960). Lime Fixation in Clayey Soils, Highway Research Board Bulletin 262, Highway Research Board, Washington, DC, pp. 20-32.

Hilt, G. H. and Davidson, D. T. (1961). Lime and Sodium Silicate Stabilization of Montmorillonite Clay Soil, Highway Research Board Bulletin 304, Highway Research Board, Washington, DC, pp. 51-64.

Ho, C. and Handy, R. L. (1963). Characteristics of Lime Retention by Montmorillonite Clays, Highway Research Record No. 29, Highway Research Board, Washington, DC, pp. 55-69.

Ho, C. and Handy, R. L. (1964). Effect of Lime on Electro-Kinetic Properties of Bentonites, Proceedings of the 12th National Conference on Clays and Clay Minerals, Pergamon Press, Oxford, UK, pp. 267-280.

Hong, H. (1967). Fatigue Characteristics of Flexible Pavements, Journal of the Highway Division, Vol. 93, No. HW1, American Society of Civil Engineers, New York, NY, pp. 43-67.

Huang, R. J. W. and Roderick, G. L. (1969). Cement Content of Soil Cement by X-Ray Fluorescence, Highway Research Record No. 263, Highway Research Board, Washington, DC, pp. 60-68.

Katti, R. K. and Barve, A. G. (1962). Effect of Inorganic Chemicals on the Consistency Properties of an Expansive Soil Sample, Bulletin 349, Highway Research Board, Washington, DC, pp. 1-8.

Kawakami, F. and Ogawa, S. (1964). Yield Stress and Modulus of Elasticity of Soil, Symposium held at Grenoble, France, Rheology and Soil Mechanics, International Union of Theoretical and Applied Mechanics, Springer-Verlag, Berlin, West Germany, pp. 354-363.

Kriezek, R. J. and Kondner, R. L. (1964). Strength Consistency Indices for a Cohesive Soil, Highway Research Record No. 48, Highway Research Board, Washington, DC, pp. 1-18.

Kumar, S. (1961). Evaluation of Shearing Characteristics of a Sample of Black Cotton Soil Stabilized with the Combinations of Portland Cement and Lime, A Master's Degree Dissertation, Indian Institute of Technology, Bombay, India, Unpublished.

Laguros, J. G. (1965). Lime-Stabilized Soil Properties and Beam Action Hypothesis, Highway Research Record No. 92, Highway Research Board, Washington, DC, pp. 12-20.

Laguros, J. G. (1972). Predictability of Physical Changes of Clay Forming Materials in Oklahoma, Final Report: Oklahoma Study No. 68-03-2, OURI Project 1677, University of Oklahoma Research Institute, Norman, Oklahoma.

Larew, H. G. and Leonards, G. A. (1962). A Strength Criterion for Repeated Loads, Proceedings of the 41st Annual Meeting, Vol. 41, Highway Research Board, Washington, DC, pp. 529-556.

Lenzen, K. H.; Yen, B. T.; Nordmark, G. E.; Yao, J. T. P.; and Munse, W. H. (1968). Analysis and Interpretation of Fatigue Data, Journal of the Structural Division, Vol. 94, No. ST12, American Society of Civil Engineers, New York, NY, pp. 2665-2677.

Marks, B. D., III and Haliburton, T. A. (1969). Subgrade Moisture Variation Studied with Nuclear Depth Gages, Highway Research Record No. 276, Highway Research Board, Washington, DC, pp. 12-24.

McDowell, C. (1966). Evaluation of Soil-Lime Stabilization Mixtures, Highway Research Record No. 139, Highway Research Board, Washington, DC, pp. 15-24.

Metcalf, J. B. and Frydman, S. (1962). A Preliminary Study of the Tensile Stresses in Stabilized Soil Pavements, Proceedings of the Australian Road Research Board, Vol. 1, Part 2, Melbourne, Australia.

Moavenzadeh, F. (1967). Asphalt Fracture, Professional Paper P67-5, School of Engineering, Massachusetts Institute of Technology, Cambridge, Massachusetts,

Moavenzadeh, F. and Carnaghi, R. A. (1966). Viscoelastic Response of Sand Asphalt Beams on Elastic Foundations Under Repeated Loading, Proceedings of the Association of the Asphalt Paving Technologists, Vol. 35, Ann Arbor, Michigan, pp. 514-528.

Nalezny, C. L. and Li, M. C. (1967). Effect of Soil Structure and Thixotropic Hardening on the Swelling Behavior of Compacted Clay Soils, Highway Research Record No. 209, Highway Research Board, Washington, DC, pp. 1-22.

Neubauer, C. H., Jr. and Thompson, M. R. (1972). Stability Properties of Uncured Lime-Treated Fine Grained Soils, Highway Research Record No. 381, Highway Research Board, Washington, DC, pp. 20-26.

Noble, D. F. (1967). Reactions and Strength Development in Portland Cement-Clay Mixtures, Highway Research Record No. 198, Highway Research Board, Washington, DC, pp. 39-56.

Peattie, K. R. (1962). A Fundamental Approach to the Design of Flexible Pavements, Proceedings of the International Conference on the Structural Design of Asphalt Pavements, University of Michigan, Ann Arbor, Michigan, pp. 487-494.

Peltier, R. (1954). Theoretical Investigation of the Brazilian Test, Bulletin No. 19, International Association of Testing and Research Laboratories for Materials and Structures (R.I.L.E.M.), Paris, France, pp. 29-69.

Pihlajavaara, S. E. (1967). Mechanical Effects of Moisture Topic 1, General Report; Paper abstract by E. Niskanen, Bulletin New Series No. 34, The International Union of Testing and Research Laboratories for Materials and Structures (R.I.L.E.M.), Paris, France, pp. 19-21.

Popovics, S. (1967). Relations Between Various Strengths of Concrete, Highway Research Record No. 210, Highway Research Board, Washington, DC, pp. 67-94.

Popovics, S. (1969). Fracture Mechanism in Concrete: How Much Do We Know?, Journal of the Engineering Mechanics Division, Vol. 95, No. EM3, American Society of Civil Engineers, New York, NY, pp. 531-544.

Pretorius, P. C. and Monismith, C. L. (1972). Fatigue Crack Formation and Propagation in Pavements Containing Soil-Cement Bases, Highway Research Record No. 407, Highway Research Board, Washington, DC, pp. 102-115.

Ranganatham, B. V. (1961). Soil Structure and Consolidation Characteristics of Black Cotton Soil, Geotechnique, Vol. XI, Institution of Civil Engineers, London, UK, pp. 333-338.

Ruff, C. G. and Ho, C. (1966). Time-Temperature Strength Reaction Product Relationships in Lime-Bentonite-Water-Mixtures, Highway Research Record No. 139, Highway Research Board, Washington, DC, pp. 42-60.

Russam, K. (1970). Subgrade Moisture Studies by the British Road Research Laboratory, Highway Research Record No. 301, Highway Research Board, Washington, DC, pp. 5-17.

Saare, E. and Nevander, L. E. (1967). Physical Effects of Moisture, Topic 2, General Report, Bulletin New Series No. 34, The International Union of Testing and Research Laboratories for Materials and Structures (R.I.L.E.M.), Paris, France, pp. 29-31.

Sauer, E. K. and Monismith, C. L. (1968). Influence of Soil Suction on Behavior of a Glacial Till Subjected to Repeated Loading, Highway Research Record No. 215, Highway Research Board, Washington, DC, pp. 8-23.

Seed, H. B.; Mitry, F. G.; Monismith, C. L.; and Chan, C.K. (1967). Prediction of Flexible Pavement Deflections from Laboratory Repeated Load Tests, National Cooperative Highway Research Program, Report 35, Highway Research Board, Washington, DC.

Sheerar, L. F. (1932). The Clays and Shales of Oklahoma, Vol. 3, No. 5, Oklahoma A&M College, Stillwater, Oklahoma.

Sherif, M. A. (1966). Deformation and Flow Properties of Clay Soils from the Viewpoint of Modern Material Science, Highway Research Record No. 119, Highway Research Board, Washington, DC, pp. 24-49.

Skempton, A. W. (1953). The Colloidal Activity of Clays, Proceedings, Vol. 1, 3rd International Conference on Soil Mechanics and Foundation Engineering, Zurich, Switzerland, pp. 57-61.

Slate, F. O. and Olsefski, S. (1963). X-Rays for Study of Internal Structure of Microcracking of Concrete, Journal Vol. 60, Proceedings of the American Concrete Institute, Detroit, Michigan, pp. 575-588.

Soderman, L. G.; Kim, Y. D.; and Milligan, V. (1968). Field and Laboratory Studies of Modulus of Elasticity of a Clay Till, Highway Research Record No. 243, Highway Research Board, Washington, DC, pp. 1-11.

Stallmeyer, J. E. and Walker, W. H. (1968). Cumulative Damage Theories and Application, Journal of the Structural Division, Vol. 94, No. ST 12, American Society of Civil Engineers, New York, NY, pp. 2739-2750.

SBEL (1970). Operating Instructions for Soil Dynamic Tester, Structural Behavior Engineering Laboratories, Inc., Phoenix, Arizona.

Taylor, H. F. W. (1966). The Chemistry of Cements, Vol. 1, Academic Press, London, UK.

Thompson, W. E. (1963). Analysis of Dynamic Behavior of Roads Subjected to Longitudinally Moving Loads, Highway Research Record No. 39, Highway Research Board, Washington, DC, pp. 1-24.

Thompson, M. R. (1966). Shear Strength and Elastic Properties of Lime-Soil Mixtures, Highway Research Record No. 139, Highway Research Board, Washington, DC, pp. 1-14.

Timoshenko, S. and Goodier, J. N. (1951). Theory of Elasticity, McGraw-Hill Book Company, New York, NY.

Townsend, F. C.; Manke, P. G.; and Parcher, J. V. (1969). Effect of Remolding on the Properties of a Lateritic Soil, Highway Research Record No. 284, Highway Research Board, Washington, DC, pp. 76-84.

Uppal, H. L. (1965). Field Study on the Movement of Moisture in Black Cotton Soils Under Road Pavements, Moisture Equilibria and Moisture Changes in Soils Beneath Covered Areas, A Symposium in Print, G. D. Aitchison, ed., Butterworths, Sydney, Australia, pp. 165-174.

Venkatasubramanian, V. (1964). Temperature Variations in a Cement Concrete Pavement and the Underlying Subgrade, Highway Research Record No. 60, Highway Research Board, Washington, DC, pp. 15-27.

Yoder, E. J. (1969). Selection of Soil Strength Values for the Design of Flexible Pavements, Highway Research Record No. 276, Highway Research Board, Washington, DC, pp. 1-13.

APPENDICES

APPENDIX A

DERIVATION OF EXPRESSIONS FOR DETERMINING THE STRESSES IN THE SPLIT TENSILE STRENGTH TEST SPECIMEN UNDER VERTICAL DIAMETRAL COMPRESSION

P = Total load applied

D = Diameter of cylinder

R = Radius of cylinder

L = Length of cylinder

Consider that the load applied, P, produces a deformation d and that the load is applied symmetrically about y axis along a distance $2x_1$. The load distribution may be assumed as a uniform load of p. Then,

$$P = p\ 2x_1\ L$$

The distance of load from the center of the specimen is y_1 and

$$y_1 = (D - d)/2$$

The stresses on an element E at (x_e, y_e) due to uniform load p acting on an elemental area dx distant x from y axis and acting vertically from both ends due to two platens

(Figure 2.3) may be written (Frocht, 1961) as:

$$ds_x = -\frac{2pdx}{\pi}\left[\frac{(y_1 - y_e)(x_e - x)^2}{[(y_1-y_e)^2+(x_e-x)^2]^2} + \frac{(y_1 + y_e)(x_e - x)^2}{[(y_1+y_e)^2+(x_e-x)^2]^2} - \sin\left(\frac{\pi}{2} + \alpha_x\right)/2R\right]$$

$$ds_y = -\frac{2pdx}{\pi}\left[\frac{(y_1 - y_e)^3}{[(y_1-y_e)^2+(x_e-x)^2]^2} + \frac{(y_1 + y_e)^3}{[(y_1+y_e)^2+(x_e-x)^2]^2} - \sin\left(\frac{\pi}{2} + \alpha_x\right)/2R\right]$$

$$dt_{xy} = \frac{2pdx}{\pi}\left[\frac{(y_1 - y_e)^2 (x_e - x)}{[(y_1-y_e)^2+(x_e-x)^2]^2} - \frac{(y_1 + y_e)^2 (x_e - x)}{[(y_1+y_e)^2+(x_e-x)^2]^2}\right]$$

where $\tan \alpha_x = x/y_1$. Set $y_1 - y_e$ equal to k_1, a constant; $y_1 + y_e$ equal to k_2, another constant; $x_e - x$ equal to u, a variable. Then,

$$dx = -du$$

$$\sin\left(\frac{\pi}{2} + \alpha_x\right)/2R = \cos \alpha_x/2R = \frac{y_1}{2R(y_1^2 + x^2)^{1/2}}$$

Then

$$ds_x = \frac{2p}{\pi}\left[\frac{k_1 u^2}{(k_1^2 + u^2)^2} + \frac{k_2 u^2}{(k_2^2 + u^2)^2}\right] du + \frac{y_1 p}{\pi R}\frac{dx}{(y_1^2 + x^2)^{1/2}}$$

$$ds_y = \frac{2p}{\pi}\left[\frac{k_1^3}{(k_1^2 + u^2)^2} + \frac{k_2^3}{(k_2^2 + u^2)^2}\right] du + \frac{y_1 p}{\pi R}\frac{dx}{(y_1^2 + x^2)^{1/2}}$$

$$dt_{xy} = -\frac{2p}{\pi}\left(\frac{k_1^2\, u}{(k_1^2 + u^2)^2} - \frac{k_2^2\, u}{(k_2^2 + u^2)^2}\right)$$

Now,

$$\int \frac{k_1 u^2\, du}{(k_1^2 + u^2)^2} = \frac{-k_1 u}{2(k_1^2 + u^2)} + \frac{k_1}{2}\int \frac{du}{(k_1^2 + u^2)} + c_1$$

$$= \frac{-k_1 u}{2(k_1^2 + u^2)} + \frac{1}{2}\text{ arc tan }\left(\frac{u}{k_1}\right) + c_1 + c_2$$

Substituting $u = x_e - x$ and evaluating integral within the limits $x = x_1$ and $x = -x_1$, definite integration yields

$$= \frac{-k_1\,(x_e - x_1)}{2[k_1^2 + (x_e - x_1)^2]} + \frac{k_1\,(x_e + x_1)}{2[k_1^2 + (x_e - x_1)^2]}$$

$$+ \frac{1}{2}\text{ arc tan }\frac{(x_e - x_1)}{k_1} - \frac{1}{2}\text{ arc tan }\frac{(x_e + x_1)}{k_1}$$

and,

$$\int \frac{k_1^3\, du}{(k_1^2 + u^2)^2} = \frac{k_1^3\, u}{2k_1^2(k_1^2 + u^2)} + \frac{k_1}{2}\int \frac{du}{(k_1^2 + u^2)} + c_3$$

$$= \frac{k_1\, u}{2(k_1^2 + u^2)} + \frac{1}{2}\text{ arc tan }\left(\frac{u}{k_1}\right) + c_2 + c_3$$

Substituting $u = x_e - x$ and evaluating integral within the limits $x = x_1$ and $x = -x_1$ definite integration yields

$$= \frac{k_1(x_e - x_1)}{2[k_1^2 + (x_e - x_1)^2]} - \frac{k_1(x_e + x_1)}{2[k_1^2 + (x_e + x_1)^2]}$$

$$+ \frac{1}{2} \arctan \frac{(x_e - x_1)}{k_1} - \frac{1}{2} \arctan \frac{(x_e - x_1)}{k_1}$$

Further, for

$$\int \frac{k_1^2 \, u \, du}{(k_1^2 + u^2)^2}, \quad \text{set} \quad k_1^2 + u^2 = t, \; 2u \, du = dt \text{ and integral}$$

is equal to

$$\frac{k_1^2}{2} \int \frac{dt}{t^2} = - \frac{k_1^2}{2t} = - \frac{k_1^2}{2(k_1^2 + u^2)}$$

Substituting $u = x_e - x$ and evaluating integral within the limits $x = x_1$ and $x = -x_1$ definite integration yields,

$$\frac{-k_1^2}{2[k_1^2 + (x_e - x_1)^2]} + \frac{k_1^2}{2[k_1^2 + (x_e + x_1)^2]}$$

and,

$$\int_{-x_1}^{x_1} \frac{y_1 \, dx}{2R(y_1^2 + x^2)^{1/2}} = \frac{y_1}{2R} \left[\ln \left[x + (y_1^2 + x^2)^{1/2} \right] \right]_{-x_1}^{x_1}$$

$$= \frac{y_1}{2R} \left[\ln \left[x_1 + (y_1^2 + x_1^2)^{1/2} \right] - \ln \left[-x_1 + (y_1^2 + x_1^2)^{1/2} \right] \right]$$

$$= \frac{y_1}{2R} \ln \frac{R + x_1}{R - x_1}, \quad \text{since } y_1^2 + x_1^2 = R^2$$

Thus, at point (x_e, y_e),

$$s_x = \frac{P}{2\pi x_1 L}\left[\frac{(y_1 - y_e)(x_e + x_1)}{(y_1-y_e)^2 + (x_e+x_1)^2} - \frac{(y_1 - y_e)(x_e - x_1)}{(y_1-y_e)^2 + (x_e-x_1)^2}\right.$$

$$+ \frac{(y_1 + y_e)(x_e + x_1)}{(y_1+y_e)^2 + (x_e+x_1)^2} - \frac{(y_1 + y_e)(x_e - x_1)}{(y_1+y_e)^2 + (x_e-x_1)^2}$$

$$+ \arctan\frac{(x_e - x_1)}{(y_1 - y_e)} - \arctan\frac{(x_e + x_1)}{(y_1 - y_e)}$$

$$+ \arctan\frac{(x_e - x_1)}{(y_1 + y_e)} - \arctan\frac{(x_e + x_1)}{(y_e + y_1)}$$

$$\left. + \frac{y_1}{R} \ln\frac{R + x_1}{R - x_1}\right]$$

$$s_y = \frac{-P}{2\pi x_1 L}\left[\frac{(y_1 - y_e)(x_e - x_1)}{(y_1-y_e)^2 + (x_e-x_1)^2} - \frac{(y_1 - y_e)(x_e + x_1)}{(y_1-y_e)^2 + (x_e+x_1)^2}\right.$$

$$+ \frac{(y_1 + y_e)(x_e - x_1)}{(y_1+y_e)^2 + (x_e-x_1)^2} - \frac{(y_1 + y_e)(x_e + x_1)}{(y_1+y_e)^2 + (x_e+x_1)^2}$$

$$+ \arctan\frac{(x_e - x_1)}{(y_1 - y_e)} - \arctan\frac{(x_e + x_1)}{(y_1 - y_e)}$$

$$+ \arctan\frac{(x_e - x_1)}{(y_1 + y_e)} - \arctan\frac{(x_e + x_1)}{(y_1 + y_e)}$$

$$\left. + \frac{y_1}{R} \ln\frac{R + x_1}{R - x_1}\right]$$

and

$$t_{xy} = \frac{P}{2\pi x_1 L}\left[\frac{(y_1 - y_e)^2}{(y_1-y_e)^2 + (x_e+x_1)^2} - \frac{(y_1 - y_e)^2}{(y_1-y_e)^2 + (x_e-x_1)^2} - \frac{(y_1 + y_e)^2}{(y_1+y_e)^2 + (x_e+x_1)^2} + \frac{(y_1 + y_e)^2}{(y_1+y_e)^2 + (x_e-x_1)^2}\right]$$

Along x axis, $y_e = 0$, therefore

$$s_{xx} = \frac{P}{2\pi x_1 L}\left[\frac{2y_1(x_e + x_1)}{y_1^2 + (x_e + x_1)^2} - \frac{2y_1(x_e - x_1)}{y_1^2 + (x_e - x_1)^2} - 2 \arctan\left(\frac{2x_1y_1}{y_1^2 + x_e^2 - x_1^2}\right) + \frac{y_1}{R} \ln \frac{R+x_1}{R-x_1}\right]$$

$$s_{yx} = \frac{P}{2\pi x_1 L}\left[-\frac{2y_1(x_e + x_1)}{y_1^2 + (x_e + x_1)^2} + \frac{2y_1(x_e - x_1)}{y_1^2 + (x_e - x_1)^2} - 2 \arctan\left(\frac{2x_1y_1}{y_1^2 + x_e^2 - x_1^2}\right) + \frac{y_1}{R} \ln \frac{R+x_1}{R-x_1}\right]$$

$$t_{xyx} = 0$$

at center $x_e = 0$, therefore

$$s_{xxc} = \frac{P}{2\pi x_1 L}\left[\frac{4x_1y_1}{R^2} - 2 \arctan\left(\frac{2x_1y_1}{y_1^2 - x_1^2}\right) + \frac{y_1}{R} \ln \frac{R+x_1}{R-x_1}\right]$$

$$s_{yxc} = \frac{-P}{2\pi x_1 L}\left[\frac{4x_1y_1}{R^2} + 2 \arctan\left(\frac{2x_1y_1}{y_1^2 - x_1^2}\right) - \frac{y_1}{R} \ln \frac{R+x_1}{R-x_1}\right]$$

at the ends $x_e = R$, therefore

$$s_{xxe} = -\frac{P}{2\pi x_1 L}\left(2 \arctan\left(\frac{x_1}{y_1}\right) - \frac{y_1}{R} \ln \frac{R+x_1}{R-x_1}\right)$$

$$s_{xye} = s_{yxc}$$

Along y axis, $x_e = 0$, therefore

$$s_{xy} = \frac{P}{2\pi x_1 L}\left(\frac{2x_1(y_1 - y_e)}{(y_1 - y_e)^2 + x_1^2} + \frac{2x_1(y_1 + y_e)}{(y_1 + y_e)^2 + x_1^2} - 2 \arctan\left(\frac{2x_1 y_1}{y_1^2 - x_1^2 - y_e^2}\right) + \frac{y_1}{R} \ln \frac{R+x_1}{R-x_1}\right)$$

$$s_{yy} = -\frac{P}{2\pi x_1 L}\left(\frac{2x_1(y_1 - y_e)}{(y_1 - y_e)^2 + x_1^2} + \frac{2x_1(y_1 + y_e)}{(y_1 + y_e)^2 + x_1^2} + 2 \arctan\left(\frac{2x_1 y_1}{y_1^2 - x_1^2 - y_e^2}\right) - \frac{y_1}{R} \ln \frac{R+x_1}{R-x_1}\right)$$

$$t_{xyy} = 0$$

at the center $y_e = 0$, therefore

$$s_{xyc} = s_{xxc}$$

$$s_{yyc} = s_{yxc}$$

at the ends $y_e = y_1$, therefore

$$s_{xye} = \frac{P}{2\pi x_1 L}\left(\frac{4x_1 y_1}{4y_1^2 + x_1^2} + 2 \arctan\left(\frac{2y_1}{x_1}\right) + \frac{y_1}{R} \ln \frac{R+x_1}{R-x_1}\right)$$

$$s_{yye} = \frac{-P}{2\pi x_1 L}\left(\frac{4x_1 y_1}{4y_1^2 + x_1^2} + 2 \arctan\left(\frac{2y_1}{x_1}\right) - \frac{y_1}{R} \ln \frac{R+x_1}{R-x_1}\right)$$

In summary,

$$s_{xxc} = \frac{P}{2\pi x_1 L}\left[\frac{4x_1y_1}{R^2} - 2 \arctan\left(\frac{2x_1y_1}{y_1^2 - x_1^2}\right) + \frac{y_1}{R} \ln \frac{R+x_1}{R-x_1}\right]$$

$$s_{yxc} = \frac{-P}{2\pi x_1 L}\left[\frac{4x_1y_1}{R^2} + 2 \arctan\left(\frac{2x_1y_1}{y_1^2 - x_1^2}\right) + \frac{y_1}{R} \ln \frac{R+x_1}{R-x_1}\right]$$

$$s_{xxe} = \frac{-P}{2\pi x_1 L}\left[2 \arctan\left(\frac{x_1}{y_1}\right) - \frac{y_1}{R} \ln \frac{R+x_1}{R-x_1}\right]$$

$$s_{yxe} = s_{xxe}$$

$$s_{xyc} = s_{xxc}$$

$$s_{yyc} = s_{yxc}$$

$$s_{xye} = \frac{P}{2\pi x_1 L}\left[\frac{4x_1y_1}{4y_1^2 + x_1^2} + 2 \arctan\left(\frac{2y_1}{x_1}\right) + \frac{y_1}{R} \ln \frac{R+x_1}{R-x_1}\right]$$

$$s_{yye} = \frac{-P}{2\pi x_1 L}\left[\frac{4x_1y_1}{4y_1^2 + x_1^2} + 2 \arctan\left(\frac{2y_1}{x_1}\right) - \frac{y_1}{R} \ln \frac{R+x_1}{R-x_1}\right]$$

$t_{xy} = 0$, along both axes.

A sample of computer program to determine these stresses and the diametral strain using IBM System 370/158 is included in the following pages.

```
      COMMON DFM(50),JDFM(50)
      J=1
  150 CONTINUE
      READ(5,1)ISM,IRPL,N,LC,IWDC,H,D
    1 FORMAT (6I3,2F10.0)
      READ(5,2)(JDFM(I),I=1,N)
    2 FORMAT(40I2)
      WRITE(6,100) ISM,IRPL
  100 FORMAT(1H1,9X,10HSHALE NO. ,3X,I3,40X,14HREPLICATE NO. ,1X,I3,/)
      WRITE(6,103)LC,IWDC
  103 FORMAT(10X,20HPERCENTAGE OF LIME  ,2X,I3,31X,25HNO. OF WET - DRY C
     1YCLES  ,2X,I3,/)
      WRITE(6,104)H,D
  104 FORMAT(10X, INITIAL HEIGHT   ,2X,F7.4,2X, INCHES ,23X, INITIAL DIA
     1METER   ,2X,F7.4,2X, INCHES ,/)
      IF(IWD-1)10,10,11
   10 WRITE(6,101)
  101 FORMAT(10X,20HTEST CONDITION   WET,/)
      GO TO 15
   11 WRITE(6,102)
  102 FORMAT(10X,20HTEST CONDITION   DRY,/)
   15 WRITE(6,105)
  105 FORMAT(///)
      WRITE(6,107)
  107 FORMAT(10X,31HSIG Y-Y-C IS SAME AS SIG Y-X-C.,15X,31HSIG X-Y-C IS
     1SAME AS SIG X-X-C.,/10X,35HAND SIG X-X-E IS SAME AS SIG Y-X-E.,//)
      WRITE(6,106)
  106 FORMAT(8X,1HI,5X,1HP,10X,9HSIG X-X-C,6X,9HSIG Y-X-C,6X,9HSIG X-X-E
     1,8X,9HSIG X-Y-E,8X,9HSIG Y-Y-E,8X,6HSTRAIN,//)
      DO 20 I=1,N
      IF(N-I) 140,25,25
   25 IF(I-12)30,30,12
   30 P=40.
      GO TO 50
   12 IF(I-24)13,13,14
   13 P=80.
```

```
      GO TO 50
   14 IF(I-36),35,35,16
   35 P=120.
      GO TO 50
   16 IF(I-45)17,17,140
   17 P=160.0
   50 CONTINUE
      DFM(I)=JDFM(I)
      DM=DFM(I)*0.0016
      IF(DM-0)20,20,60
   60 CONTINUE
       R = D/2
      Y1 = (D-DH)/2.
      X1 = SQRT((R*R)-(Y1*Y1))
      F1 = P/(2*3.14156*X1*H)
      F2 = (4*X1*Y1)/(R*R)
      F3 = (4*X1*Y1)/((4*Y1*Y1) + (X1*X1))
      F4 = (2*X1*Y1)/((Y1*Y1) - (X1*X1))
      T1=2*ATAN(F4)
      T2=2*ATAN(X1/Y1)
      T3=2*ATAN(2*Y1/X1)
      C=(Y1/R)*ALOG((R+X1)/(R-X1))
      SXXC=F1*(F2-T1+C)
      SYYC=(-F1)*(F2+T1-C)
      SXXE=(-F1)*(T2-C)
      SXYE=F1*(F3+T3+C)
      SYYE=(-F1)*(F3+T3-C)
      STN=DM/D
      WRITE(6,120)I,P,SXXC,SYXC,SXXE,SXYE,SYYE,STN
  120 FORMAT(6X,I3,3X,F5.1,1X,3(7X,F8.4), 2(6X,F10.4),6X,F6.4)
   20 CONTINUE
  140 CONTINUE
      J = J+1
      IF(J-31)150,150,160
  160 STOP
      END
```

APPENDIX B

CIRCUIT DIAGRAMS FOR ELECTRICAL CONNECTIONS

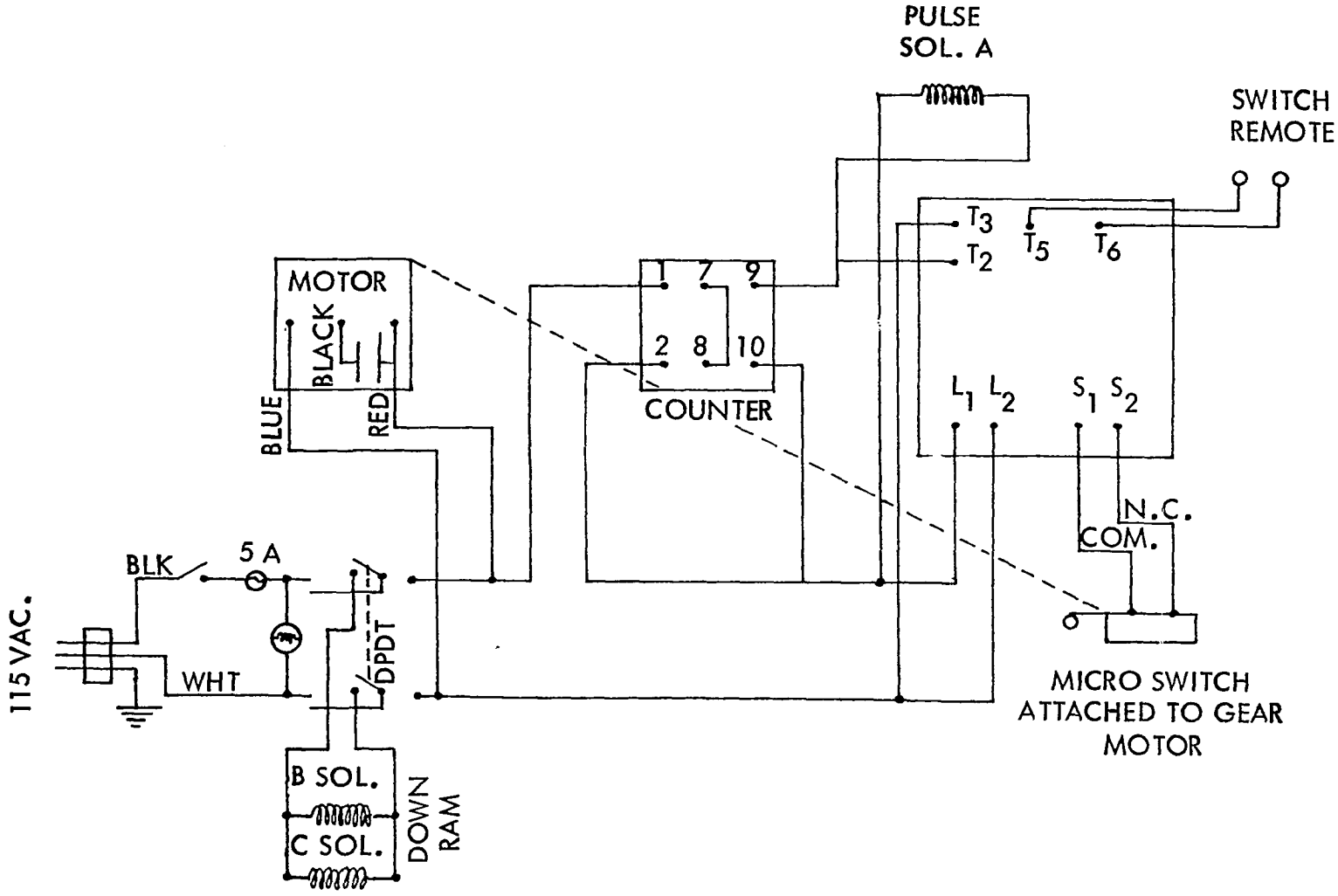


Figure B.1. Circuit diagram for SBEL Soil Dynamic Testing Machine (from reference SBEL, 1970).

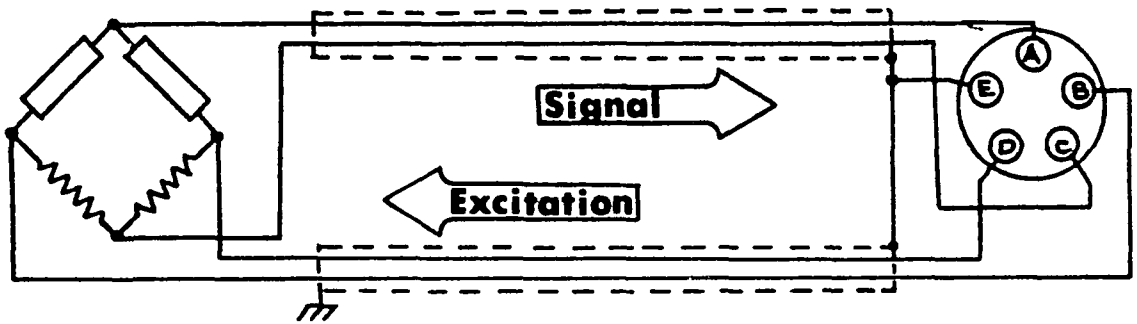


Figure B.2. Half bridge connection to preamplifier (from reference-Hewlett Packard, 1967b).

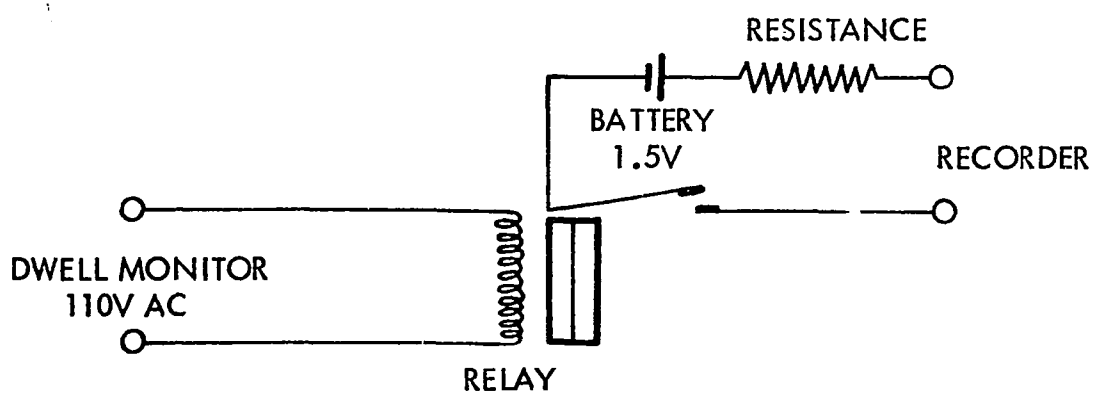


Figure B.3 Circuit diagram showing connection between dwell monitor and Atomic strip chart recorder.

APPENDIX C

SHRINKAGES OF SHALE AND SHALE LIME MIX SAMPLES

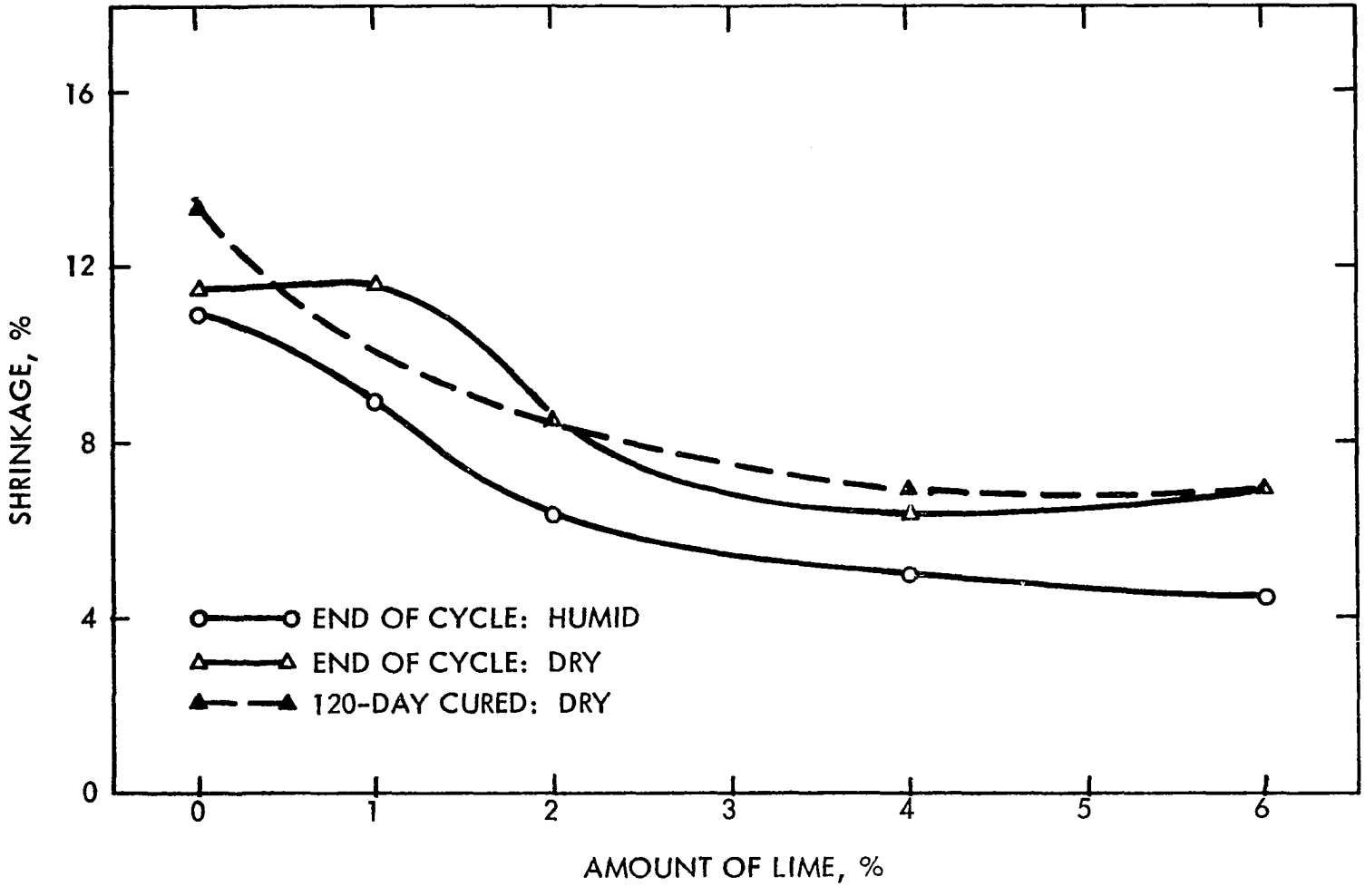


Figure C.1 Shrinkage of shale and shale lime mix samples for shale 13 at the end of wet-dry cycles and of 120-day curing.

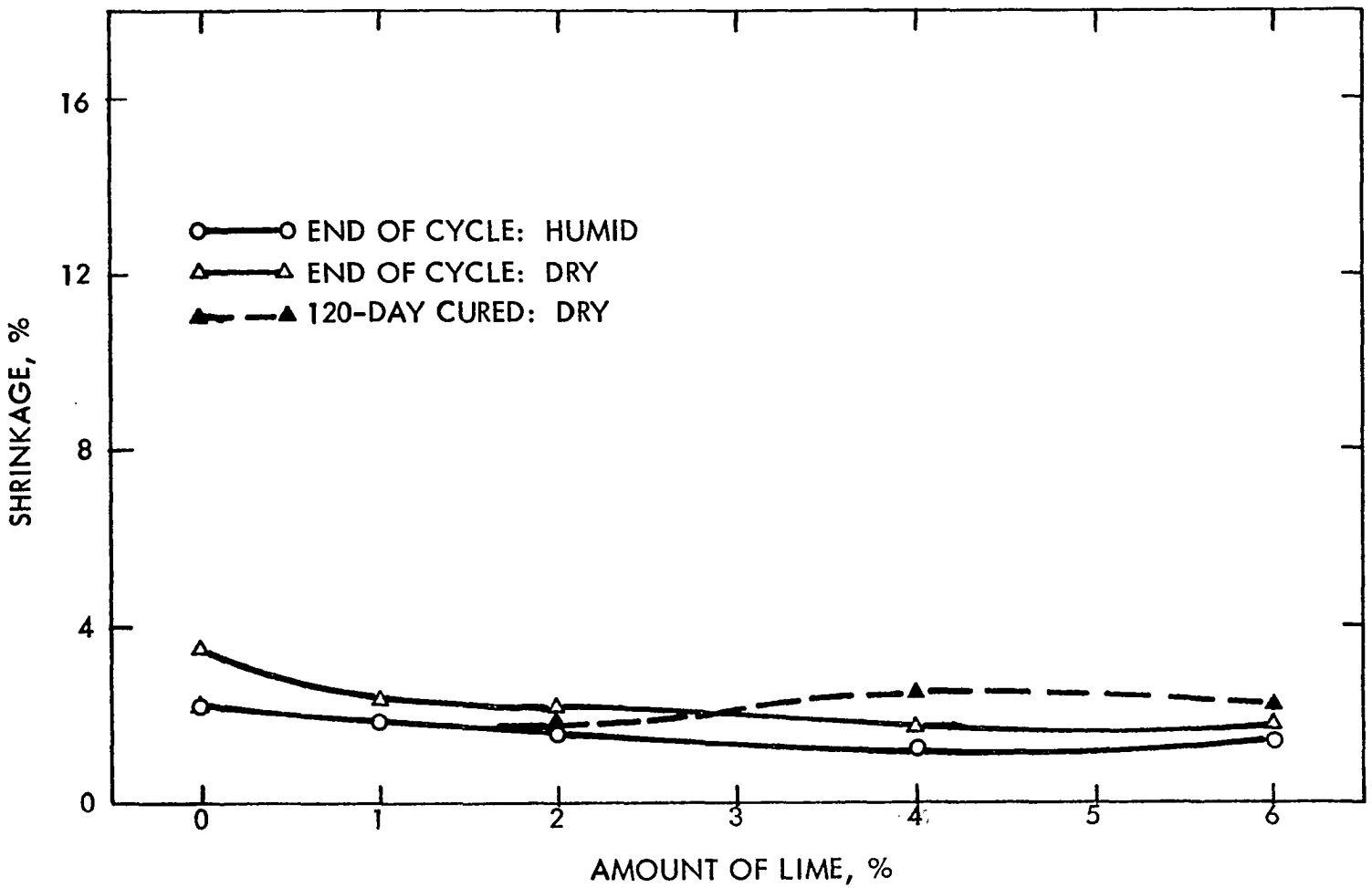


Figure C.2 Shrinkage of shale and shale lime mix samples for shale 15 at the end of wet-dry cycles and of 120-day curing.

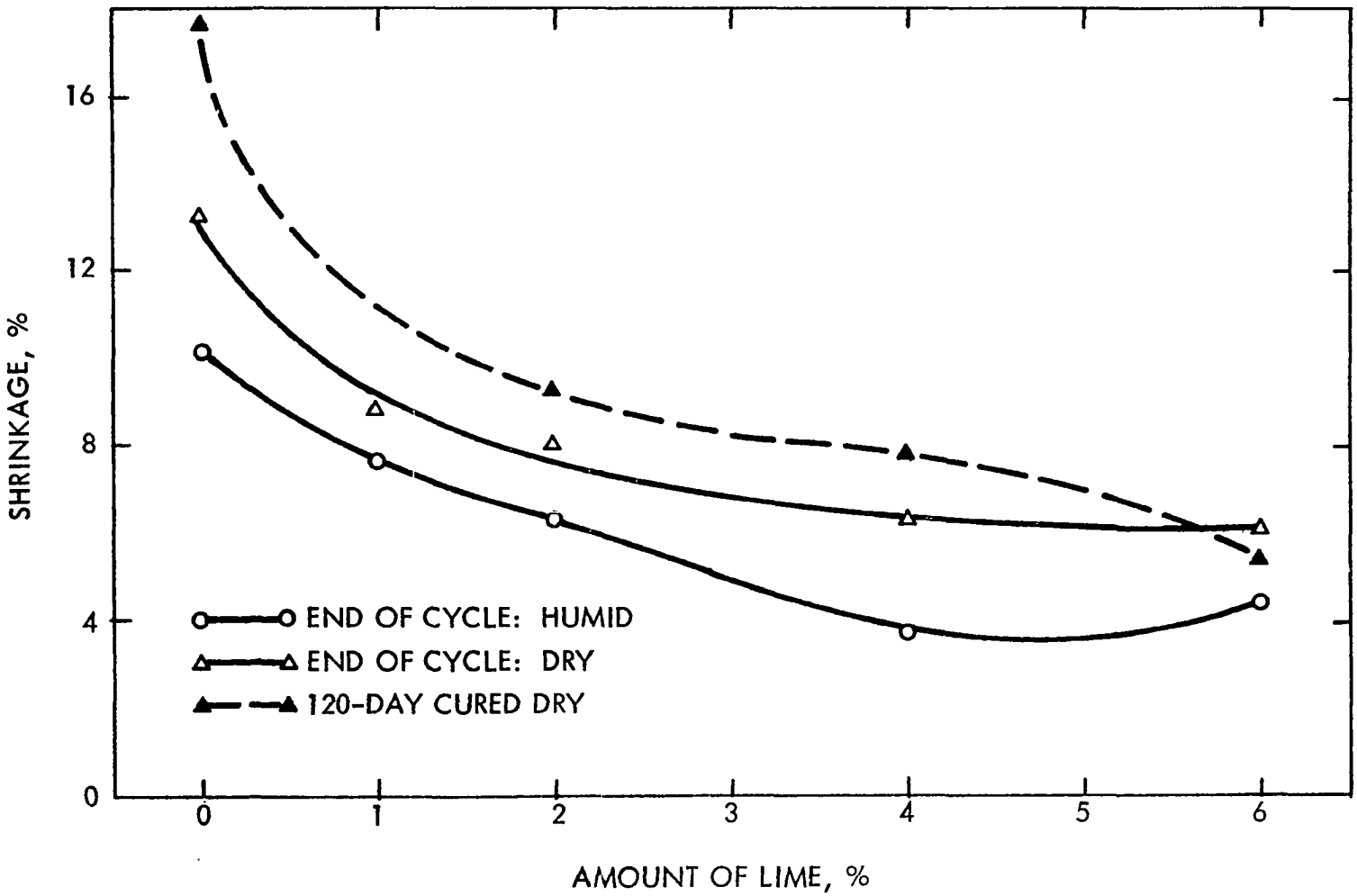


Figure C.3 Shrinkage of shale and shale lime mix samples for shale 21 at the end of wet-dry cycles and of 120-day curing.

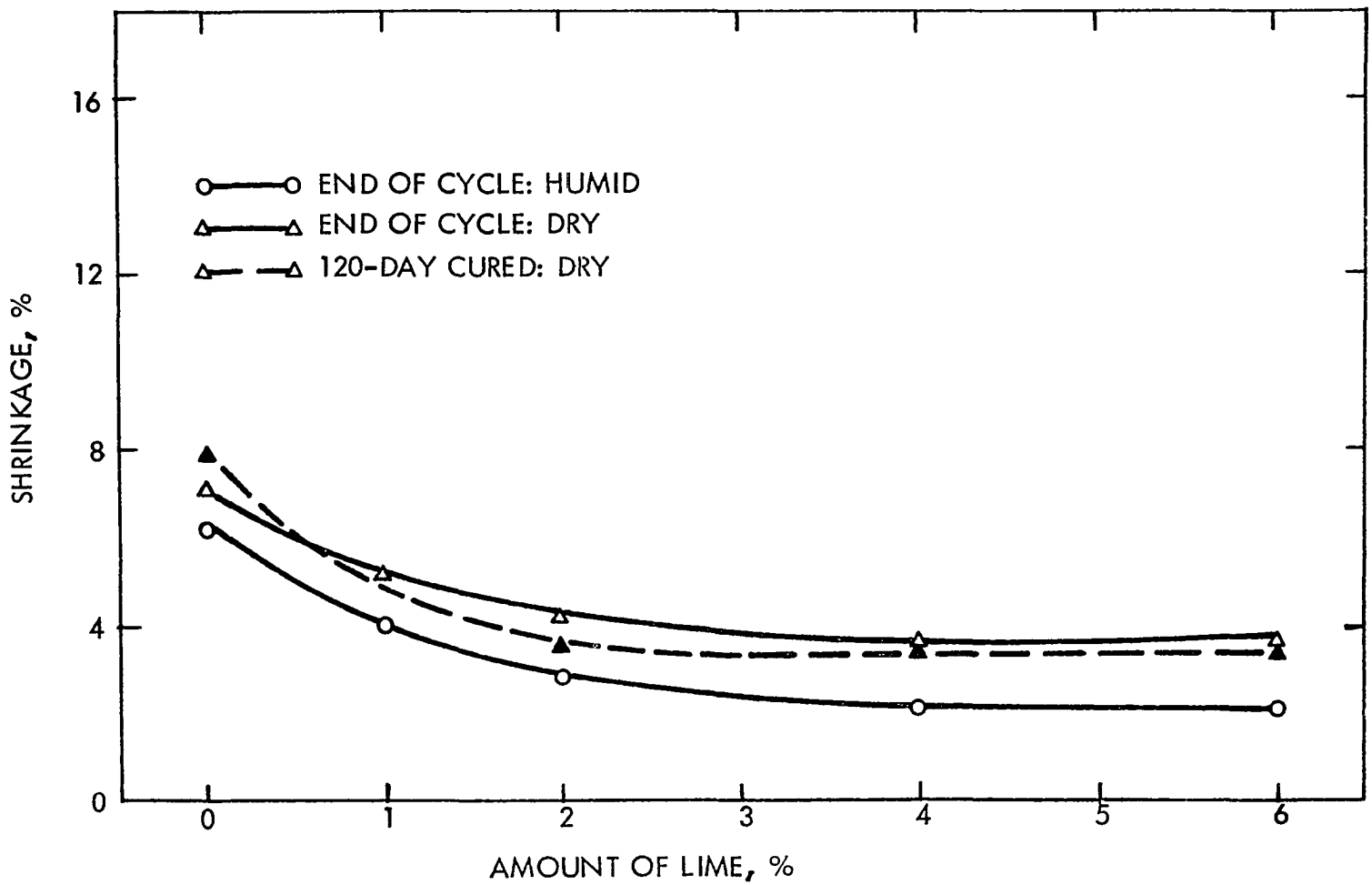


Figure C.4. Shrinkage of shale and shale lime mix samples for shale 24 at the end of wet-dry cycles and of 120-day curing.

APPENDIX D

TEST DATA FOR SHALE AND SHALE LIME MIX SAMPLES

TABLE D.1

TEST DATA FOR SHALE AND SHALE LIME MIX SAMPLES

Shale No. 13 Test Condition: Humid

No. of Wet-Dry Cycles	Amount of Lime %	Replicate	Height of Sample in.	Diam. of Sample in.	Failure Data		
					Diam. Strain x 10^{-4}	Load lb	Frequency APM[a]
0	0	1	2.922	1.352	154	40	40
		2	2.938	1.344	143	80	6
	1	1	3.016	1.344	48	40	12
		2	3.000	1.352	47	40	40
	2	1	--	--	36	70	6
		2	2.984	1.352	59	40	24
	4	1	2.984	1.352	47	40	40
		2	2.830	1.352	--	--	--
	6	1	2.891	1.352	47	40	40
		2	2.883	1.352	59	40	40
5	0	1	2.815	1.305	123	80	6
		2	2.875	1.310	110	40	40
	1	1	2.925	1.305	86	40	12
		2	2.925	1.305	--	--	--
	2	1	2.835	1.325	36	40	40
		2	2.820	1.320	85	40	40
	4	1	2.790	1.330	60	80	6
		2	2.790	1.330	60	40	40
	6	1	2.825	1.325	72	80	6
		2	2.930	1.335	72	40	12
15	0	1	2.870	1.295	86	40	40
		2	2.900	1.295	62	40	40
	1	1	2.915	1.312	73	40	6
		2	2.930	1.305	74	40	6
	2	1	2.865	1.320	73	40	6
		2	2.930	1.320	85	40	6
	4	1	2.825	1.335	72	40	12
		2	2.825	1.335	72	40	12
	6	1	2.960	1.345	--	--	--
		2	--	--	--	--	--
30	0	1	2.859	1.281	75	40	6
		2	2.875	1.297	86	40	12
	1	1	2.938	1.297	74	40	40
		2	2.938	1.297	--	--	--

TABLE D.1--Continued

No. of Wet-Dry Cycles	Amount of Lime %	Replicate	Height of Sample in.	Diam. of Sample in.	Failure Data		
					Diam. Strain x 10^{-4}	Load lb	Frequency APM[a]
30	2	1	2.922	1.313	61	40	6
		2	2.938	1.344	--	--	--
	4	1	2.938	1.328	--	--	--
		2	2.938	1.328	--	--	--
	6	1	2.938	1.328	--	--	--
		2	2.922	1.328	--	--	--
50	0	1	2.844	1.297	62	80	12
		2	--	--	--	--	--
	1	1	2.875	1.313	61	40	40
		2	2.969	1.313	73	40	12
	2	1	2.953	1.313	73	40	12
		2	2.922	1.313	85	40	6
	4	1	2.833	1.328	60	40	6
		2	2.953	1.328	--	--	--
	6	1	2.875	1.336	60	80	6
		2	2.906	1.328	--	--	--
Samples Cured for 120-Days							
	0	1	2.906	1.344	131	40	6
		2	2.891	1.344	131	40	6
	2	1	2.875	1.352	71	80	6
		2	2.883	--	59	80	6
	4	1	2.867	1.352	71	120	6
		2	2.883	1.352	71	160	12
	6	1	2.977	1.344	71	160	12
		2	2.899	1.352	95	160	12

[a]Applications per minute.

TABLE D.2

TEST DATA FOR SHALE AND SHALE LIME MIX SAMPLES
Shale No. 13 Test Condition: Dry

No. of Wet-Dry Cycles	Amount of Lime %	Replicate	Height of Sample in.	Diam. of Sample in.	Failure Data		
					Diam. Strain x 10^{-4}	Load lb	Frequency APM[a]
0	0	1	2.781	1.281	112	no failure	
		2	2.781	1.281	--	--	--
	1	1	2.875	1.289	99	no failure	
		2	2.891	1.281	100	no failure	
	2	1	2.891	1.313	73	80	40
		2	2.883	1.313	85	80	40
	4	1	2.906	1.336	48	80	40
		2	2.883	1.336	48	80	12
	6	1	2.808	1.344	60	120	12
		2	2.891	1.321	73	80	12
5	0	1	2.781	1.305	74	80	6
		2	2.797	1.313	61	80	40
	1	1	2.891	1.297	74	120	24
		2	2.891	1.297	74	80	12
	2	1	2.883	1.313	61	80	40
		2	2.790	1.315	73	80	24
	4	1	2.775	1.320	61	80	12
		2	2.760	1.325	60	40	40
	6	1	2.915	1.320	85	80	12
		2	2.915	1.320	85	80	12
15	0	1	2.815	1.310	73	80	40
		2	2.820	1.280	75	80	12
	1	1	--	--	--	--	--
		2	2.905	1.300	62	80	12
	2	1	2.870	1.315	73	80	12
		2	2.895	1.315	73	80	12
	4	1	2.905	1.315	73	80	24
		2	2.900	1.325	72	80	24
	6	1	2.845	1.325	85	80	24
		2	2.910	1.320	97	80	12
30	0	1	2.828	1.266	114	120	12
		2	2.813	1.266	88	120	12
	1	1	2.875	1.297	86	120	24
		2	2.875	1.297	74	120	12

TABLE D.2--Continued

No. of Wet-Dry Cycles	Amount of Lime %	Replicate	Height of Sample in.	Diam. of Sample in.	Failure Data		
					Diam. Strain x 10^{-4}	Load lb	Frequency APM[a]
30	2	1	2.899	1.313	73	80	24
		2	2.899	1.313	73	80	6
	4	1	2.906	1.344	71	80	6
		2	2.906	1.313	48	80	6
	6	1	2.922	1.313	73	80	12
		2	2.906	1.313	73	80	6
50	0	1	2.813	1.344	95	120	24
		2	2.797	1.344	95	120	24
	1	1	2.859	1.297	86	120	12
		2	2.875	1.297	86	120	24
	2	1	2.859	1.313	85	80	40
		2	2.922	1.305	74	120	24
	4	1	--	--	--	--	--
		2	2.859	1.313	73	80	40
	6	1	2.844	1.313	73	120	6
		2	2.844	1.313	73	80	40
Samples Cured for 120-Days							
	0	1	2.821	1.281	75	80	12
		2	2.813	1.274	--	--	--
	2	1	2.789	1.313	97	no	failure
		2	2.813	1.313	--	--	--
	4	1	2.789	1.321	95	no	failure
		2	2.875	1.313	--	--	--
	6	1	2.821	1.321	85	no	failure
		2	2.875	1.313	--	--	--

[a]Applications per minute.

TABLE D.3

TEST DATA FOR SHALE AND SHALE LIME MIX SAMPLES

Shale No. 15 Test Condition: Humid

No. of Wet-Dry Cycles	Amount of Lime %	Replicate	Height of Sample in.	Diam. of Sample in.	Failure Data		
					Diam. Strain x 10^{-4}	Load lb	Frequency APM[a]
0	0	1	3.000	1.352	--	--	--
		2	3.008	1.344	--	--	--
	1	1	3.016	1.352	--	--	--
		2	3.016	1.352	--	--	--
	2	1	3.016	1.352	--	--	--
		2	3.016	1.352	--	--	--
	4	1	3.008	1.352	--	--	--
		2	3.008	1.352	--	--	--
	6	1	3.000	1.352	--	--	--
		2	2.969	1.352	--	--	--
5	0	1	2.965	1.345	95	40	6
		2	2.975	1.340	--	--	--
	1	1	2.990	1.350	--	--	--
		2	2.975	1.350	--	--	--
	2	1	2.985	1.350	--	--	--
		2	2.975	1.350	--	--	--
	4	1	2.960	1.350	--	--	--
		2	2.955	1.350	71	40	6
	6	1	2.945	1.355	71	40	40
		2	2.960	1.350	83	40	40
15	0	1	2.965	1.345	48	40	6
		2	2.970	1.340	84	40	6
	1	1	2.990	1.355	--	--	--
		2	2.990	1.350	--	--	--
	2	1	3.000	1.355	--	--	--
		2	3.000	1.350	--	--	--
	4	1	2.975	1.345	--	--	--
		2	2.975	1.350	--	--	--
	6	1	2.945	1.345	59	40	12
		2	2.970	1.355	47	40	6
30	0	1	2.984	1.344	48	40	24
		2	2.984	1.344	48	40	6
	1	1	--	--	--	--	--
		2	2.984	1.344	--	--	--

TABLE D.3--Continued

No. of Wet-Dry Cycles	Amount of Lime %	Replicate	Height of Sample in.	Diam. of Sample in.	Failure Date		
					Diam. Strain x 10^{-4}	Load lb	Frequency APM[a]
30	2	1	--	--	--	--	--
		2	2.984	1.344	--	--	--
	4	1	2.969	1.344	--	--	--
		2	2.969	1.344	--	--	--
	6	1	2.984	1.344	60	40	12
		2	2.984	1.344	60	40	6
50	0	1	2.969	1.352	59	40	12
		2	2.969	1.352	83	40	40
	1	1	2.969	1.344	--	--	--
		2	2.969	1.344	--	--	--
	2	1	2.969	1.344	--	--	--
		2	2.969	1.344	--	--	--
	4	1	2.953	1.344	--	--	--
		2	2.969	1.344	--	--	--
	6	1	2.922	1.344	--	--	--
		2	2.930	1.344	48	40	6
Samples Cured for 120-Days							
	0	1	3.000	1.352	--	--	--
		2	2.992	1.352	--	--	--
	2	1	3,000	1.359	106	160	6
		2	3,000	1.352	--	--	--
	4	1	2.953	1.352	83	160	12
		2	2.953	1.359	--	--	--
	6	1	2.938	1.359	47	80	12
		2	--	--	47	80	12

[a]Applications per minute.

TABLE D.4

TEST DATA FOR SHALE AND SHALE LIME MIX SAMPLES

Shale No. 15 Test Condition: Dry

No. of Wet-Dry Cycles	Amount of Lime %	Replicate	Height of Sample in.	Diam. of Sample in.	Failure Data		
					Diam. Strain x 10^{-4}	Load lb	Frequency APM[a]
0	0	1	--	--	96	80	12
		2	2.969	1.328	96	80	40
	1	1	2.969	1.3 4	71	40	24
		2	2.938	1.344	71	80	12
	2	1	2.977	1.344	83	40	40
		2	2.977	1.344	71	40	12
	4	1	--	--	71	40	12
		2	2.984	1.344	83	40	12
	6	1	--	--	71	40	40
		2	2.969	1.344	71	40	40
5	0	1	2.975	1.340	84	80	6
		2	2.970	1.335	84	80	6
	1	1	2.975	1.345	71	40	6
		2	2.975	1.345	83	40	12
	2	1	2.980	1.345	83	40	24
		2	2.970	1.350	83	40	6
	4	1	2.960	1.350	95	40	24
		2	2.965	1.350	83	40	12
	6	1	2.955	1.350	71	40	40
		2	2.955	1.350	71	40	40
15	0	1	2.970	1.340	72	40	40
		2	2.970	1.340	84	40	40
	1	1	2.9 0	1.350	83	80	6
		2	2.970	1.350	71	80	6
	2	1	2.980	1.345	95	40	12
		2	2.980	1.345	83	40	40
	4	1	2.965	1.350	59	40	12
		2	2.965	1.350	83	40	40
	6	1	2.965	1.345	48	80	6
		2	2.930	1.345	59	80	6
30	0	1	2.969	1.328	72	80	12
		2	2.969	1.336	85	80	24
	1	1	2.969	1.344	71	80	6
		2	2.969	1.344	83	40	24

TABLE D.4--Continued

No. of Wet-Dry Cycles	Amount of Lime %	Replicate	Height of Sample in.	Diam. of Sample in.	Failure Data		
					Diam. Strain x 10^{-4}	Load lb	Frequency APM[a]
30	2	1	2.969	1.344	71	80	6
		2	2.969	1.344	83	40	12
	4	1	2.938	1.344	71	80	6
		2	2.969	1.344	60	80	6
	6	1	2.969	1.344	48	40	40
		2	2.969	1.344	48	80	6
50	0	1	2.938	1.328	72	80	24
		2	2.953	1.328	84	80	24
	1	1	2.984	1.344	71	40	12
		2	2.953	1.344	--	--	--
	2	1	2.984	1.344	71	80	6
		2	2.922	1.336	60	80	6
	4	1	2.922	1.344	71	80	6
		2	.2938	1.344	60	80	6
	6	1	2.906	1.344	24	40	12
		2	--	--	--	--	--
Samples Cured for 120-Days							
	0	1	2.953	1.344	83	120	6
		2	.2969	1.344	71	80	12
	2	1	2.961	1.344	71	80	40
		2	2.992	1.344	--	--	--
	4	1	2.930	1.344	72	no	failure
		2	2.930	1.344	--	--	--
	6	1	2.938	1.344	71	80	12
		2	2.953	1.344	--	--	--

[a]Applications per minute.

TABLE D.5

TEST DATA FOR SHALE AND SHALE LIME MIX SAMPLES

Shale No. 21 Test Condition: Humid

No. of Wet-Dry Cycles	Amount of Lime %	Replicate	Height of Sample in.	Diam. of Sample in.	Failure Data		
					Diam. Strain x 10^{-4}	Load lb	Frequency APM[a]
0	0	1	3.016	1.352	--	--	--
		2	3.008	1.344	--	--	--
	1	1	2.984	1.344	--	--	--
		2	2.984	1.352	--	--	--
	2	1	2.992	1.344	48	40	40
		2	2.992	1.352	59	40	40
	4	1	2.969	1.352	71	40	40
		2	3.000	1.359	47	40	40
	6	1	3.000	1.352	59	40	40
		2	2.992	1.352	71	40	40
5	0	1	2.840	1.299	87	80	12
		2	2.895	1.285	100	80	12
	1	1	2.880	1.325	72	40	40
		2	2.875	1.315	97	40	12
	2	1	2.935	1.315	--	--	--
		2	2.930	1.325	--	--	--
	4	1	2.940	1.340	--	--	--
		2	2.935	1.340	--	--	--
	6	1	2.880	1.340	72	40	6
		2	2.940	1.330	60	40	6
15	0	1	2.900	1.310	61	80	6
		2	2.900	1.305	85	80	6
	1	1	2.940	1.320	--	--	--
		2	2.875	1.310	49	40	24
	2	1	2.925	1.330	--	--	--
		2	2.900	1.330	--	--	--
	4	1	2.900	1.340	--	--	--
		2	2.875	1.335	--	--	--
	6	1	2.940	1.340	--	--	--
		2	--	--	--	--	--
30	0	1	2.906	1.313	61	80	6
		2	2.906	1.313	61	80	6
	1	1	2.938	1.313	--	--	--
		2	2.891	1.313	--	--	--

TABLE D.5--Continued

No. of Wet-Dry Cycles	Amount of Lime %	Replicate	Height of Sample in.	Diam. of Sample in.	Failure Data		
					Diam. Strain x 10^{-4}	Load lb	Frequency APM[a]
30	2	1	2.906	1.328	--	--	--
		2	2.938	1.328	--	--	--
	4	1	2.969	1.320	--	--	--
		2	2.969	1.328	--	--	--
	6	1	2.938	1.328	--	--	--
		2	2.938	1.344	--	--	--
50	0	1	2.891	1.289	74	80	24
		2	2.899	1.297	74	40	40
	1	1	2.875	1.313	73	40	6
		2	2.906	1.313	73	40	6
	2	1	2.938	1.313	--	--	--
		2	--	--	--	--	--
	4	1	2.946	1.328	--	--	--
		2	2.938	1.336	--	--	--
	6	1	2.953	1.328	--	--	--
		2	2.946	1.328	--	--	--
Samples Cured for 120-Days							
	0	1	2.969	1.344	--	--	--
		2	2.969	1.344	--	--	--
	2	1	2.992	1.352	83	80	6
		2	2.992	1.359	82	80	6
	4	1	2.938	1.352	36	80	24
		2	2.953	1.359	59	80	24
	6	1	2.969	1.352	71	120	12
		2	2.984	1.352	--	--	--

[a]Applications per minute.

TABLE D.6

TEST DATA FOR SHALE AND SHALE LIME MIX SAMPLES

Shale No. 21 Test Condition: Dry

No. of Wet-Dry Cycles	Amount of Lime %	Replicate	Height of Sample in.	Diam. of Sample in.	Failure Data		
					Diam. Strain x 10^{-4}	Load lb	Frequency APM[a]
0	0	1	2.789	1.274	151	160	12
		2	2.789	1.258	178	120	24
	1	1	2.844	1.352	118	70	12
		2	2.859	1.344	95	120	6
	2	1	2.891	1.313	61	80	12
		2	2.906	1.313	73	80	6
	4	1	2.922	1.352	--	--	--
		2	2.906	1.321	--	--	--
	6	1	2.938	1.328	59	40	24
		2	2.914	1.328	71	40	24
5	0	1	2.815	1.290	136	120	24
		2	2.820	1.285	87	40	12
	1	1	2.870	1.325	97	80	12
		2	2.865	1.305	98	80	12
	2	1	2.905	1.315	85	40	40
		2	2.900	1.310	--	--	--
	4	1	2.905	1.325	--	--	--
		2	2.905	1.325	--	--	--
	6	1	2.895	1.330	60	40	6
		2	2.905	1.330	60	40	6
15	0	1	2.880	1.295	74	120	12
		2	2.880	1.295	74	120	12
	1	1	2.870	1.305	61	80	12
		2	2.865	1.305	61	80	6
	2	1	2.895	1.340	72	80	6
		2	2.890	1.315	61	80	6
	4	1	2.825	1.325	36	40	40
		2	2.865	1.325	36	40	12
	6	1	2.915	1.325	48	40	40
		2	2.935	1.330	36	40	24
30	0	1	2.859	1.305	74	80	12
		2	2.883	1.305	98	120	24
	1	1	2.906	1.313	85	80	12
		2	2.859	1.313	85	80	40

TABLE D.6--Continued

No. of Wet-Dry Cycles	Amount of Lime %	Replicate	Height of Sample in.	Diam. of Sample in.	Failure Data		
					Diam. Strain x 10^{-4}	Load lb	Frequency APM[a]
30	2	1	2.891	1.328	84	40	40
		2	2.906	1.320	85	80	6
	4	1	2.922	1.313	--	--	--
		2	2.891	1.321	--	--	--
	6	1	2.922	1.321	61	40	40
		2	2.906	1.313	49	40	40
50	0	1	2.859	1.281	100	80	12
		2	2.859	1.281	87	80	12
	1	1	2.875	1.297	86	80	24
		2	2.844	1.289	87	80	24
	2	1	--	--	--	--	--
		2	2.891	1.313	97	80	40
	4	1	2.906	1.321	48	80	6
		2	2.906	1.321	36	80	6
	6	1	2.922	1.321	73	80	6
		2	2.914	1.328	72	40	40
Samples Cured for 120-Days							
	0	1	2.821	1.258	64	80	24
		2	2.813	1.258	--	--	--
	2	1	2.899	1.313	61	40	24
		2	2.891	1.313	73	80	24
	4	1	2.899	1.313	85	40	24
		2	2.922	1.313	73	40	24
	6	1	2.930	1.328	84	80	6
		2	2.938	1.328	84	80	6

[a]Applications per minute.

TABLE D.7

TEST DATA FOR SHALE AND SHALE LIME MIX SAMPLES

Shale No. 24 Test Condition: Humid

No. of Wet-Dry Cycles	Amount of Lime %	Replicate	Height of Sample in.	Diam. of Sample in.	Failure Data		
					Diam. Strain x 10^{-4}	Load lb	Frequency APM[a]
0	0	1	3.016	1.344	--	--	--
		2	3.000	1.344	--	--	--
	1	1	3.000	1.344	--	--	--
		2	2.953	1.344	95	40	24
	2	1	3.000	1.344	83	40	40
		2	3.000	1.352	107	40	40
	4	1	2.984	1.352	83	40	6
		2	2.977	1.352	--	--	--
	6	1	3.000	1.352	--	--	--
		2	3.000	1.352	--	--	--
5	0	1	2.910	1.352	72	40	40
		2	2.900	1.352	72	40	40
	1	1	2.900	1.340	72	40	12
		2	2.920	1.350	59	40	6
	2	1	2.850	1.345	--	--	--
		2	2.875	1.340	--	--	--
	4	1	2.845	1.345	48	40	6
		2	2.850	1.345	--	--	--
	6	1	2.850	1.350	95	40	24
		2	--	--	--	--	--
15	0	1	2.925	1.325	60	80	12
		2	2.925	1.325	60	80	6
	1	1	2.906	1.336	--	--	--
		2	2.938	1.336	--	--	--
	2	1	2.875	1.344	--	--	--
		2	--	--	--	--	--
	4	1	2.844	1.344	71	40	6
		2	2.836	1.344	--	--	--
	6	1	2.891	1.344	71	40	6
		2	2.859	1.344	60	40	12
30	0	1	2.938	1.313	61	40	40
		2	2.906	1.328	84	40	40
	1	1	2.891	1.328	--	--	--
		2	2.891	1.328	--	--	--

TABLE D.7--Continued

No. of Wet-Dry Cycles	Amount of Lime %	Replicate	Height of Sample in.	Diam. of Sample in.	Failure Data		
					Diam. Strain x 10^{-4}	Load lb	Frequency APM[a]
30	2	1	2.969	1.344	--	--	--
		2	2.883	1.344	--	--	--
	4	1	2.953	1.344	--	--	--
		2	2.859	1.344	--	--	--
	6	1	--	--	--	--	--
		2	2.859	1.344	--	--	--
50	0	1	2.922	1.313	73	80	12
		2	2.938	1.313	61	80	12
	1	1	2.969	1.328	--	--	--
		2	2.969	1.328	--	--	--
	2	1	2.961	1.336	--	--	--
		2	2.969	1.336	--	--	--
	4	1	2.891	1.344	--	--	--
		2	2.891	1.344	--	--	--
	6	1	2.891	1.344	--	--	--
		2	2.914	1.344	--	--	--
Samples Cured for 120-Days							
	0	1	2.953	1.344	--	--	--
		2	2.969	1.344	--	--	--
	2	1	2.922	1.352	71	80	12
		2	2.961	1.352	71	80	6
	4	1	2.906	1.352	59	80	24
		2	2.906	1.352	71	80	24
	6	1	2.899	1.352	59	80	24
		2	2.883	1.352	71	80	24

[a]Applications per minute.

TABLE D.8

TEST DATA FOR SHALE AND SHALE LIME MIX SAMPLES

Shale No. 24 Test Condition: Dry

No. of Wet-Dry Cycles	Amount of Lime %	Replicate	Height of Sample in.	Diam. of Sample in.	Failure Data		
					Diam. Strain x 10^{-4}	Load lb	Frequency APM[a]
0	0	1	2.914	1.313	61	160	12
		2	2.875	1.313	85	120	12
	1	1	2.938	1.328	84	80	6
		2	2.946	1.328	60	80	6
	2	1	2.946	1.344	71	40	24
		2	2.946	1.344	71	40	12
	4	1	2.875	1.344	84	40	40
		2	2.953	1.336	95	40	24
	6	1	2.946	1.344	71	40	40
		2	2.953	1.336	84	40	24
5	0	1	2.900	1.325	97	120	12
		2	2.895	1.325	107	120	12
	1	1	2.905	1.325	96	80	6
		2	2.900	1.340	72	80	24
	2	1	2.840	1.335	96	40	40
		2	2.825	1.340	84	80	6
	4	1	2.825	1.335	84	40	24
		2	2.825	1.335	84	40	40
	6	1	2.860	1.335	84	80	6
		2	2.840	1.335	84	80	6
15	0	1	2.900	1.330	96	120	6
		2	2.938	1.321	97	120	24
	1	1	2.906	1.328	96	80	24
		2	2.906	1.328	96	80	24
	2	1	2.852	1.344	95	80	12
		2	2.859	1.344	107	40	40
	4	1	2.844	1.344	83	80	6
		2	2.797	1.344	83	80	12
	6	1	2.844	1.344	83	80	12
		2	2.844	1.344	71	80	12
30	0	1	2.891	1.313	97	120	24
		2	2.906	1.313	73	120	24
	1	1	2.891	1.328	84	40	40
		2	2.844	1.328	84	40	40

TABLE D.8--Continued

No. of Wet-Dry Cycles	Amount of Lime %	Replicate	Height of Sample in.	Diam. of Sample in.	Failure Data		
					Diam. Strain x 10^{-4}	Load lb	Frequency APM[a]
30	2	1	--	--	60	40	40
		2	2.859	1.328	72	40	40
	4	1	2.844	1.328	60	80	6
		2	2.813	1.328	72	40	12
	6	1	2.844	1.328	72	80	6
		2	2.844	1.336	84	80	12
50	0	1	2.906	1.305	86	120	40
		2	2.914	1.305	112	120	40
	1	1	2.938	1.321	73	120	24
		2	2.938	1.328	72	120	6
	2	1	2.938	1.328	84	80	12
		2	2.922	1.328	72	80	12
	4	1	2.891	1.336	84	80	40
		2	2.867	1.328	84	80	40
	6	1	2.875	1.328	84	80	6
		2	2.891	1.328	72	80	6
Samples Cured for 120-Days							
	0	1	2.875	1.313	85	120	24
		2	2.899	1.313	--	--	--
	2	1	2.906	1.328	60	80	6
		2	2.891	1.336	48	80	6
	4	1	2.852	1.336	36	80	24
		2	2.821	1.336	72	80	24
	6	1	2.875	1.336	60	80	24
		2	2.891	1.336	60	80	24

[a]Applications per minute.

APPENDIX E

EFFECT OF AMOUNT OF LIME ON DIAMETRAL STRAIN OF SAMPLES

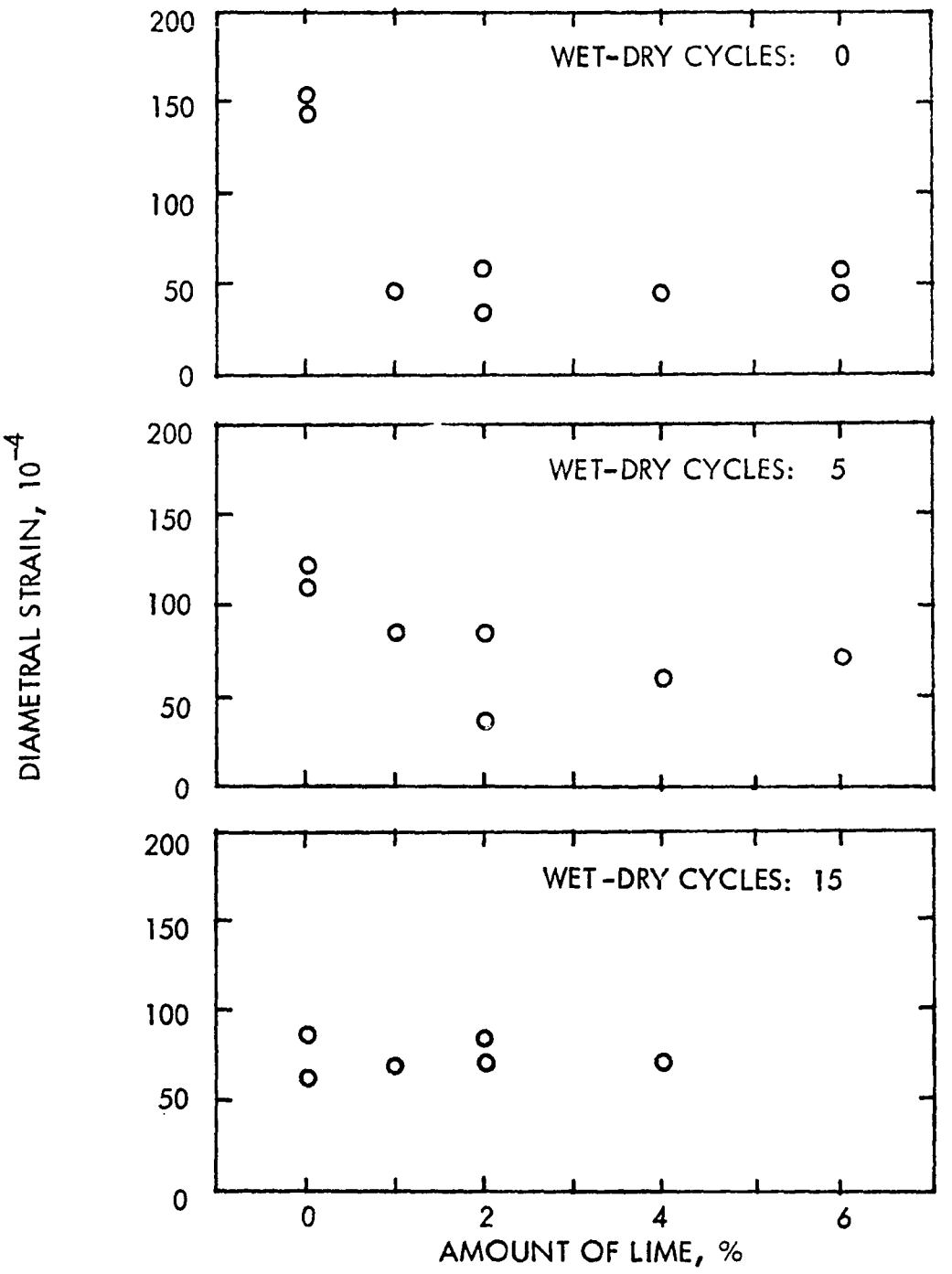


Figure E.1 Effect of amount of lime on diametral strain at failure for humid samples of shale 13.

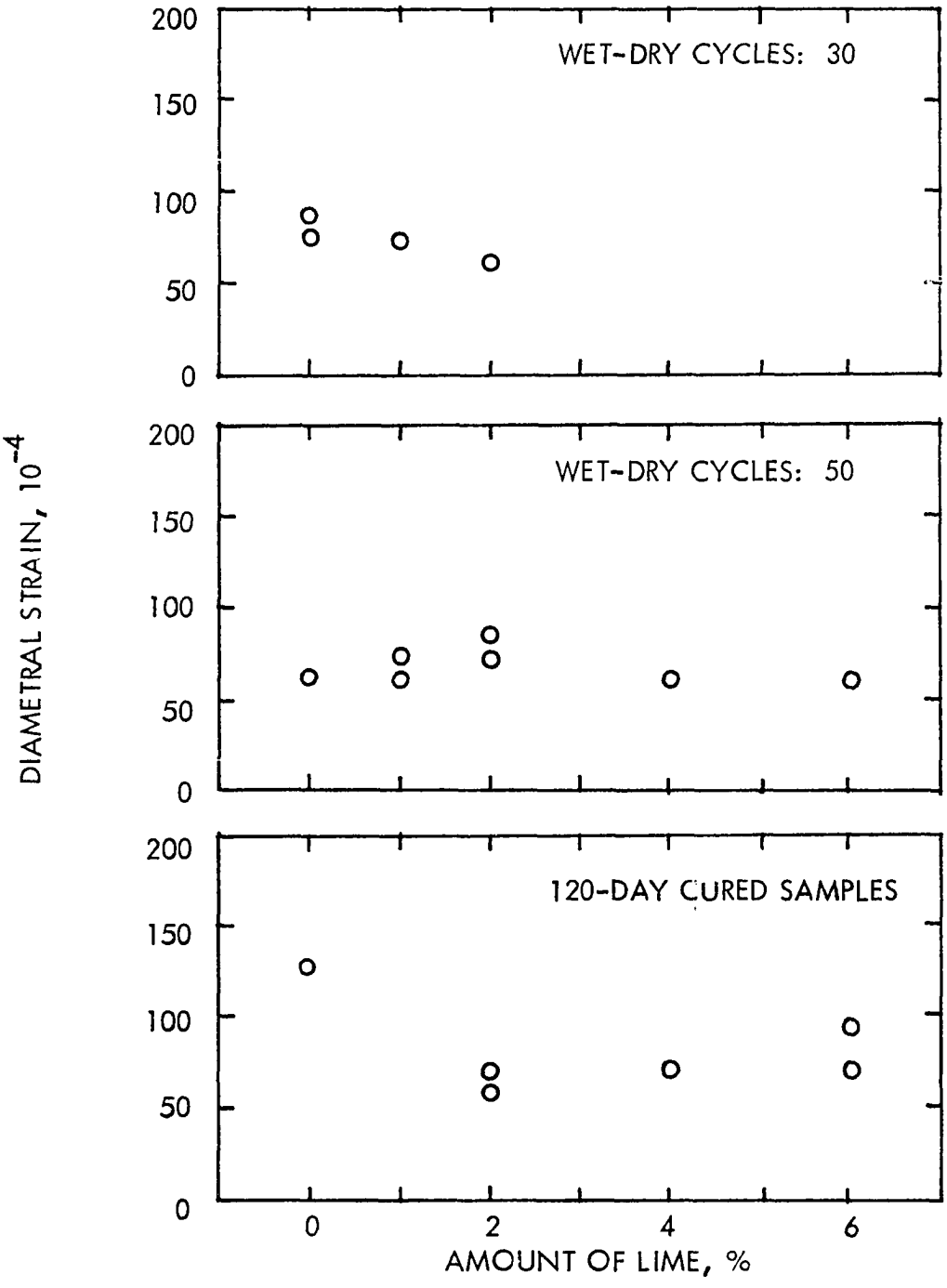


Figure E.2 Effect of amount of lime on diametral strain at failure for humid samples of shale 13.

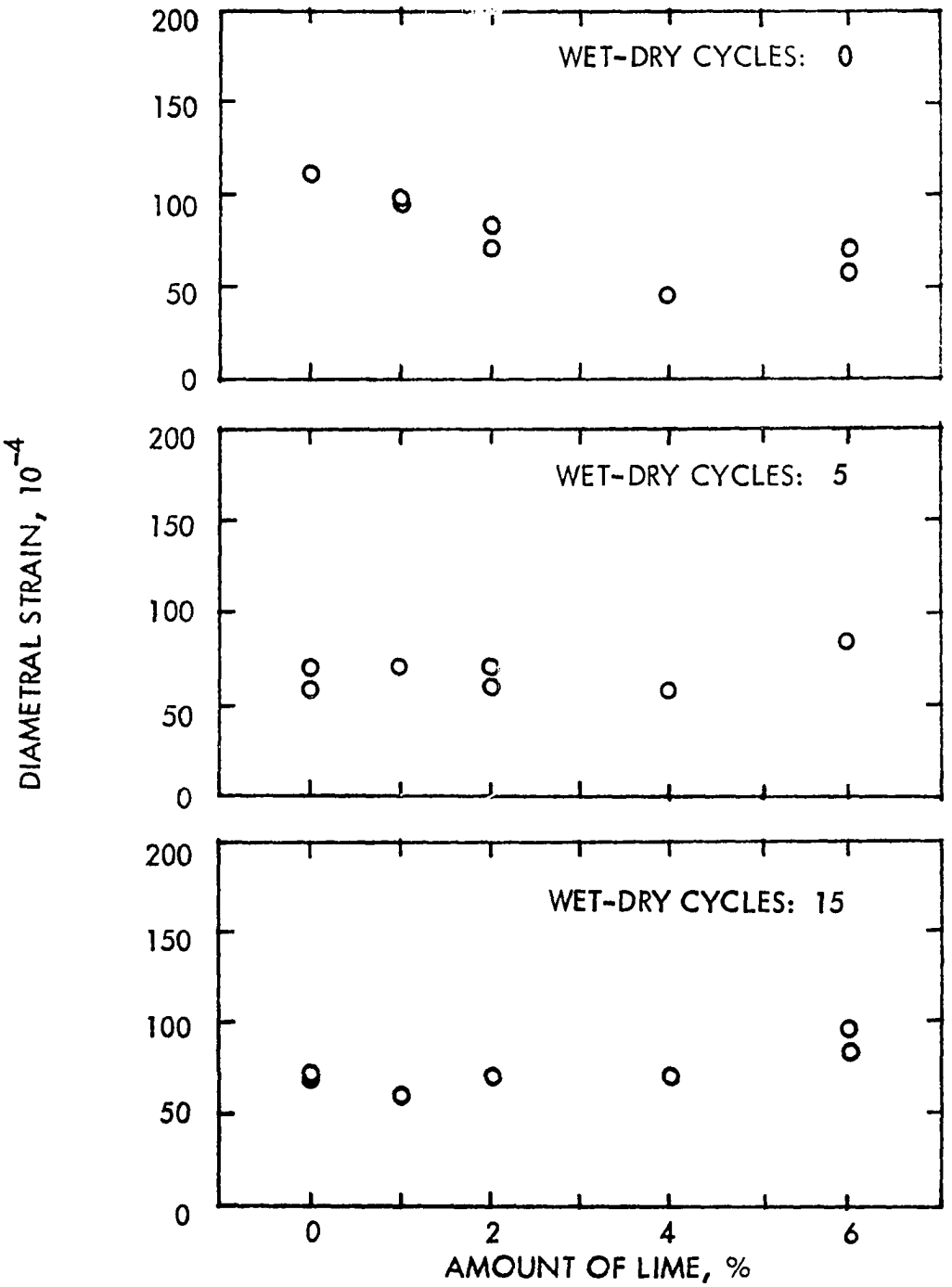


Figure E.3 Effect of amount of lime on diametral strain at failure for dry samples of shale 13.

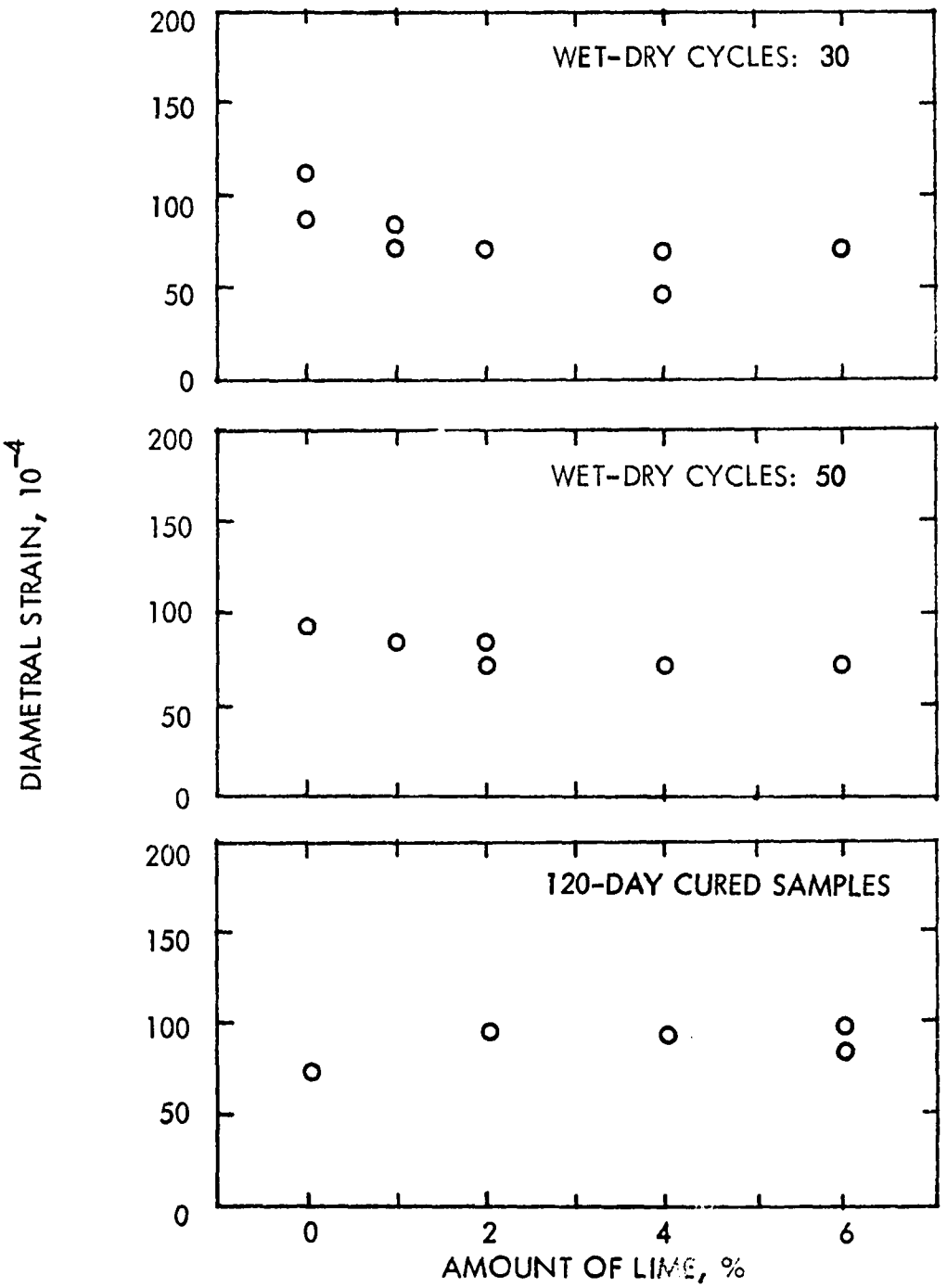


Figure E.4 Effect of amount of lime on diametral strain at failure for dry samples of shale 13.

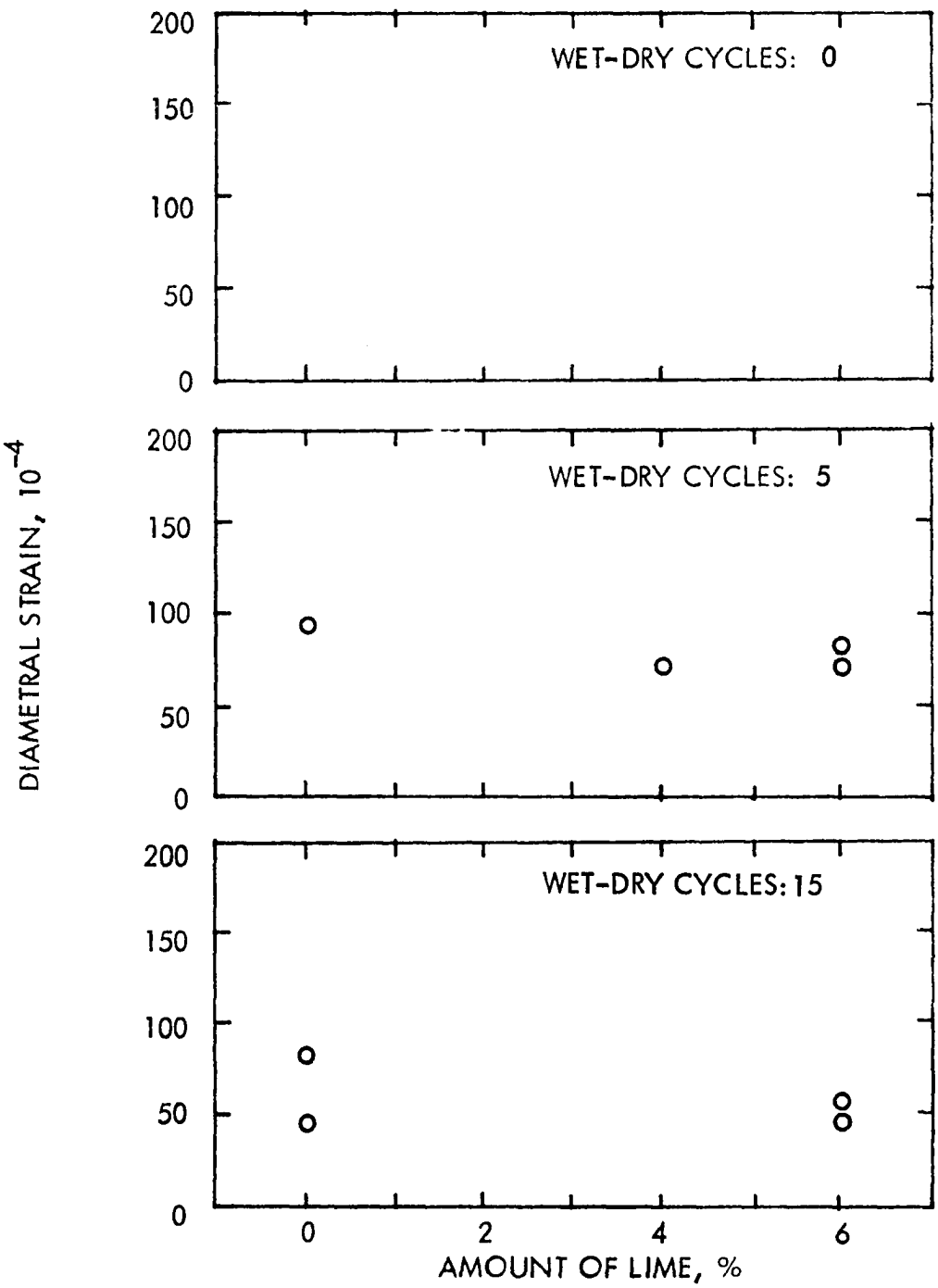


Figure E.5 Effect of amount of lime on diametral strain at failure for humid samples of shale 15.

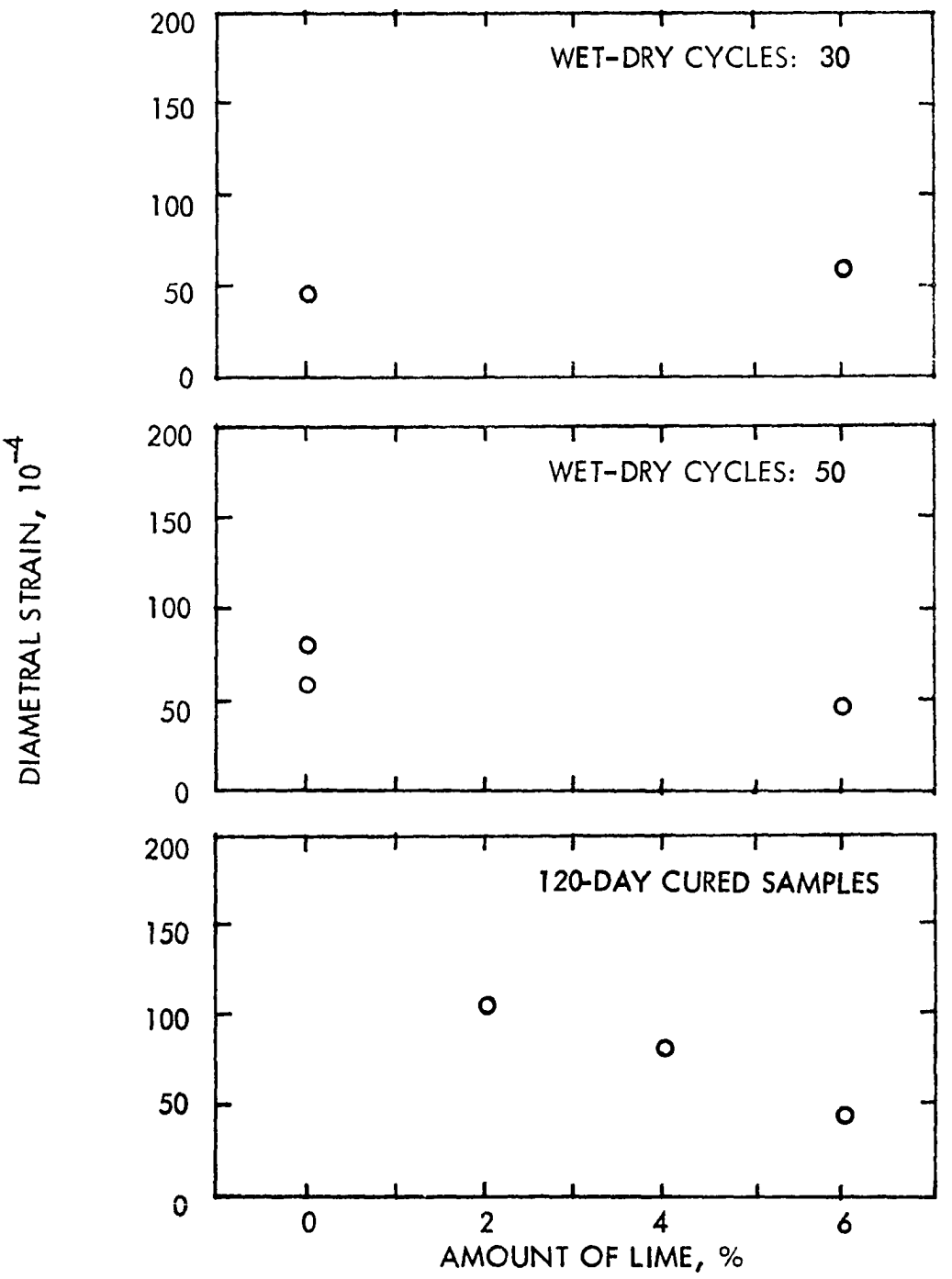


Figure E.6 Effect of amount of lime on diametral strain at failure for humid samples of shale 15.

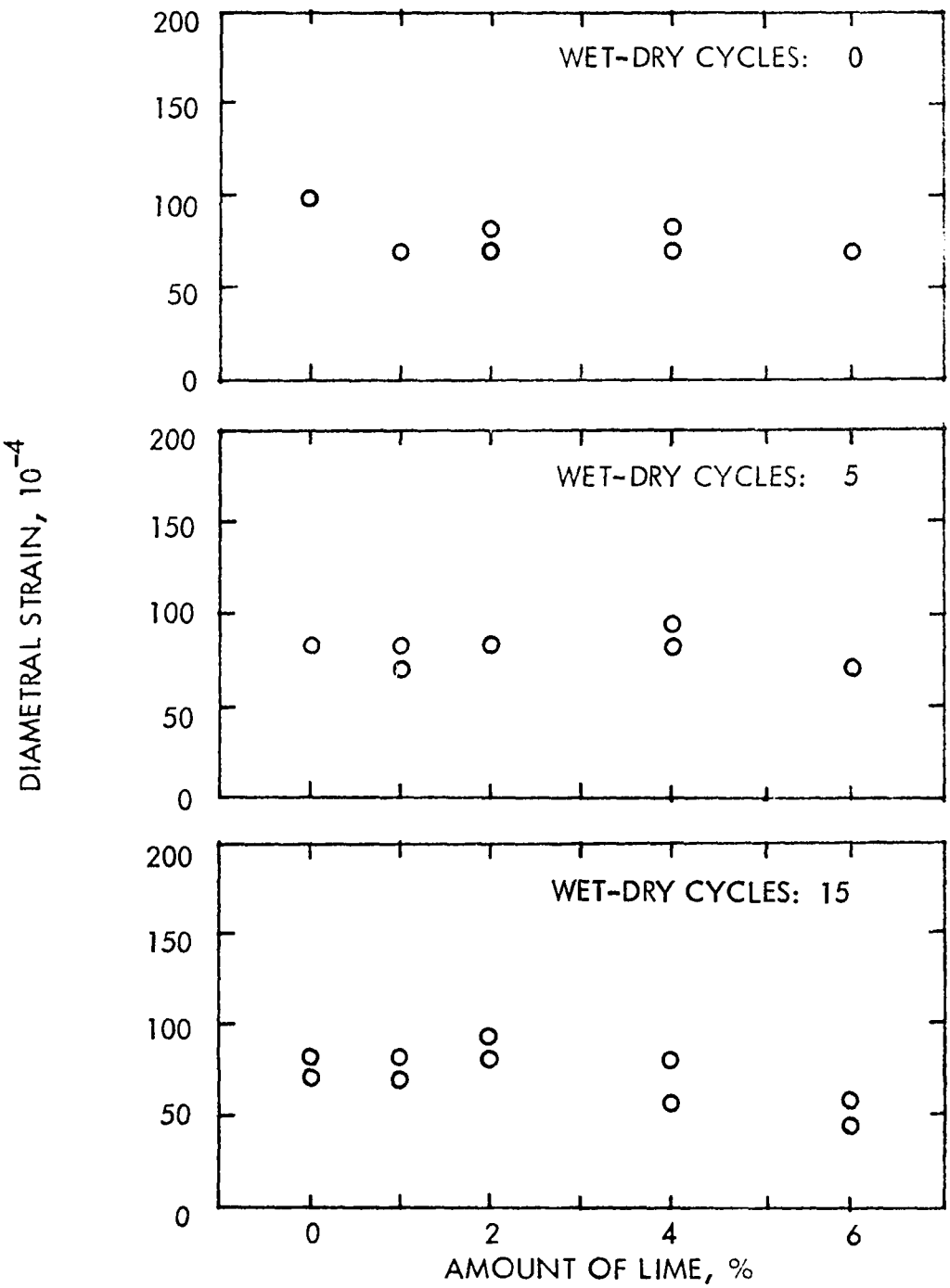


Figure E.7 Effect of amount of lime on diametral strain at failure for dry samples of shale 15.

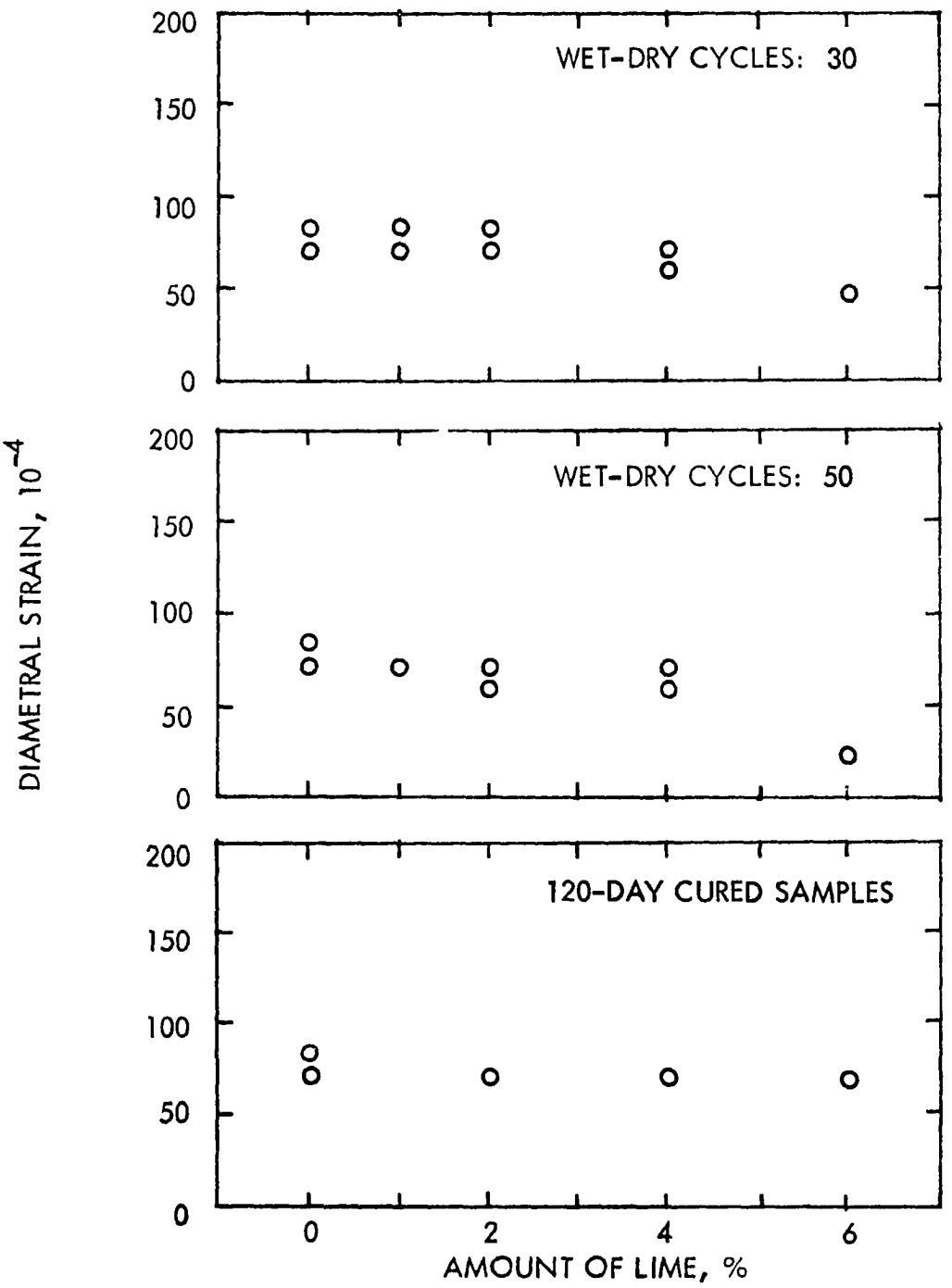


Figure E.8 Effect of amount of lime on diametral strain at failure for dry samples of shale 15.

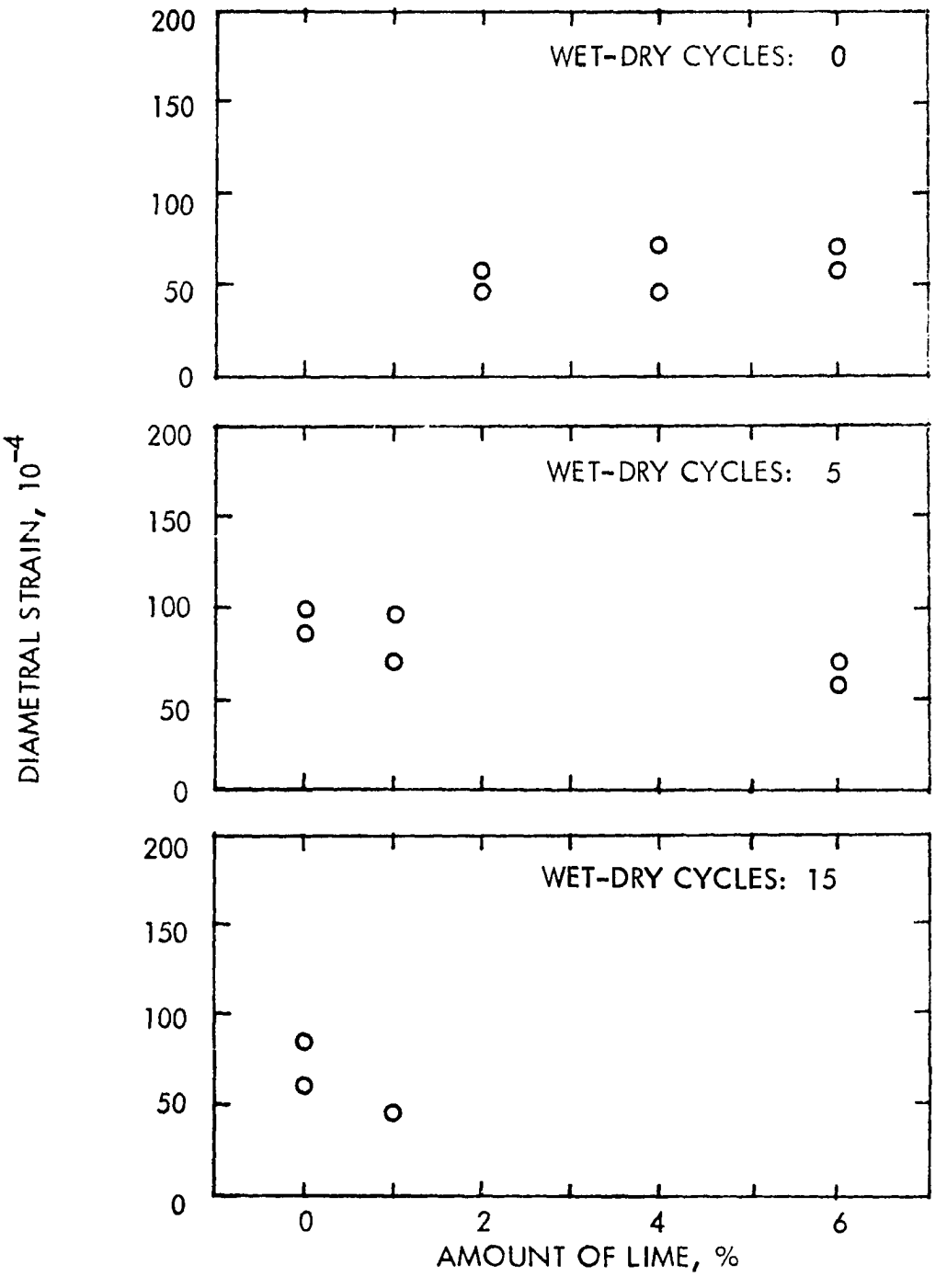


Figure E.9 Effect of amount of lime on diametral strain at failure for humid samples of shale 21.

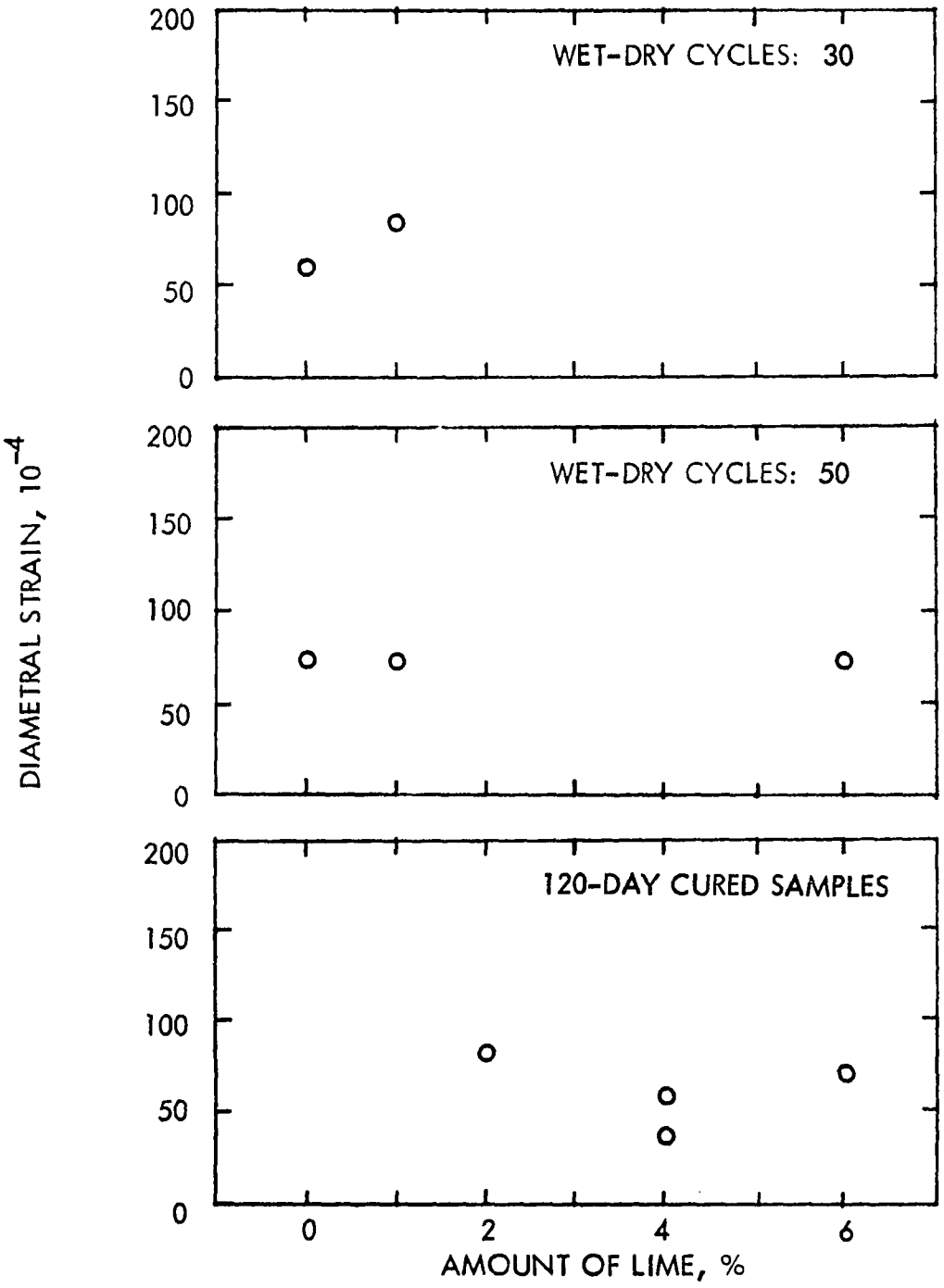


Figure E.10 Effect of amount of lime on diametral strain at failure for humid samples of shale 21.

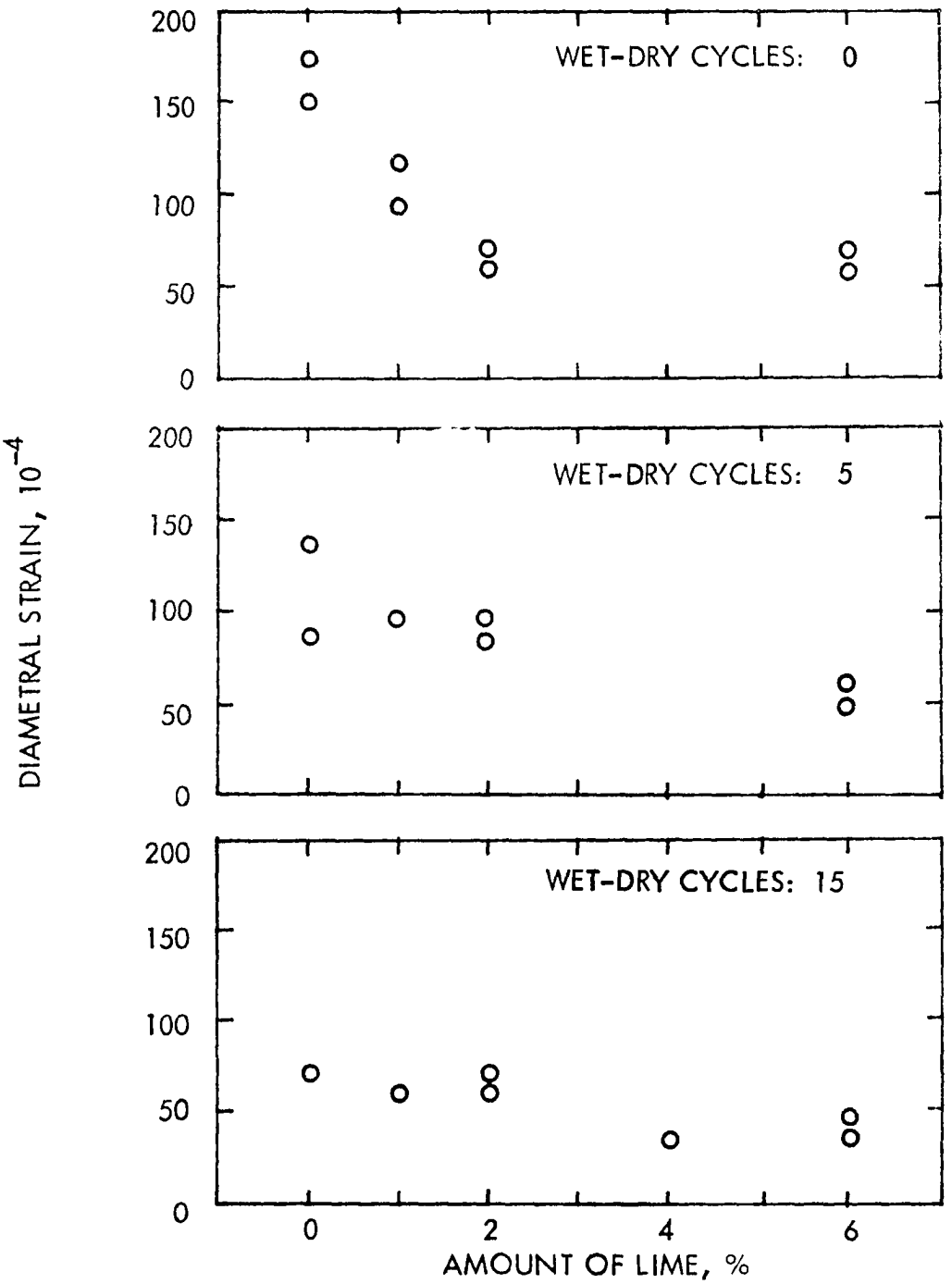


Figure E.11 Effect of amount of lime on diametral strain at failure for dry samples of shale 21.

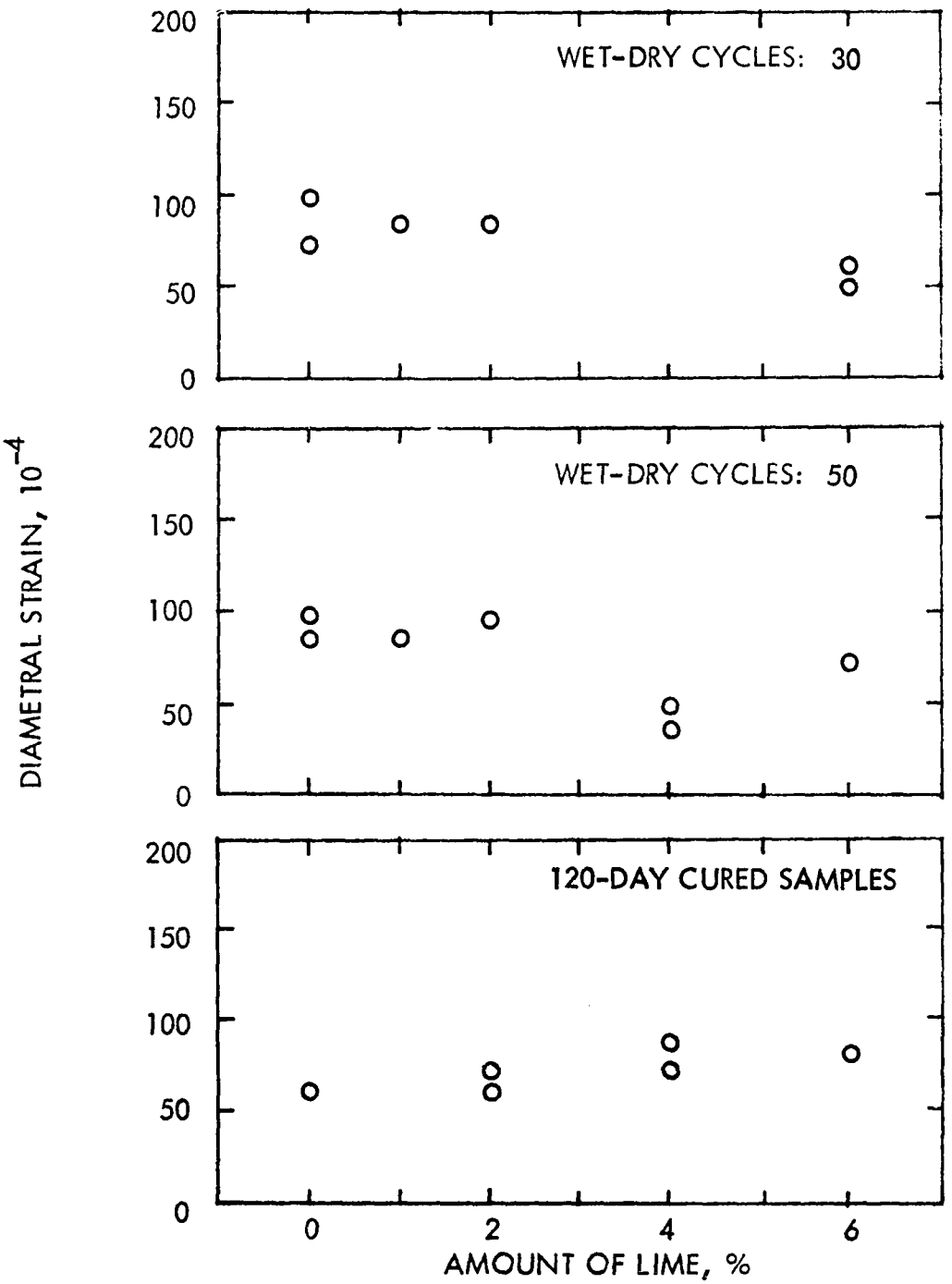


Figure E.12 Effect of amount of lime on diametral strain at failure for dry samples of shale 21.

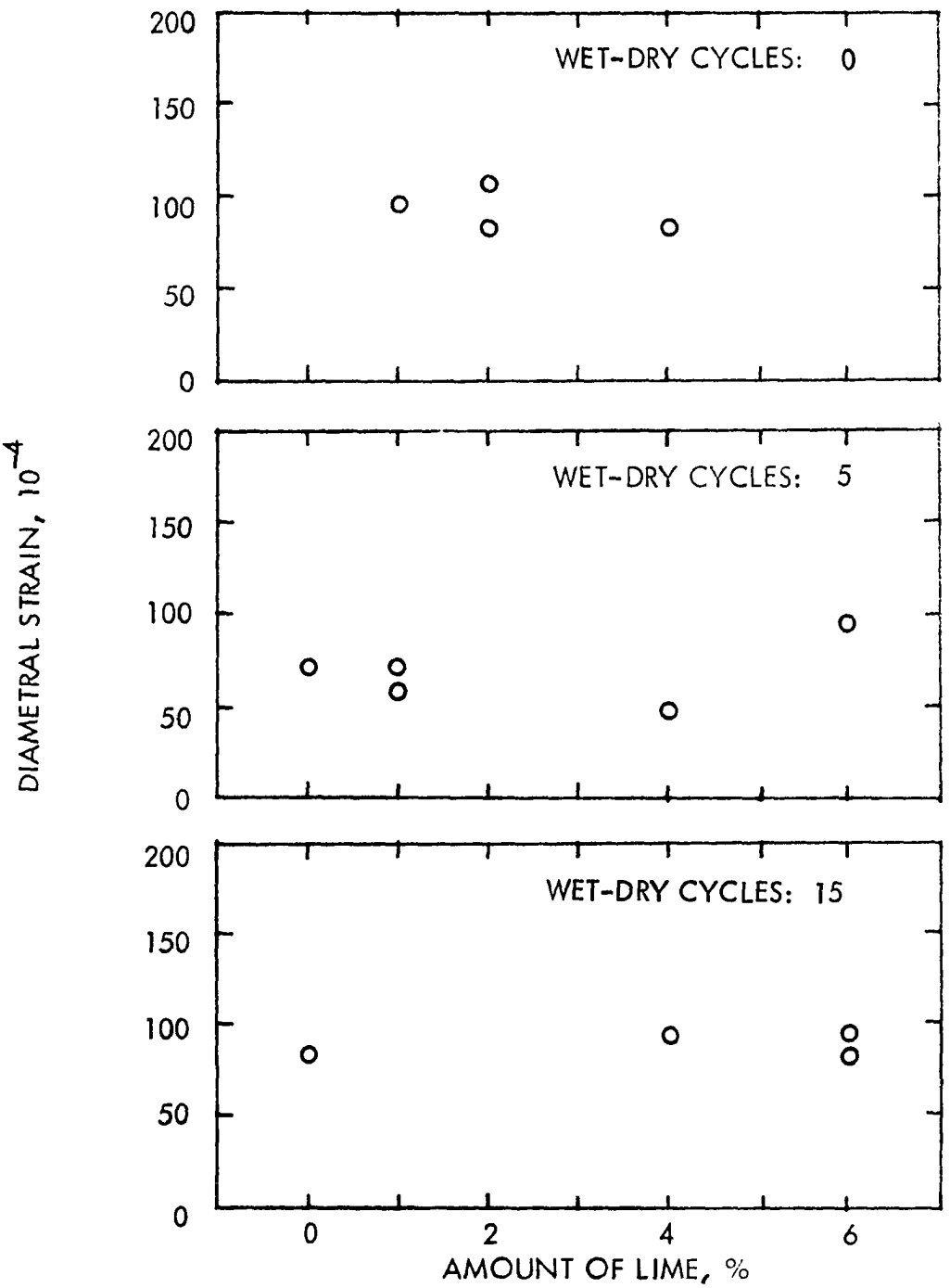


Figure E.13 Effect of amount of lime on diametral strain at failure for humid samples of shale 24.

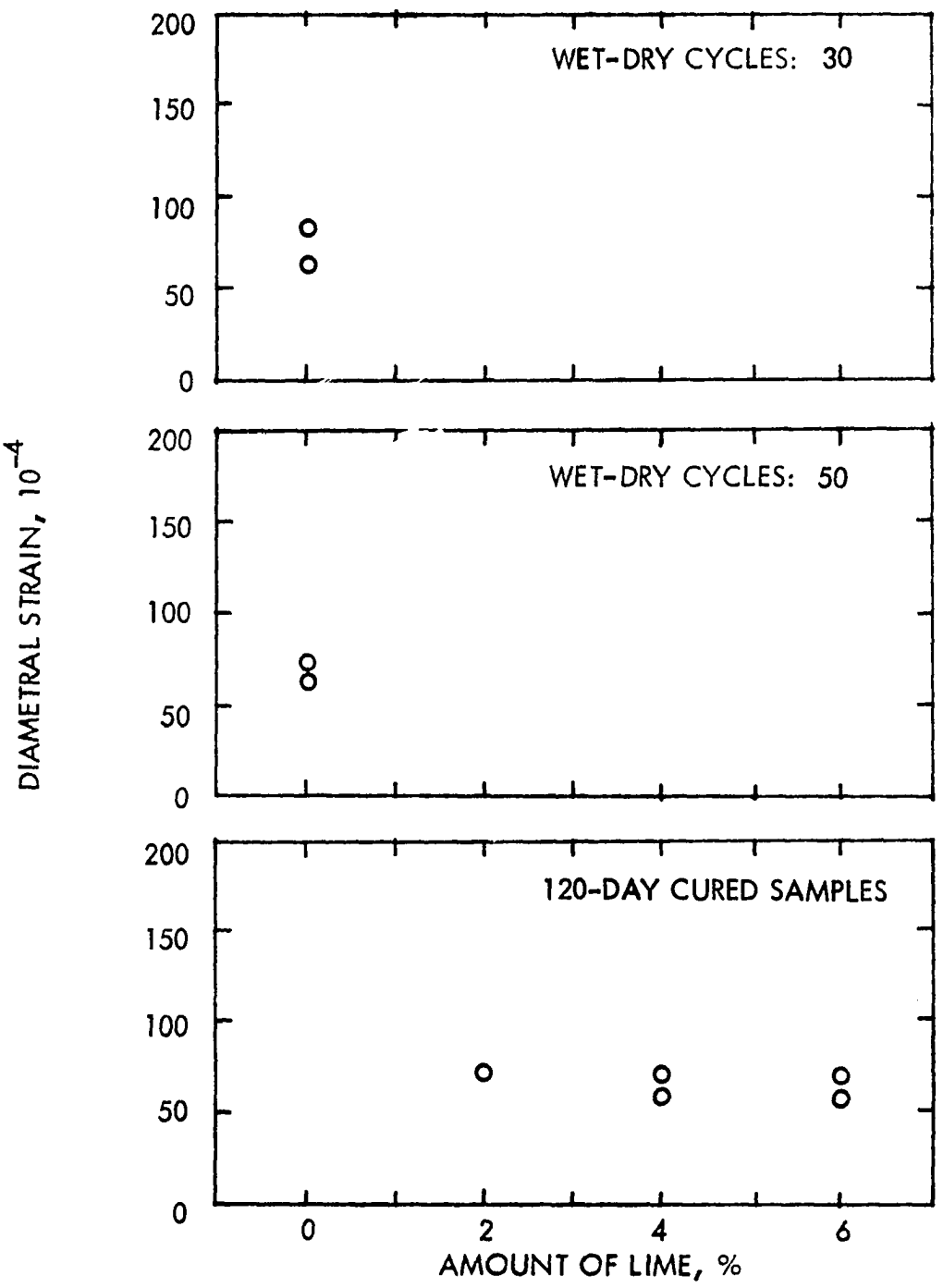


Figure E.14 Effect of amount of lime on diametral strain at failure for humid samples of shale 24.

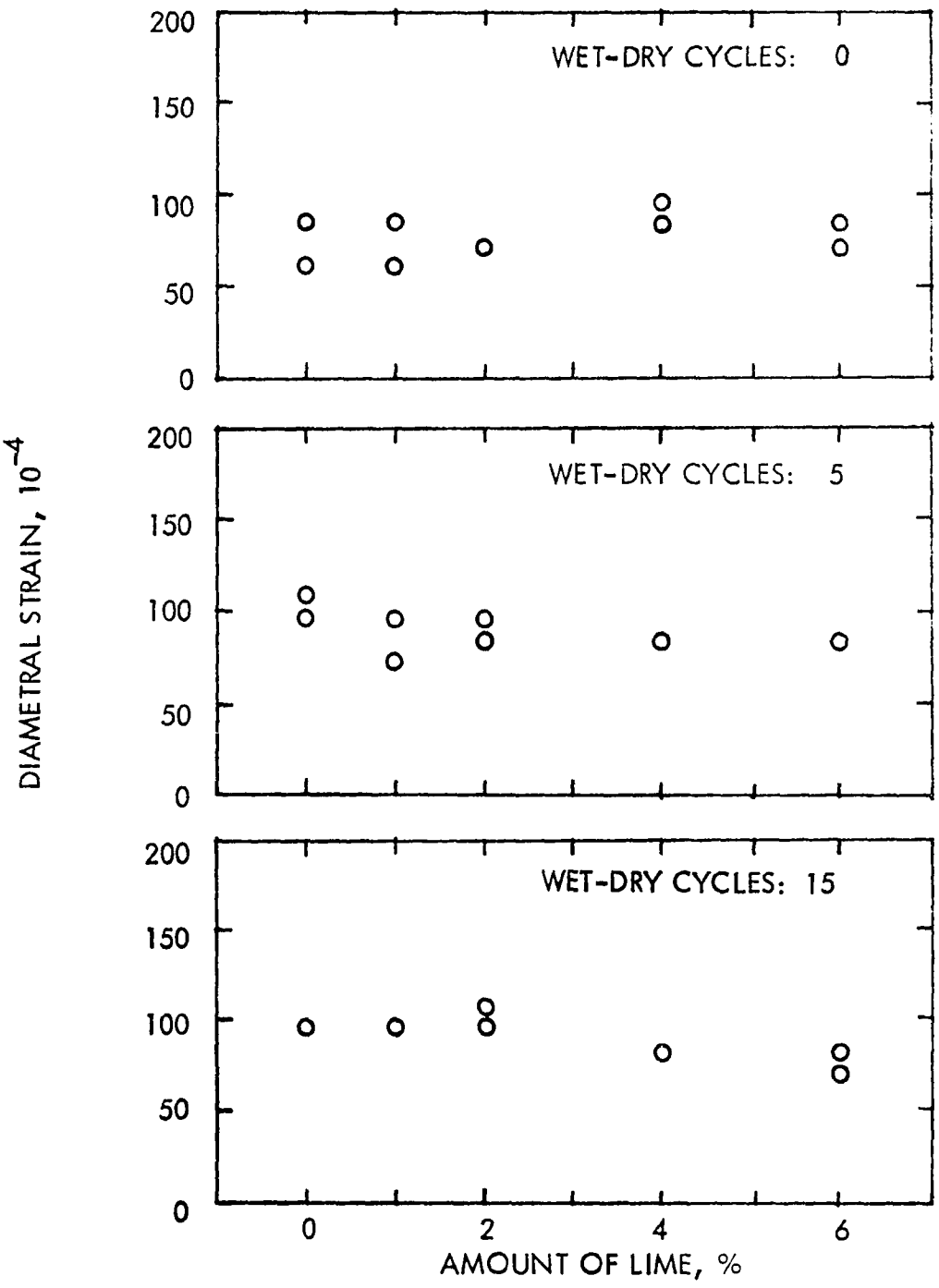


Figure E.15 Effect of amount of lime on diametral strain at failure for dry samples of shale 24.

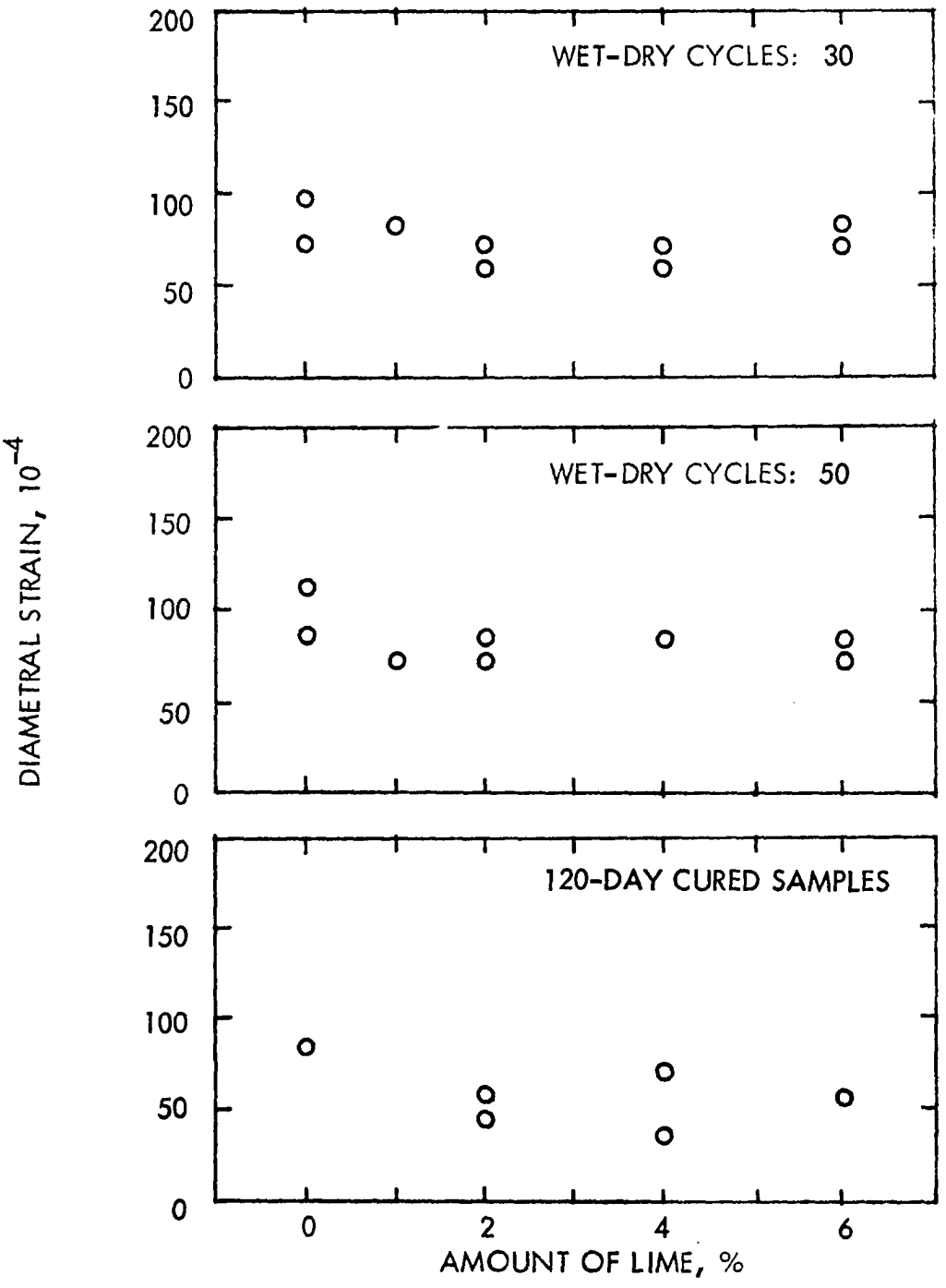


Figure E.16 Effect of amount of lime on diametral strain at failure for dry samples of shale 24.

APPENDIX F

EFFECT OF WET-DRY CYCLES ON DIAMETRAL STRAIN OF SAMPLES

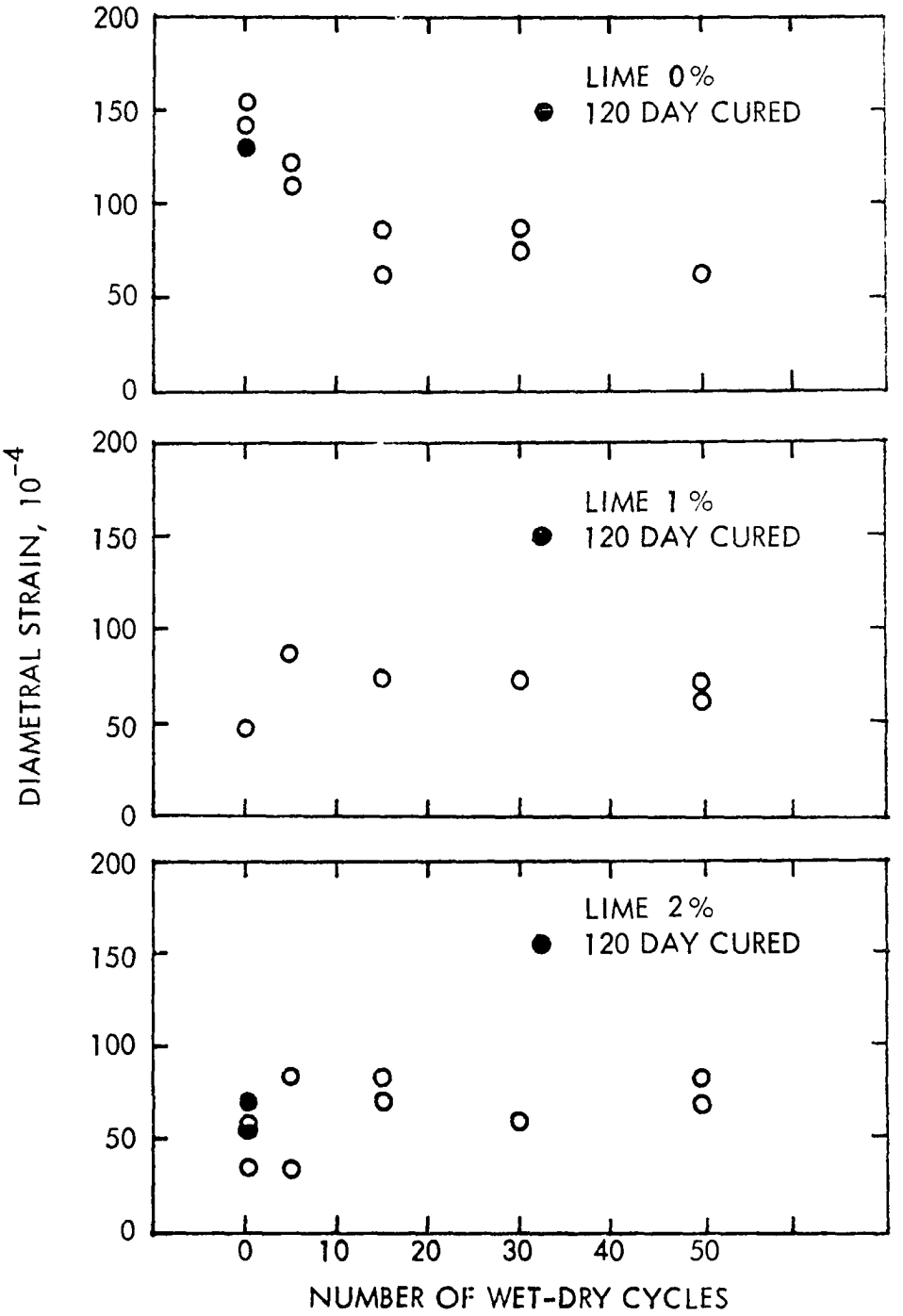


Figure F.1 Effect of wet-dry cycles on diametral strain at failure for humid samples of shale 13.

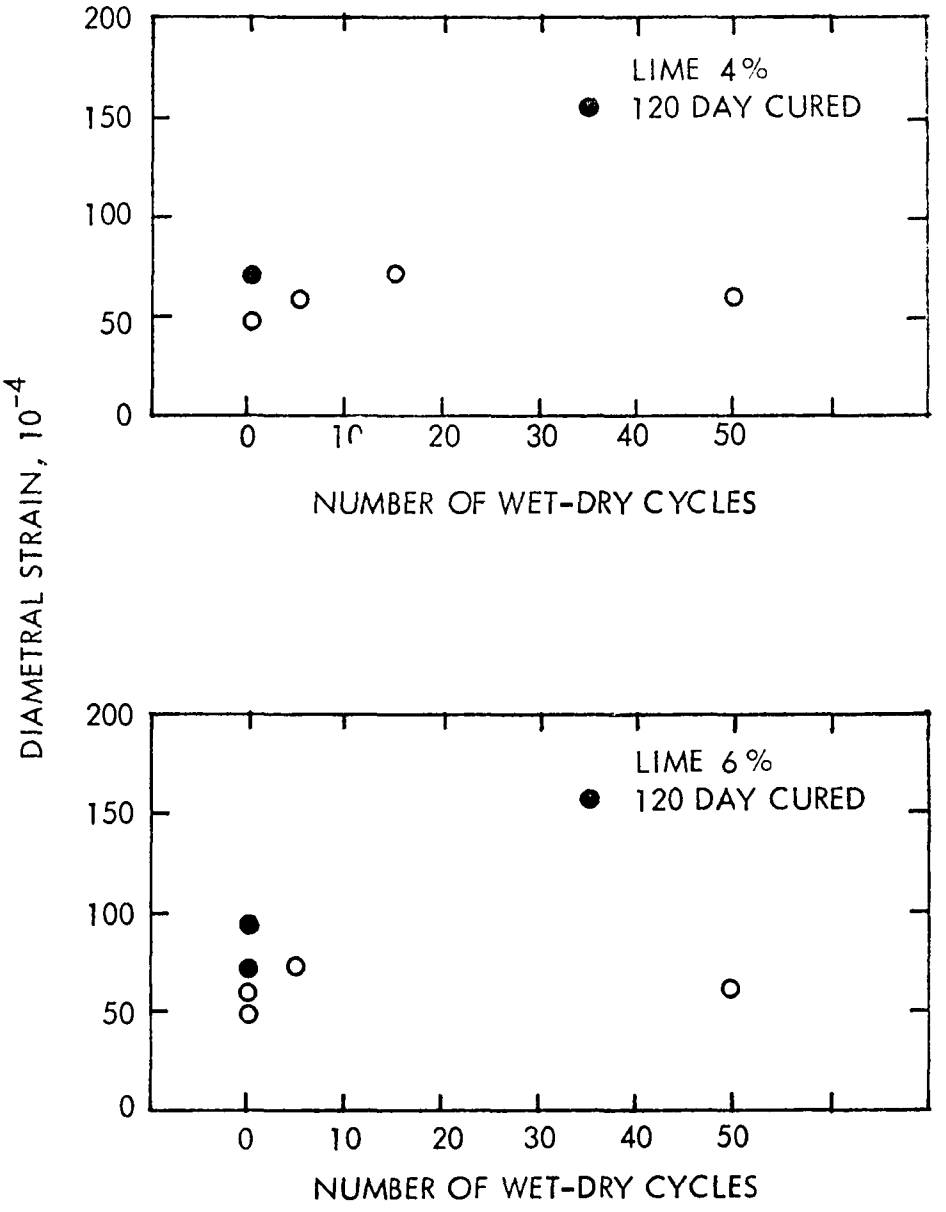


Figure F.2 Effect of wet-dry cycles on diametral strain at failure for humid samples of shale 13.

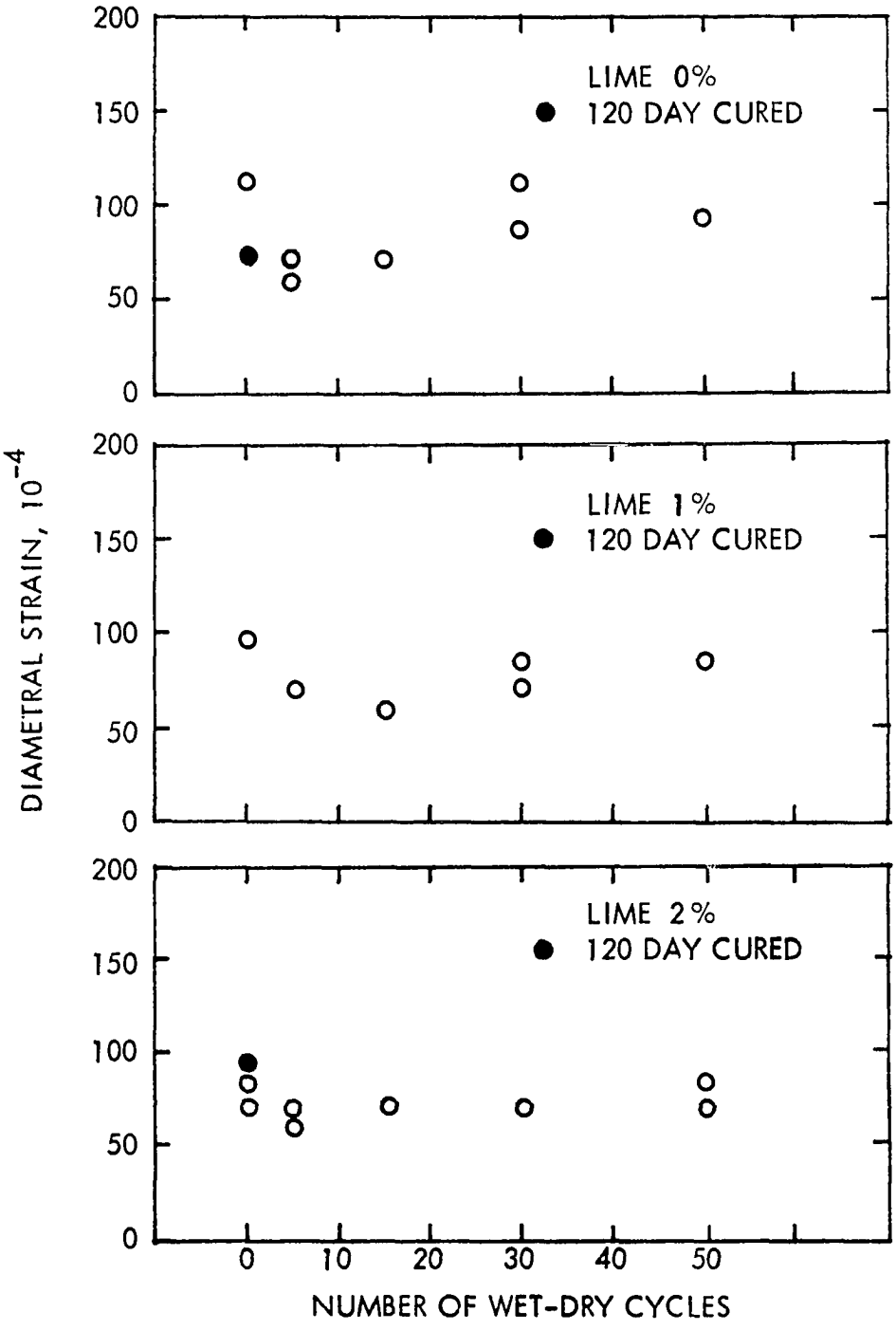


Figure F.3 Effect of wet-dry cycles on diametral strain at failure for dry samples of shale 13.

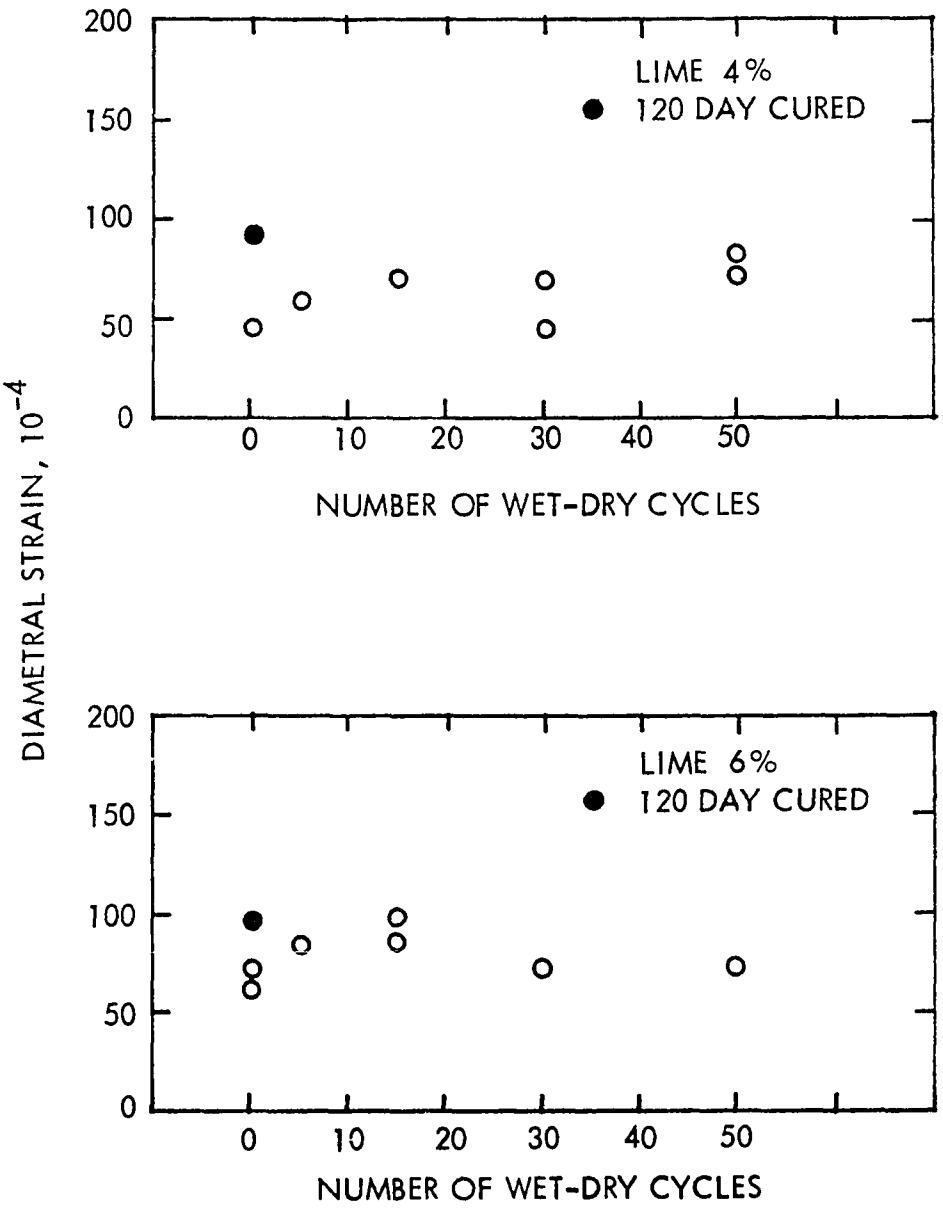


Figure F.4 Effect of wet-dry cycles on diametral strain at failure for dry samples of shale 13.

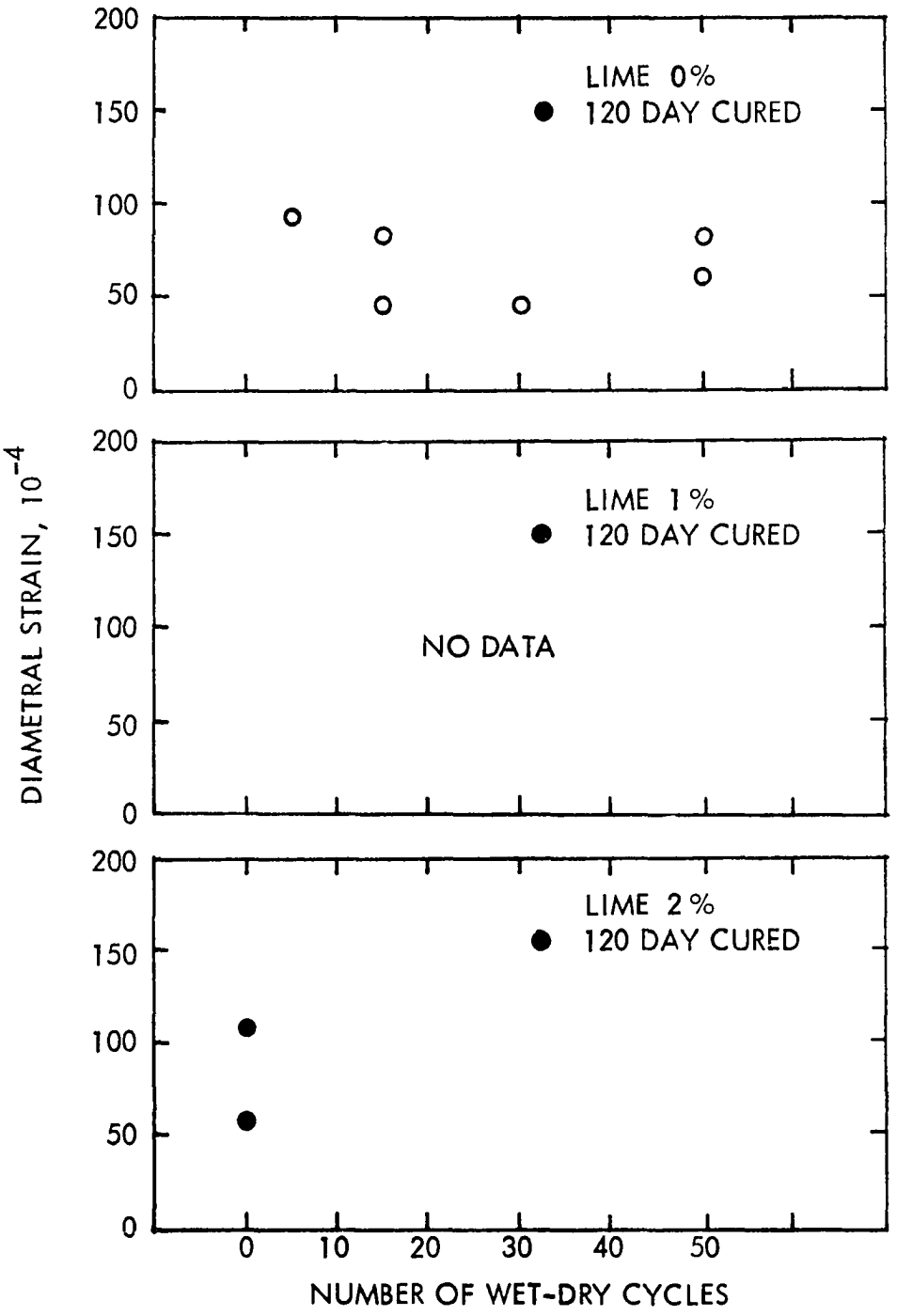


Figure E5 Effect of wet-dry cycles on diametral strain at failure for humid samples of shale 15.

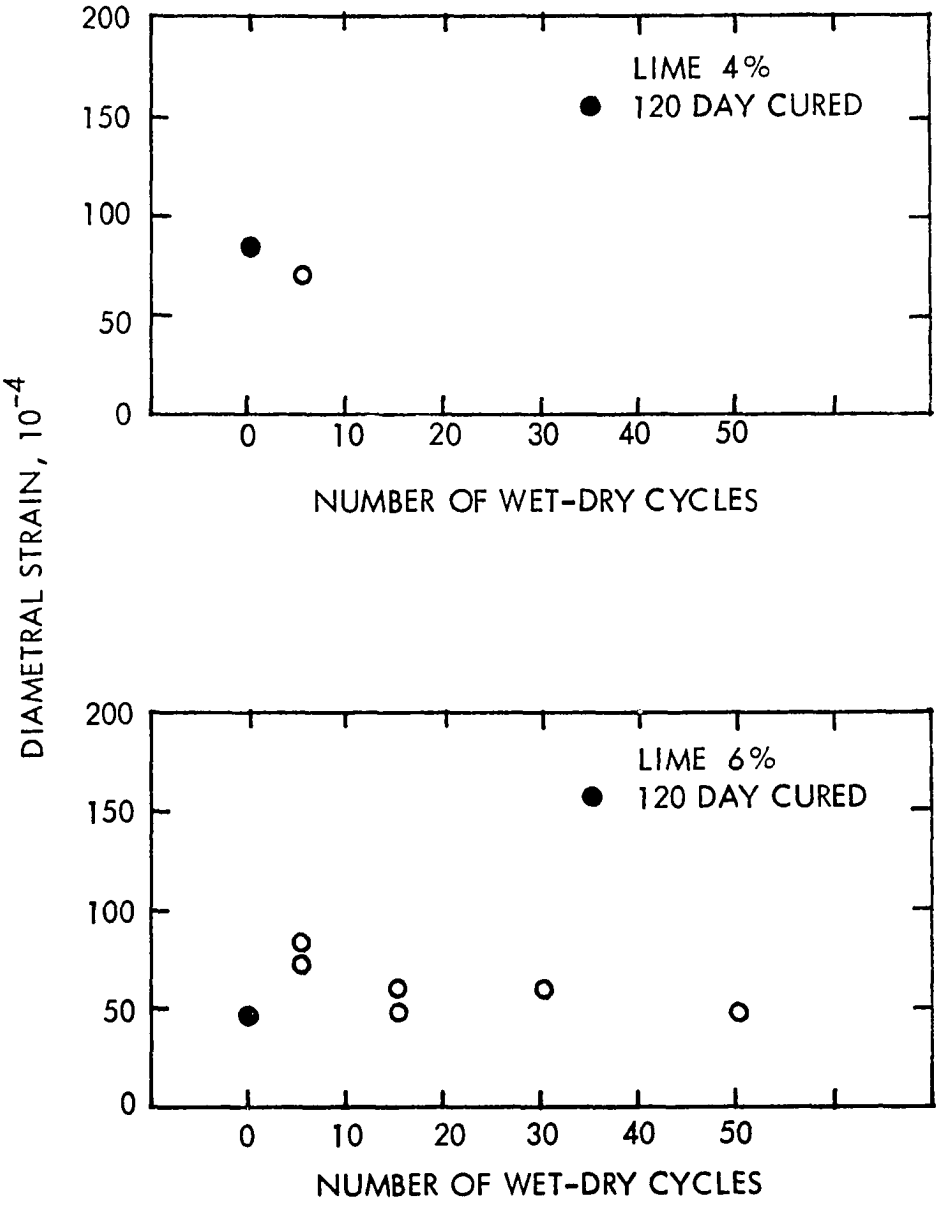


Figure F.6 Effect of wet-dry cycles on diametral strain at failure for humid samples of shale 15.

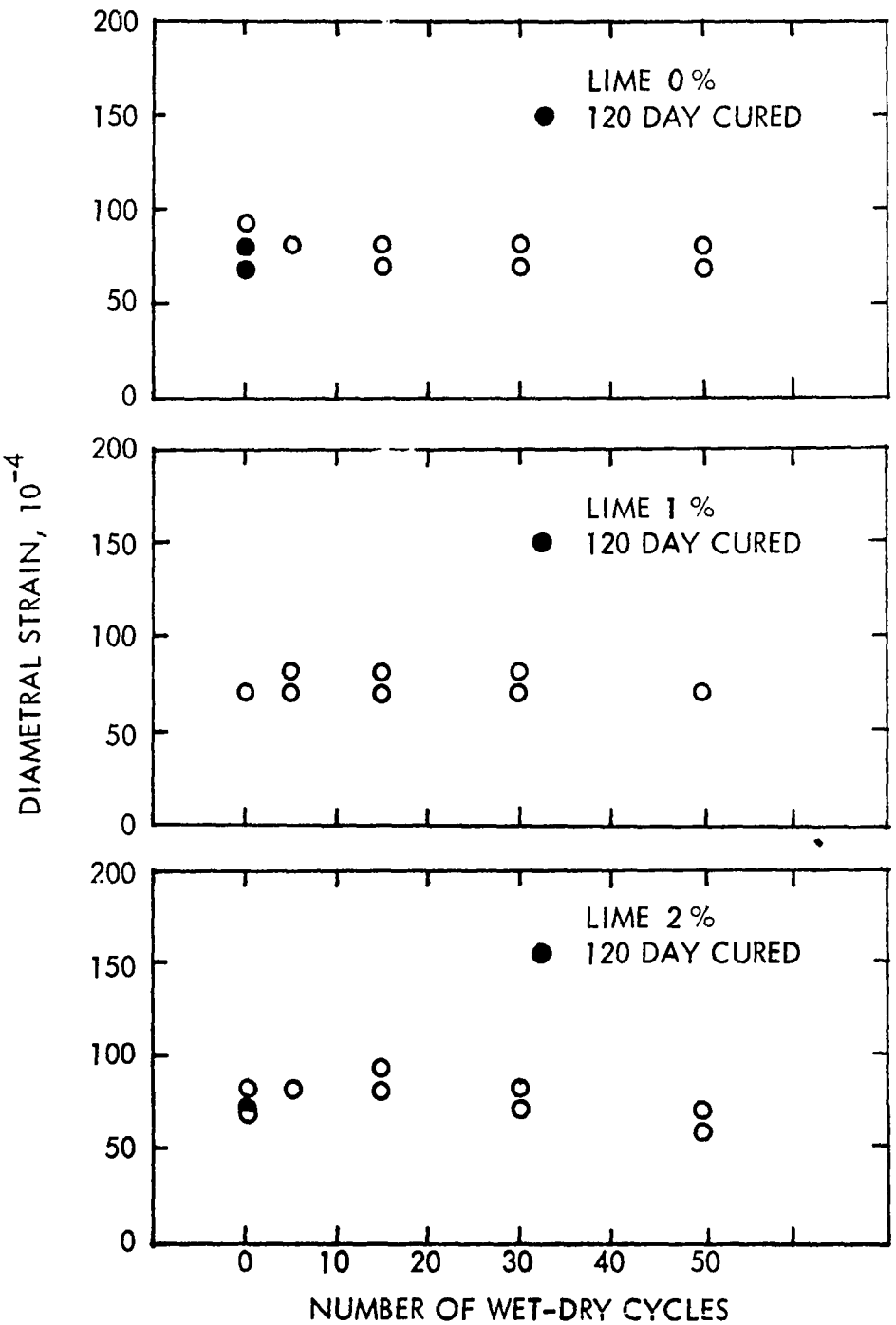


Figure E7 Effect of wet-dry cycles on diametral strain at failure for dry samples shale 15.

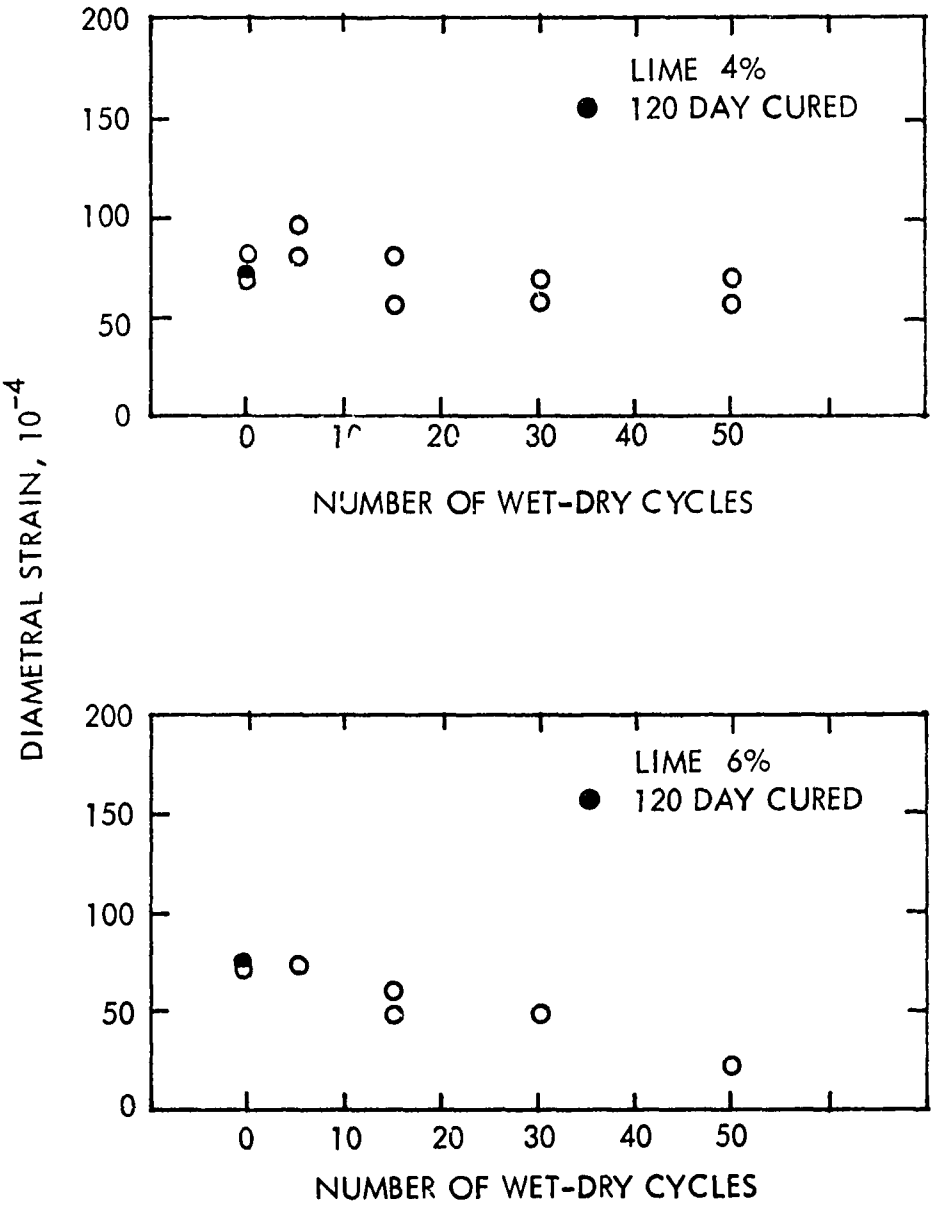


Figure F.8 Effect of wet-dry cycles on diametral strain at failure for dry samples of shale 15.

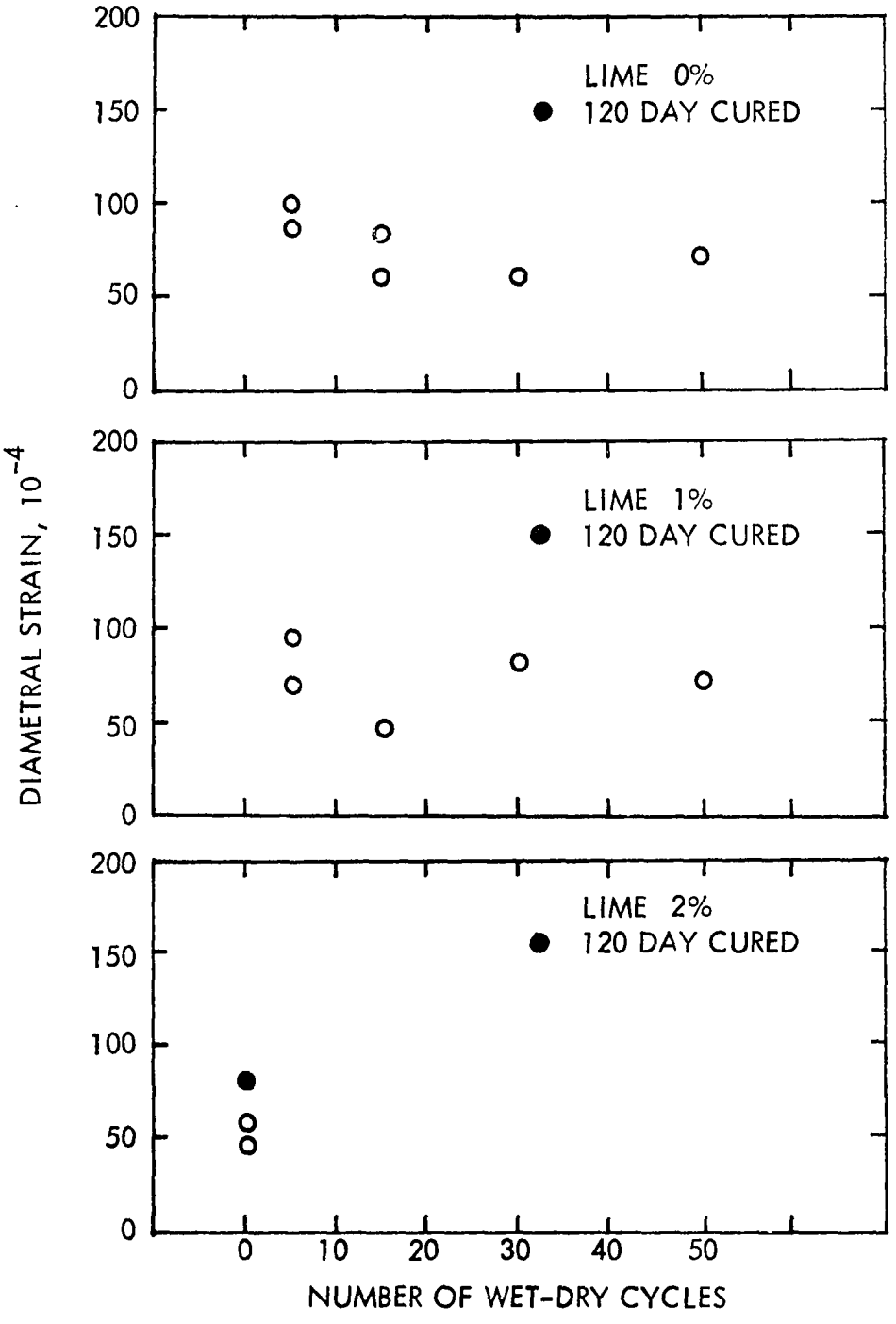


Figure F.9 Effect of wet-dry cycles on diametral strain at failure for humid samples of shale 21.

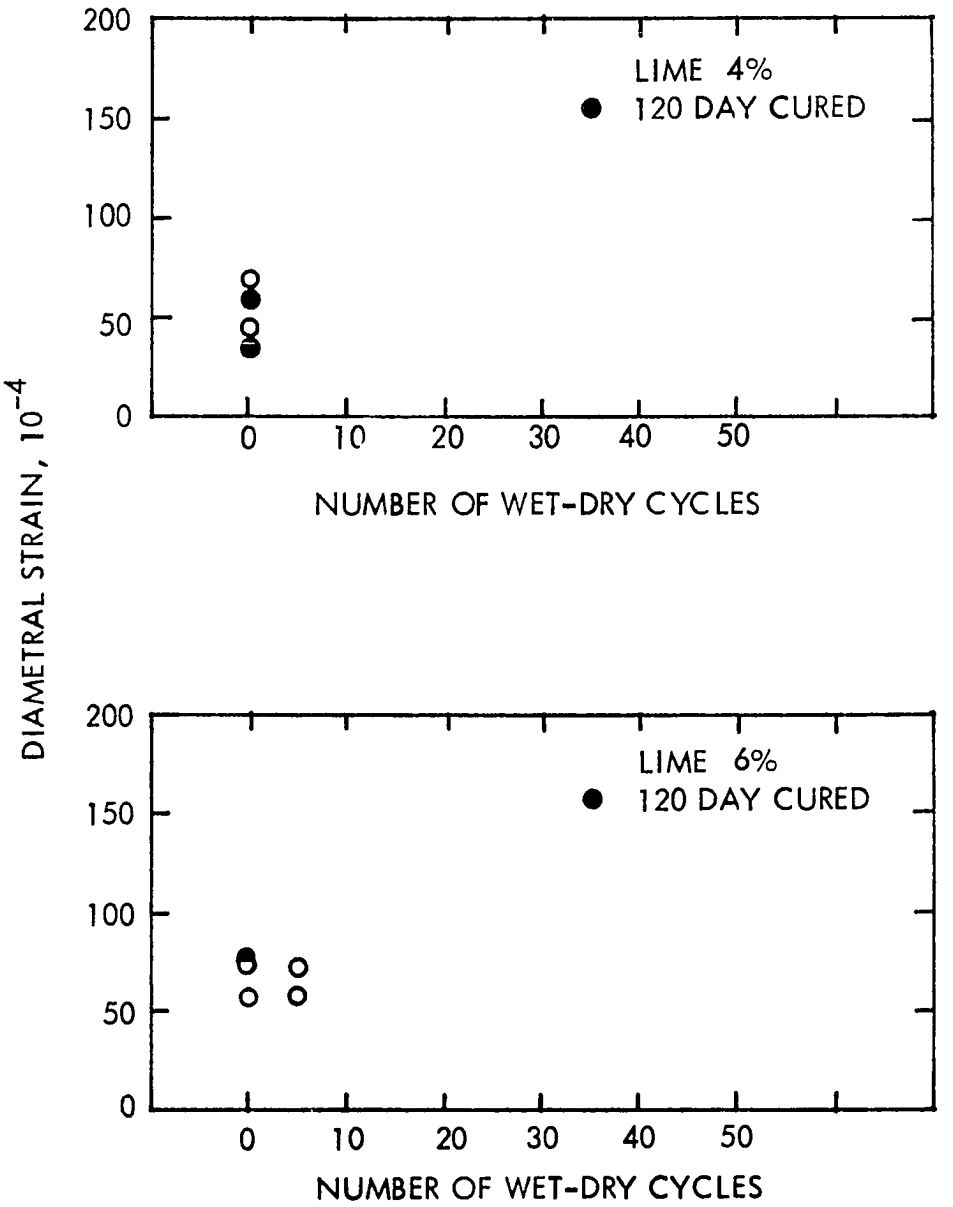


Figure F.10 Effect of wet-dry cycles on diametral strain at failure for humid samples of shale 21.

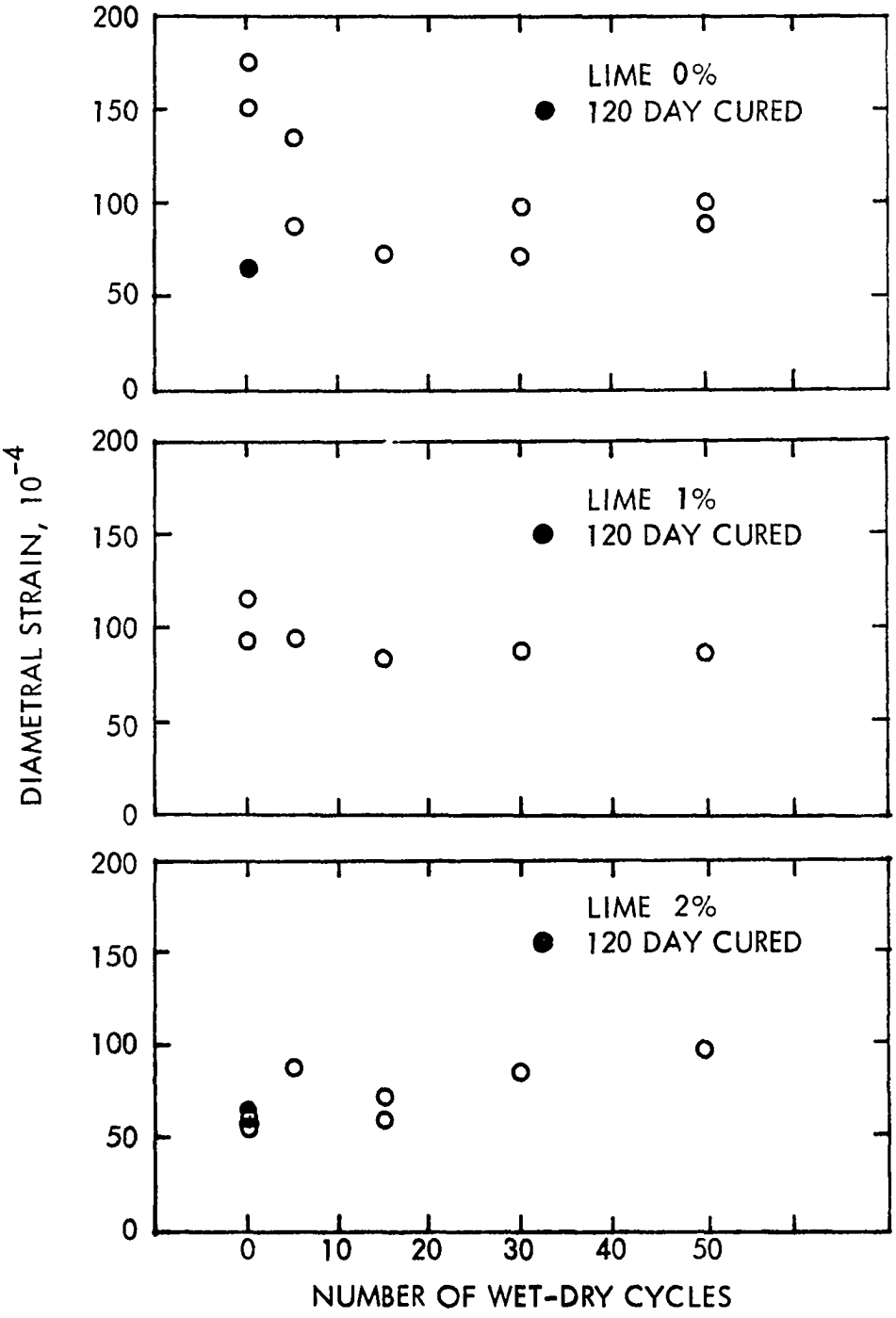


Figure F.11 Effect of wet-dry cycles on diametral strain at failure for dry samples of shale 21.

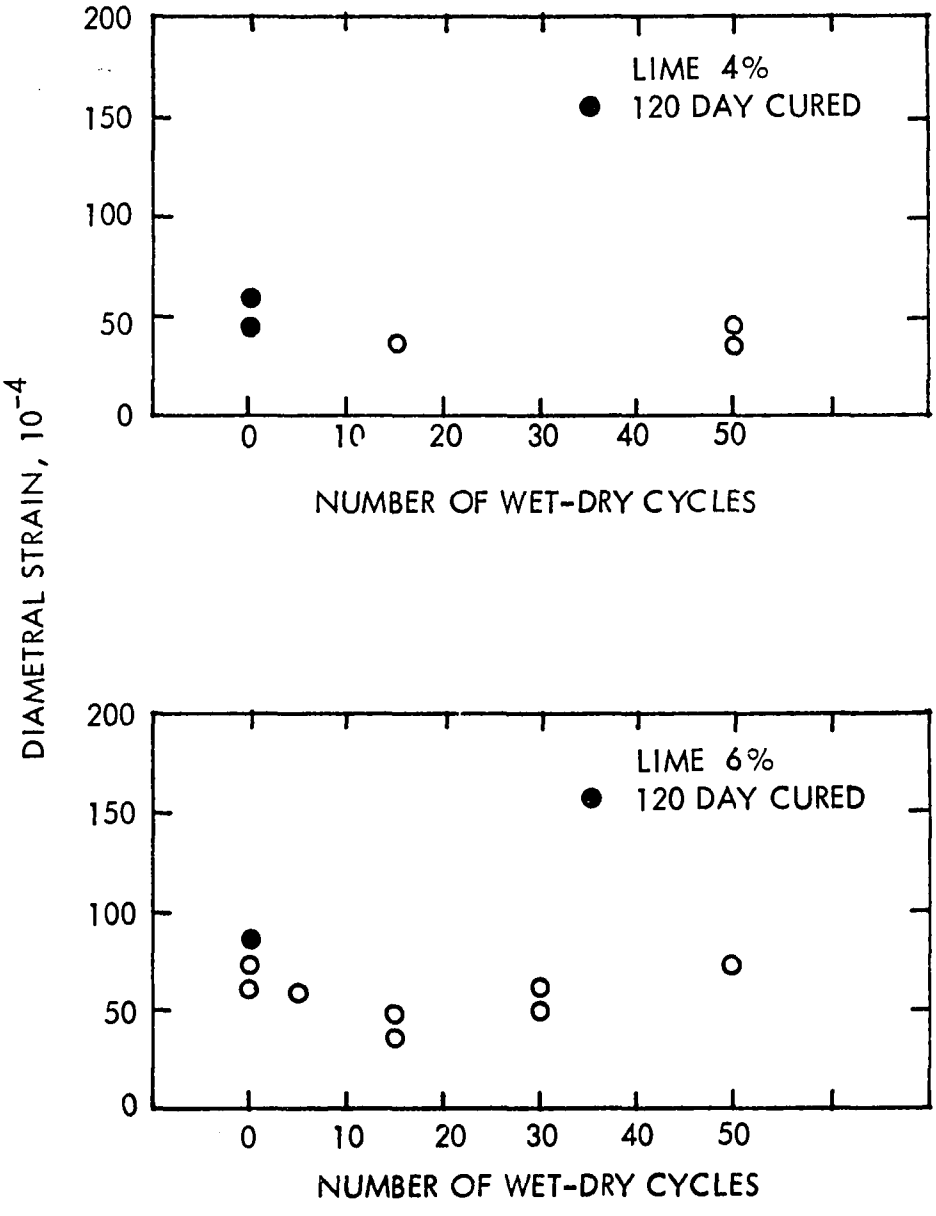


Figure F12 Effect of wet-dry cycles on diametral strain at failure for dry samples of shale 21.

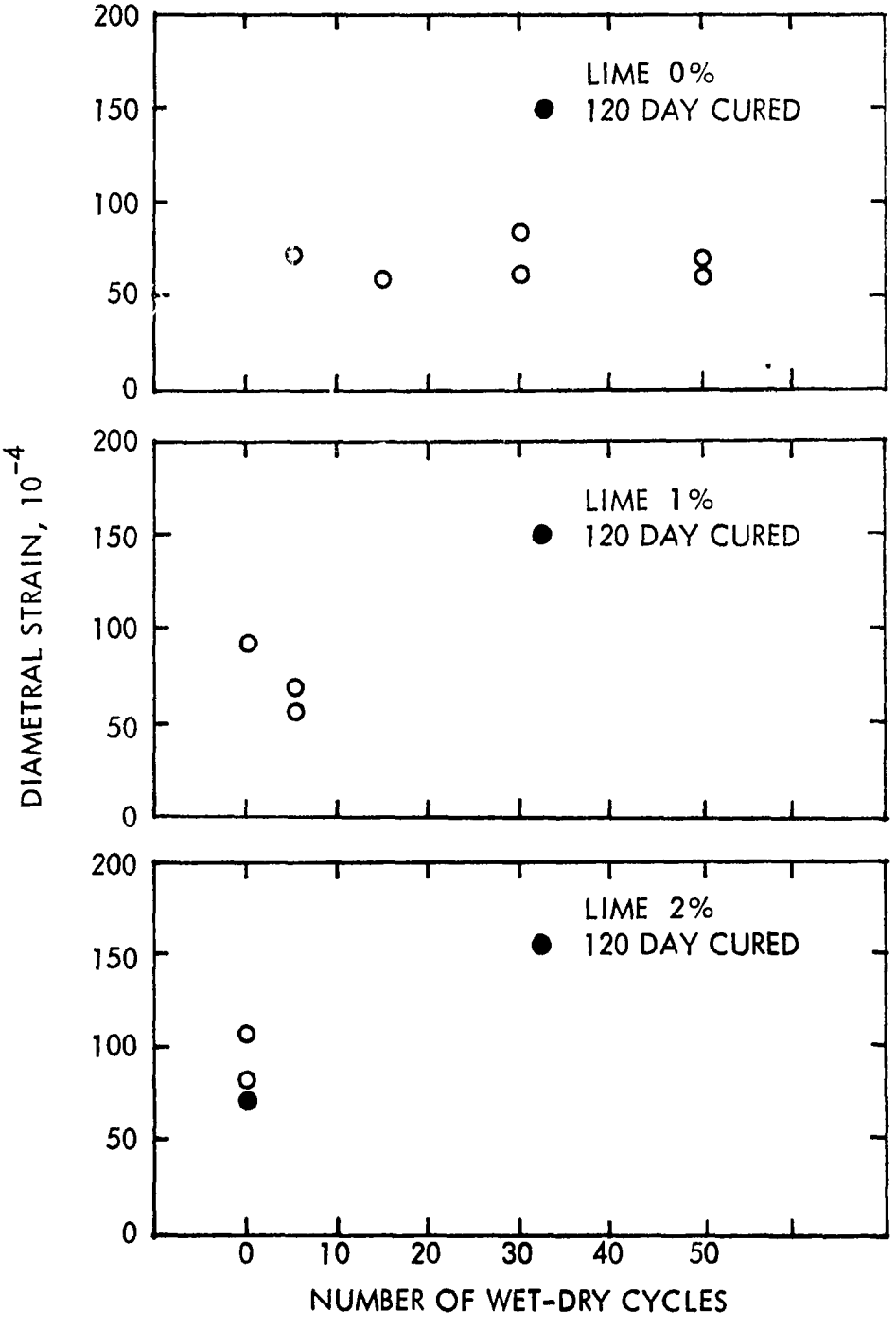


Figure F.13 Effect of wet-dry cycles on diametral strain at failure for humid samples of shale 24.

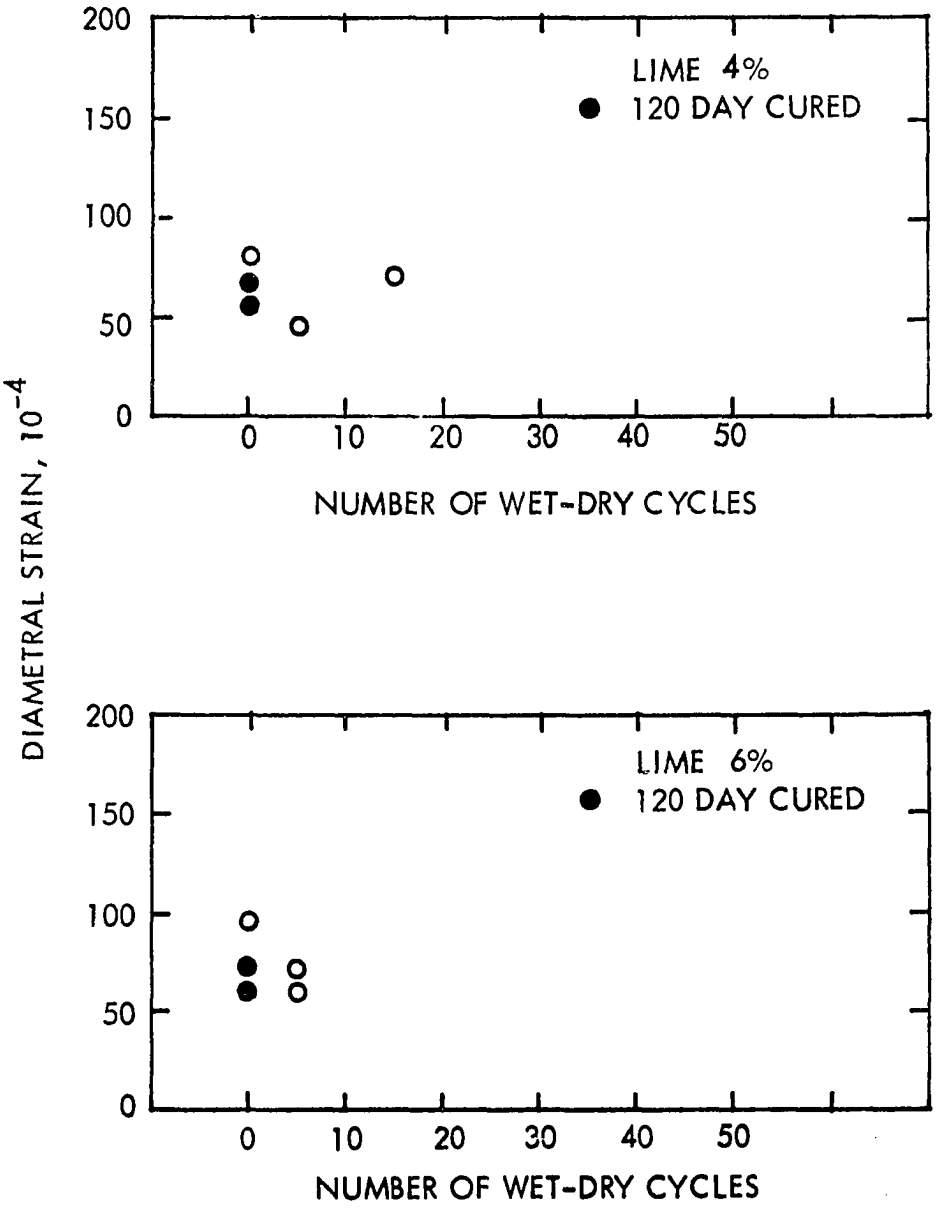


Figure F.14 Effect of wet-dry cycles on diametral strain at failure for humid samples of shale 24.

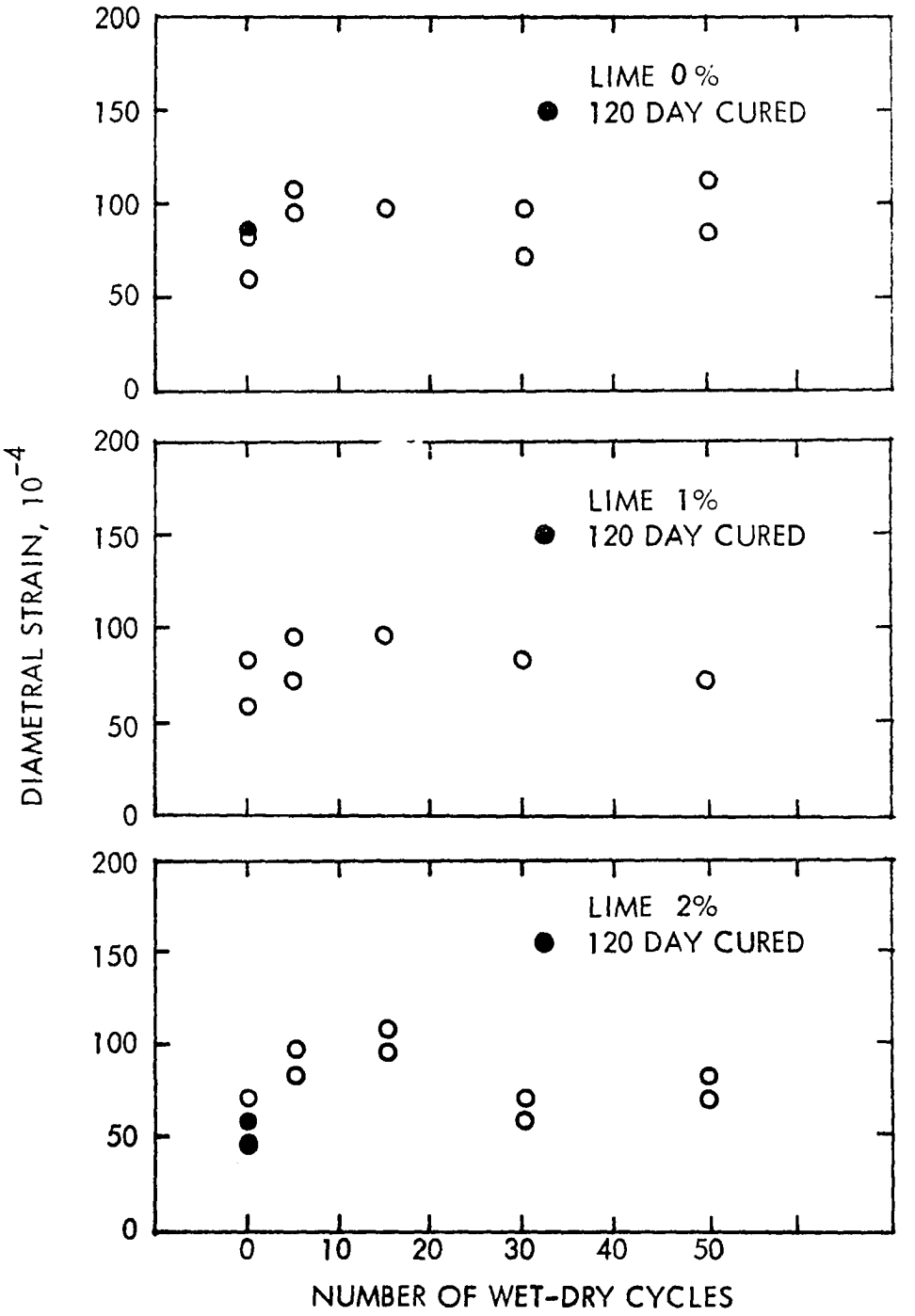
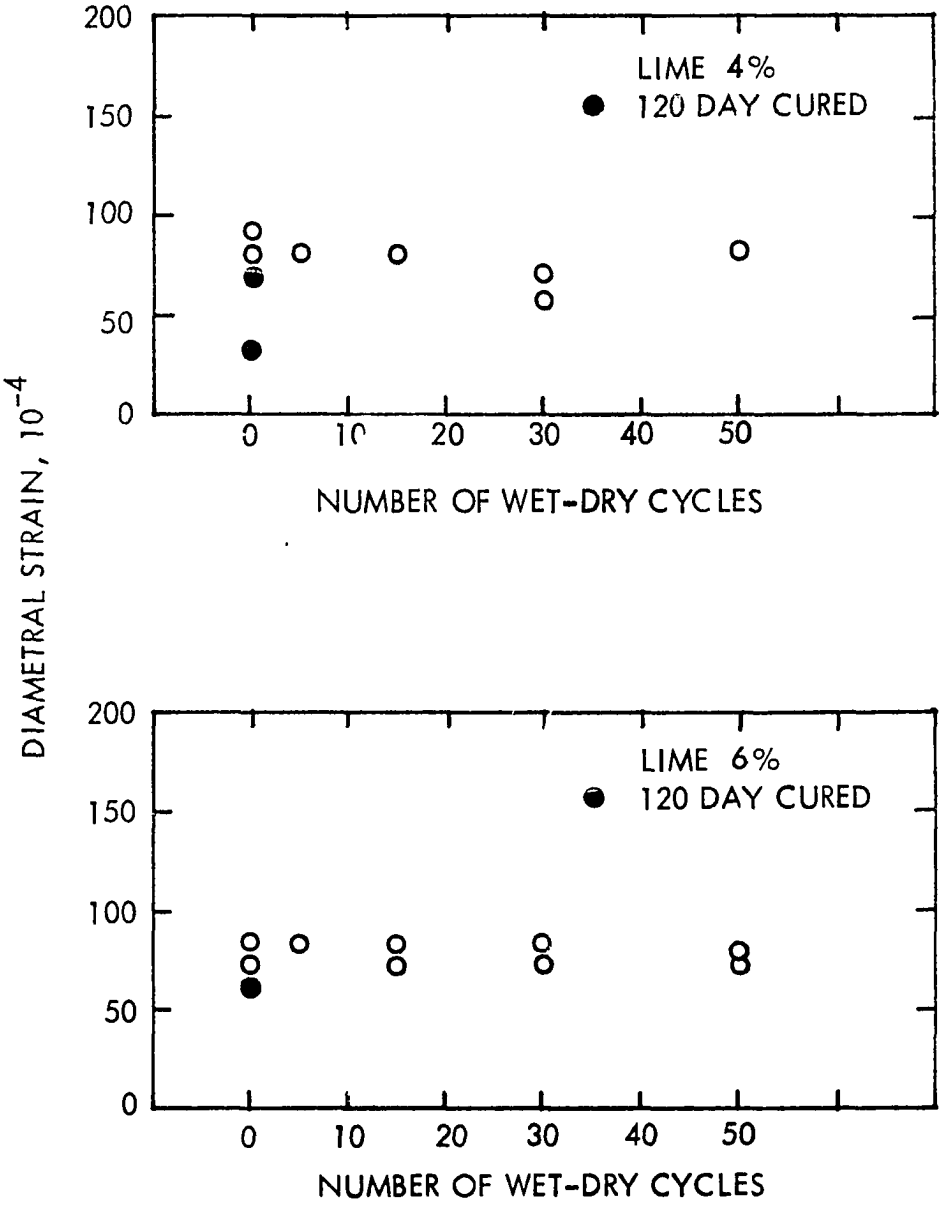


Figure F.15 Effect of wet-dry cycles on diametral strain at failure for dry samples of shale 24.



FigureF16 Effect of wet-dry cycles on diametral strain at failure for dry samples of shale 24.

APPENDIX G

EFFECTS OF AMOUNT OF LIME AND OF WET-DRY CYCLES ON THE LIQUID LIMIT VALUES OF SHALES AND SHALE LIME MIXES

TABLE G.1

EFFECTS OF AMOUNT OF LIME AND OF WET-DRY CYCLES ON THE LIQUID LIMIT VALUES OF SHALES AND SHALE LIME MIXES

Shale No.	Amount of Lime %	Test Condition[a]							
		Humid Wet-Dry Cycles				Dry Wet-Dry Cycles			
		0	15	50	LT[b]	0	15	50	LT
13	0	53	52	49	53	48	52	50	50
	1	46	45	45	--	45	47	46	--
	2	42	42	42	42	40	41	41	41
	4	38	36	36	40	35	37	35	37
	6	37	39	39	38	35	37	37	--[d]
15	0	26	25	25	26	26	25	26	24
	1	27	23	24	--	29	25	26	--
	2	29	24	25	30	28	27	29	29
	4	31	25	25	32	28	27	29	31
	6	33	24	25	--	29	29	32[c]	--
21	0	47	43	41	46	44	42	41	46
	1	38	36	36	--	37	37	38	--
	2	37	33	33	40	37	36	37	37
	4	35	31	31	--	31	32	32	--
	6	34	32	32	--	30	29	32	--
24	0	42	37	37	39	40	39	39	37
	1	39	34	34	--	38	35	36	--
	2	39	32	32	37	35	33	34	36
	4	37	30	30	37	34	31	32	34
	6	36	30	30	--	34	33	32	--

[a]Condition of sample at the time of Split Tensile Strength Testing.

[b]120-day cured sample.

[c]The underlined value indicates that considerable difficulty was experienced in determining this test value.

[d]It was not possible to determine the test value shown by two dashes (--).

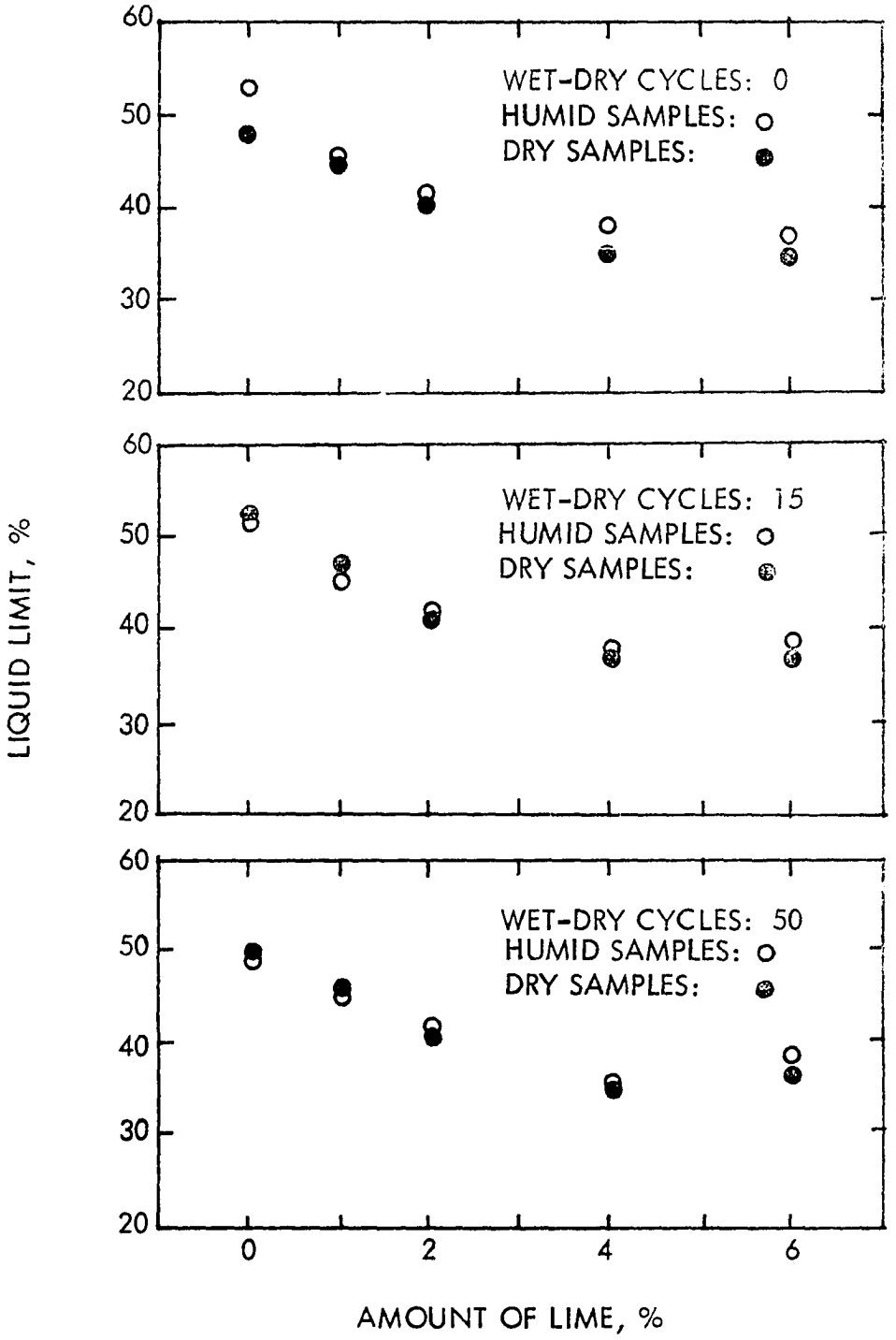


Figure G.1 Effect of amount of lime on liquid limit values for shale 13.

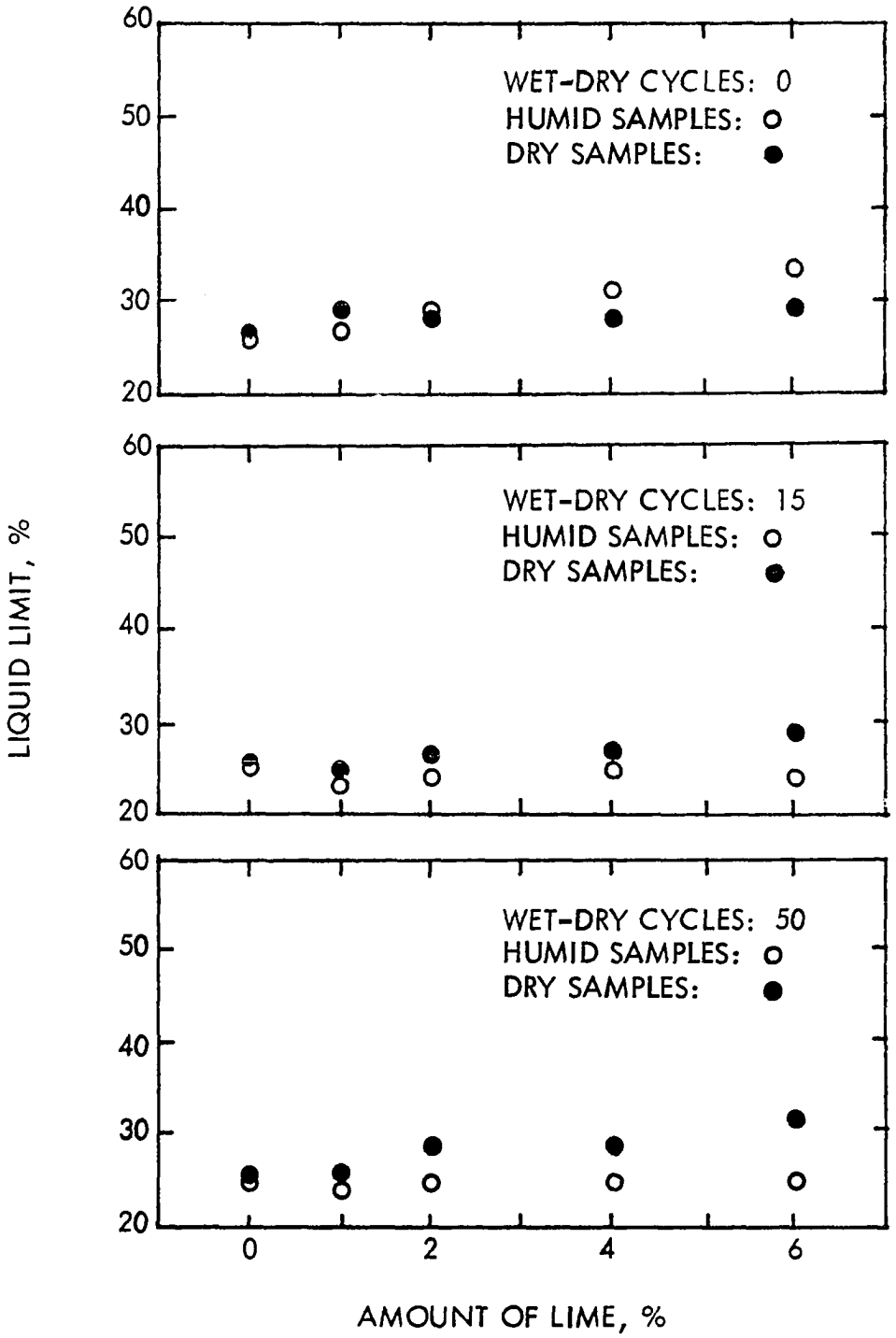


Figure G.2 Effect of amount of lime on liquid limit values for shale 15.

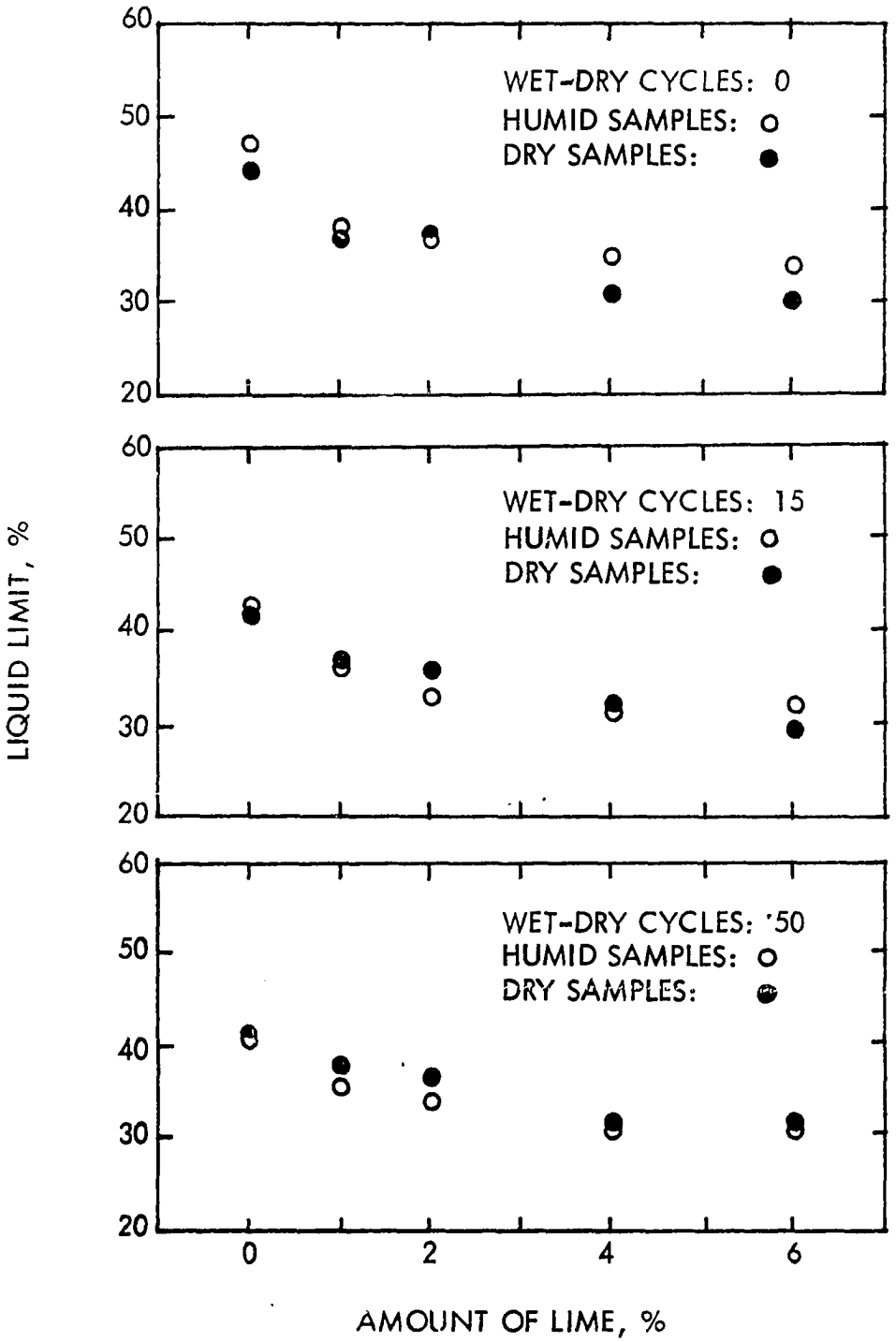


Figure G.3 Effect of amount of lime on liquid limit values for shale 21.

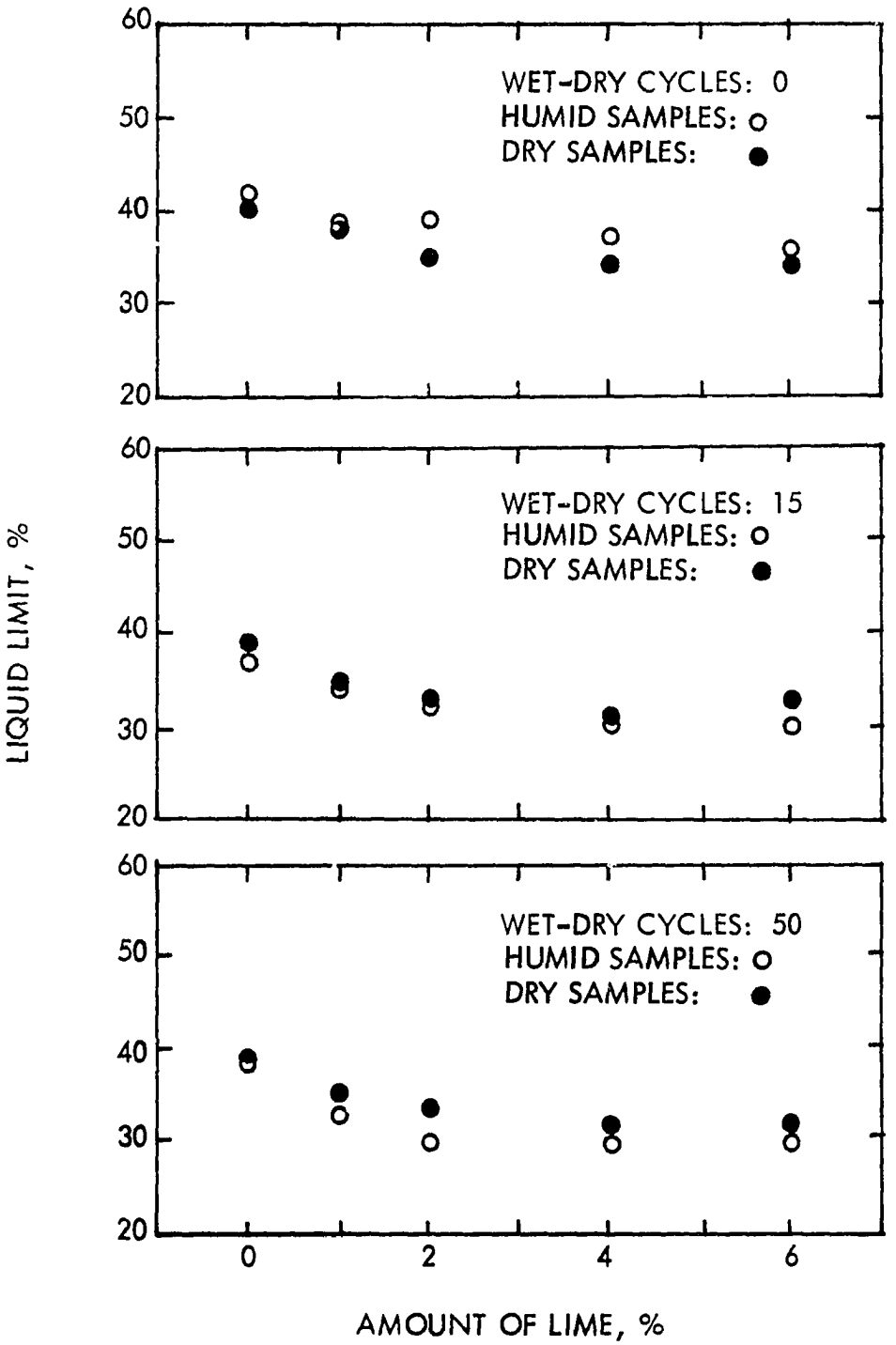


Figure G.4 Effect of amount of lime on liquid limit values for shale 24.

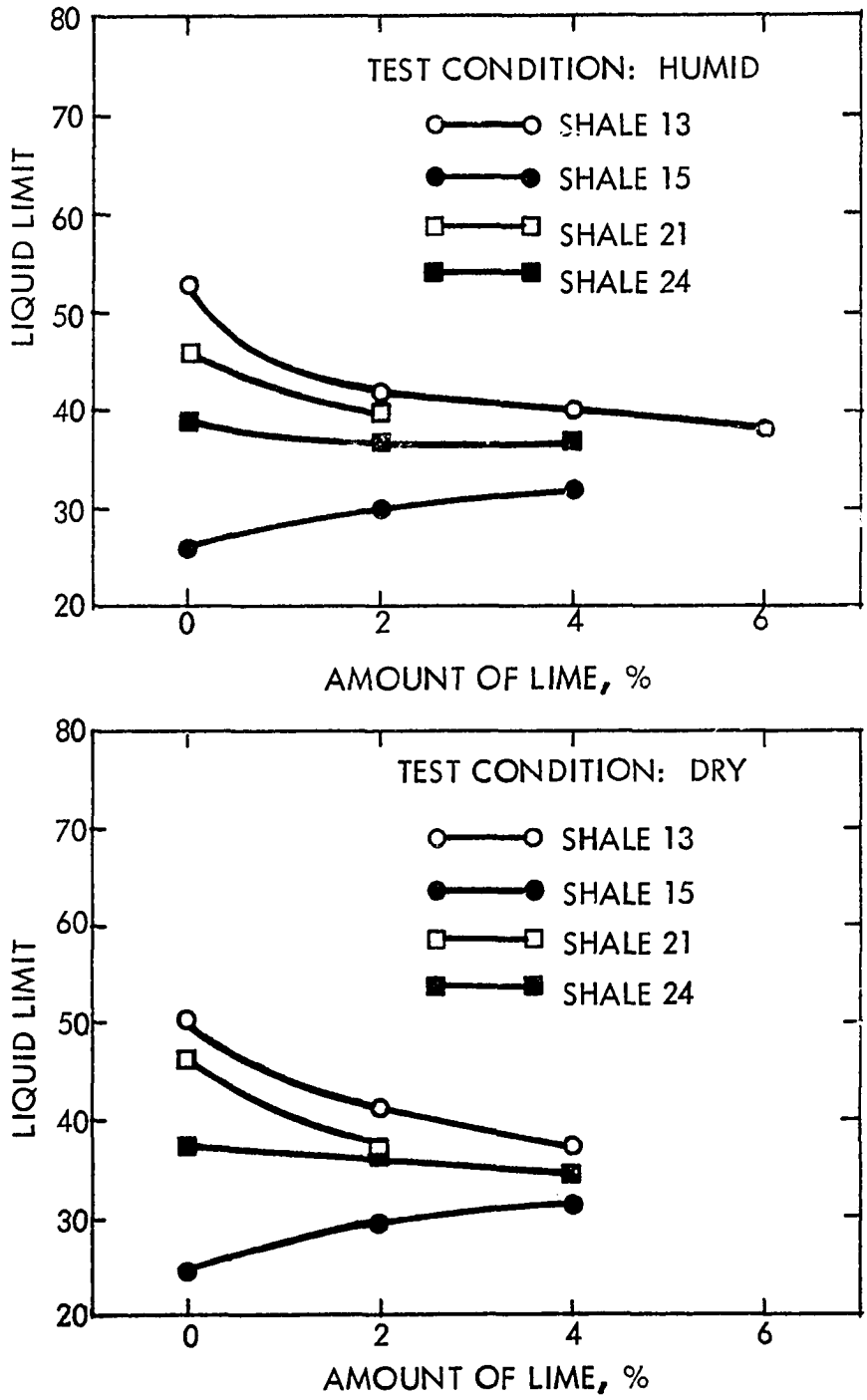


Figure G.5. Change in liquid limit values with the amount of lime for 120-day cured samples.

APPENDIX H

EFFECTS OF AMOUNT OF LIME AND OF WET-DRY CYCLES ON THE PLASTICITY INDEX VALUES OF SHALES AND SHALE LIME MIXES

TABLE H.1

EFFECTS OF AMOUNT OF LIME AND OF WET-DRY CYCLES ON THE PLASTICITY INDEX VALUES OF SHALES AND SHALE LIME MIXES

Shale No.	Amount of Lime %	Test Condition[a]							
		Humid Wet-Dry Cycles				Dry Wet-Dry Cycles			
		0	15	50	LT[b]	0	15	50	LT
13	0	31	29	29	30	28	31	32	28
	1	21	21	22	--	22	23	21	--
	2	17	16	18	15	17	15	14	13
	4	8[c]	12	13	--[d]	--	--	--	--
	6	--	13	17	--	--	--	--	--
15	0	7	6	9	8	8	8	7	8
	1	8	5	5	--	--	7	6	--
	2	--	8	7	--	--	--	--	--
	4	--	7	6	--	--	--	--	--
	6	--	--	6	--	--	--	--	--
21	0	19	16	15	20	19	17	16	18
	1	13	11	12	--	14	12	12	--
	2	10	--	10	9	--	--	--	6
	4	--	--	--	--	--	--	--	--
	6	--	--	6	--	--	--	--	--
24	0	18	14	16	15	19	15	14	12
	1	15	11	11	--	14	12	13	--
	2	14	10	8	12	10	--	10	9
	4	--	--	--	--	--	--	--	--
	6	--	--	8	--	--	--	--	--

[a]Condition of sample at the time of Split Tensile Strength Testing.

[b]120-day cured sample.

[c]The underlined value indicates that considerable difficulty was experienced in determining this test value.

[d]It was not possible to determine the test value shown by two dashes (--).

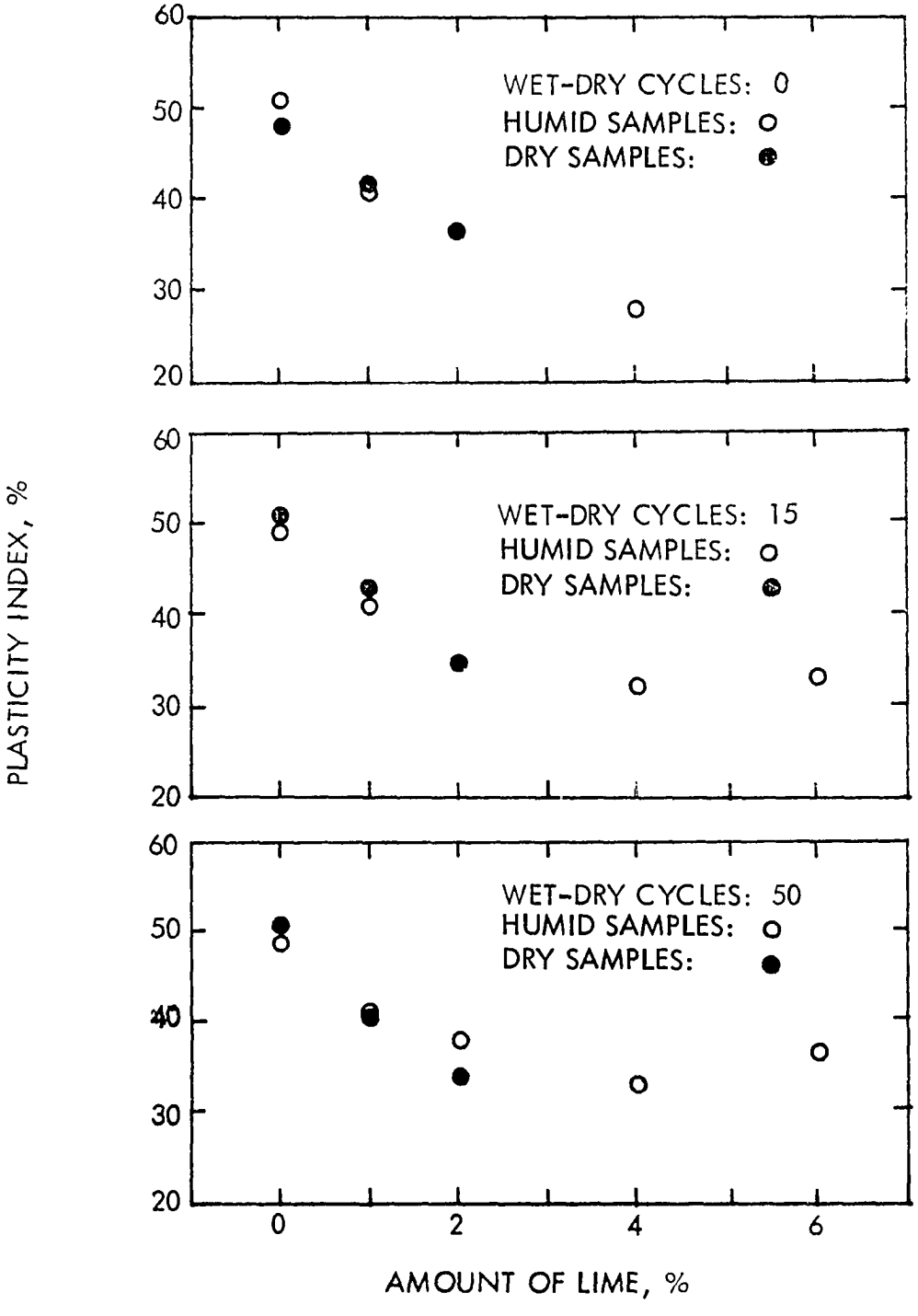


Figure H.1 Effect of amount of lime on plasticity index values for shale 13.

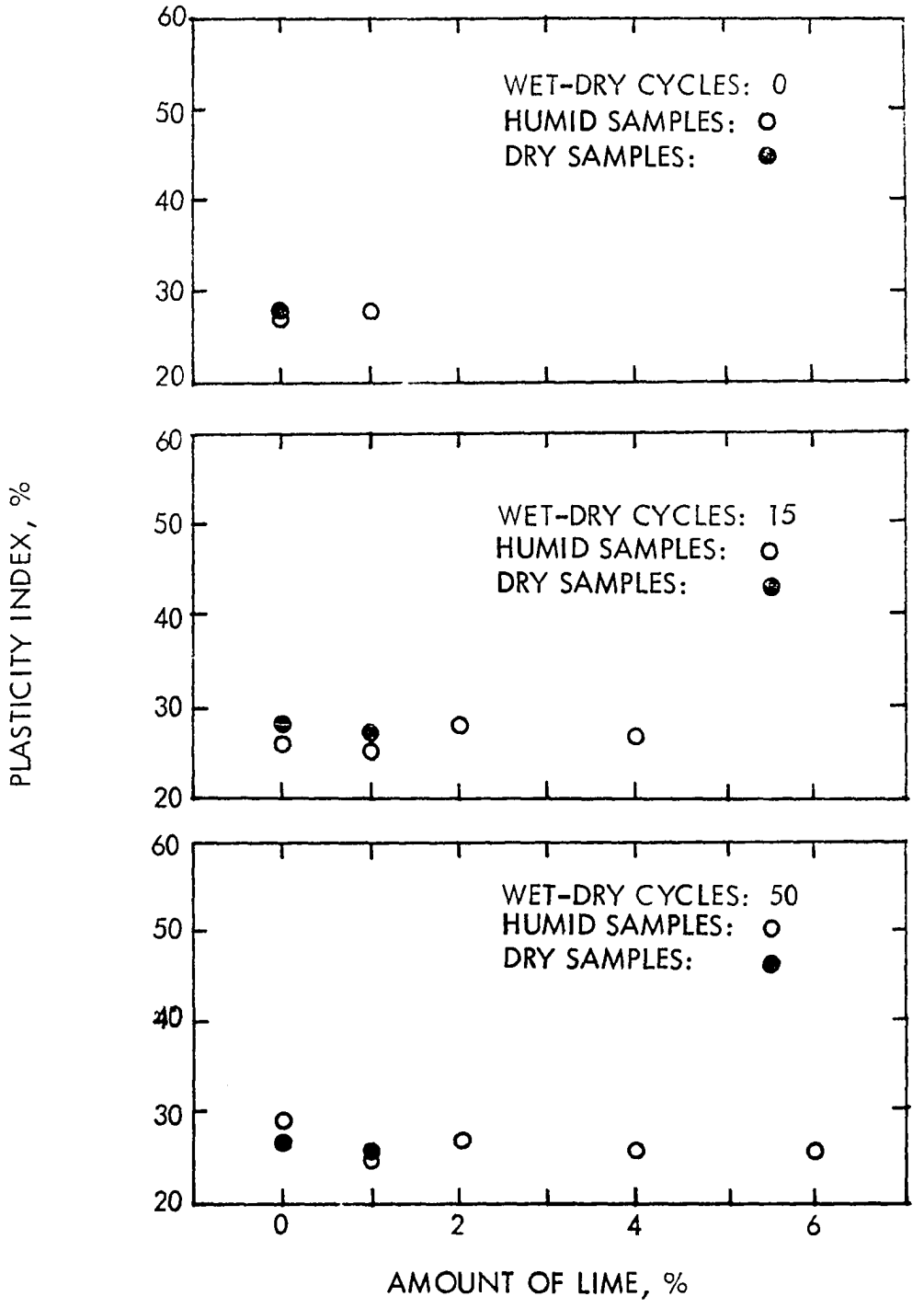


Figure H.2 Effect of amount of lime on plasticity index values for shale 15.

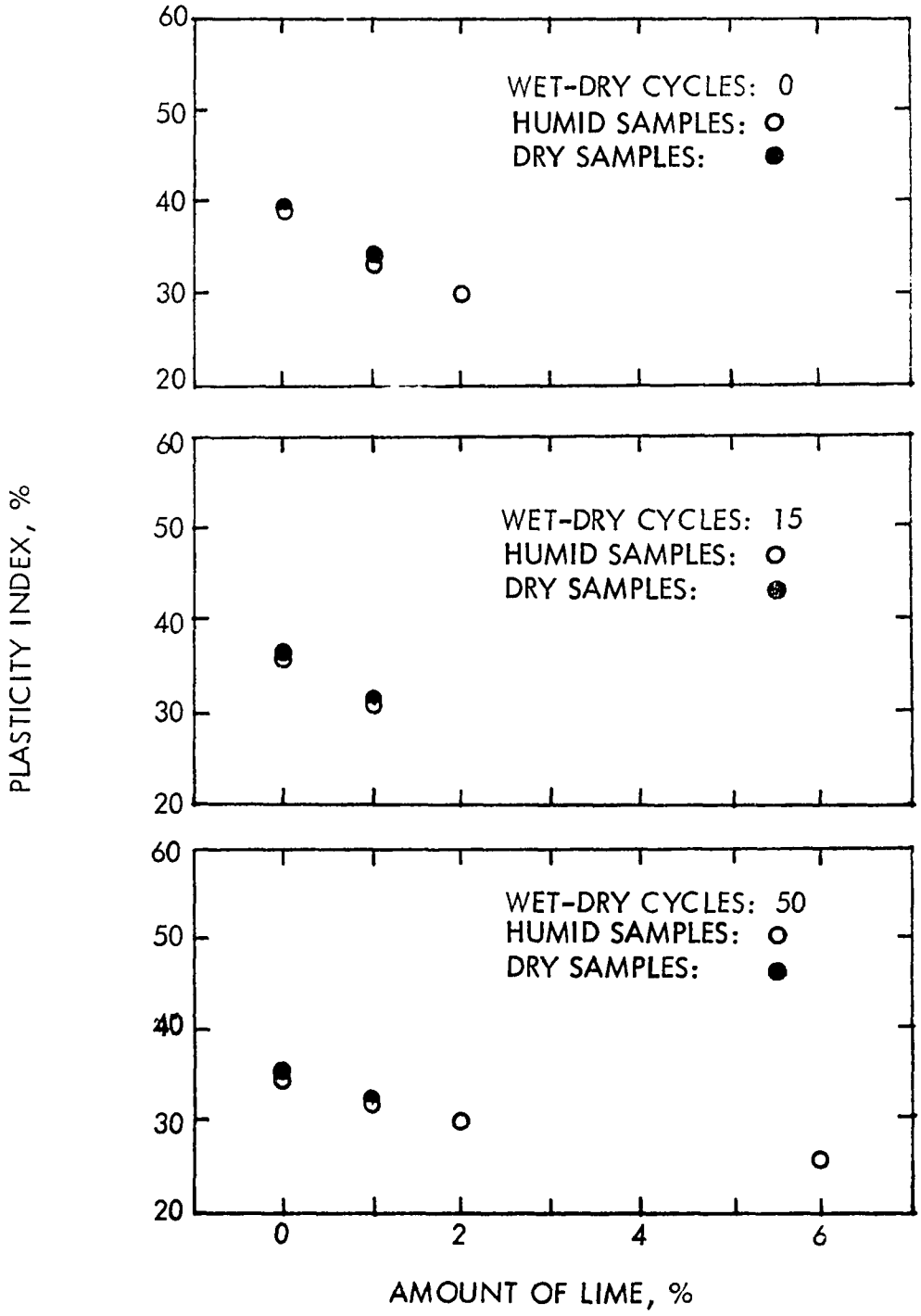


Figure H.3 Effect of amount of lime on plasticity index values for shale 21.

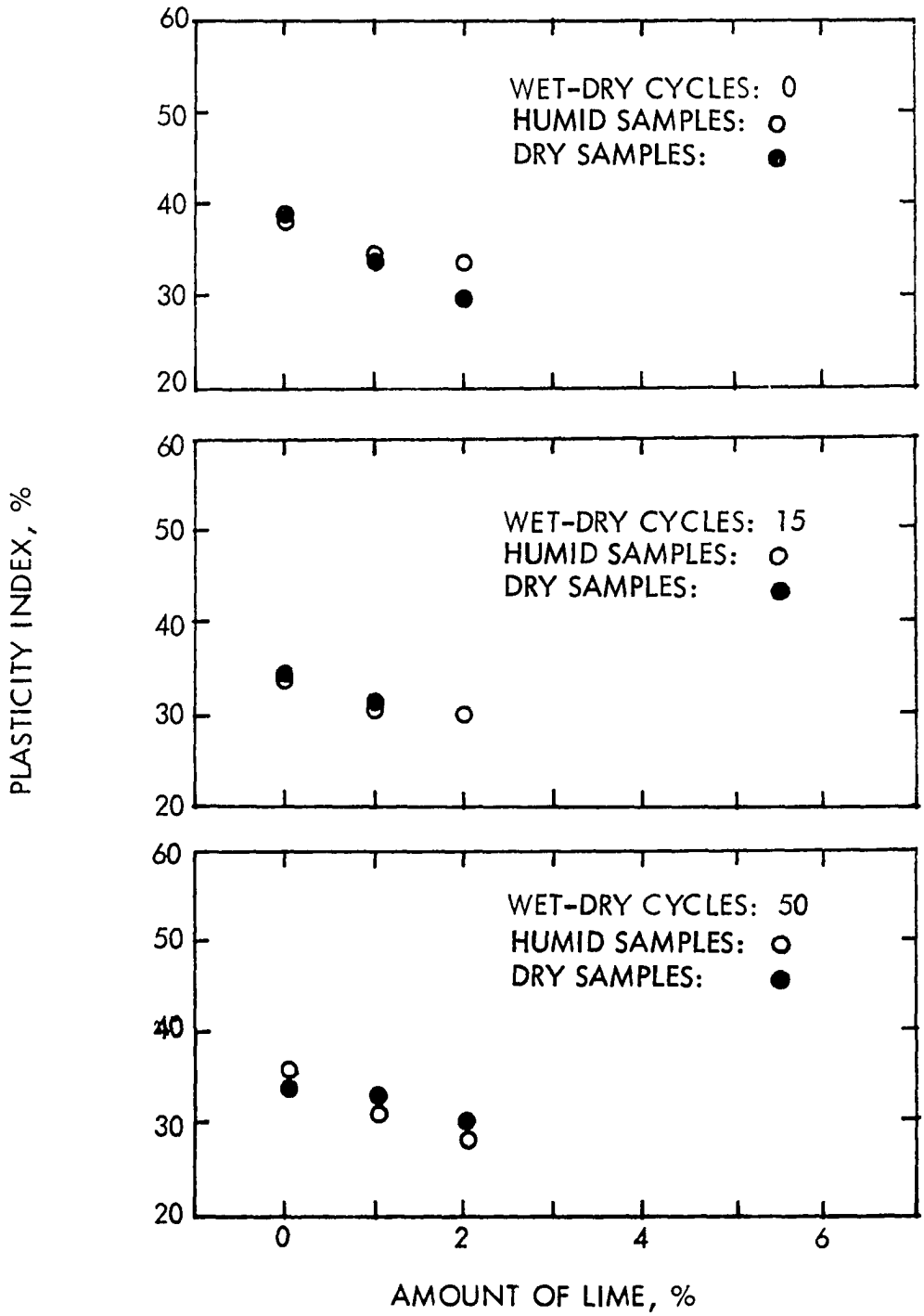


Figure H.4 Effect of amount of lime on plasticity index values for shale 24.

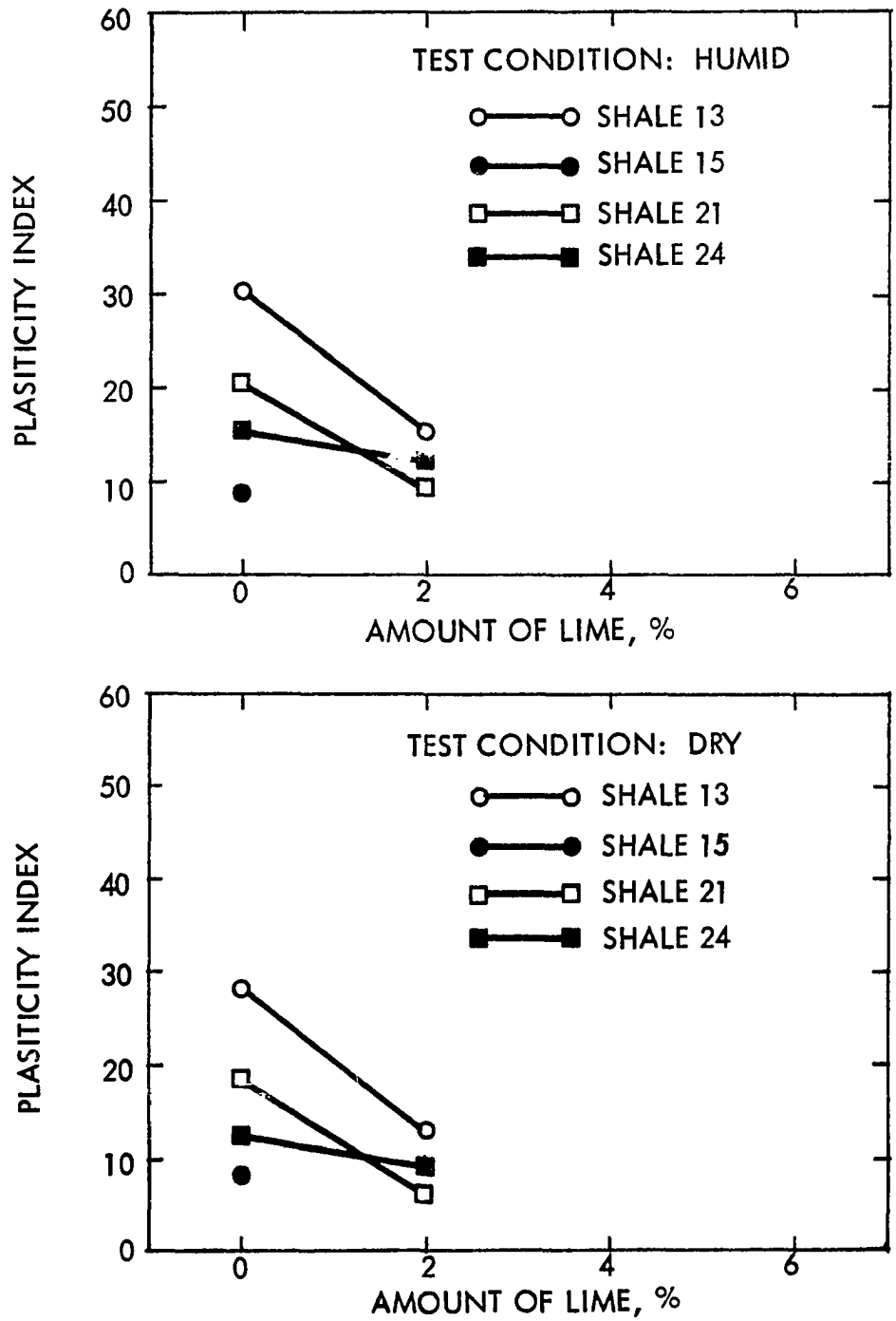


Figure H.5 Change in plasticity index values with amount of lime 120 day cured samples.